Exploring Cooperation and Competition in Molecular Chaperone Networks with Chemical Genetics and Peptide Microarrays

by

Anne Gillies

A dissertation submitted in partial fulfillment
of the requirements for the degree of
Doctor of Philosophy
(Chemical Biology)
in the University of Michigan
2013

Doctoral Committee:

Associate Professor Jason E. Gestwicki, Chair
Associate Professor Anuj Kumar
Associate Professor Duxin Sun
Associate Professor Raymond C. Trievel

Dedication

To my first and best science teacher: my dad.

Acknowledgements

This work would not have been possible without the guidance of my advisor, Dr. Jason Gestwicki. Through a deft combination of support and allowing me to find my own way, he has helped me to grow by leaps and bounds as a scientist and person. I thank him for always helping me to achieve my goals, even when those goals were constantly evolving. I would also like to thank the members of the Gestwicki lab, past and present, for creating a positive, stimulating environment to work in every day. I have learned so much from every one of you. Thank you to Andrea, Lyra, and Ashley, who welcomed me to the lab with open arms and taught me nearly everything I know, while filling the days with laughter and energy. You are all brilliant and generous with your brilliance – it was a privilege to learn from you. Thank you to Gladis for patiently teaching me how to work with yeast and for sharing stories and laughter. Thank you to the rest of the first generation who were in the lab when I arrived, Chris, Srikanth, Paul, Yoshi and Matt, for making every day fun, interesting, and educational. Thank you to Leah, whose curiosity and insight were inspirational on a daily basis ever since we joined the lab together. Victoria, I'm so glad to have had my friend as a bay mate. You were always willing to listen and help, whether it was with experiments or my life goals, and we shared many laughs – thank you. Thank you also for your hard work on the FP platform and for your thoughtful discussions on the amyloid project. Many thanks to Sharan for taking my teasing and giving it right back, for willingly acting as a medical dictionary, and for being a friend. Thank you to Laura for being a shoulder to lean on, a friend to laugh with, and a fellow grad student to

commiserate with. To the new generation – Jenny, Bryan, and Zapporah – you gave our quiet lab a kick in the pants, and it's been a delight having you around. I know the future of the lab is in great hands with you. Thank you to Tomoko, Atta, Katie, and Xiaokai, for sharing your wisdom and kindness. Tomoko, you will be missed. We have had many rotation students come through, and I was lucky enough that several were friends – Francisco Garcia, Steffen Bernard, JP Carolan, Paul Lund, David Rogawski, thank you for making my days brighter while you were around. To my two mentees, Carrie Johnson and Anne Zhang, I had a great time working with you that summer; thank you for being so joyful and enthusiastic, even when science wasn't going our way. Thank you also to Amanda Wong, whose thoughtful, intellectual approach to the amyloid array project was inspiring and enormously helpful.

I have also had the pleasure and privilege of working with many wonderful scientists throughout my time here. Thank you to Professor Kumar for always being willing to talk through my research and being generous with your time and lab space. Thank you to Professor Dickey, Dr. Jose Abisambra, Eric Tse, and Dr. Matt Scaglione for helpful conversations and sharing materials and interesting results that informed my work. Thank you to Professor Trievel and Professor Sun for your support and helpful advice as members of my committee. And thank you to Professor Anna Mapp for your wisdom, guidance, and unwavering support for my unconventional goals.

I want to thank all my friends for being my constant source of strength and humor throughout the crazy ride that is grad school. Everyone in the Chemical Biology program

formed a little family that I was so lucky to be a part of. Thank you to my four first year roommates, Emily, Nichole, Debbie, and Jess, cobbled together from a housing website, who became some of my dearest friends and shared in tears and laughter. Thank you to the Friday Night Dinner crew, led by Noah, for helping me to unwind at the end of many weeks and expanding my Ann Arbor family more than I could have dreamed. To the friends I made outside of the life sciences bubble, Stacey, Lizzi, Beth, Heather, Leslie, Erica, and Bailey, nerdy girlfriends are by far the best, and I am beyond grateful to have you. And finally, thank you to Michelle, my light, my joy, my Boston wife, for always, always being there, even when geography keeps us apart.

Throughout my education, there have been many individuals who pushed me to achieve excellence. In high school, the inspirations were legion, but I would especially like to thank Mr. Caputi, who revealed to me the wonders of the living world, Mrs. Kweskin, who taught me to find the humanity in every line of every story, and Dr. Melmed, whose belief and support was unwavering. In college, Dr. Mehl pushed me beyond my comfort zone and thus helped me discover a whole new world of possibilities. Dr. Fenlon supported and mentored me through my first fumbling attempts at lab research, and even helped me transform those fumblings into publications. Jeremy Moss helped me rediscover my joy of science through, unexpectedly, sharing his joy of film. I have been incredibly blessed with a supportive and nurturing educational environment from the beginning, and I know that I wouldn't be who I am without every bit of it. Thank you, from the bottom of my heart, to every educator that helped me on my journey.

Last but certainly not least, I want to thank my family. I am lucky enough to have a network of extended family in the Midwest, from Cleveland to Detroit to Lansing to right here in Ann Arbor, and it has been a delight to be able to see you all so often. Thank you for being a constant source of love, belief and laughter. Thank you to my brother Peter for always pushing me to think outside my usual boxes. Thank you to my little sis Meredith, one of my very best friends in the world, who is growing into a talented, confident young woman right before my eyes. Thank you to my mom, whose love and faith in my ability to tackle any challenge have kept me going. And thank you to my dad, my #1 fan, my first and best science teacher, and my port in every storm. I love you all so much.

Table of Contents

List of Figures

List of Tables

Abstract

Molecular chaperones are a class of conserved proteins that maintain proteostasis within all organisms. In order to carry out this task, chaperones bind to unfolded protein substrates and support outcomes such as folding, localization, complex assembly, aggregation prevention, and degradation. The diversity of chaperones reflects the diversity of functions they carry out within the cell. One chaperone, 70-kDa heat shock protein (Hsp70), is ubiquitously expressed and acts as a coordinating hub for a large network of co-chaperones, including J proteins, nucleotide exchange factors (NEFs), and tetratricopeptide-repeat (TPR) domain-containing proteins. The complexity of this network has posed challenges to fully understanding its many roles in cellular health and how these roles may fail in diseases of protein misfolding, such as Alzheimer's disease (AD). We have attempted to gain a more detailed understanding of these networks and the cooperation and competition that occurs within them by using techniques that allow us to probe the function of many chaperones in parallel. Using chemical genetics, we have investigated the functional roles of individual J proteins in *Saccharomyces cerevisiae*. We found that many J proteins have distinct roles in supporting certain cellular functions that cannot be compensated for by endogenous levels of other J proteins. We also designed peptide microarrays composed of peptides derived from the sequences of two model chaperone substrates, luciferase and tau. The human J protein, DNAJA2, is able to support Hsp70-mediated refolding of luciferase *in vitro*, while a highly homologous J protein, DNAJA1, is not. Binding experiments using the luciferase microarrays demonstrate that Hsp70 simulates the binding of DNAJA2, but not DNAJA1,

to a β-sheet between the domains of luciferase, suggesting that increased affinity for this binding site during luciferase refolding may be the mechanistic basis of the divergent folding abilities of these two J proteins. We also mapped the binding of 17 chaperones to tau, a protein that misfolds into amyloid fibrils in a class of neurodegenerative diseases called tauopathies, including AD. We find that chaperones generally bind a set of "hotspots" on tau, many of which are rich in residues known to be phosphorylated in AD tau or sites of mutations linked to other tauopathies. These results suggest that chaperones compete with one another and other tau binding partners, like kinases and phosphatases, to direct the metabolism of this protein in both healthy and diseased systems. Finally, we designed a peptide microarray to test the hypothesis that chaperones might preferentially bind amyloidogenic sequences in order to prevent the formation of toxic amyloid fibrils. Using this array we demonstrated that some chaperones, including Hsp70 and a subset of J proteins, have a slight but consistent preference to bind amyloid-forming peptides over normal ones. In subsequent solution-phase binding assays, we confirm this finding but also conclude that other peptide properties contribute strongly to Hsp70 binding. Taken together, these studies advance our understanding of chaperone networks and suggest novel future avenues of inquiry.

Chapter 1

The Hsp70 Multi-Protein Complex as a Drug Target

1.1 Abstract

Heat shock protein 70 (Hsp70) is a molecular chaperone that plays critical roles in protein homeostasis (proteostasis). Using cycles of ATP hydrolysis, Hsp70 binds to unfolded proteins and favors their folding. Additionally, if the protein is damaged, Hsp70 directs it to the proteasome for disposal. Thus, Hsp70 has emerged as a drug target in protein misfolding diseases, such as neurodegenerative disorders. However, competitive inhibitors of ATP binding have proven challenging to discover and, in some cases, this strategy may not be the best way to redirect Hsp70 function. Another approach is to inhibit Hsp70's interactions with important co-chaperones, such as J proteins, nucleotide exchange factors (NEFs) and tetratricopeptide repeat (TPR) domain proteins. These co-chaperones bind Hsp70 and are critical in guiding its chaperone activities, such as the selection of substrates and dictating their ultimate fate. For example, J proteins are a potentially attractive target because they help choose substrates for Hsp70. Thus, pharmacologically regulating the assembly or disassembly of Hsp70 complexes might be a powerful way to re-shape the proteome and, potentially, restore healthy proteostasis. By considering the Hsp70 complex as a composite, multi-protein drug target, we might not only develop new leads for therapeutic development but also discover new chemical probes for use in understanding Hsp70 biology.

1.2 Introduction

1.2.1 Diversity of Hsp70 Functions

Heat shock protein 70 (Hsp70) is a molecular chaperone that plays a central role in protein quality control [1, 2]. Hsp70 binds to protein substrates to assist with their folding [3, 4], degradation [5-7], transport [8], regulation [9, 10] and aggregation prevention [11]. The capacity of Hsp70 to carry out these widely divergent functions arises, in part, from three features. First, evolution has given rise to multiple homologous Hsp70 genes [12, 13]. These Hsp70s populate all of the major subcellular compartments. For example, the cytosol of human cells has two major isoforms of Hsp70, a stress-inducible form (Hsp72/HSP1A1) and a constitutive form (Hsc70/HSPA8). Similarly, BiP (HSPA5) is the form in the endoplasmic reticulum and mortalin (HSPA9) in the mitochondria. For the purposes of this thesis, "Hsp70" will often be used to broadly refer to these chaperones because they are thought to, in many cases, have similar biochemical properties. Another source of functional diversity in Hsp70s is cooperation with other chaperones, such as Hsp90 or Hsp60 [4]. Cooperation between Hsp70 and Hsp90, for example, is critical to the function of nuclear hormone receptors [8]. Finally, the full diversity of Hsp70 activities is achieved through cooperation with a large network of co-chaperones [1, 14], including J proteins, nucleotide exchange factors (NEFs), and tetratricopeptide repeat (TPR)-domain containing proteins [15]. These factors bind to Hsp70 and guide its many chaperone activities. In addition, each class of co-chaperones includes many distinct examples in mammalian cells, such that multiple J proteins, for example, compete for binding to the same site on Hsp70 (Figure 1.1).

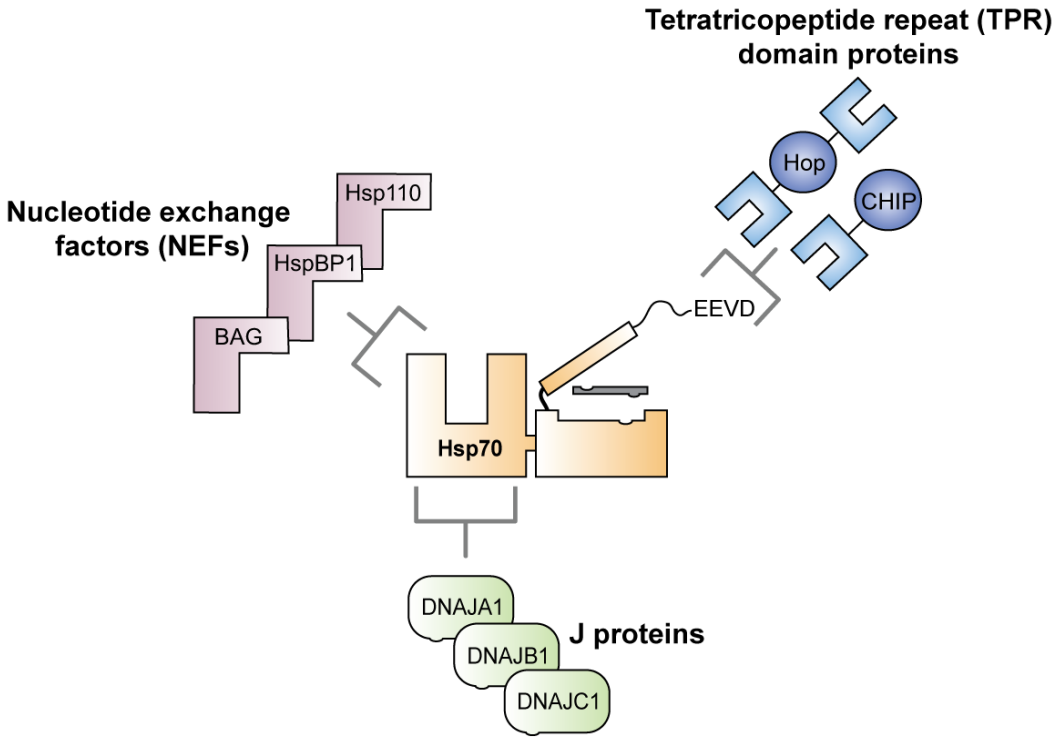

Figure 1.1. Hsp70 forms the core of a multi-protein complex and associates with numerous co-chaperones. Three distinct classes of co-chaperones, NEFs, J proteins, and TPR domain-containing proteins, interact with Hsp70 and regulate its activities. The J proteins and NEFs interact with the NBD, while the TPR domain-containing proteins bind the C-terminal disordered region. Assembly of Hsp70 complexes with different co-chaperones is believed to contribute to substrate triage and fate decisions (i.e. folding or degradation).

1.2.2 Hsp70 as a therapeutic target

Hsp70 has been implicated in multiple diseases, such as neurodegenerative disorders [16], cancer [17], and infectious disease [18]. The evidence linking Hsp70 to disease has been recently reviewed [19-21]. Despite this strong connection, relatively little progress has been made in bringing Hsp70-targeted molecules to the clinic, with only two inhibitors having been explored in clinical trials [22, 23]. One of the contributing factors to this lack of translational progress is that Hsp70's functional promiscuity makes it difficult to predict potential off-target effects. As discussed above, Hsp70 is involved in many key processes in the cell; thus, it isn't clear how therapeutics could be used to re-balance some pathological

Hsp70 functions without impacting global proteostasis. One attractive possibility may be to target the interactions between Hsp70 and its co-chaperones, because these factors are thought to diversify Hsp70's functions.

This chapter explores the structure and function of Hsp70 multi-protein complexes and evaluates recent progress in identifying compounds that selectively target the assembly/disassembly of these complexes. The underlying model is that each complex composed of an Hsp70 (*e.g.* Hsc70, Bip, *etc*) bound to a specific set of co-chaperones (*e.g.* J protein, NEF, TPR, *etc*) might be involved in a discrete aspect of chaperone biology (*e.g.* protein folding, degradation, clathrin uncoating, *etc.*). Thus, if small molecules selectively disrupted an interaction between Hsp70 and a specific co-chaperone, then only a subset of Hsp70 biology might be impacted. In other words, the complexity of this chaperone network provides a unique opportunity to influence specific subsets of protein quality control while leaving the rest unperturbed. The challenge is that it has been notoriously difficult to target protein-protein interactions [24-26], such as those between Hsp70 and its co-chaperones. However, new advances in high throughput screening (HTS) methodology are rapidly changing the landscape of discovery in this area. In fact, Hsp70 might be a particularly attractive target for deploying these methods, owing to its high number of protein-protein contacts and the importance of these interactions in guiding Hsp70 biology.

1.3 Structure and function of Hsp70 and its complexes

Hsp70 consists of two domains, a 45 kDa N-terminal nucleotide binding domain (NBD) and a 25 kDa C-terminal substrate-binding domain (SBD) connected by a short flexible

linker [27]. The NBD of Hsp70 is further divided into two subdomains, lobes I and II, that are each divided into an "A" and "B" region (Figure 1.2). These lobes form a cleft that binds ATP with a nucleotide-binding cassette that is related to hexokinase and actin [28]. Hsp70's SBD is also composed of a 15 kDa β-sandwich subdomain with a hydrophobic groove for polypeptide binding and a 10 kDa α-helical region which forms a "lid" over the polypeptide-binding site [29]. Hsp70 preferentially binds hydrophobic regions of proteins and can therefore bind newly synthesized linear peptides or exposed regions on partially unfolded proteins [3, 30]. The lack of strong sequence specificity allows Hsp70 to bind a variety of client proteins including signal transduction proteins, clathrin, nuclear hormone receptors, and cytoskeletal proteins [31, 32].

1.3.1 ATPase cycle of Hsp70

The ATPase cycle of Hsp70s has been largely studied for the prokaryotic DnaK. In this chaperone, ATP hydrolysis controls allostery between the NBD and SBD. In the ATP-bound state, Hsp70 has a low affinity for substrate and retains an "open" substrate-binding cleft, but conversion to the ADP-bound state causes the α-helical lid region to close (Figure 1.2) [33]. In DnaK, this crosstalk between the NBD and SBD appears to be bidirectional, because substrate binding also promotes nucleotide hydrolysis [33, 34]. Thus, ATP hydrolysis in Hsp70s is thought to be a major determinant of their chaperone functions. For example, mutations in the ATP-binding cassette have dramatic effects on chaperone functions *in vitro* and *in vivo* [35]. However, recent mutagenesis studies have further shown that the relationship between ATP hydrolysis and chaperone functions is indirect [35]. For

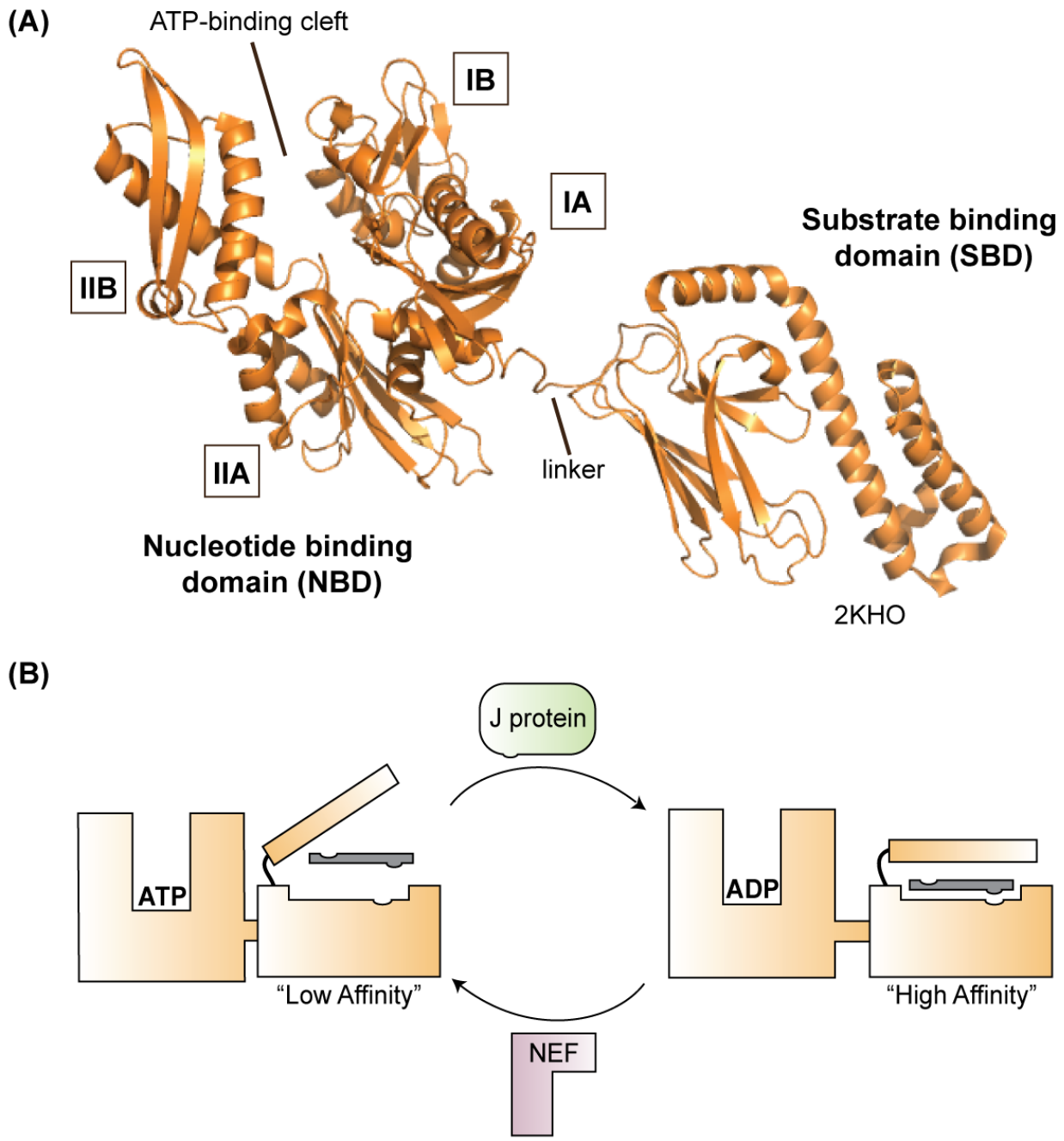

Figure 1.2. Structure and ATPase cycle of Hsp70. (A) Hsp70 is composed of a 45 kDa N-terminal nucleotide binding domain (NBD) connected to a 25 kDa substrate binding domain (SBD) by a short hydrophobic linker. The SBD is composed of a β-sandwich and an α-helical "lid" domain. The structure of the prokaryotic Hsp70, DnaK, is shown (PDB code 2KHO), but the general architecture appears to be conserved amongst prokaryotic and eukaryotic family members. (B) Schematic of ATP hydrolysis and the role of co-chaperones. Substrate binding in the SBD coupled with J-domain co-chaperone interactions in the NBD promotes ATP hydrolysis. Conformational changes associated with ATP conversion close the C-terminal "lid" and enhance affinity for the substrate. The cycle is completed when a nucleotide exchange factor interacts with the NBD and assists with ADP release.

example, some mutations in DnaK that dramatically reduce ATP turnover have only modest effects on luciferase refolding. These observations suggest that inhibiting the ATPase activity of Hsp70 might not always directly lead to proportional changes in functional outcomes, such as reduced client stability. Rather, modifying the interactions with co-chaperones might have a more predictable effect on chaperone functions [35].

1.3.2 Co-chaperones regulate Hsp70 structure and activity

The major families of co-chaperones bind to distinct interaction surfaces on Hsp70. The J protein co-chaperones bind Hsp70 at lobe IIA of the NBD and accelerate the rate of ATP hydrolysis [36]. The NEF co-chaperones bind lobes IB and IIB of Hsp70's NBD and facilitate the release of ADP, which has also been shown to accelerate Hsp70's ATPase rate [37]. TPR domain containing co-chaperones bind Hsp70's C-terminus and have been shown to modulate the fates of Hsp70 client proteins [38]. Thus, the major families of co-chaperones bind Hsp70 to regulate its enzymatic activity, its localization and its choice of substrates.

1.4 Approaches to targeting Hsp70

1.4.1 Competitive nucleotide analogues

What is the best way to chemically target Hsp70? One possible approach is to inhibit ATPase activity with competitive nucleotide analogs, as has been done with Hsp90 inhibitors [39]. The nucleotide-binding cleft of Hsp70 is well defined and relatively deep, suggesting that it might be suitable for development of inhibitors. However, Hsp70 has a

tight affinity (mid-nanomolar) for nucleotide, 300-fold better affinity than Hsp90 [40-43]. Because the cellular concentration of ATP is typically about 1-5 mM, protein targets with a tight affinity for ADP and ATP are much more difficult to inhibit than those with a weaker affinity. Further, the ATP-binding cassette in Hsp70 is highly homologous in actin and other abundant proteins. Thus, selectivity for the chaperone might be challenging. Despite these challenges, innovative work performed by a group at Vernalis has produced competitive, orthosteric inhibitors of Hsp70, using structure-based design [44]. Consistent with their design, these compounds inhibit cancer cell viability [44] and this group has even been successful at selectively targeting BiP [45]. However, Massey has reported that the path towards orthostatic, competitive inhibitors of Hsp70 is quantitatively more challenging than the parallel path to other related targets, such as Hsp90 [43]. Given these hurdles, it seems prudent to pursue additional routes to the design and discovery of potent and selective small molecule modulators targeting Hsp70.

1.4.2 Inhibitors of substrate binding

Targeting the substrate-binding cleft of Hsp70 is the next logical avenue, given the depth of the site and its known affinity for relatively low molecular mass peptides. This approach has been taken by Chaperone Technologies in their development of antibiotics. For example, a series of 18-20 amino acid peptides, including drosocin, pyrrhocoricin, and apidaecin, are known to interact with DnaK [18]. Of these peptides, pyrrhocoricin exhibited broad-spectrum antibacterial activity. Competition experiments indicated that this peptide has two binding sites on DnaK, one of which is thought to be adjacent to the substrate-binding pocket. Interestingly, pyrrhocoricin has activity against bacteria but not mammalian cells

[46], suggesting that the SBD could be leveraged to gain selectivity between different isoforms of Hsp70. While this work highlights the usefulness of SBD-targeted compounds as antibiotics, it is unclear whether this strategy could be implemented in the development of therapeutics for different Hsp70 related diseases.

1.4.3 Targeting co-chaperones and their interactions with Hsp70

Given the significant challenges associated with the targeting of either the nucleotide- or substrate-binding regions of Hsp70, additional strategies are worth pursuing. A number of additional Hsp70 inhibitors have been identified, but their mechanisms are not known yet [47-49]. To supplement this collection of compounds, targeting the PPIs between Hsp70 and its many co-chaperones may be an effective approach. In the following sections, each co-chaperone is discussed in more detail and some of the successes and challenges associated with each are outlined.

1.5 J protein co-chaperones

J proteins are a class of Hsp70 co-chaperones whose diversity in structure and function are thought to be crucial to the flexibility of the Hsp70 machinery. Evolution has dramatically expanded the cellular complement of J proteins relative to Hsp70s, such that humans have over 40 J protein-encoding genes but only 13 Hsp70 genes [50, 51]. Moreover, the co-existence of many J proteins within the cytosol and nucleus suggests that they have evolved for distinct functions [52, 53]. All J proteins share a conserved J domain that binds to Hsp70 but they diverge in other regions, perhaps providing the functional diversity needed to recruit Hsp70 into many different cellular activities. Consistent with this idea, various J

proteins have been linked to an array of pathological conditions including cancer, neurodegeneration, muscular dystrophy, and viral infection [54-58]. Thus, J proteins may be interesting targets for pharmacological targeting because they might be used to impact only a relatively narrow subset of Hsp70-dependent functions.

1.5.1 J protein structure and function

The J domain is a highly conserved structure that consists of four α-helices. The J domain interacts directly with the NBD of Hsp70 to stimulate ATP hydrolysis and allosteric conversion into a high-affinity substrate binding conformation [59-61]. For the bacterial DnaJ-DnaK interaction, the interface consists of the positively charged helix II of the J domain interacting electrostatically with the negatively charged NBD in lobes IA and IIA [36, 62-64]. J domains include an invariant His-Pro-Asp (HPD) motif in the loop between helices II and III that is required for function, perhaps by controlling the position of the helices. Though the overall four-helix architecture of the J domain is largely conserved among J proteins, subtle structural differences suggest that some functional diversity may arise from J domain interactions with Hsp70 [65]. For example, mutants in the NBD of the yeast BiP disrupt interactions with only a subset of available J proteins [66, 67]. Although speculative, these findings suggest that it might be possible to independently target specific J domains at the contact surface with Hsp70.

J proteins have been traditionally grouped into three classes based on structural homology to the *Escherichia coli* DnaJ (Figure 1.3A). Class A consists of an N-terminal J domain, a glycine-phenylalanine (G/F) rich region, a zinc finger-like region (ZFLR), a barrel topology

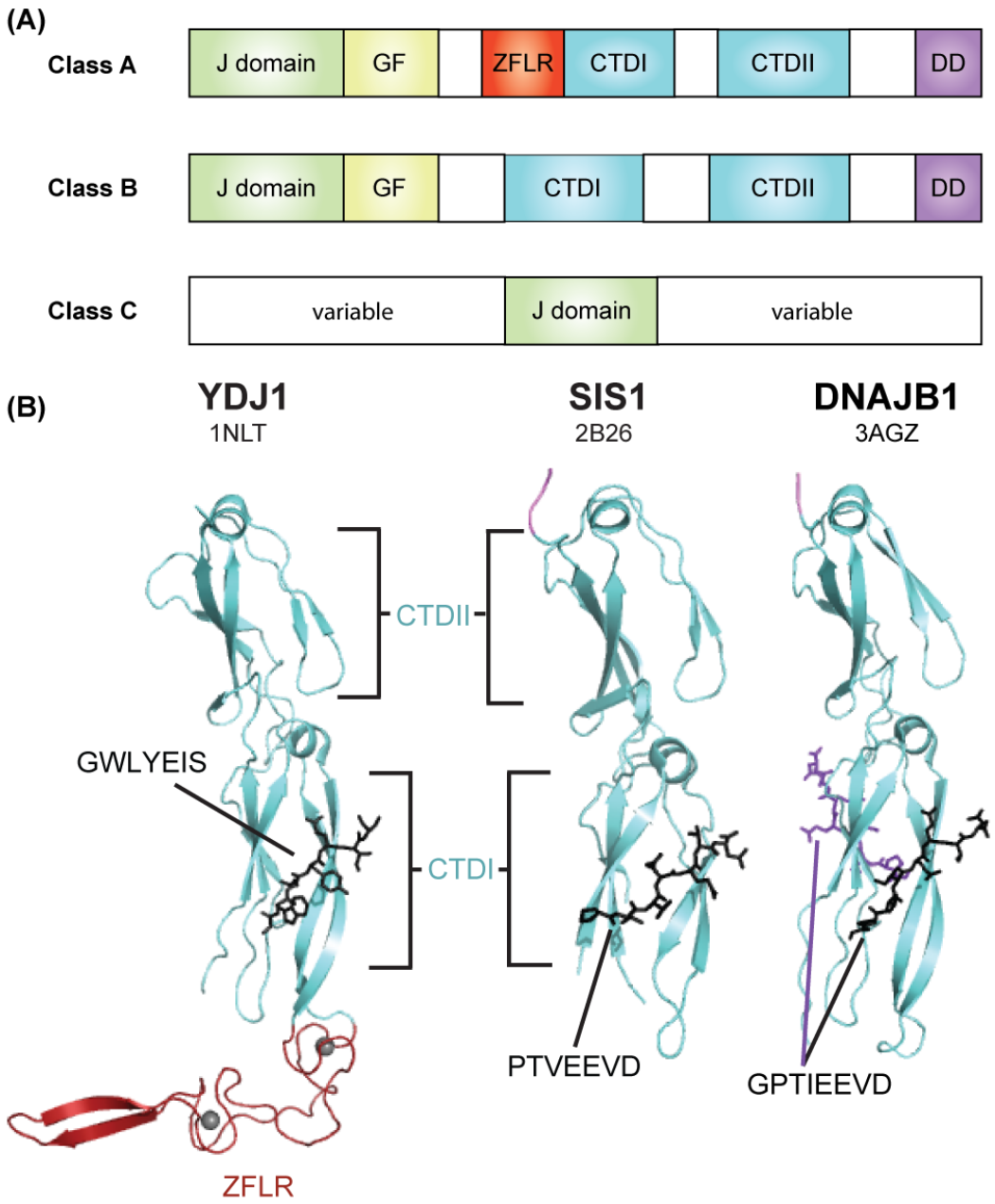

Figure 1.3. J protein co-chaperones fall into three structural classes. (A) The domain architecture of each class of J protein is depicted as a schematic beginning with the N-terminus to the left. The domain types are J domain, GF (glycine-phenylalanine rich region), ZFLR (zinc finger-like region), CTDI and II (C-terminal domain) and DD (dimerization domain). (B) The crystal structures of the C-terminal portions of Ydj1 (yeast DNAJA1), Sis1 (yeast DNAJB1) and DNAJB1 bound to peptides are shown with corresponding PDB codes. Ydj1 is bound to a peptide substrate, GWLYEIS. Sis1 and DNAJB1 are bound to peptides from the extreme C-terminus of Hsp70 (yeast and human, respectively). Two peptide binding sites are evident on DNAJB1, suggesting that class B J proteins may bind Hsp70 and substrate simultaneously. Images were prepared in PyMol.

C-terminal domain (CTD), and a dimerization domain [68, 69]. Class B has the N-terminal J domain and G/F region, lacks a ZFLR, and is more structurally variable at the C-terminus, but often contains two CTDs (CTDI and CTDII) [51]. Class C, the largest class, consists of proteins containing a J domain and with no other structural homology to DnaJ. More recently, Kampinga and Craig have provided a revised classification system based more closely on function [69]. This classification represents an important new paradigm in thinking about J proteins and it highlights the major contribution of J proteins to directing the activity of Hsp70.

1.5.2 Diversity of J protein functions

Specific functions have been described for only some of the individual J proteins and much more work is needed to clarify this area (see Chapter 2). However, some convincing and illustrative examples have been elucidated. One such is auxilin (DNAJC6), which has a C-terminal J domain and a clathrin-binding domain. This J protein is exclusively involved in the Hsc70-dependent uncoating of clathrin-coated vesicles [70-72], an activity not readily redundant with other J proteins. Similarly, DNAJC7 interacts with both Hsp70 and Hsp90 and seems to play a "recycling" role in the chaperoning of specific substrates, such as the progesterone receptor [73]. In the ER, ERdj3 (DNAJB11) works with BiP to assist with ER-associated degradation (ERAD) [74, 75]. These and other examples [76] lead to a speculative model in which individual J proteins might be responsible for each of Hsp70's specific functions. In support of this idea, a systematic study of human J proteins found that some examples are able to refold luciferase, while others inhibit aggregation of heat-denatured luciferase [53], suggesting that these co-chaperones may be specialized.

1.5.3 J proteins bind substrates directly

One prevailing model is that J proteins bind to substrates and present them to Hsp70. While this concept is likely oversimplified when applied to the large family of J proteins, the interaction of these co-chaperones with substrates seems to play a crucial role in some cases. For example, Lu and coworkers deleted the J domain of Ydj1 (yeast DNAJA1) and found that the remaining portion suppresses rhodanese aggregation on its own [77]. Later work identified a shallow hydrophobic depression on the CTDI of Sis1 (yeast DNAJB1) and found that four point mutants inhibited luciferase binding and refolding [78]. These types of studies suggest that J proteins can bind directly to substrates. Further insight into how J proteins bind to their substrates has largely been gained from peptide microarray studies. These studies have revealed that the prokaryotic DnaJ binds ~8mer peptides enriched in hydrophobic residues [79]. Interestingly, DnaJ does not discriminate between *all*-L-peptides and *all*-D-peptides with differing backbone stereochemistries, indicating that peptide binding involves side chain interactions [79, 80]. However, a crystal structure of the Ydj1 C-terminus, which is highly homologous to DnaJ, bound to the peptide GWLYEIS, suggests that the peptide forms a β-strand alongside a β-sheet in CTDI and several contacts are made with the peptide backbone [81] (Figure 1.3B). This discrepancy may be due to species differences and the general rules for J protein-substrate interactions are not yet clear. However it is reasonable to hypothesize that formation of Hsp70-J protein-substrate ternary complexes may be important in directing Hsp70 to "choose" specific substrates.

1.5.4 J proteins bind the C-terminus of Hsp70

The four C-terminal residues of Hsp70, EEVD, seem to be important in regulating Hsp70 activity and its interactions with J proteins. For example, deletion or mutation of this motif in Hsp70 prevents formation of stable Hsp70-substrate complexes and the stimulation of Hsp70 ATPase activity by DNAJB1 [82]. The EEVD motif is also crucial for Hsp70 interactions with TPR-domain containing co-chaperones (see section 1.10). Further studies with Sis1 (yeast DNAJB1) found that this J protein could bind the eight C-terminal residues of Ssa1 (yeast Hsc70) with low micromolar affinity [83, 84]. Interestingly, Ydj1 (yeast DNAJA1) could not bind the Hsp70 C-terminus, suggesting distinct mechanisms for Hsp70 regulation between the A and B classes of J proteins. A crystal structure of Sis1 (yeast DNAJB1) with the C-terminal lid of Ssa1 (yeast Hsc70) found that only the 7 terminal residues of Ssa1 were ordered and bound to Sis1 in the same binding groove used by substrate peptides in Ydj1 [84] (Figure 1.3B). However, the nature of this binding interaction is quite different. Ydj1-GWLYEIS is a mostly hydrophobic interaction, while Sis1-PTVEEVD is mediated by charge-charge interactions between four lysines in Sis1 and the EEVD motif [81, 84]. These lysines are conserved in class B J proteins but not class A, perhaps explaining Ydj1's failure to interact with the C-terminus of Ssa1 [84]. Interestingly, a crystal structure of DNAJB1 with the C-terminal octapeptide of human Hsp70 (GPTIEEVD) revealed two peptides bound to a single monomer of DNAJB1, one in the previously identified site and another in a site on the reverse side of the CTDI domain [85] (Figure 1.3B). Based on their findings and a re-examination of previous data, the authors propose that the originally identified site in class B J proteins is specific for Hsp70 binding, and the second site (which is shallow and hydrophobic) is dedicated to substrate binding.

With this in mind, they propose a model of J protein-Hsp70 activity in which one half of a J protein dimer binds Hsp70 and the other binds substrate, thus bringing the two together. This model might explain why Sis1 regulation of Hsp70 activity (e.g. luciferase refolding) requires a dimer and the Sis1 monomer is nonfunctional [82, 86]. These findings provide further evidence that ternary complexes of Hsp70 and J proteins with substrate are important for functional outcomes and perhaps substrate selection.

1.6 Roles of J proteins in disease

J proteins have been specifically implicated in the quality control of several pathologically relevant proteins, primarily in diseases of protein misfolding [87]. For example, DNAJB1 and DNAJB6 can inhibit the aggregation and toxicity of mHtt, the misfolded protein in Huntington's disease [88-90], while DNAJB1 and DNAJA1 co-localize with mHtt aggregates [91]. Interestingly, DNAJA1 over-expression increases mHtt aggregation [92], suggesting that each J protein might play a specific and sometimes opposing role in directing the fate of Hsp70 substrates. This concept is further illustrated by studies on the Hsp70 substrate, tau [93]. In this system, DNAJB1 inhibits aggregation of tau *in vitro* [94], while DNAJA1 over-expression causes proteasome-dependent degradation of tau [95]. As Hsp70 has been shown to have a direct role in the chaperoning of pathological substrates, some of these J protein phenotypes likely involve communication between Hsp70 and the J proteins, while other outcomes may be Hsp70 independent. Further work is needed to establish direct links between specific J protein-substrate interactions and phenotypic outcomes, particularly pathologically relevant ones. When these interactions are better understood, these co-chaperones may constitute viable pharmacological targets.

1.7 Efforts to target J proteins

While individual J proteins have not been pharmacologically targeted, several compounds have been developed that target the J domain-Hsp70 interaction. The first modulator of Hsp70 ATPase activity identified was 15-deoxyspergualin (DSG), a modified natural product that stimulates cytosolic Hsp70 ATP hydrolysis but does not inhibit or act synergistically with J protein stimulation [96-98]. Screens for structurally similar molecules identified R/1, a long, hydrophobic molecule that inhibits both intrinsic and J protein-stimulated ATPase activity of the yeast cytosolic Hsp70, Ssa1, and the human ER Hsp70, BiP [99] (Figure 1.4). Another class of Hsp70 modulators that acts at the J protein level is the sulfogalactosyl ceramide (SGC) mimics. SGC is a cell surface receptor that binds the NBD of multiple members of the Hsp70 family [100, 101]. Park and coworkers developed a soluble mimic of SGC called adamantylSGC (AdaSGC), which inhibits the J protein-stimulated ATPase activity of Hsc70 but not its slow intrinsic ATPase activity, suggesting that AdaSGC may directly inhibit the J domain-Hsp70 interaction [102].

1.7.1 High throughput screens provide further Hsp70-J protein modulators

More recent high throughput screening (HTS) efforts have identified additional compounds that specifically influence J protein-stimulated Hsp70 ATPase activity. For example, screening of a collection of dihydropyrimidines identified three examples, including MAL3-101, that had no effect on intrinsic Hsp70 ATP turnover but inhibited J protein-stimulated turnover [103]. Subsequent screening and structural studies showed that the dihydropyrimidines bind to a region at the J protein-Hsp70 interface [104-106]. Moreover, these studies also found that some dihydropyrimidines promote J protein activity, while

others are inhibitory. For example, 115-7c is able to stimulate the ATPase activity of Hsp70 synergistically with DnaJ [104]. 115-7c binds better to the DnaJ-DnaK complex than DnaK alone and nuclear magnetic resonance (NMR) studies found that 115-7c binds directly adjacent to the J domain-binding site on DnaK. However, the related compound 116-9e, which (similar to MAL3-101) has a diphenyl substitution on the dihydropyrimidine ring, inhibits DnaJ stimulation of ATPase activity, without impacting NEF function [104]. Interestingly, MAL3-101 seems to discriminate between J proteins, because it inhibits Ssa1 stimulation by SV40 large T Antigen (TAg), a viral J protein, but had less potent activity against the combination of Ssa1 and Ydj1. This finding suggests that it may be possible to achieve J protein-specific inhibition even by targeting the J protein-Hsp70 interface. MAL3-101 was subsequently found to have potent anti-cancer effects in a multiple myeloma cell line and mouse model [107], while other dihydropyrimidines have been found to control stability of other Hsp70 substrates, including tau, polyglutamines and Akt [48, 73, 108, 109]. This growing body of work suggests that targeting the Hsp70-J protein interface may be a productive approach for guiding Hsp70 functions. Importantly, these compounds are not generally cytotoxic and they do not activate a stress response [48, 108, 109], consistent with the idea that disrupting PPIs in the Hsp70 complex may be relatively well tolerated.

Other chemical series also appear to have activity against the Hsp70-J protein interaction and, interestingly, some of these compounds use mechanisms different than the one used by the dihydropyrimidines. For example, an HTS effort against the DnaK-DnaJ pair identified the flavinoid myricetin, which inhibits DnaJ-stimulated ATPase and substrate binding activities, without affecting intrinsic or GrpE-stimulated activity [48, 110]. NMR revealed that myricetin binds the NBD in a region between the IB and IA subdomains, which is more than 20 Å away from the J domain-binding site [110]. However, despite this distance, myricetin blocks binding of DnaJ to DnaK, suggesting that it acts through an allosteric

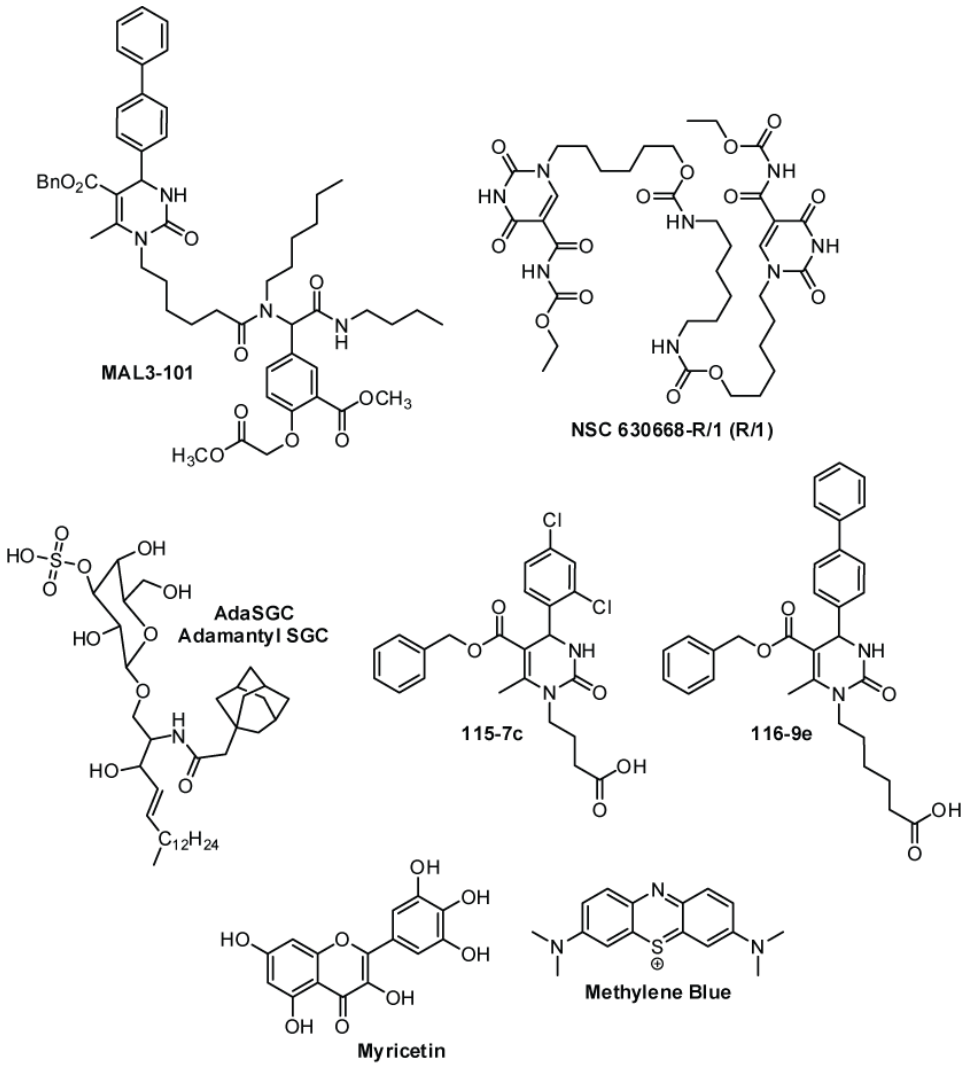

Figure 1.4. Structures of chemical modulators of the Hsp70-J protein system.

pathway. Additional HTS efforts have shown that methylene blue (MB) block J stimulation of ATP turnover *in vitro*. However, like myricetin, MB's effects in cells and animals are complex and it is likely to have targets other than Hsp70s [48, 73, 111]. Despite this complexity, MB and myricetin have clearly shown Hsp70-dependent effects on pathological substrates in cellular and animal models [48, 73, 112] and they reduce Akt levels in cancer cells [109]. Interestingly, these effects are blocked by co-administration of 115-7c, the dihydropyrimidine activator of J protein function [48], further suggesting that the Hsp70-J protein contact is critical. Finally, a larger HTS effort using more than 55,000 compounds identified that zarkulifast is also an inhibitor of the DnaK-DnaJ combination [113] and a screen of more than 300,000 compounds identified an inhibitor of TAg [114]. The binding site of these molecules is not yet known, but the results show that screening strategies can be used to identify specific inhibitors of a PPI in the Hsp70 system. Like the dihydropyrimidines, some of these are likely orthostatic, while others may be allosteric, like myricetin.

The effects of small molecules on disease-relevant Hsp70 substrates are an initial indication that this is a promising avenue of investigation. However, J protein biology is complex and more work is needed to rationally refine these studies to focus on specific J protein-Hsp70 pairs. More specifically, if a discrete Hsp70-J protein pair can be clearly attributed to a distinct pathobiology, then HTS approaches might be employed to selectively disrupt (or even promote) the key protein-protein interactions.

1.8 Nucleotide exchange factors

Nucleotide exchange factors (NEF) provide another potential "handle" for targeting the Hsp70 chaperone complex. NEFs bind Hsp70 and help to facilitate the exchange of ADP for ATP. The biochemisty of the NEF family of co-chaperones has classically been investigated using the prokaryotic NEF, GrpE, as a model [115]. However, the eukaryotic cytosol does not contain a GrpE homolog. Rather, there are three main sub-classes of human NEFs: Hsp110, HspBP1, and the BAG proteins, all of which are structurally distinct with little to no sequence homology. Consistent with their diverse structures, they also differ in their mode of binding to Hsp70s and their roles in guiding Hsp70 biology. For example, BAG2 is associated with proteasomal degradation of the Hsp70 substrate, tau, while BAG1-Hsp70 is linked to increased tau stability [116, 117]. These observations suggest that the formation of specific NEF-Hsp70 complexes may help decide the fate of Hsp70-bound substrates. Also, these observations suggest that differential disruption of specific Hsp70-NEF contacts might be beneficial in disease. For example, members of the NEF family are differentially expressed in multiple diseases, including cancer, Alzheimer's, cardiomyopathies, and ischemia [118-121], highlighting the rationale for developing chemical modulators of NEF-Hsp70 interactions.

1.8.1 Human NEF class: Hsp110

Hsp110 was originally observed and classified as a heat shock protein based on the appearance of a 110 kDa band in the lysates of Chinese Hamster Ovary (CHO) cells upon heat shock [122]. In humans the major cytosolic Hsp110 protein is called Hsp105 (HSPH1) and it has two major isoforms α and β [123]. Hsp105α is constitutively expressed and

upregulated by a variety of stressors, whereas the alternatively spliced isoform Hsp105β is only induced upon heat shock [123, 124]. Hsp110 is an evolutionary relative of the Hsp70 family and therefore it has very similar domain architecture, with the main differences including a longer acidic loop region between the β-sandwich and α-helical lid of the SBD and a larger unstructured C-terminal extension [125, 126]. Despite the structural similarity, Hsp110 only functions as a holdase (*i.e.* it maintains substrates in a stable, unaggregated form) and has no ability to refold substrates without the help of the Hsp70 machinery [126-130]. Furthermore, while Hsp110 homologs bind nucleotide, this function seems to be dispensable for their NEF activity [131]. The crystal structure of the complex between Hsp70 and yeast Hsp110, Sse1, shows that the interaction covers a large surface area involving their respective NBDs [132, 133]. This interaction between Hsp70 and Hsp110 causes several rotations in Hsp70's NBD, especially in lobe IIB [134], allowing ADP release.

1.8.2 Challenges of targeting Hsp110-Hsp70 interactions

The large buried surface area between Hsp70 and Hsp110 may make targeting this interaction difficult. The problem in PPI systems like this is that binding energy is often distributed across a large and complex topology, precluding easy inhibition by small (<500 Da) molecules. However, inhibiting PPIs with large surface areas is not unprecedented and compounds with potency values in the low nM range have been reported [135]. A common feature of previous successful strategies is that the small molecules tend to target so-called "hotspots" of the PPI, meaning that the inhibitor binds in a region on one partner containing a small number of residues that are responsible for the majority of the binding

strength [136, 137]. Thus, it will be important to identify residues that are critical to the Hsp70-Hsp110 interaction. Another common feature of successful PPI inhibitors is that they bind in allosteric sites to impact the topology of protein-protein contact surfaces from a distance. This approach lets the small molecule bind in a relatively concise pocket and impact larger surfaces to block PPIs. It seems likely that similar mechanisms will need to be employed to target the Hsp110-Hsp70 interaction.

1.8.3 Human NEF class: BAG proteins

Possible strategies to target the Hsp70-NEF interaction are illustrated by the features of the BAG family of co-chaperones, which includes BAG1-6. BAG proteins are defined by a characteristic C-terminal BAG domain that binds lobe IB and IIB of Hsp70's NBD and facilitates nucleotide release [138, 139]. This BAG domain typically consists of 110 to 124 amino acids and forms a three-helix bundle with the second and third helices providing the binding interface for Hsp70 [37, 140]. The association between the BAG domain and Hsp70 causes a 14° rotation in lobe II, which results in an opening of the nucleotide binding cleft and promotes ADP release [37]. Interestingly, while all BAG proteins interact with Hsp70 through their conserved BAG domains, their N-terminal region is highly variable. This diversity is likely to be key for pathway specificity and BAG proteins may use these domains to determine the timing and location of nucleotide-dependent delivery of Hsp70-bound cargo.

One of the major questions in this field is whether the structural differences between the major NEF classes can be exploited to produce selective inhibitors of the various families.

Similarly, can different members of the BAG family be individually targeted? Further, it isn't yet clear how many NEF functions are dependent on Hsp70 and how many are independent.

1.9 Tetratricopeptide-repeat (TPR) domain-containing proteins

Hsp70s also cooperate with a number of TPR domain-containing proteins. The TPR motif is defined by a degenerate 34 amino acid sequence that forms an amphipathic antiparallel α-helix [40, 141-144] and a TPR domain is typically assembled from 3 to 16 tandem TPR motifs. Although first identified in subunits of the anaphase promoting complex [145, 146], the TPR domain has since been found to be a common feature of protein-protein interactions, including those with Hsp70 co-chaperones.

TPR co-chaperones include a wide range of proteins that include TPR domains for binding to Hsp70 or Hsp90 and additional domains involved in other functions [40, 141-144]. For example, the TPR co-chaperone Hop (Hsp70/Hsp90 organizing protein) has three TPR domains: TPR1, TPR2A, and TPR2B. Of these domains, TPR1 and TPR2A mediate the association with Hsp70 and Hsp90, respectively [147, 148]. Thus, Hop facilitates the coordination of Hsp70 and Hsp90, ultimately allowing for the transfer of substrate between these two chaperone systems [149, 150]. This coordination allows Hop to play a central role in the folding of non-native protein substrates, such as nuclear hormone receptors [151, 152]. In contrast, the TPR co-chaperone CHIP (carboxyl terminus of Hsc70 interacting protein) is a ubiquitin E3 ligase with an effector Ubox domain [153]. This co-chaperone directs ubiquitination of Hsp70-bound substrates, marking them for proteasome-mediated

degradation [154, 155]. Thus, when Hop and CHIP compete for binding to Hsp70 through their TPR domains, they establish a choice between two opposing fates: folding *vs.* degradation. These findings clarify our understanding of the combinatorial assembly of Hsp70 complexes, in which mutually exclusive binding of Hsp70 to specific co-chaperones dictates the fate of substrates [156-158]. Taken together, these features suggest that chaperone complexes may have the potential to be chemically modulated in order to "tune" the proteome.

1.9.1 TPR-domain containing protein interactions with Hsp70

TPR co-chaperones interact with the intrinsically disordered C-terminus of Hsp70. Mutagenesis studies [148, 159, 160] and co-crystal structures of the TPR domains of Hop and CHIP with Hsp70 C-terminal peptides [147, 161] illustrate the importance of the C-terminal EEVD-COOH amino acids [159, 162]. Based on these findings, the EEVD motif of Hsp70 has been generalized as the minimal binding site for TPR co-chaperones. This motif is also present in extreme C-terminus of the evolutionarily unrelated molecular chaperone Hsp90, but not in the prokaryotic DnaK, mitochondrial, or ER-resident Hsp70 isoforms. These observations highlight the role of the EEVD motif as a recruitment element that anchors TPR co-chaperones to the cytoplasmic Hsp70 and Hsp90 chaperone systems. However, there is not much known about how TPR co-chaperones "compete" for binding to Hsp70s. Thus, compounds that block the EEVD-TPR interaction might be exciting probes for understanding chaperone biology and these compounds might be leads for drug discovery.

1.9.2 Targeting TPR-Hsp70 interactions

The development of small molecule modulators of Hsp70-TPR complexes is still in its infancy. However, in the Hsp90 system, Yi and co-workers have targeted the TPR-domain of Hop and identified pyrimidotriazinediones as inhibitors of that protein-protein interaction [163]. Additionally, derivatives of the natural product sansalvamide A have been shown to modulate Hsp90 interactions with TPR co-chaperones [164, 165]. Taken together, this work suggests that the Hsp70-TPR interactions may also be amenable to inhibition. Compared to the other PPIs (e.g. J proteins and NEFs), the interactions between TPR domains and Hsp70s are relatively more concise, which might accelerate discovery in that area. The challenges will be in understanding how to engender selectivity and guide the "choice" of TPR partner.

1.10 Future perspectives

Targeting the Hsp70 chaperone machinery is a complicated endeavor. The sheer number of interactions involved – Hsp70-substrate, Hsp70-co-chaperone, co-chaperone-substrate, etc. – is daunting. Furthermore, the nature of the interactions (often low affinity, transient, high surface area, or all of the above) poses a challenge that will require significant effort to overcome. Before attempting to disrupt any individual interaction for therapeutic purposes, it is important to understand the nature of individual interactions and their roles in both health and disease. A particular challenge of this system is that Hsp70 and its partners play a plethora of roles in normal biology, so any chemical intervention has a high probability of off-target effects. In lieu of targeting Hsp70 itself, co-chaperones provide a tantalizing route

to specificity of chaperone-targeted therapies. Further work is necessary to identify specific activities of individual co-chaperones in order to guide therapy design.

This thesis presents multiple approaches to studying chaperones as networks of cooperating and competing elements. In Chapter 2, the functional roles of 11 J proteins in *Saccharomyces cerevisiae* are probed using a chemical genetics approach. In Chapter 3, a peptide microarray platform is used to identify the binding sites of many chaperones and co-chaperones on a pathological substrate, tau, which is implicated in Alzheimer's disease and other neurodegenerative diseases. In Chapter 4, peptide microarrays are again leveraged to evaluate the binding of chaperones to peptides that are known or predicted to form the cores of amyloid fibrils. Finally, in Chapter 5, the questions raised by this work are discussed and future goals outlined.

Notes

This work was published in part as a review titled "Hsp70 Protein Complexes as Drug Targets" **2013** *Current Pharmaceutical Designs,* 19(3), 404-17. Anne Gillies, Victoria Assimon, Jennifer Rauch, and Jason Gestwicki contributed intellectually to this review.

1.11 References

[1] Mayer MP, Bukau B. Hsp70 chaperones: cellular functions and molecular mechanism. Cell Mol Life Sci, 2005; 62: 670-84.

[2] Bukau B, Weissman J, Horwich A. Molecular chaperones and protein quality control. Cell, 2006; 125: 443-51.

[3] Frydman J. Folding of newly translated proteins in vivo: the role of molecular chaperones. Annu Rev Biochem, 2001; 70: 603-47.

[4] Hartl FU, Bracher A, Hayer-Hartl M. Molecular chaperones in protein folding and proteostasis. Nature, 2011; 475: 324-32.
[5] Bercovich B, Stancovski I, Mayer A, Blumenfeld N, Laszlo A, Schwartz AL, Ciechanover A. Ubiquitin-dependent degradation of certain protein substrates in vitro requires the molecular chaperone Hsc70. J Biol Chem, 1997; 272: 9002-10.
[6] Arndt V, Rogon C, Hohfeld J. To be, or not to be--molecular chaperones in protein degradation. Cell Mol Life Sci, 2007; 64: 2525-41.
[7] Kettern N, Dreiseidler M, Tawo R, Hohfeld J. Chaperone-assisted degradation: multiple paths to destruction. Biol Chem, 2010; 391: 481-9.
[8] Pratt WB, Toft DO. Regulation of signaling protein function and trafficking by the hsp90/hsp70-based chaperone machinery. Exp Biol Med (Maywood), 2003; 228: 111-33.
[9] Gamer J, Bujard H, Bukau B. Physical interaction between heat shock proteins DnaK, DnaJ, and GrpE and the bacterial heat shock transcription factor sigma 32. Cell, 1992; 69: 833-42.
[10] Rodriguez F, Arsene-Ploetze F, Rist W, Rudiger S, Schneider-Mergener J, Mayer MP, Bukau B. Molecular basis for regulation of the heat shock transcription factor sigma32 by the DnaK and DnaJ chaperones. Mol Cell, 2008; 32: 347-58.
[11] Tyedmers J, Mogk A, Bukau B. Cellular strategies for controlling protein aggregation. Nat Rev Mol Cell Biol, 2010; 11: 777-88.
[12] Daugaard M, Rohde M, Jaattela M. The heat shock protein 70 family: Highly homologous proteins with overlapping and distinct functions. FEBS Lett, 2007; 581: 3702-10.
[13] Brocchieri L, Conway de Macario E, Macario AJ. hsp70 genes in the human genome: Conservation and differentiation patterns predict a wide array of overlapping and specialized functions. BMC Evol Biol, 2008; 8: 19.
[14] Hohfeld J, Cyr DM, Patterson C. From the cradle to the grave: molecular chaperones that may choose between folding and degradation. EMBO Rep, 2001; 2: 885-90.
[15] Meimaridou E, Gooljar SB, Chapple JP. From hatching to dispatching: the multiple cellular roles of the Hsp70 molecular chaperone machinery. J Mol Endocrinol, 2009; 42: 1-9.
[16] Broadley SA, Hartl FU. The role of molecular chaperones in human misfolding diseases. FEBS Lett, 2009; 583: 2647-53.
[17] Mosser DD, Morimoto RI. Molecular chaperones and the stress of oncogenesis. Oncogene, 2004; 23: 2907-18.
[18] Otvos L, O I, Rogers ME, Consolvo PJ, Condie BA, Lovas S, Bulet P, Blaszczyk-Thurin M. Interaction between heat shock proteins and antimicrobial peptides. Biochemistry, 2000; 39: 14150-14159.
[19] Evans CG, Chang L, Gestwicki JE. Heat shock protein 70 (hsp70) as an emerging drug target. J Med Chem, 2010; 53: 4585-602.
[20] Brodsky JL, Chiosis G. Hsp70 molecular chaperones: emerging roles in human disease and identification of small molecule modulators. Curr Top Med Chem, 2006; 6: 1215-25.
[21] Patury S, Miyata Y, Gestwicki JE. Pharmacological targeting of the Hsp70 chaperone. Curr Top Med Chem, 2009; 9: 1337-51.

[22] Propper DJ, Braybrooke JP, Taylor DJ, Lodi R, Styles P, Cramer JA, Collins WC, Levitt NC, Talbot DC, Ganesan TS, Harris AL. Phase I trial of the selective mitochondrial toxin MKT077 in chemo-resistant solid tumours. Ann Oncol, 1999; 10: 923-7.
[23] Pfister DG, Bajorin D, Motzer RJ, Scher H, Louison C, Harrison L, Shah J, Strong E, Bosl G. A phase II trial of deoxyspergualin in recurrent squamous cell head and neck cancer. Invest New Drugs, 1993; 11: 53-6.
[24] Gestwicki JE, Marinec PS. Chemical control over protein-protein interactions: beyond inhibitors. Comb Chem High Throughput Screen, 2007; 10: 667-75.
[25] Berg T. Modulation of protein-protein interactions with small organic molecules. Angew Chem Int Ed Engl, 2003; 42: 2462-81.
[26] Arkin MR, Wells JA. Small-molecule inhibitors of protein-protein interactions: progressing towards the dream. Nat Rev Drug Discov, 2004; 3: 301-17.
[27] Bertelsen EB, Chang L, Gestwicki JE, Zuiderweg ER. Solution conformation of wild-type E. coli Hsp70 (DnaK) chaperone complexed with ADP and substrate. Proc Natl Acad Sci U S A, 2009; 106: 8471-6.
[28] Bork P, Sander C, Valencia A. An ATPase domain common to prokaryotic cell cycle proteins, sugar kinases, actin, and hsp70 heat shock proteins. Proc Natl Acad Sci U S A, 1992; 89: 7290-4.
[29] Wang H, Kurochkin AV, Pang Y, Hu W, Flynn GC, Zuiderweg ER. NMR solution structure of the 21 kDa chaperone protein DnaK substrate binding domain: a preview of chaperone-protein interaction. Biochemistry, 1998; 37: 7929-40.
[30] Zhu X, Zhao X, Burkholder WF, Gragerov A, Ogata CM, Gottesman ME, Hendrickson WA. Structural analysis of substrate binding by the molecular chaperone DnaK. Science, 1996; 272: 1606-14.
[31] Young JC, Barral JM, Ulrich Hartl F. More than folding: localized functions of cytosolic chaperones. Trends Biochem Sci, 2003; 28: 541-7.
[32] Gaestel M. Molecular chaperones in signal transduction. Handb Exp Pharmacol, 2006: 93-109.
[33] Mayer MP, Schroder H, Rudiger S, Paal K, Laufen T, Bukau B. Multistep mechanism of substrate binding determines chaperone activity of Hsp70. Nat Struct Biol, 2000; 7: 586-93.
[34] Vogel M, Mayer MP, Bukau B. Allosteric regulation of Hsp70 chaperones involves a conserved interdomain linker. J Biol Chem, 2006; 281: 38705-11.
[35] Chang L, Thompson AD, Ung P, Carlson HA, Gestwicki JE. Mutagenesis reveals the complex relationships between ATPase rate and the chaperone activities of Escherichia coli heat shock protein 70 (Hsp70/DnaK). J Biol Chem, 2010; 285: 21282-91.
[36] Ahmad A, Bhattacharya A, McDonald RA, Cordes M, Ellington B, Bertelsen EB, Zuiderweg ER. Heat shock protein 70 kDa chaperone/DnaJ cochaperone complex employs an unusual dynamic interface. Proc Natl Acad Sci U S A, 2011; 108: 18966-71.
[37] Sondermann H, Scheufler C, Schneider C, Hohfeld J, Hartl FU, Moarefi I. Structure of a Bag/Hsc70 complex: convergent functional evolution of Hsp70 nucleotide exchange factors. Science, 2001; 291: 1553-7.

[38] Liu FH, Wu SJ, Hu SM, Hsiao CD, Wang C. Specific interaction of the 70-kDa heat shock cognate protein with the tetratricopeptide repeats. J Biol Chem, 1999; 274: 34425-32.
[39] Whitesell L, Lindquist SL. HSP90 and the chaperoning of cancer. Nature Reviews Cancer, 2005; 5: 761-772.
[40] Allan RK, Ratajczak T. Versatile TPR domains accommodate different modes of target protein recognition and function. Cell Stress & Chaperones, 2011; 16: 353-367.
[41] Borges JC, Ramos CHI. Spectroscopic and thermodynamic measurements of nucleotide-induced changes in the human 70-kDa heat shock cognate protein. Archives of Biochemistry and Biophysics, 2006; 452: 46-54.
[42] Williamson DS, Borgognoni J, Clay A, Daniels Z, Dokurno P, Drysdale MJ, Foloppe N, Francis GL, Graham CJ, Howes R, Macias AT, Murray JB, Parsons R, Shaw T, Surgenor AE, Terry L, Wang YK, Wood M, Massey AJ. Novel Adenosine-Derived Inhibitors of 70 kDa Heat Shock Protein, Discovered Through Structure-Based Design. Journal of Medicinal Chemistry, 2009; 52: 1510-1513.
[43] Massey AJ. ATPases as drug targets: insights from heat shock proteins 70 and 90. J Med Chem, 2010; 53: 7280-6.
[44] Massey AJ, Williamson DS, Browne H, Murray JB, Dokurno P, Shaw T, Macias AT, Daniels Z, Geoffroy S, Dopson M, Lavan P, Matassova N, Francis GL, Graham CJ, Parsons R, Wang Y, Padfield A, Comer M, Drysdale MJ, Wood M. A novel, small molecule inhibitor of Hsc70/Hsp70 potentiates Hsp90 inhibitor induced apoptosis in HCT116 colon carcinoma cells. Cancer Chemother Pharmacol, 2011; 66: 535-45.
[45] Macias AT, Williamson DS, Allen N, Borgognoni J, Clay A, Daniels Z, Dokurno P, Drysdale MJ, Francis GL, Graham CJ, Howes R, Matassova N, Murray JB, Parsons R, Shaw T, Surgenor AE, Terry L, Wang Y, Wood M, Massey AJ. Adenosine-derived inhibitors of 78 kDa glucose regulated protein (Grp78) ATPase: insights into isoform selectivity. J Med Chem, 2010; 54: 4034-41.
[46] Kragol G, Lovas S, Varadi G, Condie BA, Hoffmann R, Otvos L. The antibacterial peptide pyrrhocoricin inhibits the ATPase actions of DnaK and prevents chaperone-assisted protein folding. Biochemistry, 2001; 40: 3016-3026.
[47] Williams DR, Ko SK, Park S, Lee MR, Shin I. An apoptosis-inducing small molecule that binds to heat shock protein 70. Angew Chem Int Ed Engl, 2008; 47: 7466-9.
[48] Jinwal UK, Miyata Y, Koren J, 3rd, Jones JR, Trotter JH, Chang L, O'Leary J, Morgan D, Lee DC, Shults CL, Rousaki A, Weeber EJ, Zuiderweg ER, Gestwicki JE, Dickey CA. Chemical manipulation of hsp70 ATPase activity regulates tau stability. J Neurosci, 2009; 29: 12079-88.
[49] Cellitti J, Zhang Z, Wang S, Wu B, Yuan H, Hasegawa P, Guiney DG, Pellecchia M. Small molecule DnaK modulators targeting the beta-domain. Chem Biol Drug Des, 2009; 74: 349-57.
[50] Qiu XB, Shao YM, Miao S, Wang L. The diversity of the DnaJ/Hsp40 family, the crucial partners for Hsp70 chaperones. Cell Mol Life Sci, 2006; 63: 2560-70.
[51] Kampinga HH, Hageman J, Vos MJ, Kubota H, Tanguay RM, Bruford EA, Cheetham ME, Chen B, Hightower LE. Guidelines for the nomenclature of the human heat shock proteins. Cell Stress Chaperones, 2009; 14: 105-11.

[52] Caplan AJ, Cyr DM, Douglas MG. YDJ1p facilitates polypeptide translocation across different intracellular membranes by a conserved mechanism. Cell, 1992; 71: 1143-55.
[53] Hageman J, van Waarde MA, Zylicz A, Walerych D, Kampinga HH. The diverse members of the mammalian HSP70 machine show distinct chaperone-like activities. Biochem J, 2011; 435: 127-42.
[54] Sterrenberg JN, Blatch GL, Edkins AL. Human DNAJ in cancer and stem cells. Cancer Lett, 2011; 312: 129-42.
[55] Kalia SK, Kalia LV, McLean PJ. Molecular chaperones as rational drug targets for Parkinson's disease therapeutics. CNS Neurol Disord Drug Targets, 2010; 9: 741-53.
[56] Mitra A, Shevde LA, Samant RS. Multi-faceted role of HSP40 in cancer. Clin Exp Metastasis, 2009; 26: 559-67.
[57] Harms MB, Sommerville RB, Allred P, Bell S, Ma D, Cooper P, Lopate G, Pestronk A, Weihl CC, Baloh RH. Exome sequencing reveals DNAJB6 mutations in dominantly-inherited myopathy. Ann Neurol, 2012; 71: 407-16.
[58] Knox C, Luke GA, Blatch GL, Pesce ER. Heat shock protein 40 (Hsp40) plays a key role in the virus life cycle. Virus Res, 2011; 160: 15-24.
[59] Langer T, Lu C, Echols H, Flanagan J, Hayer MK, Hartl FU. Successive action of DnaK, DnaJ and GroEL along the pathway of chaperone-mediated protein folding. Nature, 1992; 356: 683-9.
[60] Wall D, Zylicz M, Georgopoulos C. The conserved G/F motif of the DnaJ chaperone is necessary for the activation of the substrate binding properties of the DnaK chaperone. J Biol Chem, 1995; 270: 2139-44.
[61] Szabo A, Langer T, Schroder H, Flanagan J, Bukau B, Hartl FU. The ATP hydrolysis-dependent reaction cycle of the Escherichia coli Hsp70 system DnaK, DnaJ, and GrpE. Proc Natl Acad Sci U S A, 1994; 91: 10345-9.
[62] Greene MK, Maskos K, Landry SJ. Role of the J-domain in the cooperation of Hsp40 with Hsp70. Proc Natl Acad Sci U S A, 1998; 95: 6108-13.
[63] Gassler CS, Buchberger A, Laufen T, Mayer MP, Schroder H, Valencia A, Bukau B. Mutations in the DnaK chaperone affecting interaction with the DnaJ cochaperone. Proc Natl Acad Sci U S A, 1998; 95: 15229-34.
[64] Suh WC, Burkholder WF, Lu CZ, Zhao X, Gottesman ME, Gross CA. Interaction of the Hsp70 molecular chaperone, DnaK, with its cochaperone DnaJ. Proc Natl Acad Sci U S A, 1998; 95: 15223-8.
[65] Hennessy F, Nicoll WS, Zimmermann R, Cheetham ME, Blatch GL. Not all J domains are created equal: implications for the specificity of Hsp40-Hsp70 interactions. Protein Sci, 2005; 14: 1697-709.
[66] Awad W, Estrada I, Shen Y, Hendershot LM. BiP mutants that are unable to interact with endoplasmic reticulum DnaJ proteins provide insights into interdomain interactions in BiP. Proc Natl Acad Sci U S A, 2008; 105: 1164-9.
[67] Vembar SS, Jonikas MC, Hendershot LM, Weissman JS, Brodsky JL. J domain co-chaperone specificity defines the role of BiP during protein translocation. J Biol Chem, 2010; 285: 22484-94.
[68] Cheetham ME, Caplan AJ. Structure, function and evolution of DnaJ: conservation and adaptation of chaperone function. Cell Stress Chaperones, 1998; 3: 28-36.

[69] Kampinga HH, Craig EA. The HSP70 chaperone machinery: J proteins as drivers of functional specificity. Nat Rev Mol Cell Biol, 2010; 11: 579-92.
[70] Holstein SE, Ungewickell H, Ungewickell E. Mechanism of clathrin basket dissociation: separate functions of protein domains of the DnaJ homologue auxilin. J Cell Biol, 1996; 135: 925-37.
[71] Xing Y, Bocking T, Wolf M, Grigorieff N, Kirchhausen T, Harrison SC. Structure of clathrin coat with bound Hsc70 and auxilin: mechanism of Hsc70-facilitated disassembly. EMBO J, 2010; 29: 655-65.
[72] Bocking T, Aguet F, Harrison SC, Kirchhausen T. Single-molecule analysis of a molecular disassemblase reveals the mechanism of Hsc70-driven clathrin uncoating. Nat Struct Mol Biol, 2011; 18: 295-301.
[73] Wang AM, Morishima Y, Clapp KM, Peng HM, Pratt WB, Gestwicki JE, Osawa Y, Lieberman AP. Inhibition of hsp70 by methylene blue affects signaling protein function and ubiquitination and modulates polyglutamine protein degradation. J Biol Chem, 2010; 285: 15714-23.
[74] Nakanishi K, Kamiguchi K, Torigoe T, Nabeta C, Hirohashi Y, Asanuma H, Tobioka H, Koge N, Harada O, Tamura Y, Nagano H, Yano S, Chiba S, Matsumoto H, Sato N. Localization and function in endoplasmic reticulum stress tolerance of ERdj3, a new member of Hsp40 family protein. Cell Stress Chaperones, 2004; 9: 253-64.
[75] Shen Y, Hendershot LM. ERdj3, a stress-inducible endoplasmic reticulum DnaJ homologue, serves as a cofactor for BiP's interactions with unfolded substrates. Mol Biol Cell, 2005; 16: 40-50.
[76] Fan CY, Lee S, Ren HY, Cyr DM. Exchangeable chaperone modules contribute to specification of type I and type II Hsp40 cellular function. Mol Biol Cell, 2004; 15: 761-73.
[77] Lu Z, Cyr DM. The conserved carboxyl terminus and zinc finger-like domain of the co-chaperone Ydj1 assist Hsp70 in protein folding. J Biol Chem, 1998; 273: 5970-8.
[78] Lee S, Fan CY, Younger JM, Ren H, Cyr DM. Identification of essential residues in the type II Hsp40 Sis1 that function in polypeptide binding. J Biol Chem, 2002; 277: 21675-82.
[79] Rudiger S, Schneider-Mergener J, Bukau B. Its substrate specificity characterizes the DnaJ co-chaperone as a scanning factor for the DnaK chaperone. EMBO J, 2001; 20: 1042-50.
[80] Feifel B, Schonfeld HJ, Christen P. D-peptide ligands for the co-chaperone DnaJ. J Biol Chem, 1998; 273: 11999-2002.
[81] Li J, Qian X, Sha B. The crystal structure of the yeast Hsp40 Ydj1 complexed with its peptide substrate. Structure, 2003; 11: 1475-83.
[82] Freeman BC, Myers MP, Schumacher R, Morimoto RI. Identification of a regulatory motif in Hsp70 that affects ATPase activity, substrate binding and interaction with HDJ-1. EMBO J, 1995; 14: 2281-92.
[83] Qian X, Hou W, Zhengang L, Sha B. Direct interactions between molecular chaperones heat-shock protein (Hsp) 70 and Hsp40: yeast Hsp70 Ssa1 binds the extreme C-terminal region of yeast Hsp40 Sis1. Biochem J, 2002; 361: 27-34.
[84] Li J, Wu Y, Qian X, Sha B. Crystal structure of yeast Sis1 peptide-binding fragment and Hsp70 Ssa1 C-terminal complex. Biochem J, 2006; 398: 353-60.

[85] Suzuki H, Noguchi S, Arakawa H, Tokida T, Hashimoto M, Satow Y. Peptide-binding sites as revealed by the crystal structures of the human Hsp40 Hdj1 C-terminal domain in complex with the octapeptide from human Hsp70. Biochemistry, 2010; 49: 8577-84.
[86] Sha B, Lee S, Cyr DM. The crystal structure of the peptide-binding fragment from the yeast Hsp40 protein Sis1. Structure, 2000; 8: 799-807.
[87] Arawaka S, Machiya Y, Kato T. Heat shock proteins as suppressors of accumulation of toxic prefibrillar intermediates and misfolded proteins in neurodegenerative diseases. Curr Pharm Biotechnol, 2010; 11: 158-66.
[88] Jana NR, Tanaka M, Wang G, Nukina N. Polyglutamine length-dependent interaction of Hsp40 and Hsp70 family chaperones with truncated N-terminal huntingtin: their role in suppression of aggregation and cellular toxicity. Hum Mol Genet, 2000; 9: 2009-18.
[89] Zhou H, Li SH, Li XJ. Chaperone suppression of cellular toxicity of huntingtin is independent of polyglutamine aggregation. J Biol Chem, 2001; 276: 48417-24.
[90] Chuang JZ, Zhou H, Zhu M, Li SH, Li XJ, Sung CH. Characterization of a brain-enriched chaperone, MRJ, that inhibits Huntingtin aggregation and toxicity independently. J Biol Chem, 2002; 277: 19831-8.
[91] Hay DG, Sathasivam K, Tobaben S, Stahl B, Marber M, Mestril R, Mahal A, Smith DL, Woodman B, Bates GP. Progressive decrease in chaperone protein levels in a mouse model of Huntington's disease and induction of stress proteins as a therapeutic approach. Hum Mol Genet, 2004; 13: 1389-405.
[92] Wyttenbach A, Carmichael J, Swartz J, Furlong RA, Narain Y, Rankin J, Rubinsztein DC. Effects of heat shock, heat shock protein 40 (HDJ-2), and proteasome inhibition on protein aggregation in cellular models of Huntington's disease. Proc Natl Acad Sci U S A, 2000; 97: 2898-903.
[93] Miyata Y, Koren J, Kiray J, Dickey CA, Gestwicki JE. Molecular chaperones and regulation of tau quality control: strategies for drug discovery in tauopathies. Future Med Chem, 2011; 3: 1523-37.
[94] Sahara N, Maeda S, Yoshiike Y, Mizoroki T, Yamashita S, Murayama M, Park JM, Saito Y, Murayama S, Takashima A. Molecular chaperone-mediated tau protein metabolism counteracts the formation of granular tau oligomers in human brain. J Neurosci Res, 2007; 85: 3098-108.
[95] Abisambra JF, Jinwal UK, Suntharalingam A, Arulselvam K, Brady S, Cockman M, Jin Y, Zhang B, Dickey CA. DnaJA1 Antagonizes Constitutive Hsp70-Mediated Stabilization of Tau. J Mol Biol, 2012.
[96] Nadler SG, Tepper MA, Schacter B, Mazzucco CE. Interaction of the immunosuppressant deoxyspergualin with a member of the Hsp70 family of heat shock proteins. Science, 1992; 258: 484-6.
[97] Brodsky JL. Selectivity of the molecular chaperone-specific immunosuppressive agent 15-deoxyspergualin: modulation of Hsc70 ATPase activity without compromising DnaJ chaperone interactions. Biochem Pharmacol, 1999; 57: 877-80.
[98] Nadeau K, Nadler SG, Saulnier M, Tepper MA, Walsh CT. Quantitation of the interaction of the immunosuppressant deoxyspergualin and analogs with Hsc70 and Hsp90. Biochemistry, 1994; 33: 2561-7.

[99] Fewell SW, Day BW, Brodsky JL. Identification of an inhibitor of hsc70-mediated protein translocation and ATP hydrolysis. J Biol Chem, 2001; 276: 910-4.
[100] Mamelak D, Mylvaganam M, Whetstone H, Hartmann E, Lennarz W, Wyrick PB, Raulston J, Han H, Hoffman P, Lingwood CA. Hsp70s contain a specific sulfogalactolipid binding site. Differential aglycone influence on sulfogalactosyl ceramide binding by recombinant prokaryotic and eukaryotic hsp70 family members. Biochemistry, 2001; 40: 3572-82.
[101] Mamelak D, Lingwood C. The ATPase domain of hsp70 possesses a unique binding specificity for 3'-sulfogalactolipids. J Biol Chem, 2001; 276: 449-56.
[102] Park HJ, Mylvaganum M, McPherson A, Fewell SW, Brodsky JL, Lingwood CA. A soluble sulfogalactosyl ceramide mimic promotes Delta F508 CFTR escape from endoplasmic reticulum associated degradation. Chem Biol, 2009; 16: 461-70.
[103] Fewell SW, Smith CM, Lyon MA, Dumitrescu TP, Wipf P, Day BW, Brodsky JL. Small molecule modulators of endogenous and co-chaperone-stimulated Hsp70 ATPase activity. J Biol Chem, 2004; 279: 51131-40.
[104] Wisen S, Bertelsen EB, Thompson AD, Patury S, Ung P, Chang L, Evans CG, Walter GM, Wipf P, Carlson HA, Brodsky JL, Zuiderweg ER, Gestwicki JE. Binding of a small molecule at a protein-protein interface regulates the chaperone activity of hsp70-hsp40. ACS Chem Biol, 2010; 5: 611-22.
[105] Chang L, Bertelsen EB, Wisen S, Larsen EM, Zuiderweg ER, Gestwicki JE. High-throughput screen for small molecules that modulate the ATPase activity of the molecular chaperone DnaK. Anal Biochem, 2008; 372: 167-76.
[106] Wisen S, Androsavich J, Evans CG, Chang L, Gestwicki JE. Chemical modulators of heat shock protein 70 (Hsp70) by sequential, microwave-accelerated reactions on solid phase. Bioorg Med Chem Lett, 2008; 18: 60-5.
[107] Braunstein MJ, Scott SS, Scott CM, Behrman S, Walter P, Wipf P, Coplan JD, Chrico W, Joseph D, Brodsky JL, Batuman O. Antimyeloma Effects of the Heat Shock Protein 70 Molecular Chaperone Inhibitor MAL3-101. J Oncol, 2011; 2011: 232037.
[108] Walter GM, Smith MC, Wisen S, Basrur V, Elenitoba-Johnson KS, Duennwald ML, Kumar A, Gestwicki JE. Ordered assembly of heat shock proteins, Hsp26, Hsp70, Hsp90, and Hsp104, on expanded polyglutamine fragments revealed by chemical probes. J Biol Chem, 2011; 286: 40486-93.
[109] Koren J, 3rd, Jinwal UK, Jin Y, O'Leary J, Jones JR, Johnson AG, Blair LJ, Abisambra JF, Chang L, Miyata Y, Cheng AM, Guo J, Cheng JQ, Gestwicki JE, Dickey CA. Facilitating Akt clearance via manipulation of Hsp70 activity and levels. J Biol Chem, 2010; 285: 2498-505.
[110] Chang L, Miyata Y, Ung PM, Bertelsen EB, McQuade TJ, Carlson HA, Zuiderweg ER, Gestwicki JE. Chemical screens against a reconstituted multiprotein complex: myricetin blocks DnaJ regulation of DnaK through an allosteric mechanism. Chem Biol, 2011; 18: 210-21.
[111] Congdon EE, Wu JW, Myeku N, Figueroa YH, Herman M, Marinec PS, Gestwicki JE, Dickey CA, Yu WH, Duff K. Methylthioninium chloride (methylene blue) induces autophagy and attenuates tauopathy in vitro and in vivo. Autophagy, 2012; 8.

[112] O'Leary JC, 3rd, Li Q, Marinec P, Blair LJ, Congdon EE, Johnson AG, Jinwal UK, Koren J, 3rd, Jones JR, Kraft C, Peters M, Abisambra JF, Duff KE, Weeber EJ, Gestwicki JE, Dickey CA. Phenothiazine-mediated rescue of cognition in tau transgenic mice requires neuroprotection and reduced soluble tau burden. Mol Neurodegener, 2010; 5: 45.
[113] Miyata Y, Chang L, Bainor A, McQuade TJ, Walczak CP, Zhang Y, Larsen MJ, Kirchhoff P, Gestwicki JE. High-throughput screen for Escherichia coli heat shock protein 70 (Hsp70/DnaK): ATPase assay in low volume by exploiting energy transfer. J Biomol Screen, 2010; 15: 1211-9.
[114] Seguin SP, Evans CW, Nebane-Akah M, McKellip S, Ananthan S, Tower NA, Sosa M, Rasmussen L, White EL, Maki BE, Matharu DS, Golden JE, Aube J, Brodsky JL, Noah JW. High-throughput screening identifies a bisphenol inhibitor of SV40 large T antigen ATPase activity. J Biomol Screen, 2012; 17: 194-203.
[115] Harrison C. GrpE, a nucleotide exchange factor for DnaK. Cell Stress Chaperones, 2003; 8: 218-24.
[116] Carrettiero DC, Hernandez I, Neveu P, Papagiannakopoulos T, Kosik KS. The cochaperone BAG2 sweeps paired helical filament- insoluble tau from the microtubule. J Neurosci, 2009; 29: 2151-61.
[117] Elliott E, Tsvetkov P, Ginzburg I. BAG-1 associates with Hsc70.Tau complex and regulates the proteasomal degradation of Tau protein. J Biol Chem, 2007; 282: 37276-84.
[118] Souza AP, Albuquerque C, Torronteguy C, Frasson A, Maito F, Pereira L, Duval da Silva V, Zerwes F, Raynes D, Guerriero V, Bonorino C. HspBP1 levels are elevated in breast tumor tissue and inversely related to tumor aggressiveness. Cell Stress Chaperones, 2009; 14: 301-10.
[119] Elliott E, Laufer O, Ginzburg I. BAG-1M is up-regulated in hippocampus of Alzheimer's disease patients and associates with tau and APP proteins. J Neurochem, 2009; 109: 1168-78.
[120] Knoll R, Hoshijima M, Hoffman HM, Person V, Lorenzen-Schmidt I, Bang ML, Hayashi T, Shiga N, Yasukawa H, Schaper W, McKenna W, Yokoyama M, Schork NJ, Omens JH, McCulloch AD, Kimura A, Gregorio CC, Poller W, Schaper J, Schultheiss HP, Chien KR. The cardiac mechanical stretch sensor machinery involves a Z disc complex that is defective in a subset of human dilated cardiomyopathy. Cell, 2002; 111: 943-55.
[121] Nakamura J, Fujimoto M, Yasuda K, Takeda K, Akira S, Hatayama T, Takagi Y, Nozaki K, Hosokawa N, Nagata K. Targeted disruption of Hsp110/105 gene protects against ischemic stress. Stroke, 2008; 39: 2853-9.
[122] Subjeck JR, Sciandra JJ, Chao CF, Johnson RJ. Heat shock proteins and biological response to hyperthermia. Br J Cancer Suppl, 1982; 5: 127-31.
[123] Ishihara K, Yasuda K, Hatayama T. Molecular cloning, expression and localization of human 105 kDa heat shock protein, hsp105. Biochim Biophys Acta, 1999; 1444: 138-42.
[124] Wakatsuki T, Hatayama T. Characteristic expression of 105-kDa heat shock protein (HSP105) in various tissues of nonstressed and heat-stressed rats. Biol Pharm Bull, 1998; 21: 905-10.

[125] Liu Q, Hendrickson WA. Insights into Hsp70 chaperone activity from a crystal structure of the yeast Hsp110 Sse1. Cell, 2007; 131: 106-20.
[126] Oh HJ, Easton D, Murawski M, Kaneko Y, Subjeck JR. The chaperoning activity of hsp110. Identification of functional domains by use of targeted deletions. J Biol Chem, 1999; 274: 15712-8.
[127] Dragovic Z, Broadley SA, Shomura Y, Bracher A, Hartl FU. Molecular chaperones of the Hsp110 family act as nucleotide exchange factors of Hsp70s. EMBO J, 2006; 25: 2519-28.
[128] Goeckeler JL, Stephens A, Lee P, Caplan AJ, Brodsky JL. Overexpression of yeast Hsp110 homolog Sse1p suppresses ydj1-151 thermosensitivity and restores Hsp90-dependent activity. Mol Biol Cell, 2002; 13: 2760-70.
[129] Oh HJ, Chen X, Subjeck JR. Hsp110 protects heat-denatured proteins and confers cellular thermoresistance. J Biol Chem, 1997; 272: 31636-40.
[130] Yamagishi N, Yokota M, Yasuda K, Saito Y, Nagata K, Hatayama T. Characterization of stress sensitivity and chaperone activity of Hsp105 in mammalian cells. Biochem Biophys Res Commun, 2011; 409: 90-5.
[131] Shaner L, Trott A, Goeckeler JL, Brodsky JL, Morano KA. The function of the yeast molecular chaperone Sse1 is mechanistically distinct from the closely related hsp70 family. J Biol Chem, 2004; 279: 21992-2001.
[132] Schuermann JP, Jiang J, Cuellar J, Llorca O, Wang L, Gimenez LE, Jin S, Taylor AB, Demeler B, Morano KA, Hart PJ, Valpuesta JM, Lafer EM, Sousa R. Structure of the Hsp110:Hsc70 nucleotide exchange machine. Mol Cell, 2008; 31: 232-43.
[133] Polier S, Dragovic Z, Hartl FU, Bracher A. Structural basis for the cooperation of Hsp70 and Hsp110 chaperones in protein folding. Cell, 2008; 133: 1068-79.
[134] Hendrickson WA, Liu Q. Exchange we can believe in. Structure, 2008; 16: 1153-5.
[135] Wilson CG, Arkin MR. Small-molecule inhibitors of IL-2/IL-2R: lessons learned and applied. Curr Top Microbiol Immunol, 2011; 348: 25-59.
[136] DeLano WL, Ultsch MH, de Vos AM, Wells JA. Convergent solutions to binding at a protein-protein interface. Science, 2000; 287: 1279-83.
[137] Wells JA, McClendon CL. Reaching for high-hanging fruit in drug discovery at protein-protein interfaces. Nature, 2007; 450: 1001-9.
[138] Takayama S, Xie Z, Reed JC. An evolutionarily conserved family of Hsp70/Hsc70 molecular chaperone regulators. J Biol Chem, 1999; 274: 781-6.
[139] Takayama S, Bimston DN, Matsuzawa S, Freeman BC, Aime-Sempe C, Xie Z, Morimoto RI, Reed JC. BAG-1 modulates the chaperone activity of Hsp70/Hsc70. EMBO J, 1997; 16: 4887-96.
[140] Briknarova K, Takayama S, Brive L, Havert ML, Knee DA, Velasco J, Homma S, Cabezas E, Stuart J, Hoyt DW, Satterthwait AC, Llinas M, Reed JC, Ely KR. Structural analysis of BAG1 cochaperone and its interactions with Hsc70 heat shock protein. Nat Struct Biol, 2001; 8: 349-52.
[141] Goebl M, Yanagida M. THE TPR SNAP HELIX - A NOVEL PROTEIN REPEAT MOTIF FROM MITOSIS TO TRANSCRIPTION. Trends in Biochemical Sciences, 1991; 16: 173-177.
[142] Lamb JR, Tugendreich S, Hieter P. Tetratrico peptide repeat interactions: to TPR or not to TPR? Trends in Biochemical Sciences, 1995; 20: 257-259.

[143] Blatch GL, Lässle M, Zetter BR, Kundra V. Isolation of a mouse cDNA encoding mSTI1, a stress-inducible protein containing the TPR motif. Gene, 1997; 194: 277-282.
[144] D'Andrea LD, Regan L. TPR proteins: the versatile helix. Trends in Biochemical Sciences, 2003; 28: 655-662.
[145] Sikorski RS, Boguski MS, Goebl M, Hieter P. A repeating amino acid motif in CDC23 defines a family of proteins and a new relationship among genes required for mitosis and RNA synthesis. Cell, 1990; 60: 307-317.
[146] Hirano T, Kinoshita N, Morikawa K, Yanagida M. Snap helix with knob and hole: Essential repeats in S. pombe nuclear protein nuc2 +. Cell, 1990; 60: 319-328.
[147] Scheufler C, Brinker A, Bourenkov G, Pegoraro S, Moroder L, Bartunik H, Hartl FU, Moarefi I. Structure of TPR domain-peptide complexes: Critical elements in the assembly of the Hsp70-Hsp90 multichaperone machine. Cell, 2000; 101: 199-210.
[148] Brinker A, Scheufler C, von der Mulbe F, Fleckenstein B, Herrmann C, Jung G, Moarefi I, Hartl FU. Ligand discrimination by TPR domains - Relevance and selectivity of EEVD-recognition in Hsp70 center dot Hop center dot Hsp90 complexes. Journal of Biological Chemistry, 2002; 277: 19265-19275.
[149] Chen S, Smith DF. Hop as an adaptor in the heat shock protein 70 (Hsp70) and hsp90 chaperone machinery. J Biol Chem, 1998; 273: 35194-200.
[150] Morishima Y, Murphy PJ, Li DP, Sanchez ER, Pratt WB. Stepwise assembly of a glucocorticoid receptor.hsp90 heterocomplex resolves two sequential ATP-dependent events involving first hsp70 and then hsp90 in opening of the steroid binding pocket. J Biol Chem, 2000; 275: 18054-60.
[151] Hutchison KA, Dittmar KD, Czar MJ, Pratt WB. Proof that hsp70 is required for assembly of the glucocorticoid receptor into a heterocomplex with hsp90. J Biol Chem, 1994; 269: 5043-9.
[152] Smith DF. Dynamics of heat shock protein 90-progesterone receptor binding and the disactivation loop model for steroid receptor complexes. Mol Endocrinol, 1993; 7: 1418-29.
[153] Zhang M, Windheim M, Roe SM, Peggie M, Cohen P, Prodromou C, Pearl LH. Chaperoned ubiquitylation--crystal structures of the CHIP U box E3 ubiquitin ligase and a CHIP-Ubc13-Uev1a complex. Mol Cell, 2005; 20: 525-38.
[154] Connell P, Ballinger CA, Jiang J, Wu Y, Thompson LJ, Hohfeld J, Patterson C. The co-chaperone CHIP regulates protein triage decisions mediated by heat-shock proteins. Nat Cell Biol, 2001; 3: 93-6.
[155] Qian SB, McDonough H, Boellmann F, Cyr DM, Patterson C. CHIP-mediated stress recovery by sequential ubiquitination of substrates and Hsp70. Nature, 2006; 440: 551-5.
[156] Young JC, Barral JM, Hartl FU. More than folding: localized functions of cytosolic chaperones. Trends in Biochemical Sciences, 2003; 28: 541-547.
[157] Meimaridou E, Gooljar SB, Chapple JP. From hatching to dispatching: the multiple cellular roles of the Hsp70 molecular chaperone machinery. Journal of Molecular Endocrinology, 2009; 42: 1-9.
[158] Hohfeld J, Cyr DM, Patterson C. From the cradle to the grave: molecular chaperones that may choose between folding and degradation. Embo Reports, 2001; 2: 885-890.

[159] Wu SJ, Liu FH, Hu SM, Wang C. Different combinations of the heat-shock cognate protein 70 (hsc70) C-terminal functional groups are utilized to interact with distinct tetratricopeptide repeat-containing proteins. Biochemical Journal, 2001; 359: 419-426.
[160] Ballinger CA, Connell P, Wu YX, Hu ZY, Thompson LJ, Yin LY, Patterson C. Identification of CHIP, a novel tetratricopeptide repeat-containing protein that interacts with heat shock proteins and negatively regulates chaperone functions. Molecular and Cellular Biology, 1999; 19: 4535-4545.
[161] Wang L, Liu Y-T, Hao R, Chen L, Chang Z, Wang H-R, Wang Z-X, Wu J-W. Molecular Mechanism of the Negative Regulation of Smad1/5 Protein by Carboxyl Terminus of Hsc70-interacting Protein (CHIP). Journal of Biological Chemistry, 2011; 286.
[162] Liu FH, Wu SJ, Hu SM, Hsiao CD, Wang C. Specific interaction of the 70-kDa heat shock cognate protein with the tetratricopeptide repeats. Journal of Biological Chemistry, 1999; 274: 34425-34432.
[163] Yi F, Zhu PJ, Southall N, Inglese J, Austin CP, Zheng W, Regan L. An AlphaScreen (TM)-Based High-Throughput Screen to Identify Inhibitors of Hsp90-Cochaperone Interaction. Journal of Biomolecular Screening, 2009; 14: 273-281.
[164] Vasko RC, Rodriguez RA, Cunningham CN, Ardi VC, Agard DA, McAlpine SR. Mechanistic Studies of Sansalvamide A-Amide: An Allosteric Modulator of Hsp90. Acs Medicinal Chemistry Letters, 2010; 1: 4-8.
[165] Ardi VC, Alexander LD, Johnson VA, McAlpine SR. Macrocycles That Inhibit the Binding between Heat Shock Protein 90 and TPR-Containing Proteins. Acs Chemical Biology, 2011; 6: 1357-1366.

Chapter 2

Synthetic Lethal Interactions in Yeast Reveal Functional Roles of J Protein Co-chaperones

2.1 Abstract

J proteins are a diverse family of co-chaperones that cooperate with heat shock protein 70 (Hsp70) to coordinate protein quality control, especially in response to cellular stress. Current models suggest that individual J proteins might play roles in recruiting Hsp70s to specific functions, such as maintaining cell wall integrity or promoting ribosome biogenesis. However, relatively few stresses have been used to test this model and, as a result, only a few specific activities have been identified. To expand our understanding of the J protein network, we used a synthetic lethal approach in which 11 *Saccharomyces cerevisiae* deletion strains were treated with 12 well-characterized chemical inhibitors. The results defined new roles for specific J proteins in major signaling pathways. For example, an important role for Swa2 in cell wall integrity was identified and activities of the under-explored Jjj1, Apj1, Jjj3 and Caj1 proteins were suggested. More generally, these findings support a model in which some J proteins, such as Ydj1 and Zuo1, play "generalist" roles, while others, such as Apj1 and Jjj2, are "specialists", having roles in relatively few pathways. Together, these results provide new insight into the network of J proteins.

2.2 Introduction

2.2.1 Hsp70 and J proteins in *S. cerevisiae*

In *Saccharomyces cerevisiae*, there are two cytosolic classes of Hsp70: Ssa (Ssa1-4) and Ssb (Ssb1-2). Expression of only one of each class is required to support near wild type viability, underscoring the high structural and functional homology among Hsp70 isoforms [1].

The dramatic expansion of the J proteins in higher organisms, especially compared to the relatively few Hsp70s, suggests that a larger pool of more specialized J proteins supports greater cellular complexity. Prevailing models suggest that combinations of an individual J protein with an Hsp70 might yield a complex with the ability to perform specific tasks or engage with specific subsets of substrates. In support of this idea, recent efforts have identified roles for individual J proteins in a handful of specific cellular tasks. For example, Swa2, the *S. ceresvisiae* ortholog of human auxilin, uncoats clathrin coated vesicles and is required for cortical ER inheritance [2, 3]. This activity is not readily recovered by over-expression of other J proteins, suggesting that Swa2 is specialized for this Hsp70 function. Similarly, Jjj3 is a J protein that is essential for diphthamide synthesis [4]. In contrast to these "specialist" J proteins, *S. cerevisiae* has also retained "generalists", such as Ydj1 and Sis1, which maintain protein quality control in the cytosol by helping Hsp70 fold proteins [5]. A systematic study of cytosolic *S. cerevisiae* J proteins using deletion mutants confirmed that some J proteins play essential roles during thermal stress, while others are apparently redundant for this activity [1]. These observations suggest that other J proteins might be important under specific biological or environmental conditions.

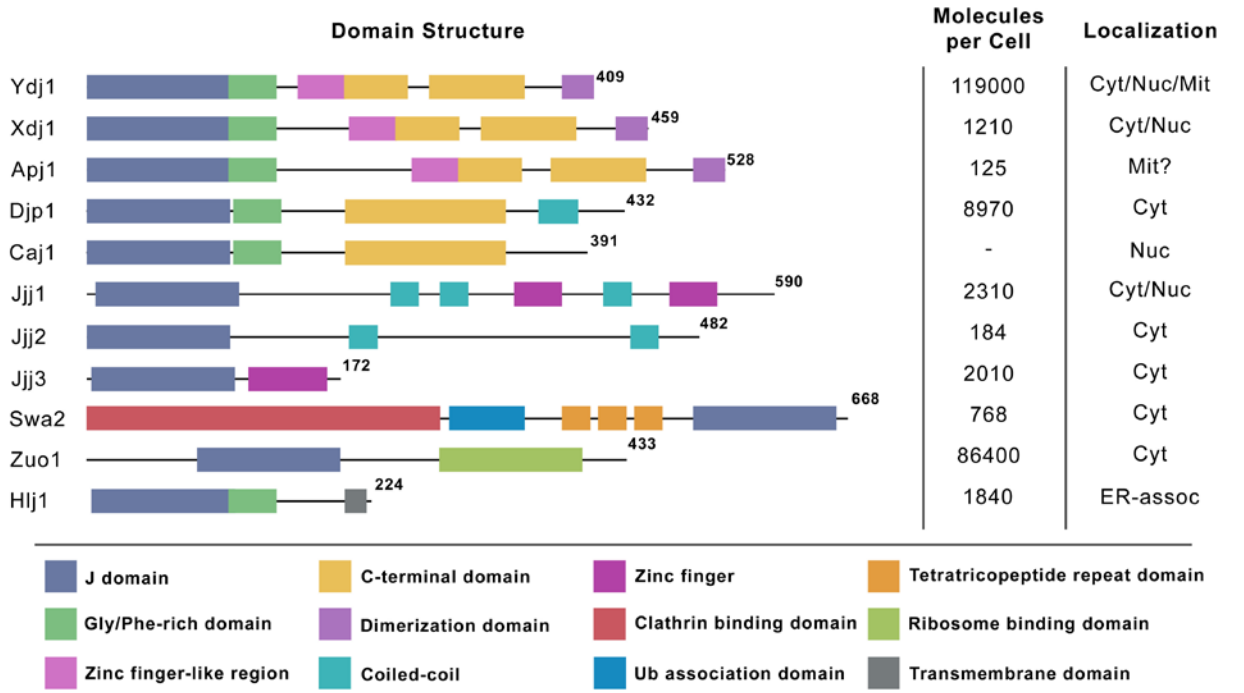

Table 2.1. Domain structure of J proteins Eleven J proteins were tested for synthetic lethal interactions. Molecules per cell determined by Ghaemmaghami *et al.*, 2003. Localization is in some cases predicted. Figure adapted from Kampinga and Craig, 2010.

2.2.2 Elucidation of J protein functional roles in *S. cerevisiae*

We envisioned that a synthetic lethal approach might enable assignment of cellular roles to individual J proteins. Using deletions of the 11 cytosolic J proteins in *S. cerevisiae* [1, 6, 7], we tested the effects of twelve well-characterized chemical inhibitors that act in specific cellular pathways, such as cell wall synthesis and translation (Table 2.1), on growth [6, 8]. We found that some J proteins, such as Ydj1, are multidrug resistance genes, required to buffer the cell against a diverse array of stressors. Others confer resistance to only a subset of the compounds, suggesting functions in specific pathways. Three J proteins had no synthetic lethal interactions and they may either be redundant or have specific functions in pathways not targeted by the twelve compounds. These findings define new biological roles for individual J proteins, results that could facilitate their functional classification and provide new opportunities for their use as drug targets.

Compound	Target
Hygromycin B	Translation; 30S ribosomal subunit formation
Cycloheximide	Translation elongation
Rapamycin	TOR1/TOR2 signaling
Caffeine	TOR1 signaling; cell wall; other kinases
Calcofluor White	Cell wall integrity (CWI) pathway
Congo Red	Cell wall integrity (CWI) pathway
Fluconazole	Ergosterol biosynthesis (plasma membrane)
17-AAG	Hsp90
Camptothecin	Topoisomerase I
Hydroxyurea	Ribonucleotide reductase
FK-506	Calcineurin
Wortmannin	Phosphatidylinositol kinase

Table 2.2. Compounds with known antifungal activity tested for synthetic lethal interactions with J proteins in *S. cerevisiae.*

2.3 Results

2.3.1 Selection of J proteins and chemical probes for synthetic lethal analysis

Eleven *S. cerevisiae* deletion mutants of cytosolic and nuclear J proteins were selected to carry out chemical genetic investigations [1] (Table 2.1). These J proteins represent 3 members of class I, 2 of class II and 6 of class III. In addition, twelve compounds targeting diverse cellular processes were chosen [6, 7] (Table 2.2). Yeast strains were spotted in five-fold dilutions on rich media agar containing a sublethal concentration of each compound and grown for three days. As a secondary assay, yeast growth in liquid was also assessed using optical density (OD) values monitored for 10 hours, when all strains had reached stationary phase. Compounds that reduced growth of a J protein deletion strain in either assay were scored as synthetic lethal interactions.

2.3.2 Ydj1

Ydj1 is an abundant J protein that partners with Hsp70s (Ssa1-4 in yeast) to carry out general protein quality control in the cytosol [9, 10]. Consistent with this activity, deletion

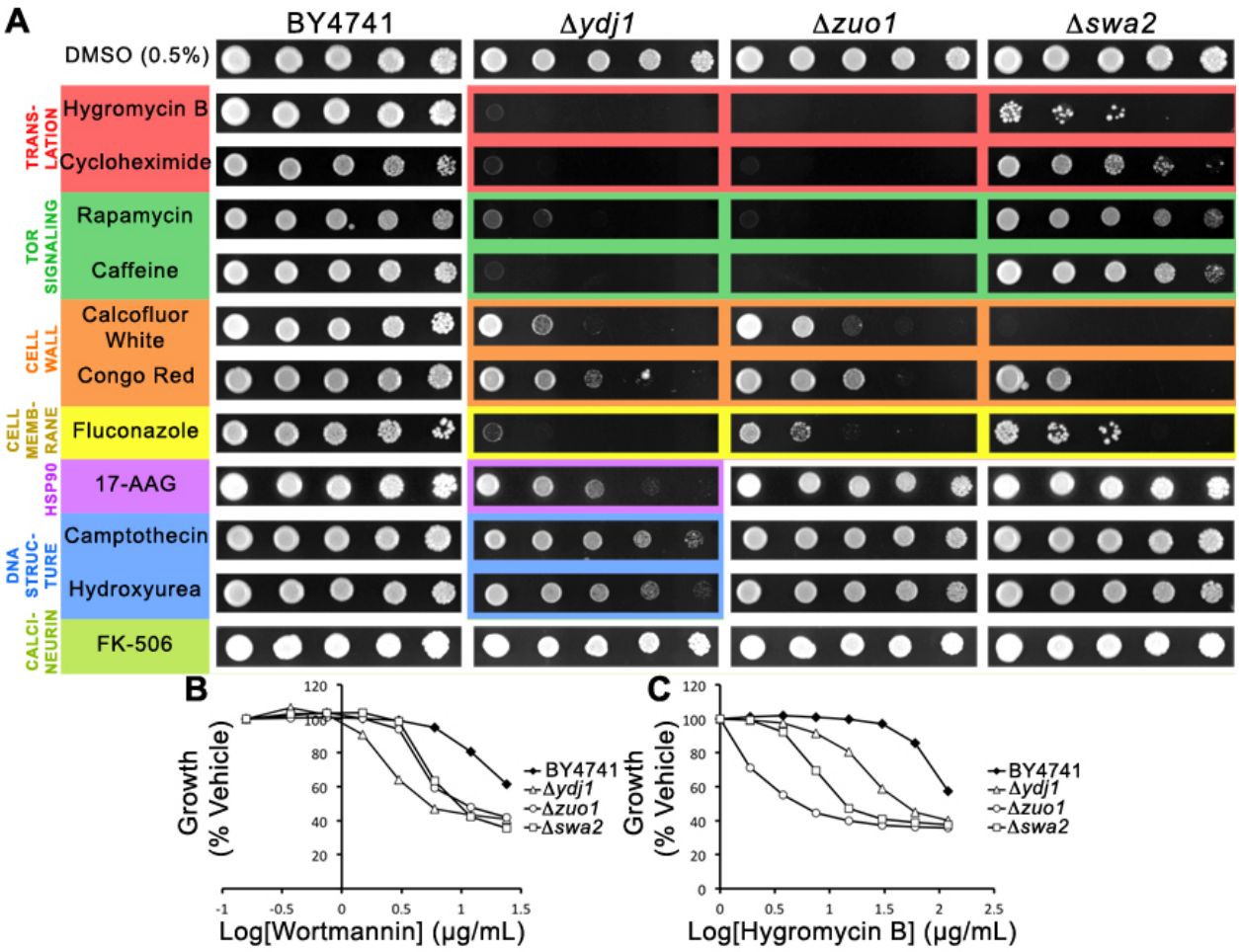

Figure 2.1. J proteins Ydj1, Zuo1, and Swa2 are involved in many cellular processes. A) Five-fold dilutions of BY4741, *Δydj1*, *Δzuo1*, or *Δswa2* were plated on rich medium containing DMSO or compound (see Materials and Methods for concentrations) and grown for 72 hours at 30°C. Images are representative of 3 replicates. B-C) Cultures were grown to saturation, diluted to OD_{600} = 0.15, and transferred to a 96-well plate containing two-fold dilutions of (B) wortmannin (24-0 μg/mL) or (C) hygromycin B (120-0 μg/mL) in DMSO (final concentration 2%). Plates were incubated with shaking at 30°C for 10 hours. At 10 hours, OD_{600} values were recorded and normalized to the OD_{600} with DMSO alone for each strain. See Appendix 2.1 for results with other compounds.

of Ydj1 resulted in sensitivity to nearly every compound tested (Figure 2.1A). Δ*ydj1* cells were particularly sensitive to translation inhibitors, fluconazole, rapamycin and caffeine (Figure 2.1A). Furthermore, Δ*ydj1* was very sensitive to wortmannin, an inhibitor of PI kinases, in the liquid growth assay (Figure 2.1B). Together, these results suggest that Ydj1 may play an important role in supporting the integrity of kinase signaling networks, perhaps by stabilizing the enzymes. On the other hand, Δ*ydj1* was only moderately sensitive to cell

wall stressors, suggesting that cells lacking Ydj1 can still maintain the cell wall integrity (CWI) pathway. Finally, Δ*ydj1* was the only strain tested that was mildly sensitive to the stressors of DNA maintenance, hydroxyurea and camptothecin. This result suggests that the J proteins (and, by extension, the Hsp70 machinery) may not be responsible for stability or function in that system.

2.3.3 Zuo1

Zuo1 is a ribosome-associated J protein that plays roles in nascent protein folding and ribosomal assembly [11-13]. Deletion of Zuo1 resulted in marked sensitivity to seven compounds (Figure 2.1A). The sensitivity profile of Δ*zuo1* was similar to that of Ydj1, which is unexpected because they have markedly different localization patterns and domain structures (Table 2.1). For example, Δ*zuo1* was acutely sensitive to fluconazole, rapamycin, caffeine, and wortmannin (Figure 2.1A,B) and these cells also had moderate sensitivity to cell wall perturbing compounds. It seems possible that the similar sensitivities of Δ*zuo1* and Δ*ydj1* cells may reflect their activities at different stages in the same processes. For example, Zuo1 might be important in initial folding of a kinase, while Ydj1 might be important in final maturation. However, Δ*zuo1* cells do not share the growth defect of Δ*ydj1* cells, so it may be that Ydj1's role is more critical to a wider range of substrates. Consistent with this idea, Δ*zuo1* was not sensitive to inhibitors of Hsp90, DNA-modifying enzymes or calcineurin. Another possibility is based on the observations that Zuo1 promotes expression of the drug exporter Pdr5 [14, 15]. The absence of Zuo1 may therefore allow accumulation of the specific drugs exported by Pdr5, which includes fluconazole (Figure 2.1A). Finally, as expected, Δ*zuo1* cells were not viable in the presence of compounds that inhibit translation

(Figure 2.1A,C). In healthy cells, Zuo1 may confer tolerance to cycloheximide and hygromycin B by helping to disassemble arrested ribosomes and assemble new ones, and in its absence the cells cannot recover from the accumulation of arrested ribosomes.

2.3.4 Swa2

Swa2 functions with Hsp70s in the removal of clathrin from vesicles [2] and it has essential roles in cortical ER inheritance [3]. In addition to its J domain and clathrin-binding domain, Swa2 includes three tetratricopeptide (TPR) motifs and a ubiquitin-binding domain [16]. Deletion of Swa2 caused sensitivity to 6 compounds (Figure 2.1A), including weak sensitivity to caffeine and rapamycin and severe responses to calcofluor white, congo red, fluconazole, and hygromycin B. Lesser sensitivity was also observed in the presence of cycloheximide, caffeine, and rapamycin. The acute sensitivity of Δ*swa2* to cell wall perturbing agents suggests that Swa2 may have a role, whether direct or indirect, in cell wall assembly or integrity. CW and CR induce upregulation of the cell wall integrity (CWI) pathway, but caffeine causes cell wall defects independent of the CWI pathway [17, 18]. The severe sensitivity of Δ*swa2* to CW and CR but not caffeine thus suggests a specific defect in the cell's ability to mount a CWI response in the absence of Swa2. This may be due to impaired trafficking of cell wall components or CWI pathway members as a result of accumulated clathrin coated transport vesicles, or it could be another uncharacterized function of Swa2.

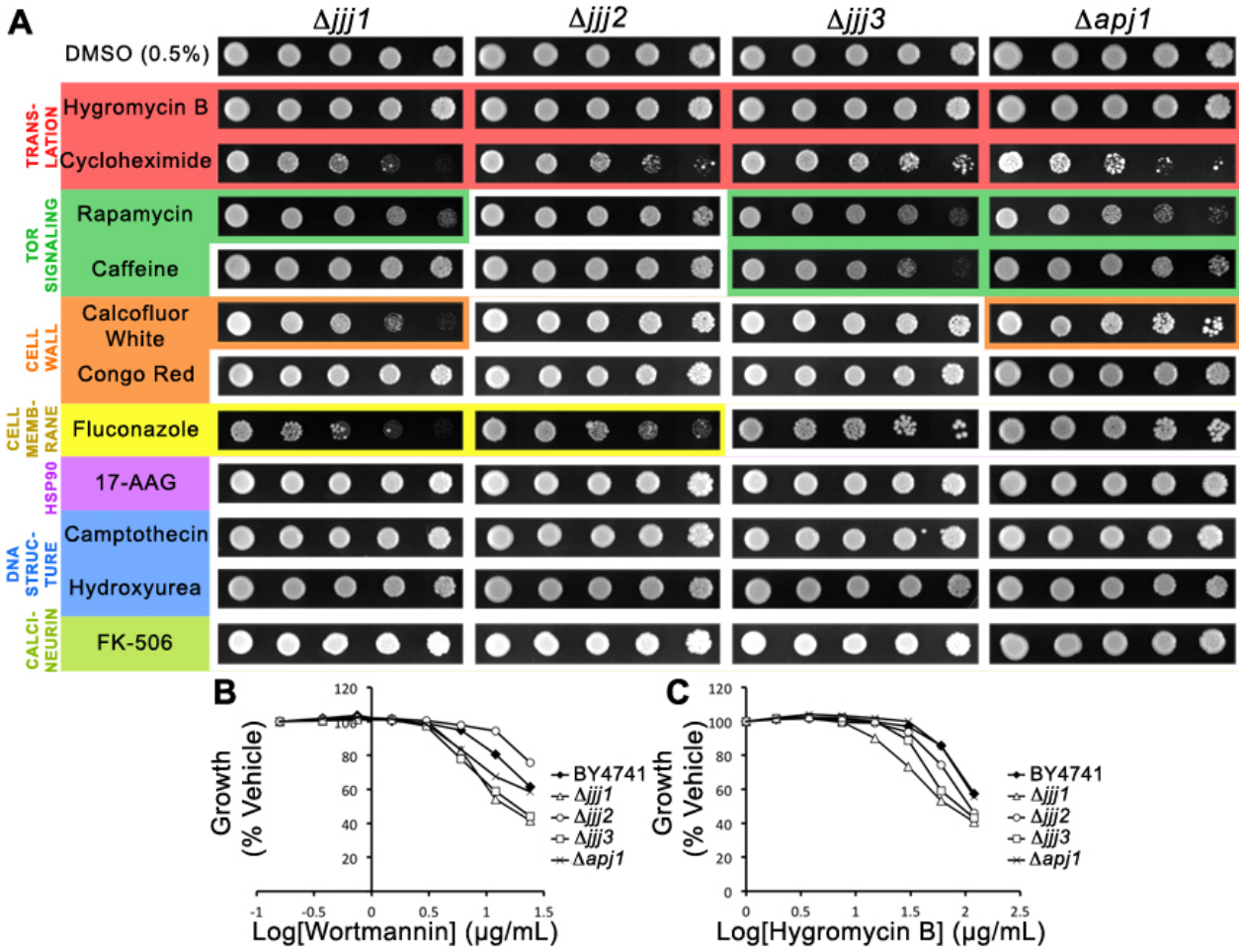

Figure 2.2. J proteins Jjj1, Jjj2, Jjj3, and Apj1 have more specific functional roles. A) Five-fold dilutions of *Δjjj1*, *Δjjj2*, *Δjjj3*, or *Δapj1* were plated on rich medium containing DMSO or compound and grown for 72 hours at 30°C. B,C) Strains were grown in liquid YPD in the presence of (B) wortmannin (24-0 μg/mL) or (C) hygromycin B (120-0 μg/mL) in DMSO (final concentration 2%).

2.3.5 Jjj1

Jjj1 is a specialized J protein that plays a role in 60S ribosomal subunit biogenesis [19, 20] and perhaps other aspects of ribosome turnover [13]. Deletion of this J protein conferred mild sensitivity to calcofluor white, rapamycin, cycloheximide, and fluconazole in the spot assay and hygromycin B and wortmannin in the liquid assay (Figure 2.2). Previous work has demonstrated that growth defects resulting from Jjj1 deletion cannot be ameliorated by

any other J protein [1]. On the other hand, overexpression of Jjj1 can partially rescue the slow growth of Δ*zuo1* cells, which is thought to be due to its ability to recruit Ssa1 (the cytosolic yeast Hsp70) to the ribosome when Zuo1 is not present to recruit Ssb1/2 [13]. Further enforcing this relationship between Jjj1 and Zuo1, their deletions confer sensitivity to nearly the same compounds in our experiments. However, loss of Jjj1 is less detrimental, as the phenotype of Δ*jjj1* cells is uniformly less dramatic. The differences in phenotype severity are consistent with their copy numbers; Jjj1 exists as only 2310 molecules per cell, while Zuo1 has 86400 copies and is possibly associated with every ribosome. Together, these finding are consistent with Jjj1 and Zuo1 having partially overlapping functions in ribosome function.

2.3.6 Jjj3

Jjj3 is one of the five genes required for synthesis of diphthamide (DT), a posttranslational modification of translation elongation factor 2 (EF2) [4]. Studies of the human ortholog of Jjj3, Dph4, found that it is an iron-binding enzyme that is capable of participating in redox processes, and it was confirmed that Jjj3 also possesses these properties [21]. In fact, one of the enzymes responsible for DT synthesis, Dph2, contains an iron-sulfur cluster, and it is likely that Dph4/Jjj3 cooperates with Dph2 [21]. In our synthetic lethal screen, deletion of Jjj3 conferred mild sensitivity to the TOR-targeting compounds, rapamycin and caffeine, and the translation inhibitor, cycloheximide (Figure 2A). Mild sensitivity of Δ*jjj3* to hygromycin B and wortmannin in the liquid assay was also observed (Figure 2.2B,C). These results clearly demonstrate that DT synthesis is not the only process in which Jjj3 is involved. Perhaps consistent with this model, Jjj3 is partially colocalized to the perinuclear

site of diphthamide synthesis, but there is a significant portion of the Jjj3 pool that associates with the broader cytoskeleton [22]. Interestingly, protein microarray studies suggest that Jjj3 physically interacts with 8 kinases [23] and it was one of only 24/4200 proteins that interacted with 8 or more kinases, including kinases involved in the PKC pathway, septin behavior, cell cycle progression, and transcriptional activation [23]. Together, the previous observations and these synthetic lethal studies suggest that Jjj3 may have broad roles as a redox partner.

2.3.7 Apj1

Deletion of Apj1 conferred mild sensitivity to caffeine, rapamycin, cyclohexmide, calcofluor white, and wortmannin (Figure 2.2). The identification of phenotypes deriving from deletion of this J protein is remarkable given its extremely low abundance – there are merely 125 copies of Apj1 in the cell [24]. This low number suggests that this J protein may need to be localized in order to carry out its functions. Indeed, Apj1 has been identified in stringent analyses of the mitochondrial proteome [25, 26]. Apj1 is a class I J protein and it is highly homologous to Ydj1 (35% identity). It is therefore unsurprising that overexpression of Apj1 can rescue loss of Ydj1 in functions such as prion propagation [27]. However, deletion of Apj1 confers two interesting phenotypes: suppressed RNA replication of flock house virus [28] and hypersensitivity to mutant huntingtin (mHtt) [29]. Though the phenotypes identified to date do not point to a clear single function of Apj1, it is evident that this J protein plays roles that cannot be fully compensated for by endogenous levels of other J proteins, perhaps because of its mitochondrial localization.

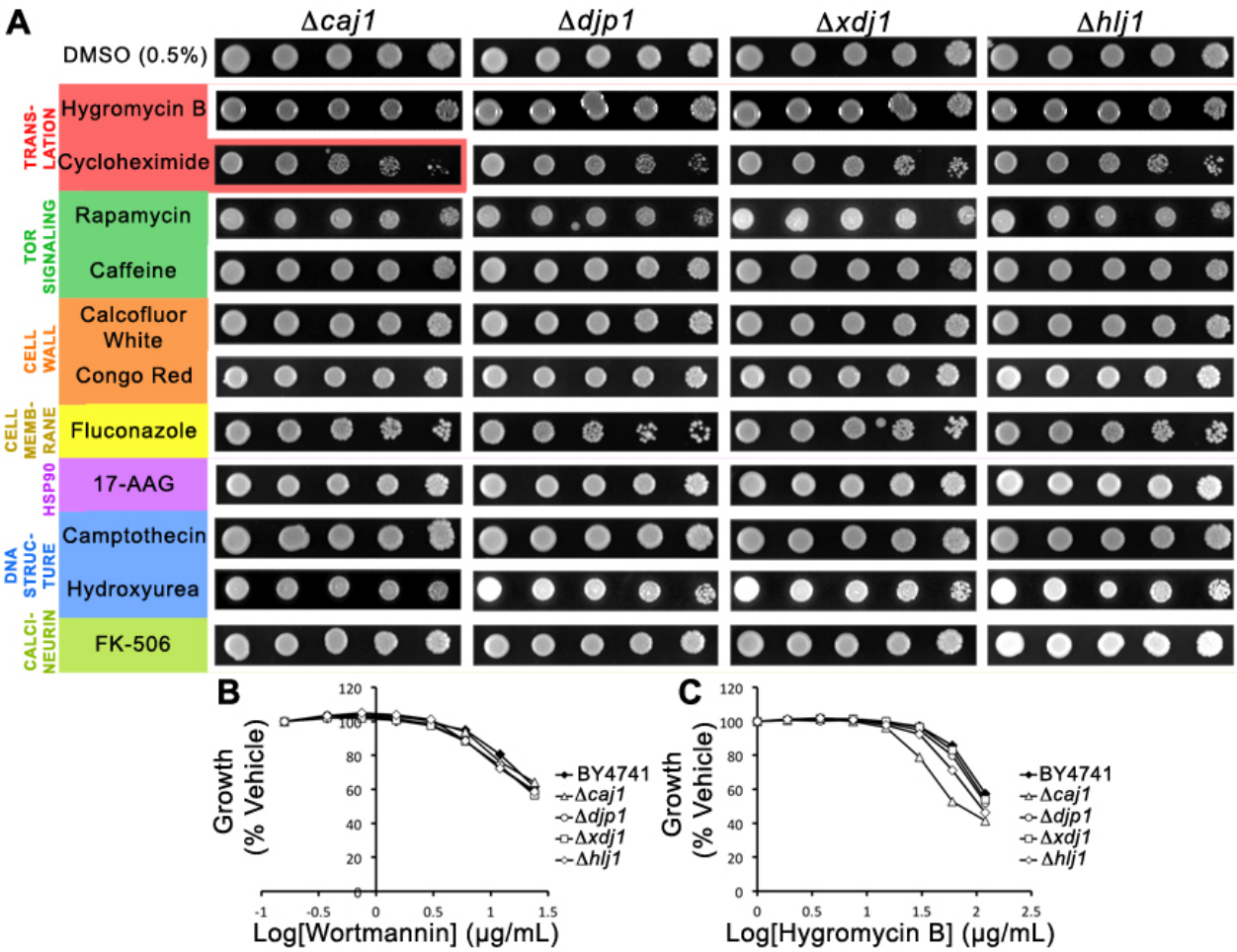

Figure 2.3. J proteins Caj1, Djp1, Xdj1 and Hlj1 have non-essential or redundant roles. A) Five-fold dilutions of *Δcaj1*, *Δdjp1*, *Δxdj1*, or *Δhlj1* were plated on rich medium containing DMSO or compound and grown for 72 hours at 30°C. B,C) Strains were grown in liquid YPD in the presence of (B) wortmannin (24-0 μg/mL) or (C) hygromycin B (120-0 μg/mL) in DMSO (final concentration 2%).

2.3.8 Jjj2

Jjj2 is another low-abundance J protein (182 copies) [24], although no specific sub-cellular localization has been reported. It is a class III protein with no predicted domains other than the J domain. Deletion of Jjj2 conferred sensitivity to cycloheximide and fluconazole (Figure 2.2). These are the only two compounds tested that are exported by the PDR5 transporter, suggesting that Jjj2 may support transporter expression or function, although this idea remains untested.

2.3.9 Caj1

Caj1 is thought to be located in the nucleus [30, 31] but is otherwise uncharacterized. In our synthetic lethal screen, *Δcaj1* cells were largely indistinguishable from wild type, with only mild phenotypes in the presence of cycloheximide in the spot assay and hygromycin B in the liquid assay (Figure 3A, C). A previous large-scale chemical genetic screen also identified Δ*caj1* as sensitive to cycloheximide [8], and together these findings suggest that Caj1 may be involved in transcription.

2.3.10 J proteins with no observed synthetic lethal interactions

These three J proteins exhibited no phenotypes in any of the conditions tested (Figure 3), suggesting that they either have roles in pathways not tested by these twelve compounds or that they are redundant under these conditions. It is known that Djp1 has a role in peroxisomal protein import, and it may be that this J protein is highly specialized for this role and no others [32]. Also, Xdj1 may not be expressed [33].

2.3.11 Hsp70s

J proteins cooperate with Hsp70s to maintain protein quality control. When we treated *Δssa1*, *Δssa2*, or *Δssa4* cells with the twelve chemical inhibitors, no apparent growth defects were observed (data not shown). These studies suggest that the Ssa proteins are redundant under these conditions. In light of this conclusion, the phenotypes resulting from deletion of individual J proteins are striking and highlight their functional diversity.

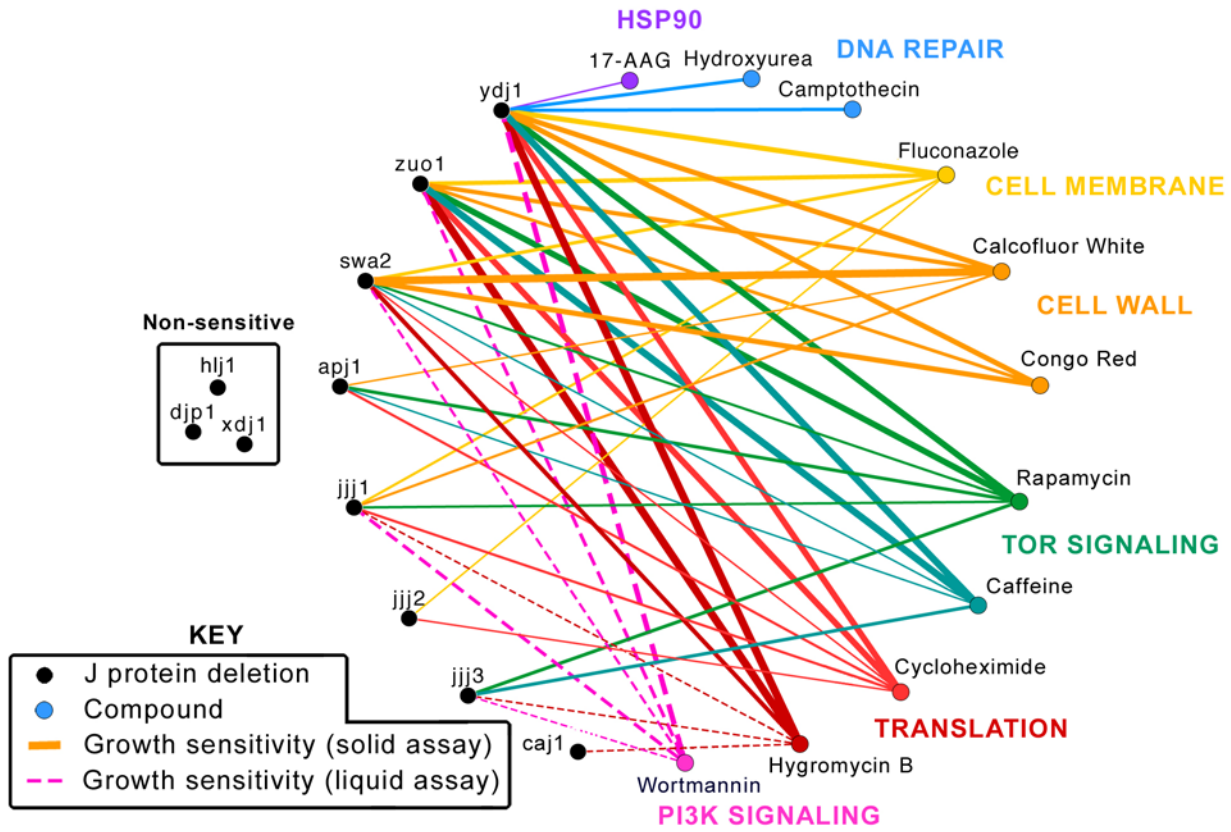

Figure 2.4. Yeast J proteins have widely varied functional roles and importance to cellular health. J proteins (black circles) are connected to compounds (colored circles) with which they exhibited a synthetic lethal interaction. Thickness of lines indicates severity of growth sensitivity phenotype. Solid lines represent interactions identified using the solid media assay and dotted lines represent interactions identified exclusively in the liquid assay.

2.4 Discussion

These results provide additional details to the J protein network (Figure 4). Specifically, some J proteins, such as Ydj1 and Zuo1, have profiles that suggest broad roles in multiple cellular pathways, while others, such as Apj1 and Jjj2, seem to have focused cellular responsibilities. Although the current synthetic lethal analysis is certainly not inclusive of all possible stress conditions, these studies are supportive of a model in which J proteins have evolved to maintain a wide array of cellular processes, allowing Hsp70s to be recruited into many different types of biology.

What do these results reveal about J proteins in disease? One interesting possibility comes from comparing these findings to the results of experiments in which proteotoxic stress (e.g. over-expression of misfolded proteins) was used to evaluate J protein activity. Specifically, Jjj3 over-expression has been shown to suppress the toxicity of polyglutamine-expanded huntingtin (Htt) [34]. This finding has direct relevance to our results because TOR inhibition activates autophagy and clearance of mHtt [35, 36] and we found that *Δjjj3* cells are sensitive to rapamycin. Similarly, we found that Apj1 is sensitive to rapamycin and this J protein is also upregulated in cells expressing mHtt [34]. Thus, pharmacological targeting of individual J proteins or specific Hsp70-J protein combinations [37, 38] may be a compelling approach.

2.5 Experimental Methods

2.5.1 Materials

Compounds were dissolved in dimethylsulfoxide (DMSO, Sigma Aldrich) or weighed out (caffeine and hydroxyurea) and added to yeast peptone-dextrose (YPD, Teknova) rich media plates to the following final concentrations: hygromycin B (InvivoGen, 50 μg/mL), cycloheximide (Sigma Aldrich, 0.25 μg/mL), rapamycin (LC Laboratories, 0.021 μg/mL), caffeine (Sigma Aldrich, 5 mM), calcofluor white (Sigma Aldrich. 20 μg/mL), congo red (Fluka, 20 μg/mL), fluconazole (Santa Cruz, 5 μg/mL), 17-AAG (LC Laboratories, 25 μg/mL), camptothecin (Santa Cruz, 25 μg/mL), hydroxyurea (Santa Cruz, 100 mM), FK-506 (LC Laboratories, 4 μg/mL).

2.5.2 Yeast spot growth assay

Yeast knockout strains were purchased from Open Biosystems (Thermo Scientific) in the BY4741 background (*MAT***a** *his3Δ1 leu2Δ0 met15Δ0 ura3Δ0*). Wild type and knockout strains were grown overnight in 5 mL YPD cultures. Cells were diluted to OD_{600} = 0.5 and 5-fold dilutions made in YPD. A micropipette was used to spot 3 µL of cells onto plates containing DMSO (1%) or compound. Plates were inverted and incubated for 72 hours at 30°C, then imaged.

2.5.3 Yeast liquid growth assay

Compounds were dissolved in DMSO to 50 times the following final concentrations: wortmannin (24 µg/mL), hygromycin B (120 µg/mL), and calcofluor white (200 µg/mL). Two-fold serial dilutions were carried out in 96-well PCR plates (BioExpress), then 2 µL of each solution was transferred to a flat-bottom clear 96-well plate (CytoOne) using a multichannel micropipette. Yeast strains were grown overnight in 5 mL YPD cultures and diluted to OD_{600} = 0.15 in YPD, then 100 µL was added to each well of the plate. Plates were covered and incubated with shaking (200 RPM) at 30°C for 10 hours. OD_{600} values were measured using a microplate reader (Molecular Devices).

Notes

This work was published in full as a journal article: Gillies, A. T.; Taylor, R.; Gestwicki, J.E. "Synthetic lethal interactions in yeast reveal functional roles of J protein co-chaperones," **2012** *Molecular Biosystems*, 8(11), 2901-8. Anne Gillies and Rebecca Taylor carried out the experiments.

2.6 References

[1] Sahi C, Craig EA. Network of general and specialty J protein chaperones of the yeast cytosol. Proc Natl Acad Sci U S A, 2007; 104: 7163-8.

[2] Gall WE, Higginbotham MA, Chen C, Ingram MF, Cyr DM, Graham TR. The auxilin-like phosphoprotein Swa2p is required for clathrin function in yeast. Curr Biol, 2000; 10: 1349-58.

[3] Du Y, Pypaert M, Novick P, Ferro-Novick S. Aux1p/Swa2p is required for cortical endoplasmic reticulum inheritance in Saccharomyces cerevisiae. Mol Biol Cell, 2001; 12: 2614-28.

[4] Liu S, Milne GT, Kuremsky JG, Fink GR, Leppla SH. Identification of the proteins required for biosynthesis of diphthamide, the target of bacterial ADP-ribosylating toxins on translation elongation factor 2. Mol Cell Biol, 2004; 24: 9487-97.

[5] Kampinga HH, Craig EA. The HSP70 chaperone machinery: J proteins as drivers of functional specificity. Nat Rev Mol Cell Biol, 2010; 11: 579-92.

[6] Parsons AB, Brost RL, Ding H, Li Z, Zhang C, Sheikh B, Brown GW, Kane PM, Hughes TR, Boone C. Integration of chemical-genetic and genetic interaction data links bioactive compounds to cellular target pathways. Nat Biotechnol, 2004; 22: 62-9.

[7] Parsons AB, Lopez A, Givoni IE, Williams DE, Gray CA, Porter J, Chua G, Sopko R, Brost RL, Ho CH, Wang J, Ketela T, Brenner C, Brill JA, Fernandez GE, Lorenz TC, Payne GS, Ishihara S, Ohya Y, Andrews B, Hughes TR, Frey BJ, Graham TR, Andersen RJ, Boone C. Exploring the mode-of-action of bioactive compounds by chemical-genetic profiling in yeast. Cell, 2006; 126: 611-25.

[8] Alamgir M, Erukova V, Jessulat M, Azizi A, Golshani A. Chemical-genetic profile analysis of five inhibitory compounds in yeast. BMC Chem Biol, 2010; 10: 6.

[9] Caplan AJ, Douglas MG. Characterization of YDJ1: a yeast homologue of the bacterial dnaJ protein. J Cell Biol, 1991; 114: 609-21.

[10] Becker J, Walter W, Yan W, Craig EA. Functional interaction of cytosolic hsp70 and a DnaJ-related protein, Ydj1p, in protein translocation in vivo. Mol Cell Biol, 1996; 16: 4378-86.

[11] Gautschi M, Lilie H, Funfschilling U, Mun A, Ross S, Lithgow T, Rucknagel P, Rospert S. RAC, a stable ribosome-associated complex in yeast formed by the DnaK-DnaJ homologs Ssz1p and zuotin. Proc Natl Acad Sci U S A, 2001; 98: 3762-7.

[12] Huang P, Gautschi M, Walter W, Rospert S, Craig EA. The Hsp70 Ssz1 modulates the function of the ribosome-associated J-protein Zuo1. Nat Struct Mol Biol, 2005; 12: 497-504.

[13] Albanese V, Reissmann S, Frydman J. A ribosome-anchored chaperone network that facilitates eukaryotic ribosome biogenesis. J Cell Biol, 2010; 189: 69-81.

[14] Eisenman HC, Craig EA. Activation of pleiotropic drug resistance by the J-protein and Hsp70-related proteins, Zuo1 and Ssz1. Mol Microbiol, 2004; 53: 335-44.

[15] Prunuske AJ, Waltner JK, Kuhn P, Gu B, Craig EA. Role for the molecular chaperones Zuo1 and Ssz1 in quorum sensing via activation of the transcription factor Pdr1. Proc Natl Acad Sci U S A, 2012; 109: 472-7.

[16] Xiao J, Kim LS, Graham TR. Dissection of Swa2p/Auxilin Domain Requirements for Cochaperoning Hsp70 Clathrin-uncoating Activity In Vivo. Molecular Biology of the Cell, 2006; 17: 3281-3290.
[17] Garcia R, Bermejo C, Grau C, Perez R, Rodriguez-Pena JM, Francois J, Nombela C, Arroyo J. The global transcriptional response to transient cell wall damage in Saccharomyces cerevisiae and its regulation by the cell integrity signaling pathway. J Biol Chem, 2004; 279: 15183-95.
[18] Kuranda K, Leberre V, Sokol S, Palamarczyk G, Francois J. Investigating the caffeine effects in the yeast Saccharomyces cerevisiae brings new insights into the connection between TOR, PKC and Ras/cAMP signalling pathways. Mol Microbiol, 2006; 61: 1147-66.
[19] Meyer AE, Hung NJ, Yang P, Johnson AW, Craig EA. The specialized cytosolic J-protein, Jjj1, functions in 60S ribosomal subunit biogenesis. Proc Natl Acad Sci U S A, 2007; 104: 1558-63.
[20] Meyer AE, Hoover LA, Craig EA. The cytosolic J-protein, Jjj1, and Rei1 function in the removal of the pre-60 S subunit factor Arx1. J Biol Chem, 2010; 285: 961-8.
[21] Thakur A, Chitoor B, Goswami AV, Pareek G, Atreya HS, D'Silva P. Structure and Mechanistic Insights into Novel Iron-mediated Moonlighting Functions of Human J-protein Cochaperone, Dph4. J Biol Chem, 2012; 287: 13194-205.
[22] Webb TR, Cross SH, McKie L, Edgar R, Vizor L, Harrison J, Peters J, Jackson IJ. Diphthamide modification of eEF2 requires a J-domain protein and is essential for normal development. J Cell Sci, 2008; 121: 3140-5.
[23] Fasolo J, Sboner A, Sun MG, Yu H, Chen R, Sharon D, Kim PM, Gerstein M, Snyder M. Diverse protein kinase interactions identified by protein microarrays reveal novel connections between cellular processes. Genes Dev, 2011; 25: 767-78.
[24] Ghaemmaghami S, Huh WK, Bower K, Howson RW, Belle A, Dephoure N, O'Shea EK, Weissman JS. Global analysis of protein expression in yeast. Nature, 2003; 425: 737-41.
[25] Reinders J, Zahedi RP, Pfanner N, Meisinger C, Sickmann A. Toward the complete yeast mitochondrial proteome: multidimensional separation techniques for mitochondrial proteomics. J Proteome Res, 2006; 5: 1543-54.
[26] Sickmann A, Reinders J, Wagner Y, Joppich C, Zahedi R, Meyer HE, Schonfisch B, Perschil I, Chacinska A, Guiard B, Rehling P, Pfanner N, Meisinger C. The proteome of Saccharomyces cerevisiae mitochondria. Proc Natl Acad Sci U S A, 2003; 100: 13207-12.
[27] Hines JK, Li X, Du Z, Higurashi T, Li L, Craig EA. [SWI], the prion formed by the chromatin remodeling factor Swi1, is highly sensitive to alterations in Hsp70 chaperone system activity. PLoS Genet, 2011; 7: e1001309.
[28] Weeks SA, Shield WP, Sahi C, Craig EA, Rospert S, Miller DJ. A targeted analysis of cellular chaperones reveals contrasting roles for heat shock protein 70 in flock house virus RNA replication. J Virol, 2010; 84: 330-9.
[29] Willingham S, Outeiro TF, DeVit MJ, Lindquist SL, Muchowski PJ. Yeast genes that enhance the toxicity of a mutant huntingtin fragment or alpha-synuclein. Science, 2003; 302: 1769-72.

[30] Mukai H, Shuntoh H, Chang CD, Asami M, Ueno M, Suzuki K, Kuno T. Isolation and characterization of CAJ1, a novel yeast homolog of dnaJ. Gene, 1994; 145: 125-7.
[31] Walsh P, Bursac D, Law YC, Cyr D, Lithgow T. The J-protein family: modulating protein assembly, disassembly and translocation. EMBO Rep, 2004; 5: 567-71.
[32] Hettema EH, Ruigrok CC, Koerkamp MG, van den Berg M, Tabak HF, Distel B, Braakman I. The cytosolic DnaJ-like protein djp1p is involved specifically in peroxisomal protein import. J Cell Biol, 1998; 142: 421-34.
[33] Schwarz E, Westermann B, Caplan AJ, Ludwig G, Neupert W. XDJ1, a gene encoding a novel non-essential DnaJ homologue from Saccharomyces cerevisiae. Gene, 1994; 145: 121-4.
[34] Tauber E, Miller-Fleming L, Mason RP, Kwan W, Clapp J, Butler NJ, Outeiro TF, Muchowski PJ, Giorgini F. Functional gene expression profiling in yeast implicates translational dysfunction in mutant huntingtin toxicity. J Biol Chem, 2011; 286: 410-9.
[35] Hyrskyluoto A, Reijonen S, Kivinen J, Lindholm D, Korhonen L. GADD34 mediates cytoprotective autophagy in mutant huntingtin expressing cells via the mTOR pathway. Exp Cell Res, 2012; 318: 33-42.
[36] Roscic A, Baldo B, Crochemore C, Marcellin D, Paganetti P. Induction of autophagy with catalytic mTOR inhibitors reduces huntingtin aggregates in a neuronal cell model. J Neurochem, 2011; 119: 398-407.
[37] Evans CG, Chang L, Gestwicki JE. Heat shock protein 70 (hsp70) as an emerging drug target. J Med Chem, 2010; 53: 4585-602.
[38] Patury S, Miyata Y, Gestwicki JE. Pharmacological targeting of the Hsp70 chaperone. Curr Top Med Chem, 2009; 9: 1337-51.

Chapter 3

Peptide Microarrays Map the Binding Sites of Chaperones on Luciferase and Tau

3.1 Abstract

Molecular chaperones interact with unfolded proteins and promote a variety of outcomes, including folding, proteasomal degradation and autophagy. The mechanisms by which chaperones work together to carry out these functions are poorly understood. Current models suggest that the "choice" of chaperones and co-chaperones that bind the protein might dictate the outcomes, as discussed in Chapter 1. In this chapter, we used peptide microarrays to investigate the binding of purified chaperones to peptides derived from two substrates, firefly luciferase and microtubule associated protein tau (MAPT/tau). We found that the J proteins DNAJA2 and DNAJA1 have similar binding sites on luciferase, but that Hsc70 stimulated binding of DNAJA2 (not DNAJA1) to one of these sites. These results could help explain why DNAJA2 is capable of assisting Hsc70 in refolding luciferase, while DNAJA1 is not. To understand how a broader collection of chaperones might converge on a protein, we also mapped the binding of 17 chaperones to peptides derived from tau. We found that many chaperones, including Hsc70, Hsp72 and Hsp90, bind to "hotspots" on tau and that pro-stabilizing and pro-degradation chaperones share similar binding sites. These results provide new models for how competition between chaperones might play an important role in regulating tau homeostasis.

3.2 Introduction

Members of the Hsp70 and Hsp90 families of chaperones and some of their associated co-chaperones bind directly to protein substrates (see Chapter 1). It is unknown how Hsp70s, Hsp90s and their co-chaperones come together on a single substrate – do they compete for the same binding sites? Do they bind simultaneously? How many binding sites for chaperones are present within a single, unfolded substrate? How do the locations and types of these physical interactions promote outcomes such as folding or targeting for degradation? In order to develop models for how these complexes form and how they cooperate during protein triage, we hypothesize that it will be necessary to understand the binding sites for chaperones on protein substrates. In this Chapter, we map the binding of chaperones and co-chaperones to peptides derived from two well-characterized substrates of the Hsp70 system: luciferase and tau.

3.2.1 Luciferase is a model substrate for Hsp70 chaperone system

Firefly luciferase has been used extensively to study chaperone function. Denatured luciferase is only weakly able to fold in the absence of chaperones and refolded luciferase can be conveniently measured by luminescence. Chaperone systems composed of a purified Hsp70, a J-protein and a nucleotide exchange factor (NEF), will refold denatured luciferase in the presence of ATP [1-3]. This model system has been used to explore the mechanisms of chaperone cooperation, especially the role of the J protein co-chaperones. For example, refolding is successful when denatured luciferase is incubated with the J protein and Hsc70 added later, but not vice versa, suggesting that the J protein can bind and stabilize the unfolded substrate in the absence of Hsc70 [4]. J protein-luciferase interactions are in fact

necessary for productive luciferase refolding, as J domain-mediated stimulation of Hsp70 ATPase activity is insufficient to catalyze folding [5]. However, not all J proteins are equally capable of supporting luciferase refolding. Ydj1 (yeast DNAJA1) is twice as competent in this system as Sis1 (yeast DNAJB1) [6, 7], which might be because Sis1 lacks the ZFLR domain (Figure 1.3B) [7]. In fact, point mutants in the two zinc-binding domains in the Ydj1 ZFLR nearly abolish luciferase refolding [8] and crosslinking experiments identified direct interactions between the ZFLR of DnaJ (*E. coli* DNAJA1) and luciferase [5]. These studies on luciferase suggest that J proteins interact directly with substrates using contacts in multiple domains, including the ZFLR and CTDI (Figure 1.3B).

Additional studies using denatured luciferase have suggested that J protein domain structure is not the only determinant of luciferase refolding ability. For example, human DNAJA2, but not its close homolog, DNAJA1, can efficiently support luciferase refolding *in vitro* [9, 10] and in cells [11]. The ZFLR domains of these J proteins are 57% identical and the CTDs are 55% identical, so modest sequence differences might be sufficient to specialize these co-chaperones for interactions with different substrates. We explored this question using genetics in Chapter 2. However, a deeper understanding of the molecular details of chaperone binding to luciferase would provide important insights into the mechanism of chaperone-mediated refolding.

3.2.2 Tau aggregation is a hallmark of Alzheimer's disease

Tau is a natively unfolded protein that forms aggregates characteristic of a class of neurodegenerative diseases called tauopathies, including Alzheimer's disease (AD),

frontotemporal dementia (FTD), progressive supranuclear palsy (PSP), and Pick's disease (PD) [12-14]. Tau belongs to a class of microtubule-associated proteins (MAPs) and in healthy cells functions to facilitate microtubule assembly and regulate microtubule dynamics [15-17]. Though normal tau has only transient secondary structure and is highly soluble, it is able to undergo a structural conversion into rigid, ordered amyloid fibrils, termed paired helical filaments (PHFs) [18-22]. This conversion is thought to be one of the major pathological events of AD and other tauopathies, as the accumulation of intracellular tau deposits (neurofibrillary tangles, NFTs) correlates with cognitive decline and neuron loss [23-25]. The other major feature of AD, plagues composed of another protein called amyloid-β (Aβ), has long been thought to be the primary underlying cause of AD, partly due to the identification of disease-linked mutations in amyloid precursor protein (APP), which is cleaved to release Aβ [26, 27]. However, recent evidence has shown that tau plays an equally important role in AD pathology and that Aβ toxicity is actually dependent on tau [28-31]. Furthermore, identification of over 40 mutations in the tau gene in cases of FTD, collectively termed frontotemporal dementia and Parkinsonism linked to chromosome-17 (FTDP-17), demonstrates that tau can be a direct cause of neurodegeneration [32-34].

Despite extensive research, the mechanism of tau toxicity is not well understood. Toxicity likely arises from a combination of loss of normal function and gain of pathological function upon formation of tau aggregates [35]. As pre-formed tau PHFs are not inherently neurotoxic, and may indeed constitute a mechanism by which the cell tries to protect itself, it appears that an intermediate stage of aggregation (e.g. tau oligomers) may constitute the toxic species [36]. In healthy neurons, tau is tightly regulated by a host of post-translational

modifications, including phosphorylation, nitration, ubiquitination, and others. Hyperphosphorylation is one of the most striking characteristics of tauopathies, suggesting that tau becomes dangerously disregulated [37, 38]. Approximately 45 phosphorylated residues have been identified in tau PHFs, including Ser, Thr, and Tyr residues. Many kinases are candidates for tau phosphorylation, including proline-directed (SP/TP) kinases such as glycogen synthase kinase-3 (GSK3), KXGS-motif recognizing kinases like microtubule affinity-regulating kinase (MARK), and non-receptor tyrosine kinases (Fyn, c-Abl) [37]. Hyperphosphorylation reduces the affinity of tau for microtubules and increases its propensity to aggregate into PHFs [39]. Another outcome of the disregulation of tau is that it is mislocalized in tauopathies, moving from the axon into the somatodendritic compartment and perhaps leading to excitotoxicity through activation of Fyn, a non-receptor tyrosine kinase linked to Aβ toxicity that can also phosphorylate tau [31, 40]. In tauopathies, tau also undergoes a host of truncations by caspases and other proteases that seem to enhance its toxicity [41, 42].

In the adult brain, tau is expressed as six isoforms resulting from the alternative splicing of three exons. Two inserts of unknown function near the N-terminus give rise to three different variants (0N, 1N, 2N), and the presence or absence of the second of four imperfect repeats in the C-terminal repeat domain gives rise to two further variants (3R and 4R) (Figure 3.1). The repeat domain is also called the microtubule-binding region (MTBR) as it governs the interaction of tau with microtubules, though other parts of tau appear to be important for regulating this interaction as well. Another distinct region of tau is called the proline-rich domain, immediately upstream of the repeat domain. The most abundant

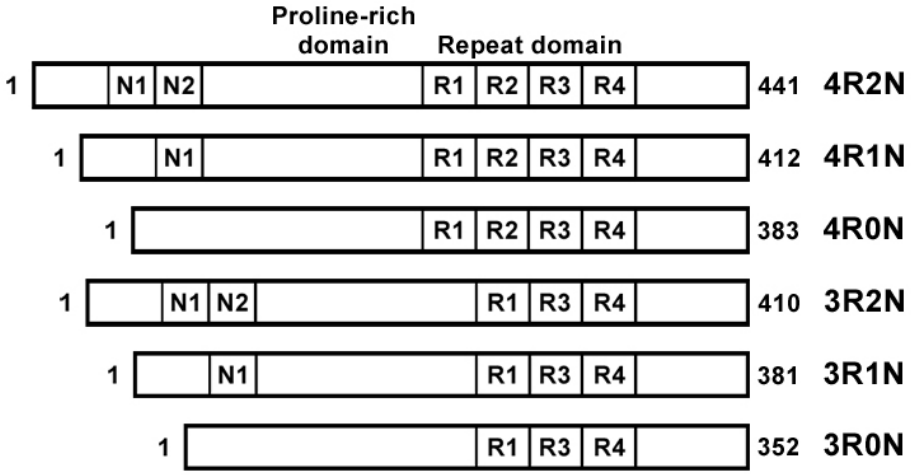

Figure 3.1. Tau domains and isoforms. Tau is expressed as six isoforms resulting from alternative splicing of two N-terminal inserts (N1, exon 2; N2, exon 3) and one of four imperfect repeats (R2, exon 10).

isoform of tau in the brain is 4R2N (also known as hTau40) and thus most biochemical studies have been carried out on this isoform, a 441 residue, 40 kDa protein. Despite the presence of these clear domains, the regulation and functions of tau cannot be easily pinned down to specific regions of the protein. For example, post-translational modifications and intermolecular interactions occur at residues throughout the entirety of the tau molecule, with different modifications and interactions often competing for similar sites [37, 43]. This complexity is the basis of our difficulty in understanding the fundamental biology of tau and its pathological mechanisms.

3.2.3 Chaperones regulate normal tau and play a role in tauopathies

Tau provides a medically important model substrate for understanding chaperone functions. Hsc70 and Hsp90, along with many of their co-chaperones, directly interact with tau and regulate its functions and homeostasis [44-46]. Hsp72 and Hsp90 work together with the E3 ligase CHIP to target tau for proteasomal degradation (see Chapter 1), while other co-chaperones favor re-binding of free tau to microtubules [47-49]. Over-expression of different

members of the J protein, NEF and FK506-binding protein (FKBP) classes of co-chaperones have distinct effects on tau stability [46, 50]. Further, the small heat shock protein, Hsp27, reduces tau pathology [51]. Together, these observations suggest that interplay between chaperones and co-chaperones regulates the normal and disease-associated functions of tau, including its turnover, aggregation and association with microtubules. In tauopathies, this quality control system appears to be dysfunctional or insufficient. An understanding of individual chaperone interactions with tau would provide critical insight into the regulation of this system and, perhaps, provide new opportunities for drug discovery

The binding of chaperones to tau has been explored in a number of recent studies. Sarkar and coworkers used a truncation approach to identify two binding sites for Hsc70 and Hsp72 on tau: ^{275}VQIINKK^{281} and ^{306}VQIVYK^{311}, located in R2 and R3 respectively [52]. These hexapeptides are very interesting because they comprise the backbone of the amyloid fibril structure at the core of PHFs (see Chapter 4) [53, 54]. This region is also involved in binding to microtubules [55], suggesting that binding of tau to either microtubules or Hsp70s might limit its aggregation into PHFs. However, mutations in the two chaperone-mediated autophagy (CMA) targeting motifs in R4 also abolish binding of tau by Hsc70, suggesting that tau-Hsc70 interactions are more complex [56]. Our group recently reported that Hsp72 and Hsp90 compete for tau binding through shared binding sites, but that unique Hsp72 binding sites allow it to outcompete Hsp90 *in vitro*, suggesting that varied expression levels of these chaperones may play a role in tau metabolism [48]. Further, we also recently showed that Hsc70 and Hsp72 have different effects on tau stability in cells, despite shared binding sites measured by NMR [57].

In this chapter, we explore the binding of chaperones to luciferase and tau using peptide microarrays. In these studies, we were interested in exploring how different classes of chaperones might cooperate or compete for binding to these proteins. By understanding how chaperones and co-chaperones converge on these proteins, we might provide insight into the logic and mechanisms of protein quality control.

3.2.4 Studying protein-protein interactions with peptide microarrays

Peptide microarrays were developed to study interactions of proteins with peptides in a high density format [58]. In this method, peptides are immobilized on a cellulose membrane or a glass slide and bound protein is detected using HRP-conjugated or fluorescent antibodies. In the glass slide format, binding is qualitatively determined by the amount of fluorescence at each peptide, similar to the commonly used DNA microarrays. Rüdiger and co-workers have used this method to study binding of DnaK (bacterial Hsc70) and DnaJ (bacterial DNAJA1) to luciferase and other substrates [59, 60]. Peptide arrays were also used to determined sites of DnaJ and DnaK interaction with the σ^{32} subunit of RNA polymerase [61] and the binding sites of human DNAJA1 and Hsc70 on luciferase [62].

In this chapter, we used peptide microarrays to explore how chaperones interact with luciferase and tau. In the case of luciferase, we were particularly interested in why DNAJA1 and DNAJA2 might differ in their ability to refold luciferase and we hypothesized that these co-chaperones might differ in their recruitment of Hsc70. We found that Hsc70, DNAJA1, and DNAJA2 have similar binding sites on luciferase, but that Hsc70 stimulates binding of DNAJA2, but not DNAJA1, to a specific region of luciferase (413-439).

We also explored binding of 17 different chaperones and co-chaperones to tau. These studies provided the first comprehensive map of chaperone binding to a protein substrate and yielded a complex map of interactions. Broadly, we found that chaperones tended to bind "hotspots" on the N-terminus, proline-rich and repeat domains of tau. We discuss the implications of these interactions on the function and homeostasis of tau and new models of chaperone cooperation are proposed.

3.3 Results

3.3.1 Luciferase peptide microarray design

In order to identify the binding sites of Hsc70, DNAJA1, and DNAJA2 on luciferase, we designed a peptide microarray that scans the sequence of luciferase. The array consists of 15 amino acid (AA) peptides with 4 AA steps along the sequence for a total of 135 peptides (Appendix 3.1). This degree of overlap was chosen to strike a balance between binding site coverage and the number of peptides to be synthesized. Each microarray printed on a glass microscrope slide consists of the peptide library printed in triplicate.

The arrays were incubated with chaperones bearing a polyhistidine (His6x) tag. Bound chaperones were then detected with a fluorescently labeled anti-His6x antibody (see the Methods section for details). Fluorescence was detected using a GenePix 4100A microarray scanner and background-corrected intensity values were generated for each spot. The three signals for each peptide on the array were averaged and these values were used to identify "binders" and compare binding sites between chaperones.

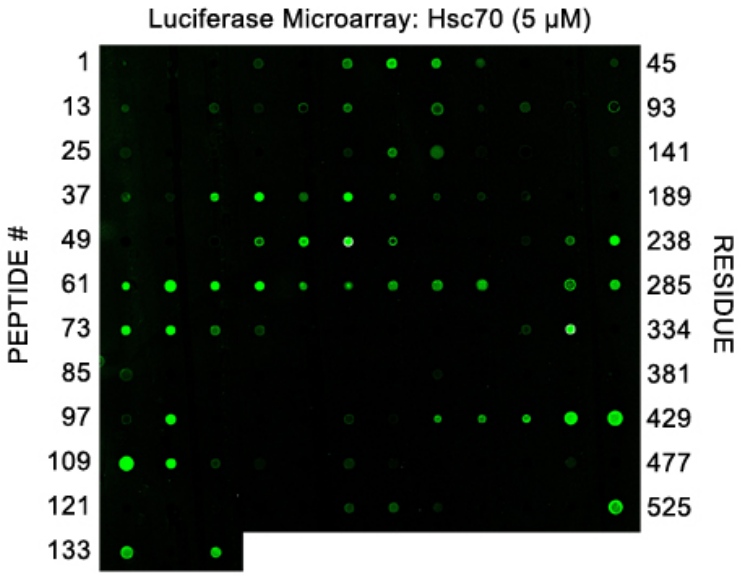

Figure 3.2. Example of raw luciferase peptide microarray data. Peptides derived from the primary sequence of luciferase (15 AA, 4 AA steps) were covalently immobilized on a glass slide. Peptide numbers are indicated on the left and N-terminal residues of the peptides are indicated on the right. The array was incubated with His6x-tagged chaperone (in this case Hsc70, 5 μM) then fluorescently labeled (HiLyte555) anti-His6x antibody (1:1000). Array was scanned using a GenePix 4100a Microarray Scanner.

3.3.2 Chaperones bind to several long continuous regions on luciferase

On our luciferase arrays, all of the chaperones and chaperone mixtures tested exhibited qualitatively similar binding patterns. These consisted of long series of consecutive peptides with bright signal interspersed with stretches of little to no signal (Figure 3.2). The length of these stretches (4 to 12 peptides) and the 4 AA steps between peptides means that no amino acids are shared among all of the peptides in a stretch of binding. Therefore, they cannot point to a minimal binding site. However, the gradual increase and decrease of fluorescence intensity in these regions suggests that the central peptides may contain the most important residues. In general, our data suggests that Hsc70 and J proteins interact with larger regions of luciferase than the 7-13 AA peptide substrates usually discussed for these chaperones and, further, that these binding sites are not limited to hydrophobic AAs [63, 64]. This finding

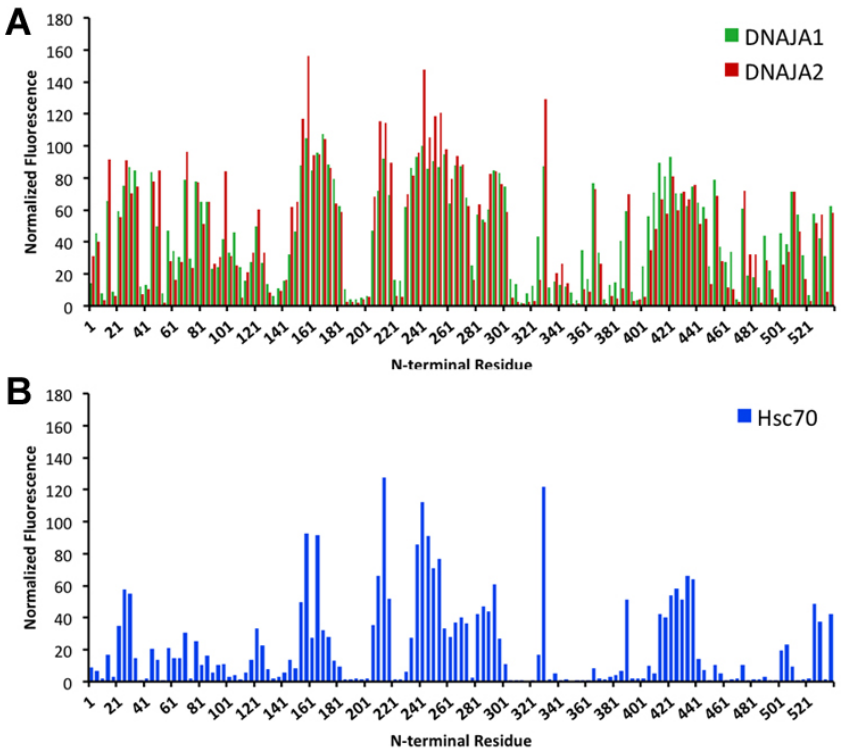

Figure 3.3. Binding of Class A J proteins and Hsc70 to luciferase peptide microarray. Normalized fluorescence values of representative binding experiments for DNAJA1, DNAJA2, and Hsc70 on the peptide microarrays are shown. Values are averages of three replicates on one array; error bars ommitted for clarity. (A) DNAJA1 and DNAJA2 have nearly identical binding patterns. (B) Hsc70 has a similar binding pattern to the J proteins, with some differences in relative intensities.

could suggest either that multiple chaperones bind together on denatured luciferase or that a single chaperone has a more complicated interaction with substrate than previously thought.

3.3.3 DNAJA1 and DNAJA2 have nearly identical binding sites on luciferase

We found that DNAJA1 and DNAJA2 had nearly identical binding patterns, both in peptide identity and relative intensity (Figure 3.3A). Thus, the functional differences between these co-chaperones are not due to their ability to bind to distinct sites. Interestingly, our studies using glass slides revealed additional binding sites for DNAJA1

beyond those originally identified using cellulose arrays [62]. Both studies identified strong luciferase binding sites at 259-280 and 415-436 (Figure 3.3A).

The binding pattern of Hsc70 was similar to those of the J proteins (Figure 3.3B), suggesting that these interactions may be competitive. The relative intensity of many Hsc70 binding sites tended to be reduced compared to the J protein signals, suggesting that its affinity may be weaker [65]. There were some sites unique to the J proteins, i.e. near the N- and C-termini, but the lack of continuous series of sites suggests that these sites may be false positives. The five binding sites previously identified for Hsc70 [62] (19-37, 67-82, 208-223, 433-451, and 523-538) were confirmed by our data with the exception of 67-82, though this region was bound by DNAJA1 and DNAJA2. In summary, our data confirms previously identified binding sites and identifies a number of novel interactions.

3.3.4 Hsp70 influences the binding of DNAJA2 but not DNAJA1 to luciferase

We envisioned that peptide arrays could be a good platform for understanding how chaperones converge on peptide substrates. For luciferase, we were specifically interested in whether Hsc70 might impact the binding of DNAJA1 or DNAJA2. To test this idea, we co-incubated the J proteins with untagged Hsp70 in the presence of ATP or ADP. We repeated each experiment in duplicate and compared all possible pairs. We then evaluated the statistical significance of the changes using CyberT [66, 67]. These studies revealed that Hsp70 stimulated binding of DNAJA2 to a series of four peptides comprising residues 413-439 ($p < 0.05$), while DNAJA1 was unaffected (Figure 3.4). This effect was not dependent on nucleotide (data not shown). We conclude that Hsc70 promotes the binding of DNAJA2

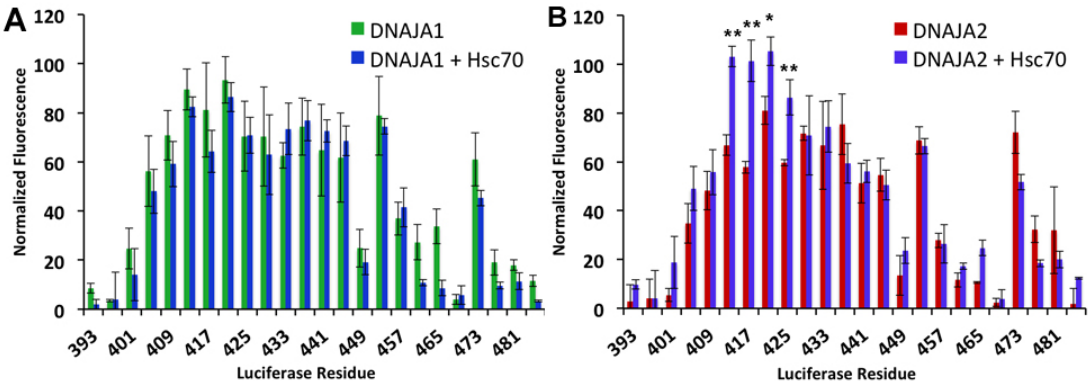

Figure 3.4. Hsc70 stimulates DNAJA2, but not DNAJA1, binding to residues 413-439 of luciferase. His6x-tagged DNAJA1 (A) or DNAJA2 (B) was incubated alone or with untagged Hsc70 on the luciferase microarray. Normalized fluorescence values are shown for each J protein with and without Hsc70. Values are averages of three replicates on an array; error bars represent the SD. Only peptides 393-485 are shown for clarity. Statistical analysis was performed with CyberT. (* $p < 0.05$, ** $p < 0.01$)

to residues 413-439 in luciferase, and DNAJA2 binding may play a particularly important role in productive luciferase refolding. When the binding sites were mapped onto a surface of folded luciferase, we found that most of the sites bound by DNAJA2 (green) are on surface exposed α-helices, but residues 413-439 comprise two strands of a β-sheet located at the interface between the two domains of luciferase (Figure 3.5). Thus, it is possible that Hsc70-promoted DNAJA2 binding to this region facilitates inter-domain folding or limits inter-domain aggregation.

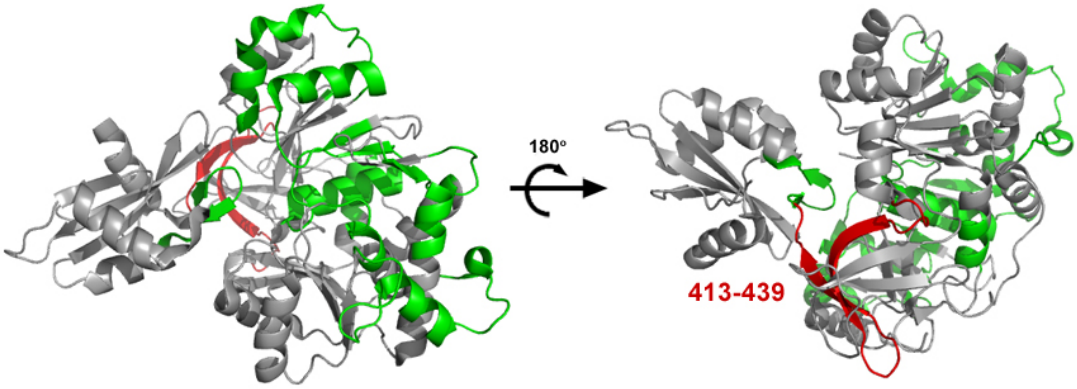

Figure 3.5. DNAJA2 binding sites on luciferase. The structure of luciferase is shown with the regions bound by DNAJA2 highlighted in green (unaffected by Hsc70) and red (increased by Hsc70). PDB ID 4G37

3.3.5 Properties of luciferase peptides bound by Hsc70 and J proteins

Next, we examined the physicochemical properties of the peptides bound by DNAJA1, DNAJA2 and Hsc70. In these studies, we examined the correlation of raw fluorescence with eight properties of the array peptides: aliphatic index [68], hydrophobicity (GRAVY score [69]), average molecular weight of amino acids, number of aromatic residues (Tyr, Phe, Trp), calculated isoelectric point (pI) [70], net charge at pH 7.2, number of basic residues (Arg, Lys), and number of acidic residues (Glu, Asp). Surprisingly, no correlation was observed with peptide hydrophobicity (Table 3.1). Instead, the strongest preference for all three chaperones was to bind bulky and aromatic residues. Additionally, a slight preference against aliphatic peptides was observed. While DNAJA1 and DNAJA2 did not exhibit any correlation with overall charge or charged residues, Hsc70 showed a slight preference for higher pI values, positive charge at pH 7.2, and against acidic residues. These results challenge the limited characterization of Hsc70 binding sites as comprising a hydrophobic core flanked by basic residues [63]. Our results suggest that

	DjA1		DjA2		Hsc70	
	Corr	R^2	*Corr*	R^2	*Corr*	R^2
Aliphatic index	**-**	**0.05**	**-**	**0.04**	**-**	**0.05**
GRAVY		0.0002		0.01		0.003
Avg AA MW	**+**	**0.28**	**+**	**0.24**	**+**	**0.20**
n Aromatics	**+**	**0.51**	**+**	**0.48**	**+**	**0.36**
Calc pI		0.001		0.005	**+**	**0.10**
Charge at pH 7.2		0.007		0.0001	**+**	**0.06**
n(R+K)		0.007		0.007		0.01
n(D+E)		0.002		0.01	**-**	**0.07**

Table 3.1. Properties of luciferase peptides bound by chaperones. Fluorescence values were plotted against 8 peptide properties and fit by linear regression. DNAJA1, DNAJA2, and Hsc70 had positive correlations with average AA molecular weight and number of aromatic residues and negative correlations with aliphatic index. Additionally, Hsc70 correlated positively with calculated pI and charge at physiological pH, negatively with number of acidic residues. No correlation was observed with hydrophobicity (GRAVY).

hydrophobicity has minimal predictive value for Hsc70 and J protein binding, while side chain bulk and aromaticity are positively correlated, at least in the case of firefly luciferase.

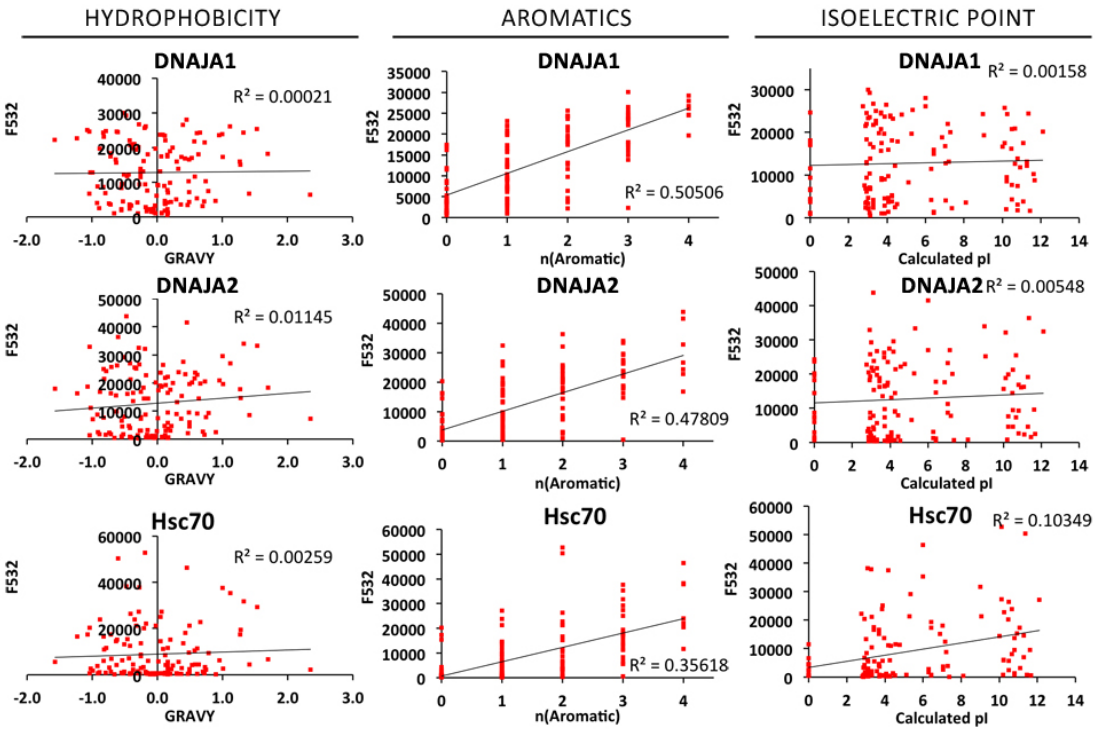

Figure 3.6. Correlation of microarray fluorescence values with luciferase peptide properties. The raw fluorescence values of DNAJA1, DNAJA2, and Hsc70 binding to the luciferase peptide microarrays were plotted against properties of the peptides. Linear regressions and R^2 values are shown on each plot. No correlation was observed with GRAVY scores (hydrophobicity), but all three chaperones preferred aromatic residues. Hsc70 showed a slight preference for higher pI values.

3.3.6 Design of tau microarrays

In order to determine the binding sites of chaperones on tau, another microarray was designed with the same principles as used in the creation of the luciferase array: 15 AA peptides with 4 AA steps for a total of 187 tau peptides (Appendix 3.2). Additionally, 7 phosphomimetic peptides were designed incorporating a glutamic acid (or two) in place of Ser/Thr residues whose phosphorylation is known to impact chaperone interactions with tau (Table 3.2). The tau array encompasses peptides from the longest isoform of tau, which is only expressed in the peripheral nervous system (PNS) (758 AA). For this chapter, we

Name	Sequence	Phospho site	Unphos. Pep ID
P1	GYSSPGEPGEPGSRS	S202/T205	196
P2	GYSSPGEPGTPGSRS	S202	196
P3	PGSPGEPGSRSRTPS	T205	200
P4	VKSKIGETENLKHQP	S262	256
P5	DRVQSKIGELDNITH	S356	348
P6	HGAEIVYKEPVVSGD	S396	388
P7	SPVVSGDTEPRHLSN	S404	396

Table 3.2. Phosphomimetic peptides on tau array. Seven peptides were designed with the residues marked in green mutated to Glu to mimic Ser/Thr phosphorylation. These peptides are named P1-P7 (left column). Corresponding unphosphorylated peptides are indicated in the fourth column.

focus on the results from the 4R2N isoform (441 AA), which is most implicated in tauopathies.

As in the luciferase arrays, His-tagged chaperones were incubated with the tau arrays and fluorescence images acquired. Two sample array images are shown in Figure 3.7 to provide a visual comparison of the results obtained from two representative chaperones: DNAJA1 and Hsp27. As a control, the array was incubated with a fluorescent anti-His6x antibody alone and positive labeling was excluded from future analyses (red squares in Figure 3.7). Peptides that are derived from the PNS isoform are denoted by the orange region in Figure 3.7.

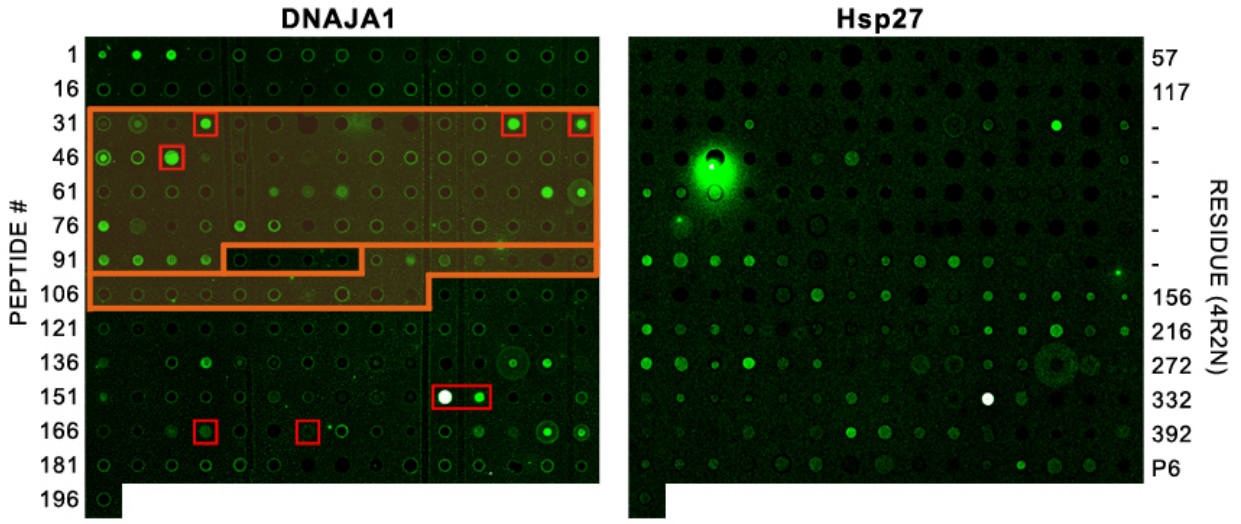

Figure 3.7. Tau peptide microarray raw images. Single arrays (one of three on a slide) from two different experiments (DNAJA1 and Hsp27) are shown. Slides were incubated with His6x-tagged DNAJA1 (3 μM) or Hsp27 (10 μM) followed by HiLyte555-labeled anti-His6x antibody and scanned at 532 nm with 5 μm resolution. On the left array, false positives (determined by binding to antibody alone) are marked with red squares. Peptides corresponding to PNS tau only are boxed and shaded in orange. Peptide numbers for the full array are marked on the left; on the right, N-terminal residues of 4R2N-only peptides are identified.

3.3.7 Map of chaperone binding sites on tau

Using the tau peptide microarrays, we have mapped the binding of 17 chaperones (Figure 3.8). These results provide an unprecedented examination of the binding of chaperones to a single protein substrate and a number of initial observations are striking.

First, the binding sites on tau were relatively short and most were only composed of three to four consecutive peptides. Thus, the "footprints" of chaperone interactions with tau were smaller and more localized than the binding sites on luciferase. This difference might arise from the fact that tau is an intrinsically disordered, highly soluble protein that does not have a globular core. Thus, unlike luciferase, it does not require broad chaperone binding in the unfolded state to prevent aggregation.

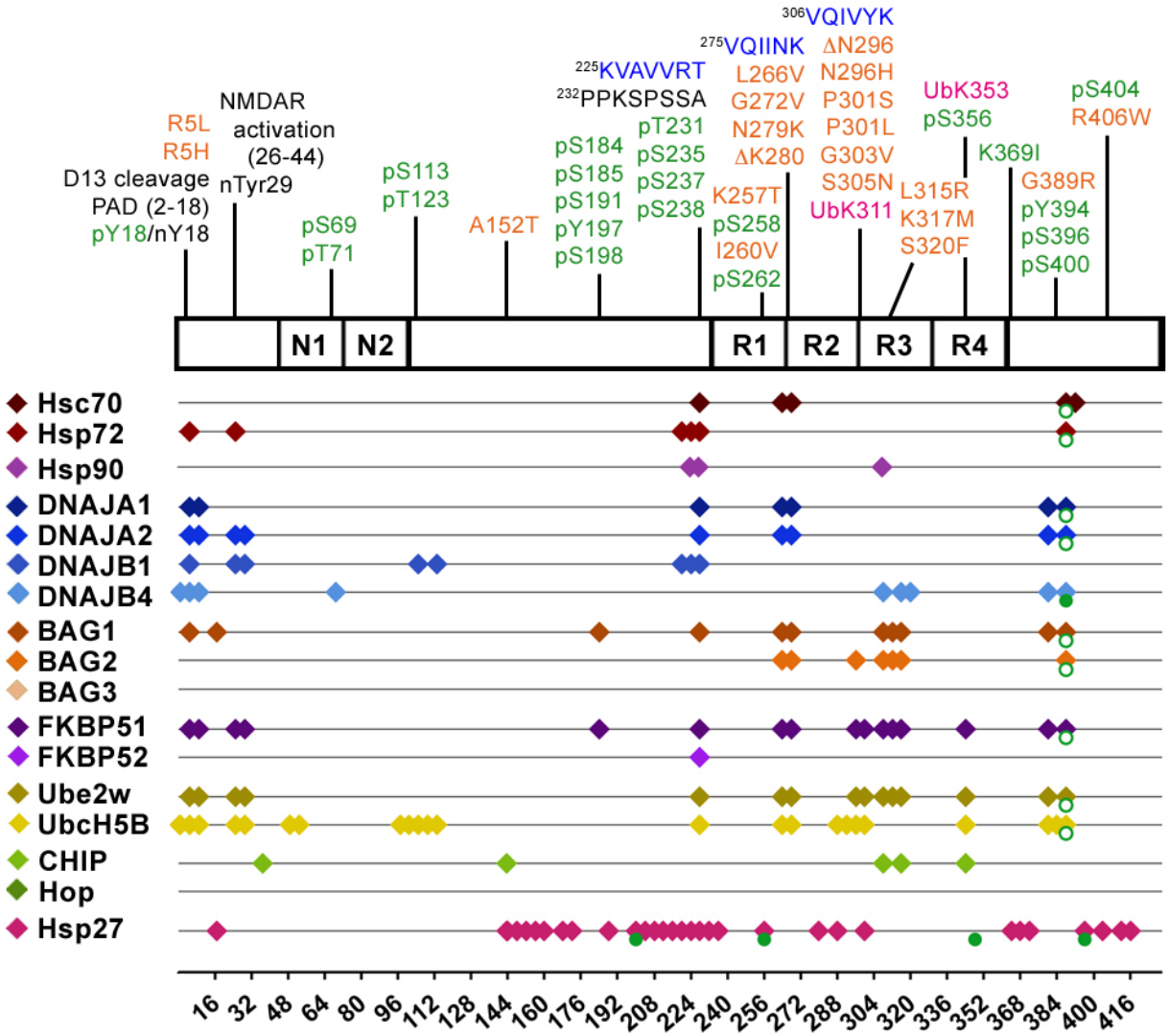

Figure 3.8. Map of chaperone binding sites on tau identified by peptide microarray. Peptides bound by 17 chaperones on a peptide microarray scanning the sequence of 4R2N tau are marked by colored diamonds, each representing a 15AA peptide. Green circles denote corresponding phosphomimetic peptides (P1-P6); ○: unbound, ●: bound. Features of the bound peptides are noted above on a schematic of tau; these features are discussed in detail in the text. Green: residue phosphorylated in PHF tau from AD brain. Orange: mutation associated with FTDP-17. Blue: microtubule binding site. Pink: ubiquitination site

Another feature of this map is that there appear to be a limited set of "hotspots" for chaperone interactions. For example, the extreme N-terminus of tau was a binding site for the J proteins, Hsp72 (but not Hsc70), BAG1, FKBP51, and the E2 ubiquitin conjugating enzymes Ube2w and UbcH5B. The N-terminus of tau has recently emerged as an important region for normal function and it has been implicated in the pathological cascade of tau

aggregation. Our data suggest that chaperones may be involved in regulating these functions, which is a possibility that has not been appreciated previously. Other "hotspots" included a portion of the proline-rich domain immediately upstream of R1, the ^{275}VQIINKK^{281} motif in R2, and a section of the C-terminal region including several phosphorylation sites. The possible implications for these interactions will be discussed below.

Peptide 228 (^{228}VVRTPPKSPSSAKSR^{242}) in the proline-rich domain emerged as a binder for the majority of the chaperones tested and it was often the brightest spot on the array. This peptide includes half of the ^{225}KVAVVRT^{231} motif, which is involved in microtubule binding and transiently occupies β structure in solution [71-73]. It also contains a PXXP motif (^{233}PKSP^{236}), which act as interaction sites for the SH3 domains of Src family tyrosine kinases [74] and a region, ^{232}PPKSPSSA^{239}, that transiently occupies polyproline II helical structure [72]. Moreover, this peptide encompasses four residues that have been found to be phosphorylated in AD (Thr231, Ser235, Ser237, and Ser238) [37]. Phosphorylation of Thr231 and Ser235 impairs microtubule binding [35, 75], suggesting an important interplay between microtubule interactions, chaperone binding and post-translational modifications. Finally, this sequence contains the binding site of the peptidyl-prolyl isomerase Pin1 (^{231}TPPKSP^{236} with Thr231 phosphorylation required), which induces a conformational change in tau that promotes its binding to microtubules [37, 76, 77]. This region of tau is involved in many different interactions and our findings provide evidence that chaperones might be involved in further regulating these contacts. Further validation by other biophysical methods, such as NMR and ITC, will be required to further explore this

possibility. Nevertheless, intriguing (and hypothesis building) possibilities are suggested by closer examination of the peptide array results and the following sections focus on the findings for each family of chaperones.

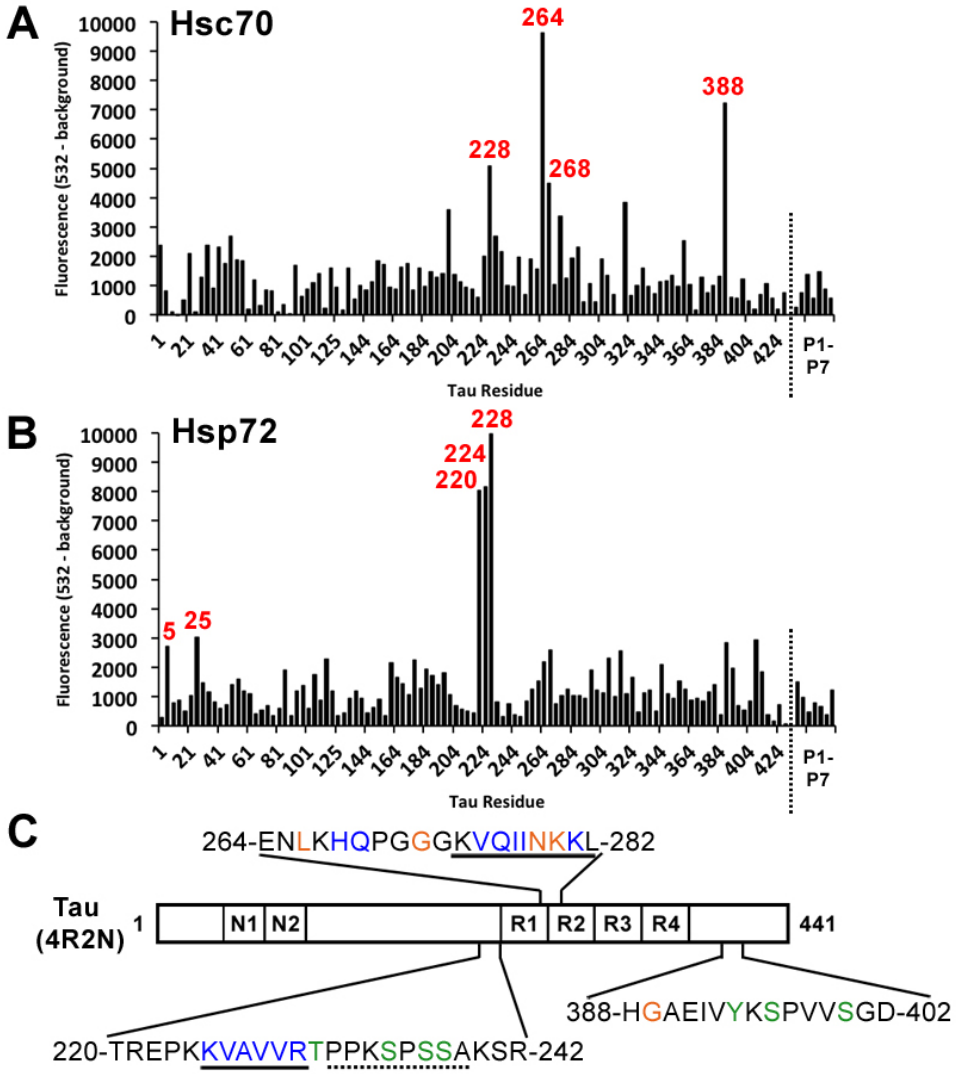

Figure 3.9. Hsc70 and Hsp72 binding sites on tau array. Fluorescence intensities of Hsc70 (A) and Hsp72 (B) bound to the tau microarray are plotted by peptide ID (numbered according to N-terminal tau residue). Binders confirmed by experimental replicates are numbered in red. (C) Diagram of 4R2N tau with sequences of notable binding sites and important features highlighted. Blue: MT binding site (Mukrasch 2009). Green: residue phosphorylated in AD (Hanger 2009). Orange: site of mutation associated with FTDP-17 (Gasparini 2007). Underlined: transient secondary structure identified by NMR (solid: β-sheet; dashed: polyproline II helix).

3.3.8 Tau binding sites for the "core" chaperones: Hsp72, Hsc70 and Hsp90

Our lab has previously reported binding sites for Hsp72 and Hsp90 on tau [48]. In that study, we found that Hsp72 had four binding sites on tau, two of which were shared with Hsp90, while Hsp90 had no unique binding sites. In an ELISA binding assay, Hsp72 was able to compete with Hsp90 for tau binding, but Hsp90 was unable to compete with Hsp72, providing supporting evidence for the array data. The present work refines the array findings and introduces results for Hsc70, the constitutively expressed isoform of Hsp72.

The intensity values for representative Hsc70 and Hsp72 experiments are shown in Figure 3.9. For clarity, only peptides corresponding to the 4R2N isoform of tau are shown in the graph. Each experiment was replicated 2 to 3 times, and these replicates informed the selection of the reproducible binders reported in Figure 3.8. When the data is viewed in this way, it is readily apparent that the binders vary widely in intensity. Features of some of the binding sites are highlighted in Figure 3.9C.

3.3.9 Hsp72 binds a microtubule-binding site upstream of the repeat domain

Hsp72 bound to three peptides spanning residues 220-242 (Figure 3.9B). The region 220-242 is located in the proline-rich domain upstream of the repeats. It includes the ^{225}KVAVVRT^{231} motif, which has β–structure 18% of the time [72] and is one of four regions that interact with microtubules [71, 72]. Thus, the interaction of Hsp72 with this region may play a central role in its ability to modulate the interaction of tau with microtubules.

In contrast to Hsp72, Hsc70 bound relatively weakly to this region, especially the upstream residues. This result suggests that Hsc70 may not interact directly with the ^{225}KVAVVRT^{231} motif. However, it retained some affinity for the polyproline helix, ^{232}PPKSPSSA^{239} and phosphorylated residues Thr231, Ser235, Ser237, and Ser238 (as discussed in Section 3.3.7). We have recently found that Hsc70 and Hsp72 have distinct effects on tau stability [57] and these array findings suggest that the binding to the KVAVVRT region may be involved in this difference.

3.3.10 Hsc70 binds ^{275}VQIINKK^{281}, a hexapeptide involved in PHF formation

The strongest binding site for Hsc70 was the two peptides spanning residues 264-282 in the repeat domain. These peptides were not bound by Hsp72 or Hsp90, which is interesting because Hsc70 has been implicated in restoring tau binding to microtubules, while Hsp72 and Hsp90 are linked to tau degradation. The 264-282 region comprises the end of R1, including the characteristic PGGG motif found in all four repeats, and the beginning of R2, including ^{275}VQIINKK^{281}. The shared residues between the two peptides are ^{268}HQPGGGKVQII^{278}. Interestingly, Hsc70 did not bind peptide 272 (which immediately follows these two peptides) even though it includes the full ^{275}VQIINKK^{281} motif, which could mean that Hsc70 binding of this motif requires additional upstream residues. This requirement was not tested by Sarkar and coworkers, as their work demonstrated the necessity of the VQI(I/V) motif and not its sufficiency [52]. Thus, additional studies will be required to better understand these interactions. This part of tau, especially the ^{275}VQIINKK^{281} motif (dubbed PHF6*), is important for function and it is involved in microtubule binding, heparin binding, and forming the core of PHFs [54, 55]. The

interaction of Hsc70 with this region thus likely plays an important regulatory role, perhaps allowing Hsc70 to control the interacting partners of tau. Another important feature of this region is that it is contains four mutations linked to FTDP-17 [34]. Three of these mutations are L266V, G272V and N279K, all of which cause increased tau aggregation and moderately reduced microtubule assembly competence [34, 78]. Interestingly, while G272V binds normally to microtubules, N279K exhibits dramatically attenuated binding, suggesting different mechanisms for disregulation by these two mutations [78]. Another mutation in this region is ΔK280, which is associated with dramatically enhanced tau aggregation and reduced microtubule affinity [78, 79]. Additionally, K280 has been identified as the primary target of acetylation, a post-translational modification that appears to be used to dynamically regulate tau [80, 81]. Ac-K280 tau has significantly reduced affinity for microtubules and is strongly correlated with pathological tau PHFs [81]. Thus, our results suggest that Hsc70 may compete with acetyltransferases and act as one of the regulators of tau acetylation.

3.3.11 Hsc70 binds a C-terminal region rich in phosphorylated residues

Another strong binding site for Hsc70 is the region 388-402, which only weakly bound to Hsp72. This C-terminal site is located adjacent to the repeats and it contains three residues that have been found to be phosphorylated in AD brains: Tyr394, Ser396 and Ser400 [37]. Tyr394 phosphorylation is only found in PHFs isolated from AD brain, not soluble tau from healthy brain [82-84]. Phosphorylation at Ser396/Ser404 comprises the epitope of an antibody called PHF-1 and has thus been extensively used as a marker of hyperphosphorylated tau [85]. *In vitro* studies have found that phosphorylation at

Ser396/Ser404 leads to increased tau aggregation [75, 86-88]. Furthermore, tau phosphorylated at S396/S404 is targeted for chaperone-mediated proteasomal degradation [89]. Interestingly, neither Hsc70 nor Hsp72 bound the phosphomimetic peptide P6, which is the same as peptide 388-402 except for a S396E mutation (see Table 3.2). This result suggests that Hsc70 might only associate with this section of tau only when Ser396 is unphosphorylated, though the effect of phosphorylation of the other residues in this region is unknown. Secondly, this peptide includes the site of a mutation associated with FTDP-17, G389R [34, 90]. This mutation impairs microtubule binding, but its effect on *in vitro* aggregation has not been determined [34]. Thirdly, the peptide includes the motif ^{393}VYK^{395}, which was found to be able to form fibrils in isolation and it also enhanced the aggregation of the PHF6 and PHF6* peptides [91]. This sequence is likely the nucleating region that allows the C-terminal tail of tau to form straight filaments in isolation from the rest of tau [92]. However, the mutation Y394K in the context of 4R2N tau did not affect the kinetics of PHF formation, suggesting that this motif is not directly involved in the aggregation of full length tau [91]. Nevertheless, its similarity with the known Hsc70 binding site, ^{306}VQIVYK^{311}, may form the basis of Hsc70's interaction with this binding site. It is known that the C-terminus of tau interacts with the repeat domain, forming part of the "paperclip" conformation [93], so interaction of Hsc70 with the bending region may serve as a handle to control this intra-molecular interaction. Deleting this region of tau (392-421) blocks the ability of an N-terminal fragment of tau (1-196) to inhibit the polymerization of full-length tau, suggesting that interactions between the N-terminus and this C-terminal region may play an important role in fibrillization [94].

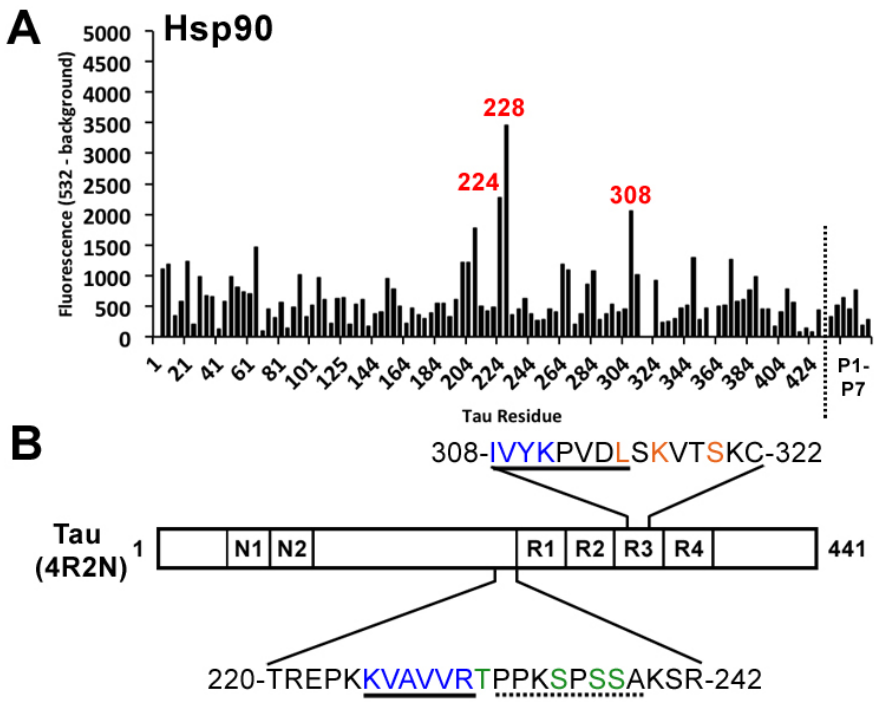

Figure 3.10. Hsp90α binding sites on tau array. Fluorescence intensities of Hsp90α (A) bound to the tau microarray are plotted by peptide ID (numbered according to N-terminal tau residue). Binders confirmed by experimental replicates are numbered in red. (C) Diagram of 4R2N tau with sequences of notable binding sites and important features highlighted. Blue: MT binding site (Mukrasch 2009). Green: residue phosphorylated in AD (Hanger 2009). Underlined: transient secondary structure identified by NMR (solid: β-sheet; dashed: polyproline II helix).

3.3.12 Hsp90 has no unique binding sites

The binding spots for Hsp90 are overlapping with those of Hsp72, spanning residues 224-242 and thus including the ^{225}KVAVVRT^{231} and ^{232}PPKSPSSA^{239} motifs and the phosphorylated residues Thr231, Ser235, Ser237, and Ser238 (Figure 3.10). Therefore, Hsp90 has no unique binding sites on tau and may interact with tau only after it is "handed" over by Hsp72, as our group has previously suggested [48].

3.3.13 Distinct binding patterns of Hsc70, Hsp72, and Hsp90 reflect functional differences

The marked differences in the binding sites for Hsp72 and Hsc70 may partially explain the functional differences in how the chaperones regulate tau homeostasis. Association of Hsc70 with tau is increased after microtubule destabilization, suggesting that Hsc70 preferentially interacts with free tau [95]. Recent work has shown that over-expression of Hsc70 favors tau accumulation, while Hsp72 causes increased tau clearance through proteasomal degradation [57]. Interestingly, this work also found that Hsc70 and tau were strongly synergistic for microtubule assembly, while Hsp72 did not have this effect [57]. Chimeras between Hsc70 and Hsp72 confirmed that the functional differences were determined by the identity of the C-terminal domain of the Hsp70 family members. Consistent with this finding, the Hsp72-tau complex was able to recruit the E3 ubiquitin ligase CHIP while Hsc70-tau was not. Further, our recent studies suggest that the Hsp72-tau complex converts to an Hsp90-tau complex during chemically-induced degradation of tau [48]. As discussed in Chapter 1, CHIP binds the C-terminus of Hsp70 and Hsp90 family members. Thus, our array findings suggest that differences in the chaperone-binding sites (and possibly their affinities) direct tau to its various fates: binding to microtubules or being shuttled to the proteasome for degradation.

3.3.14 J proteins bind both shared and distinct regions of tau

The binding of four J proteins to tau was evaluated using the microarrays (Figure 3.8). DNAJA1 and DNAJA2 had strikingly similar binding patterns, much as they did on the luciferase microarrays. The only discrepancy was in the region 25-43, but the functional

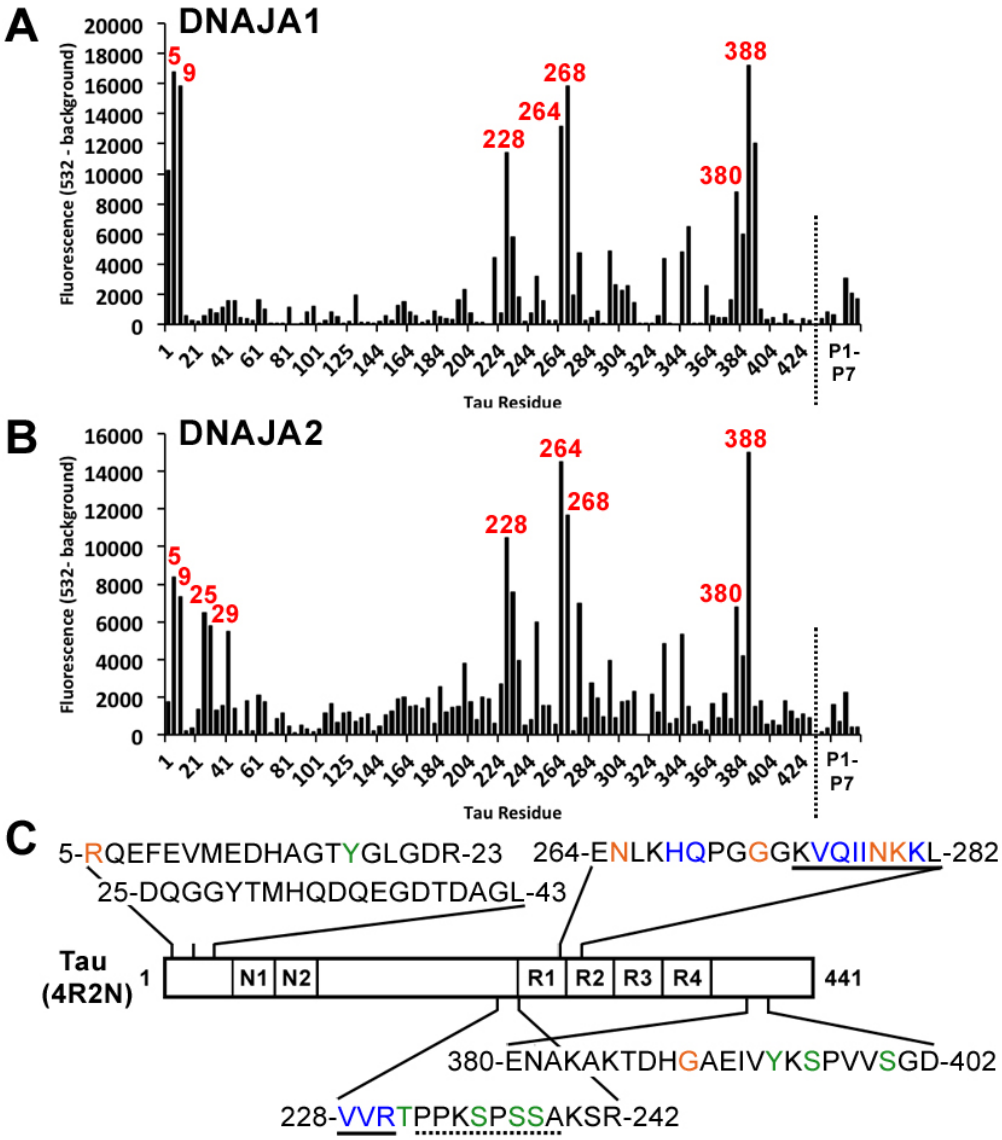

Figure 3.11. DNAJA1 and DNAJA2 binding sites on tau array. Fluorescence intensities of DNAJA1 (A) and DNAJA2 (B) bound to the tau microarray are plotted by peptide ID. Binders confirmed by experimental replicates are numbered in red. (C) Diagram of 4R2N tau with sequences of notable binding sites and important features highlighted. Blue: MT binding site (Mukrasch 2009). Green: residue phosphorylated in AD (Hanger 2009). Orange: site of mutation associated with FTDP-17 (Gasparini 2007). Underlined: transient secondary structure identified by NMR (solid: β-sheet; dashed: polyproline II helix).

significance of this difference is not known. DNAJB1 and DNAJB4 each shared some binding sites with the Class A J proteins and each other, but also had unique binding sites. The potential implications of these interactions will be discussed in the next sections.

3.3.15 J proteins bind the N-terminus of tau, a crucial structural and functional element

A striking feature of these results is that all four J proteins bind the extreme N-terminus of tau (Figure 3.8). Specifically, DNAJA1, DNAJA2 and DNAJB4 bind the second and third peptides, spanning residues 5-23, while DNAJB1 binds 5-19. In addition, DNAJA2 and DNAJB1 bind a second region from 25-43 (Figures 3.11 and 3.12). The overlap between the peptides suggests that the two binding sites include ^{5}RQEFEVMEDHAGTYG^{19} (all four J proteins) and ^{29}QDQEGDTDAGL^{39} (DNAJA2 and B1). These two neighboring sites might afford two "handles" for J proteins to bind tau. These events might occur in concert with Hsp72, because this chaperone also bound these two sites (Figure 3.9B).

The interaction of J proteins with the N-terminus of tau is intriguing because this region has been implicated in its function, structure, regulation, and pathology. Two mutations in this region, R5H and R5L, have been identified in cases of FTDP-17 and PSP [33, 96, 97]. The R5L mutation causes increased tau fibrillization and longer filaments [98, 99]. On the other hand, deletion of residues 2-18 results in drastically slowed *in vitro* tau fibrillization with a concomitant decrease in fibril length [98]. R5L also inhibits retrograde axonal transport by disrupting the interaction between tau and the dynactin complex [100]. Two caspase cleavage sites have been reported that result in a truncated N-terminus: caspase-6 cleaves after Asp13, while an unknown caspase may cleave after Asp25 [41, 101, 102]. Loss of the N-terminus is observed during later stages of AD progression and correlates with caspase-3 cleavage of the C-terminus at Asp421 [101]. Based on these observations, current models of tau processing suggest that cleavage of the N-terminus may reflect an attempt at self-

protection by the cell. Thus, binding of J proteins to this site might help regulate the timing and extent of the cleavage events.

Although tau is a natively unstructured protein, a growing body of evidence demonstrates that parts of the protein adopt a discrete set of conformations [72, 93]. Importantly for this discussion, the N-terminus is directly involved in these conformations. The major conformation occupied in solution is termed a "paperclip" and was deduced from FRET measurements [93]. The paperclip consists of the C-terminus folded over to interact with the repeat domain, while the N-terminus folds over to interact with the C-terminus (but not the repeat domain) [93]. Additionally, conformation-specific antibodies have been discovered that recognize discontinuous epitopes, and some of these epitopes include the N-terminus. For example, the MC-1 and Alz-50 antibodies both have epitopes that include the N-terminus and R3 [103, 104]. These antibodies recognize tau in early AD pathology but not healthy brains, and can recognize soluble tau that is competent for PHF formation, suggesting that the N-terminal interaction with the repeat domain represents an early step in neurotoxic tau aggregation [105]. Furthermore, FRET studies found that a mutant form of tau including 7 Glu residues in place of known pathological Ser/Thr phosphorylation sites adopted a compacted form of the paperclip conformation, including the N-terminus approaching the repeat domain, and exhibited dramatically increased reactivity to the MC-1 antibody (though not Alz-50) [106]. These findings provide a possible structural link between known pathological phosphorylation events and the increased propensity of hyperphosphorylated tau to form PHFs.

In addition to its involvement in structure of tau, the N-terminus has been directly implicated in mechanisms of neurotoxicity. One study found that filamentous, but not soluble, tau can inhibit anterograde (kinesin-dependent) fast axonal transport (FAT) [107]. A soluble N-terminal fragment of tau was able to recapitulate this inhibition, and the effect required residues 2-18, suggesting that this part of the N-terminus becomes exposed upon fibril formation and is then available to inhibit FAT [107]. The same group later found that residues 2-18 constitute a phosphatase activating domain (PAD) that directly activates protein phosphatase 1 (PP1), which in turn activates GSK3, causing phosphorylation of kinesin and anterograde FAT inhibition [108]. Many of the pathological signatures of AD are consistent with FAT inhibition, suggesting that this toxic gain-of-function upon tau aggregation could constitute a major mechanism of pathology [108]. Interestingly, both Hsp72 and phosphorylation of the N-terminus (pTyr18) have been found to prevent c inhibition by tau, suggesting that this interaction is regulated by post-translational modifications and the chaperone machinery [109, 110]. Tau toxicity in primary neuronal cultures has been traced to arise from residues 26-44, which cause NMDAR-dependent excitotoxic cell death [111]. This mechanism of toxicity also involves activation of extracellular regulated kinases (ERK1/2) and calpain, which in turn causes cleavage of tau to a 17 kDa fragment that may correlate to residues 45-230 [111]. The dramatic and complicated neurodegeneration that follows tau aggregation may result from some combination of these effects, which notably arise from neighboring but non-overlapping sites, reminiscent of the two binding sites observed for J proteins, as discussed above.

The N-terminus is also subject to post-translational modifications. Tyr18 is a target for phosphorylation by the tyrosine kinase Fyn, and it has been shown that phosphorylation of this residue is important for interaction with the SH2 domain of Fyn itself [37, 112]. Of the four Tyr residues subject to nitration by peroxynitrite ($ONOO^-$), Tyr18 and Tyr29 are preferentially nitrated [113]. Nitration of Tyr18 dramatically reduces the rate and amount of fibrillization, while nitration of Tyr29 has a moderate effect on rate and results in longer fibrils formed [114]. Tau nitration occurs during the course of AD and other tauopathies [115] and, specifically, nitrated Tyr29 has been detected in tau from diseased brains but not normal controls [116].

This body of research demonstrates that the N-terminus of tau may play a central role in the pathology of AD and other tauopathies. Our studies suggest that J proteins may have a unique role in regulating the N-terminus of tau and its many interactions. This hypothesis is supported by the finding that over-expression of DNAJA1 promotes degradation of tau independently of Hsp70 [50]. Thus, we hypothesize that J protein binding to residues 5-19 may inhibit the activation of PP1 and the consequential inhibition of FAT. Similarly, binding to 29-39 may prevent activation of extrasynaptic NMDARs and excitotoxic signaling. These interactions could also compete with, or be inhibited by, post-translational modifications (phosphorylation and nitration). Based on their binding to the N terminus, J proteins could also modulate the conformations of tau. It is known that DNAJA1 expression is 47% reduced in AD brains [50], perhaps creating a dis-equilibrium in the types of J proteins bound to tau.

3.3.16 Class A J proteins bind the repeat domain and C-terminus of tau

Other than the minor variation between DNAJA1 and DNAJA2 in binding the N-terminus, the two J proteins have identical binding sites in the rest of the protein. This shared binding pattern is also highly similar to that of Hsc70, which may indicate cooperation between the constitutive Hsc70 and the class A J proteins. These binding sites include peptide 228, the two peptides encompassing the ^{275}VQIINKK^{281} motif, and peptide 388, which contains three phosphorylation sites. Like Hsc70, DNAJA1 and DNAJA2 did not interact with P6 containing the Ser396 phosphorylation mimic, further suggesting that phosphorylation of this region may inhibit chaperone interactions. Unlike Hsc70, DNAJA1 and DNAJA2 both bound peptide 380-394, immediately upstream of the phosphorylation-rich region. The only functional connection identified for this region is that the first four residues comprise the end of a heparin-binding region, 372-383, identified by NMR (Mukrasch 2007). It is unclear what functional relevance this binding site may have for J proteins, though it may serve as an anchoring site for class A J proteins through which they can recruit Hsc70.

3.3.17 Class B J proteins have distinct binding sites throughout the length of tau

Beyond the N-terminus, DNAJB1 and DNAJB4 bind distinct sites on tau (Figure 3.12). The most robust binding site for DNAJB1 is residues 220-242, which is also a binding site for Hsp72 and Hsp90 (see Section 3.3.7). DNAJB1 has a unique binding site in the region between the N-terminal inserts and the proline rich domain, peptides 105 and 113. The discontinuous nature of these peptides makes it difficult to draw conclusions about the presence of a single site or two discrete sites. This region encompasses two known

phosphorylation sites – S113 and T123 – and a region ([114]LEDEAAGHVT[123]) that has alpha helical character by NMR [37, 72].

DNAJB4 binds strongly to peptide 69-83, spanning the end of N1 and the beginning of N2,

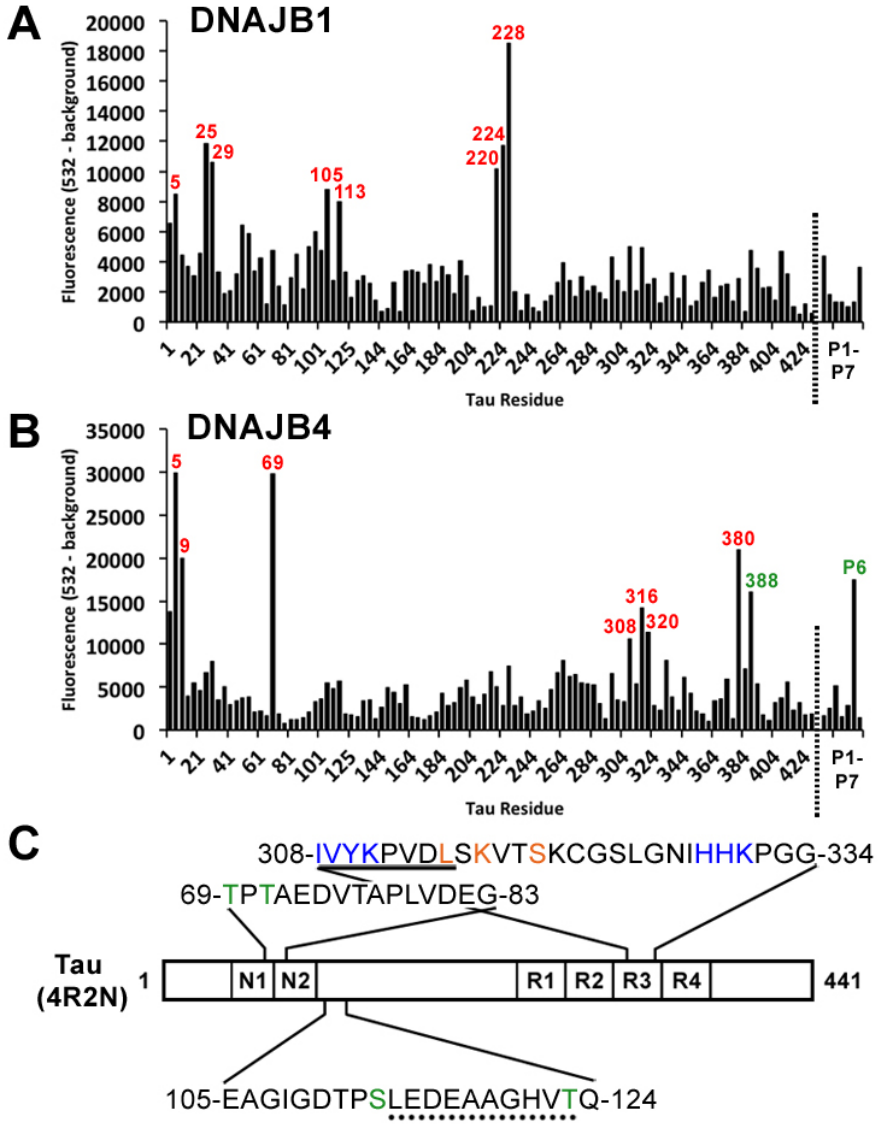

Figure 3.12. DNAJB1 and DNAJB4 binding sites on tau array. Fluorescence intensities of DNAJB1 (A) and DNAJB4 (B) bound to the tau microarray are plotted by peptide ID. Binders confirmed by experimental replicates are numbered in red (except for peptide 388, colored in green with its phosphomimetic P6). (C) Diagram of 4R2N tau with sequences of notable binding sites and important features highlighted. Green: residue phosphorylated in AD (Hanger 2009). Orange: site of mutation associated with FTDP-17 (Gasparini 2007). Underlined: transient secondary structure identified by NMR (solid: β-sheet; round dashed: α helix).

which is a region that was not identified for any other chaperone (Figure 3.8). This peptide includes two known phosphorylation sites – Ser69 and Thr71 – but its role in tau biology is not clear. DNAJB4 also weakly binds three peptides in the repeat domain, 308, 316, and 320, encompassing residues 308-334 which correspond with most of R3. R3 has been found to interact with the N-terminus, and this interaction comprises the MC-1 conformational epitope that signals an early pathological form of tau [103, 104, 106]. DNAJB4 may therefore be able to regulate this interaction. Additionally, this section of R3 contains three mutations identified in cases of FTDP-17 (L315R, K317M, and S320F), while an additional three mutations occur immediately downstream (G335V, Q336R, V337M), underscoring the importance of R3 in tau function and pathology [34].

Finally, DNAJB4 interacts with two C-terminal peptides, 380 and 388, which are also bound by the two class A J proteins tested. Interestingly, DNAJB4 was the only chaperone to bind the phosphomimetic peptide P6 (S396E). This suggests that DNAJB4 may be able to interact with tau even when it is phosphorylated, distinguishing it from other chaperones. This finding needs to be expanded to investigate other phosphorylation sites within DNAJB4's binding sites on tau – Ser69, Thr72, Tyr394, Ser400, and combinations thereof.

3.3.18 BAG1 binds multiple regions of tau rich in residues phosphorylated in AD

As discussed in Chapter 1, the BAG proteins are co-chaperones of Hsc70/Hsp70 that facilitate nucleotide and substrate release. In neuronal cell culture, BAG1 promotes accumulation of tau, an effect that is accentuated by Hsp70 induction, and in the absence of BAG1, tau is degraded by the proteasome [117]. One of the three BAG1 isoforms, BAG1M,

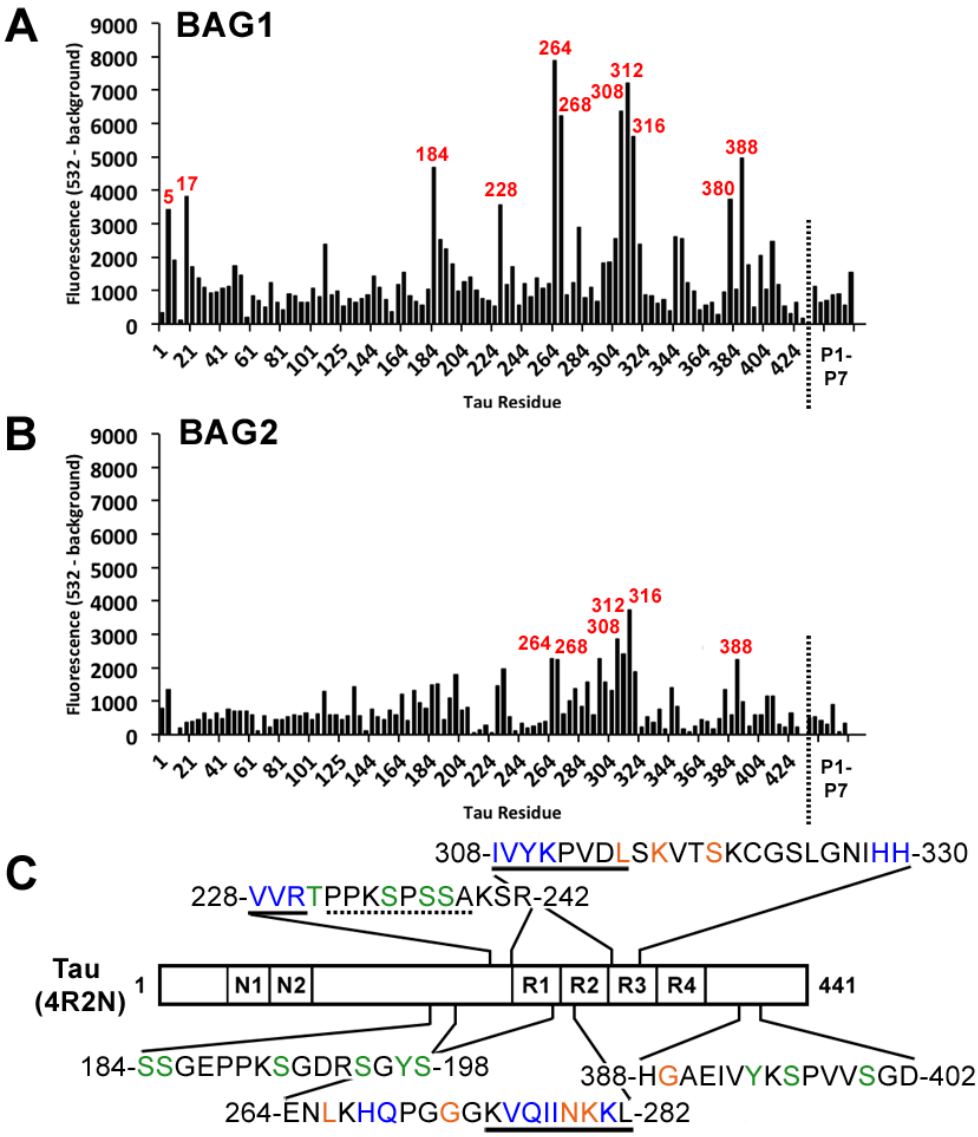

Figure 3.13. BAG1 and BAG2 binding sites on tau array. Fluorescence intensities of BAG1 (A) and BAG2 (B) bound to the tau microarray are plotted by peptide ID. Binders confirmed by experimental replicates are numbered in red. (C) Diagram of 4R2N tau with sequences of notable binding sites and important features highlighted. Blue: MT binding site (Mukrasch 2009). Green: residue phosphorylated in AD (Hanger 2009). Orange: site of mutation associated with FTDP-17 (Gasparini 2007). Underlined: transient secondary structure identified by NMR (solid: β-sheet; dashed: polyproline II helix).

is significantly upregulated in AD [118] and all three isoforms of BAG1 interact with tau in an Hsc70-dependent manner [117]. Further, a direct interaction between BAG1 and tau has been observed in our laboratory (Jennifer Rauch, unpublished data).

On our tau microarray, BAG1 has a unique binding pattern relative to other chaperones, but its individual binding sites are all shared with at least one other chaperone (Figure 3.8). A plot of the intensities reveals that the strongest binding sites are 264-282 (containing the ^{275}VQIINKK^{281} motif) and 308-330, comprising most of R3 (Figure 3.13). Interestingly, these sites are both rich in FTDP-17 linked tau mutations, encompassing a combined 7 mutations (L266V, G272V, N279K, ΔK280, L315R, K317M, and S320F) [34]. Other binding sites are mostly individual peptides and are found throughout the length of tau: the N-terminus (peptides 5 and 17), the proline-rich domain (peptide 184), the polyproline helix upstream of the repeat domain (peptide 228), and the C-terminus (peptides 380 and 388). BAG1 did not bind P6 despite binding 388, suggesting the interaction may be inhibited by phosphorylation. The functional significance of all of these binding sites has been discussed above, with the exception of peptide 184. This peptide falls between the two stretches of PXXP motifs responsible for interactions with the SH3 domains of kinases. It is rich in residues that undergo phosphorylation in AD, including Ser184, Ser185, Ser191, Tyr197, and Ser198. Interestingly, BAG1 knockdown leads to hyperphosphorylation of the tau that escapes proteasomal degradation, suggesting that BAG1 may play a role in regulating tau phosphorylation [117]. Our data suggests that, as BAG1 binds multiple regions rich in AD-related phosphorylation targets, part of this role could be competing with kinases for binding to their target residues in both the proline-rich domain and the C-terminal domain.

The binding of tau by two other BAG proteins, BAG2 and BAG3, was investigated using the microarrays. Unfortunately, the insolubility of BAG2 prevented definitive conclusions

(Figure 3.13), but some weak binding was observed at residues 264-282 and 308-330 in the repeat domain. BAG3 was soluble and it clearly did not bind tau.

The shared binding sites of BAG1 and BAG2 are intriguing since they have opposing roles in the regulation of tau. While BAG1 overexpression causes tau accumulation, BAG2 overexpression promotes proteasome-mediated, but ubiquitin-independent, degradation of tau, particularly aggregated and phosphorylated tau [119]. Furthermore, BAG1 and Hsc70 associate with free tau in the cytosol, while BAG2 and Hsc70 form a complex with tau on the microtubule [117, 119]. The shared binding sites for BAG1 and BAG2 could allow for a balance between these two opposing regulatory mediators.

3.3.19 FKBP51 and FKBP52 have markedly different tau binding profiles

FKBP51 and FKBP52 are immunophilins important for immune cell activation [120, 121]. These proteins also interact with Hsp90 through their TPR domains and have peptidyl-prolyl *cis-trans* isomerase (PPIase) activity. Both have been implicated in the regulation of tau, but despite their high homology, they appear to have opposing roles, much like BAG1 and BAG2 [122]. FKBP51 stabilizes tau by preventing ubiquitination and promoting dephosphorylation [123]. FKBP52 prevents tau accumulation and antagonizes microtubule assembly, while FKBP51 and tau have synergistic effects on microtubule assembly [123-125]. Both directly bind tau in the absence of other chaperones [123, 125]. The PPIase domain of FKBP51 has been shown to isomerize proline residues in tau, but the functional role of FKBP52's PPIase domain has not been demonstrated [123]. Because of the

intriguing roles of these chaperones in tau regulation, they were both tested on the tau microarray.

FKBP51 and FKBP52 had very different binding patterns (Figure 3.14). While FKBP51

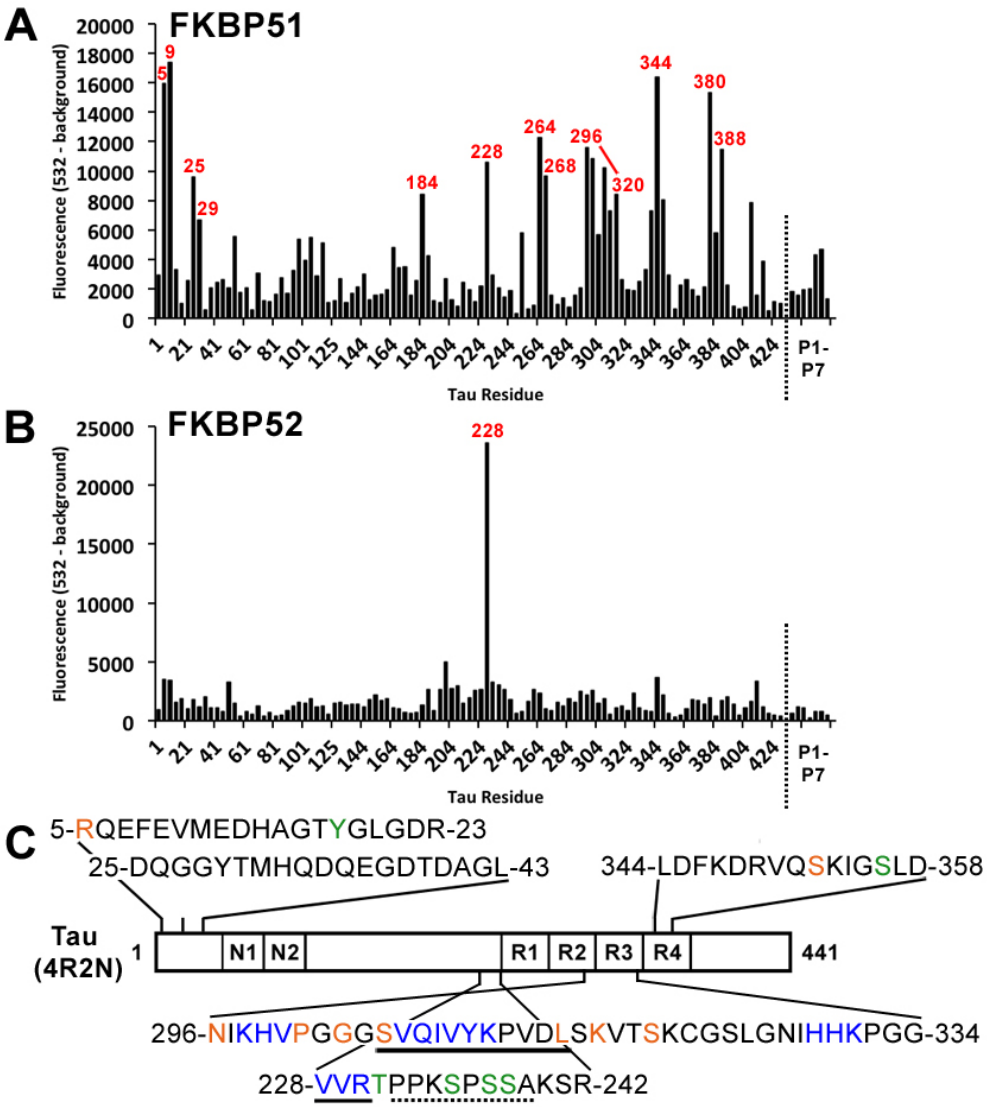

Figure 3.14. FKBP51 and FKBP52 binding sites on tau array. Fluorescence intensities of FKBP51 (A) and FKBP52 (B) bound to the tau microarray are plotted by peptide ID. Binders confirmed by experimental replicates are numbered in red. (C) Diagram of 4R2N tau with sequences of notable binding sites and important features highlighted. Blue: MT binding site (Mukrasch 2009). Green: residue phosphorylated in AD (Hanger 2009). Orange: site of mutation associated with FTDP-17 (Gasparini 2007). Underlined: transient secondary structure identified by NMR (solid: β-sheet; dashed: polyproline II helix).

bound eight different regions on tau, FKBP52 bound a single peptide in the proline-rich region. The peptide bound by FKBP52, which was also bound by FKBP51, was peptide 228 (see Section 3.3.7) and this interaction has been confirmed by NMR (Chad Dickey, personal communication). This finding further suggests that residues 228-242 in tau constitutes a central regulatory handle for the chaperone network.

In contrast to FKBP52, FKBP51 bound sites throughout the length of tau. Its binding pattern was strikingly similar to that of BAG1 (Figure 3.8), which is especially interesting given that both co-chaperones stabilize tau. The strongest site for FKBP51 binding was near the N-terminus at residues 5-23. The other binding sites included peptide 184 in the polyproline rich region (a binding site shared only with BAG1), 264-282 (beginning of R2), 296-330 (all of R3), 344-358 (within R4) and peptides 380 and 388 (C-terminus). While BAG1 also bound 308-330, the FKBP51 binding site is longer, extending to include 296-308 and thus the full ^{306}VQIVYK^{311} motif. This segment is also the site of six FTDP-17 mutations (ΔN296, N296H, P301S, P301L, G303V, S305N) [34]. Combined with the 7 mutations bound by BAG1 (see above), a mutation in peptide 388 (G389R), and two mutations near the N-terminus (R5L and R5H), FKBP51 binds a total of 16 FTDP-17 mutation sites, a significant portion of the ~40 known tau gene mutations. This result suggests that FKBP51 binding to tau may be impaired in many tauopathies, perhaps contributing to pathology.

While most of the FKBP51 binding sites were shared with BAG1, residues 344-358 were unique to FKBP51. This peptide contains a KXGS phosphorylation site, Ser 356; phosphorylation of this residue blocks microtubule binding and provides resistance to

chaperone-mediated degradation (see below) [89, 126]. This region also contains one of the motifs recognized by Hsc70 for chaperone-mediated autophagy, ^{347}KDRVQ^{351}, though binding of this site by Hsc70 was not observed in our experiments [56]. Thus, FKBP51 might serve as a handle for Hsc70-mediated recognition of tau for autophagy. FKBP51 shares this binding site with the degradation chaperones (CHIP, Ube2w and UbcH5, see below) suggesting a competition between the pro-stabilizing and pro-degradation arms of the chaperone machine.

3.3.20 CHIP, UbcH5B, and Ube2w cooperate to ubiquitinate tau in AD

The E3 ubiquitin ligase CHIP and the E2 ubiquitin-conjugating enzyme UbcH5B, in cooperation with the constitutive Hsc70/Hsp90 chaperone machinery, have been identified to play a key role in the processing of tau [127-129]. Tau lesions in various tauopathies are immunoreactive for ubiquitin [130]. Additionally, tau extracted from AD brain can be ubiquitinated *in vitro* by CHIP and UbcH5B, but tau from healthy brain cannot [127]. This disparity was traced to the phosphorylation state of tau; specifically, tau phosphorylated at proline-directed residues (by GSK3B and Cdk5; e.g. Ser202, Ser205, Ser396, and Ser404) can be ubiquitinated, while unphosphorylated tau cannot [47, 127]. However, tau phosphorylated at KXGS motifs (pS262/S356) is resistant to chaperone-mediated proteasomal degradation [89]. Interestingly, CHIP overexpression is protective against cell death caused by hyperphosphorylated (proline-directed) tau [127]. Inhibition of the proteasome along with tau, GSK3B, and CHIP co-expression causes accumulation of aggregates containing ubiquitinated hyperphosphorylated tau; however, these aggregates are not cytotoxic, suggesting that ubiquitination and sequestration of tau into aggregates may

constitute a protective mechanism. Indeed, deletion of CHIP in mice causes the accumulation of soluble, hyperphosphorylated, non-ubiquitinated tau, but no aggregates ever form, even when P301L mutant tau is expressed, suggesting that ubiquitination is a necessary signal for tau aggregate formation [89]. Misregulation or decay of this system may be an important pathological event.

CHIP directly interacts with tau, though neither the U-box or TPR domains of CHIP are sufficient for this interaction, suggesting that CHIP may engage in a multivalent interaction with tau [128]. Attempts at mapping the CHIP binding site(s) on tau found that CHIP interacted best with tau(156-373), encompassing the proline-rich domain and the repeats, while CHIP was also able to bind tau(249-441) [128]. CHIP binding of tau is abrogated by MARK phosphorylation of S262/S356 or mutation of these residues to alanine, which could suggest that the hydroxyl side chains of the Ser residues are themselves important, either for direct interaction with CHIP or maintaining a tau conformation conducive to CHIP binding [47].

Tau immunoprecipitated from AD brain by the MC-1 antibody has been found to be poly-ubiquitinated at three lysines in the repeat domain (K254, K311, K353) (Figure 3.15, pink dots) [131]. Notably, K353 is very close to one of the MARK phosphorylation sites, S356. In order to determine whether UbcH5B has site-selectivity for ubiquitination of tau in the absence of CHIP, tau was incubated *in vitro* with UbcH5B for 18 hours; this tau was found to be ubiquitinated at no less than 17 lysine residues (including the three previously identified) scattered throughout the length of tau (Figure 3.15, purple dots) (Matthew

Scaglione, personal communication). This suggests that CHIP may direct UbcH5B's activity towards the three lysines in the repeat domain, though the mechanism of this targeting is unknown. Furthermore, another E2 involved in the regulation of CHIP, Ube2w, has been found to specifically monoubiquitinate tau at the N-terminal amine (Matthew Scaglione, personal communication) [132]. Interestingly, this form of ubiquitinated tau is unable to form aggregates, suggesting that the two different types of ubiquitination may have functional differences *in vivo*, thus providing an explanation as to why two separate E2s are used. We investigated the binding of CHIP, UbcH5B, and Ube2w to the tau microarray to determine to what extent binding site(s) might contribute to the differential tau ubiquination activity of these two E2-E3 pairs.

3.3.21 E2s cooperate with CHIP and compete with stabilizing co-chaperones

The E2 ligases Ube2w and UbcH5B had strikingly similar binding patterns on the tau array (Figure 3.15). This finding suggests that binding sites alone cannot account for the disparate tau ubiquitination carried out by these E2s and that some other variable must affect site selectivity, perhaps other proteins or the conformational state of tau. The strongest binding site for both is peptide 228-242 in the proline rich region, which is just upstream of one of the AD ubiquitination sites, K254. They also both interact with the N-terminus at the sites identified for J proteins and FKBP51, 5-23 and 25-43. Furthermore, both have nearly the same pattern of rather weak binding to various sites in all four repeats of the repeat domain and the C-terminus. The only marked difference between the two E2s is that UbcH5 has two unique binding sites in the N-terminal half of tau: 49-67 and 97-124. Neither of these sites was identified for any other chaperone save for some overlap with DNAJB1 in the

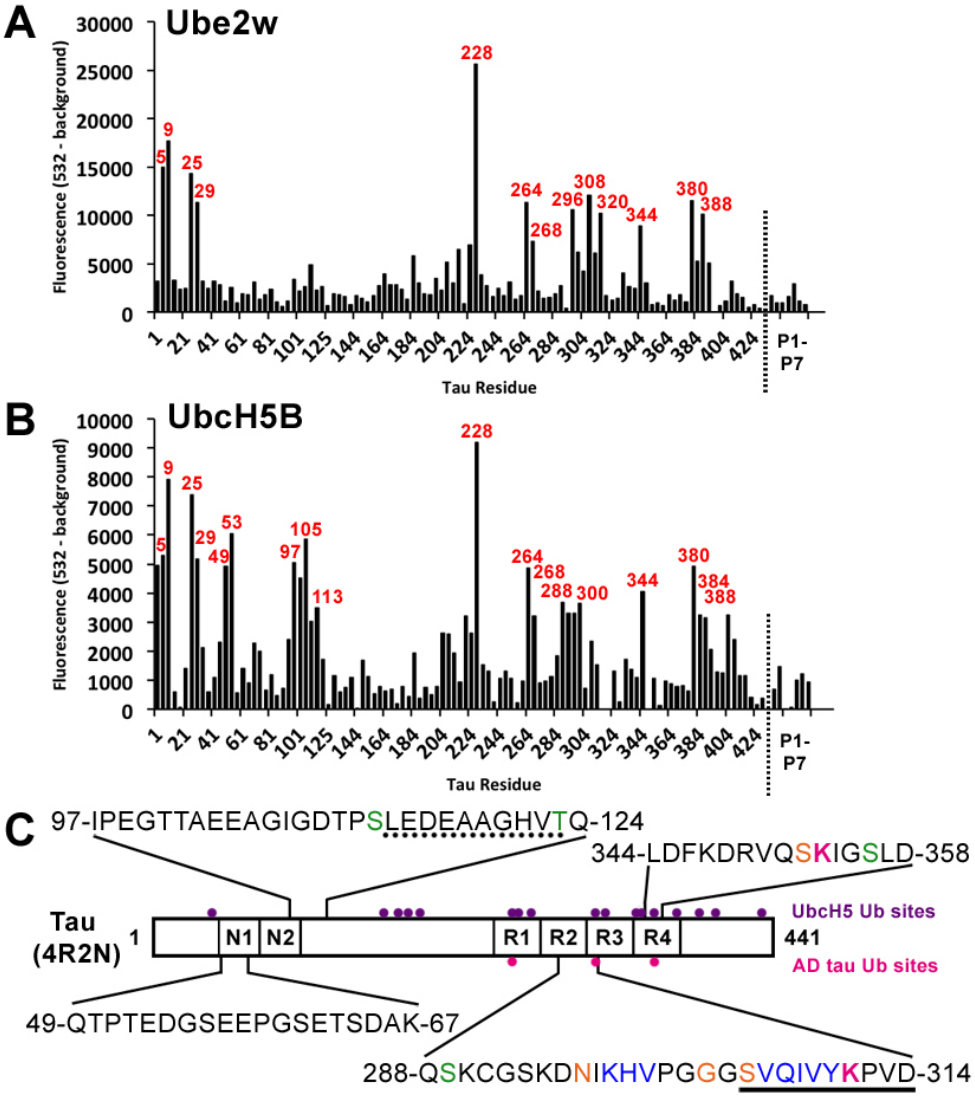

Figure 3.15. Ube2w and UbcH5B binding sites on tau array. Fluorescence intensities of Ube2w (A) and UbcH5B (B) bound to the tau microarray are plotted by peptide ID. Binders confirmed by experimental replicates are numbered in red. (C) Diagram of 4R2N tau with sequences of notable binding sites and important features highlighted. Blue: MT binding site (Mukrasch 2009). Green: residue phosphorylated in AD (Hanger 2009). Orange: site of mutation associated with FTDP-17 (Gasparini 2007). Underlined: transient secondary structure identified by NMR (solid: β-sheet; dashed: polyproline II helix).

latter site. The functional role of these sites is not clear as they do not include lysines ubiquitinated either by UbcH5B alone or in AD tau, but they may allow UbcH5B to interact with a specific conformation of tau that is due to be marked by ubiquitination.

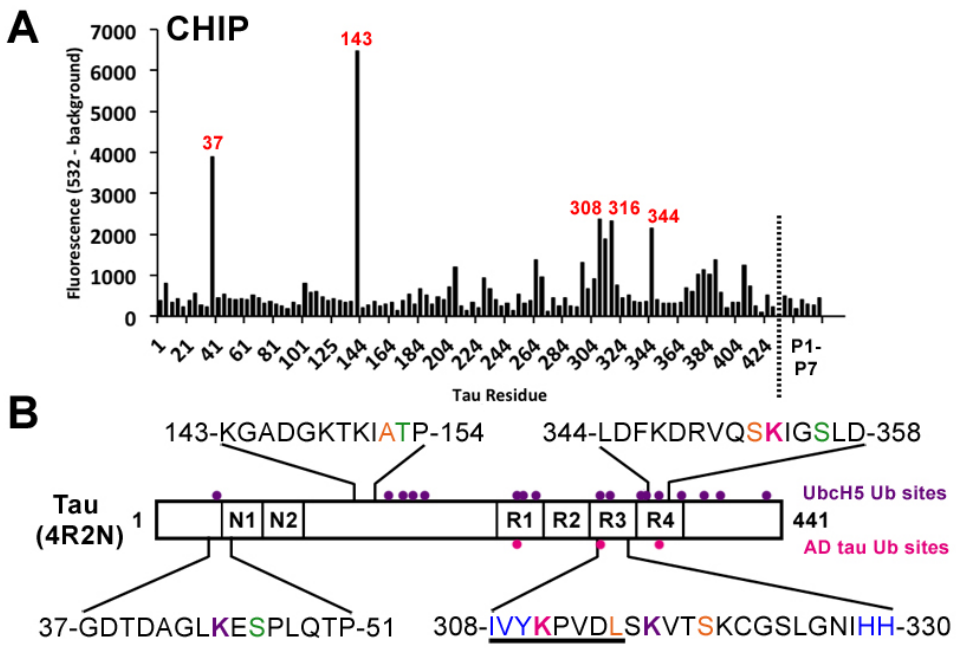

Figure 3.16. CHIP binding sites on tau array. Fluorescence intensities of CHIP (A) bound to the tau microarray are plotted by peptide ID. Binders confirmed by experimental replicates are numbered in red. (B) Diagram of 4R2N tau with sequences of notable binding sites and important features highlighted. Blue: MT binding site (Mukrasch 2009). Green: residue phosphorylated in AD (Hanger 2009). Orange: site of mutation associated with FTDP-17 (Gasparini 2007). Purple (dots and residues): lysines ubiquitinated by UbcH5 *in vitro* without CHIP. Pink (dots and residues): lysines ubiquitinated in PHF tau from AD brain (Cripps 2006) Underlined: transient secondary structure identified by NMR (solid: β-sheet; dashed: polyproline II helix).

The E3 ligase CHIP had a markedly different interaction pattern from the E2s (Figure 3.16). It bound two peptides, 37-51 and 143-154, with high intensity in three experimental replicates. Neither is identified for any other chaperone in our dataset. Peptide 37 does not have distinguishing features beyond a single phosphorylated residue, S46, but given the general importance of the N-terminus in tau biology (see Section 3.3.15), this binding site could have an important role in regulating tau. Peptide 143 comes with a caveat: this peptide on the array begins with three residues from the PNS isoform of tau, and the next peptide on the array, which also contains the full 143-154 sequence, was not bound by CHIP, suggesting that this interaction could be an experimental artifact. If it is a genuine

CHIP binding site, this sequence is interesting because it contains a recently identified tau mutation, A152T, linked with increased risk for FTDs and AD [133]. This mutation causes significant impairment in microtubule assembly but, unlike most other tau mutations, slightly attenuates PHF formation. On the other hand, an increase in oligomer formation is observed, suggesting a possible toxic gain of function as oligomers are thought to be more neurotoxic than full filaments [36, 133]. The location of this mutation, distant from sites generally understood to govern MT binding and PHF formation, suggests an as yet unknown role for this region of tau in influencing these activities.

The fact that both UbcH5B and CHIP had two unique and neighboring binding sites in the N-terminal projection domain, a region that is largely devoid of other chaperone interactions, suggests that this region could act as a specific handle for ubiquination. During tau's conformational switching, it is conceivable that this region could approach the repeat domain where AD tau ubiquitination occurs [131]. CHIP also weakly bound two regions in the repeat domain: 308-330 and 344-358. Notably, these two regions include two of the AD ubiquitination sites, K311 and K353. UbcH5 bound 288-314, also encompassing K311 but including the region upstream of this residue, while CHIP binding includes the region downstream, suggesting a possible pair of binding sites that could allow the two to collaborate in ubiquitination of K311. On the other hand, UbcH5 and CHIP both bound peptide 344 but not any neighboring peptides, suggesting a different mode of cooperation for ubiquitination of K353. This peptide also includes S356, one of the MARK-phosphorylated residues that prevents CHIP ubiquitination of tau and chaperone-mediated degradation [47, 89]. One of our phosphomimetic peptides, P5, includes a S356E mutation; however, this

peptide has the same sequence as peptide 348, which was not bound by CHIP or the E2s either, so this cannot be taken as clear evidence that S356 phosphorylation directly blocks CHIP interaction; further experiments, perhaps using peptide 344, are necessary to resolve this question. No binding was observed to any peptides containing the other MARK-phosphorylated residue, S262, or the corresponding phosphomimetic peptide (P4).

The binding of another TPR-containing chaperone, Hop, was also tested on the tau array. Hop is comprised solely of TPR domains and serves to coordinate Hsc70 and Hsp90 by interacting with both of them simultaneously. No evidence of Hop interacting with tau has been reported, and indeed, we observed no binding to the array (Figure 3.8), suggesting that the interactions observed for CHIP, and likely the other chaperones, represent specific interactions.

The interaction patterns of Ube2w and UbcH5B bear a striking resemblance to those of FKBP51 and BAG1, both of which are stabilizing co-chaperones that prevent proteasomal degradation of tau [117, 123] (Figure 3.8). This suggests that direct competition could mediate triage decisions by the co-chaperone machinery and that factors such as phosphorylation, conformation of tau, and other chaperones bound may determine which co-chaperones dominate in a given context. This data provides specific sequences within tau that may be used to probe the finer details of tau triage.

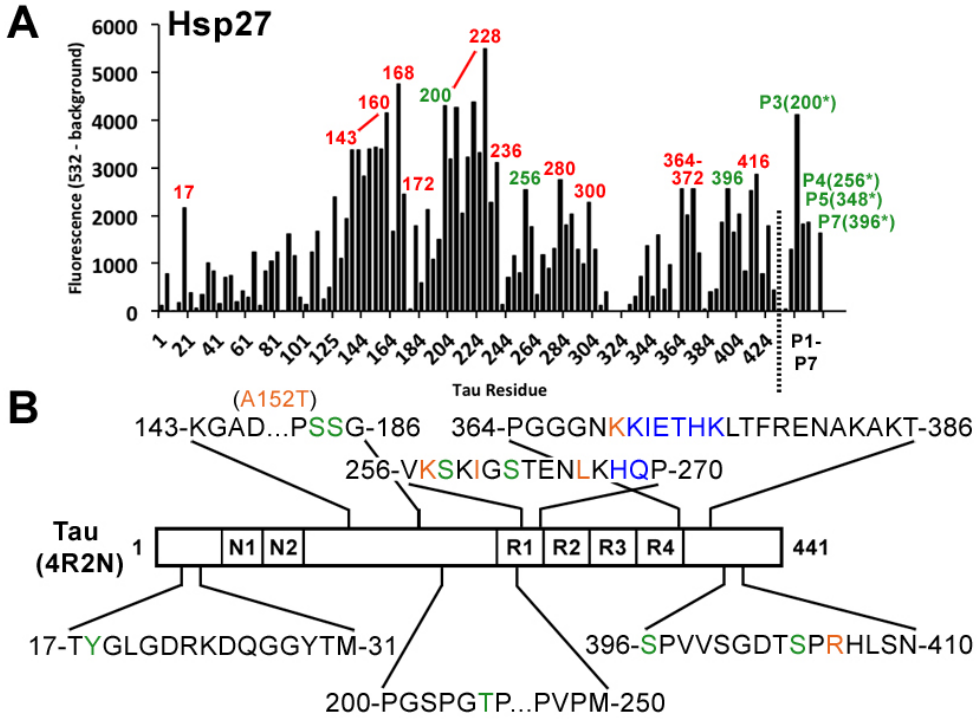

Figure 3.17. Hsp27 binding sites on tau array. Fluorescence intensities of Hsp27 (A) bound to the tau microarray are plotted by peptide ID. Binders confirmed by experimental replicates are numbered in red except for those whose corresponding phosphomimetics were bound, which are colored in green. (C) Diagram of 4R2N tau with sequences of notable binding sites and important features highlighted. Blue: MT binding site (Mukrasch 2009). Green: residue phosphorylated in AD (Hanger 2009). Orange: site of mutation associated with FTDP-17 (Gasparini 2007). Underlined: transient secondary structure identified by NMR (solid: β-sheet; dashed: polyproline II helix).

3.3.22 Hsp27 binds extensive regions of the proline-rich domain and C-terminus of tau

Hsp27 is a member of the small heat shock protein family that preferentially interacts with hyperphosphorylated tau (either GSK3β treated or derived from AD brain) [51]. Hsp27 is regulated by phosphorylation, which alters its oligomeric state and chaperone functions. Delivery of wild type Hsp27 to tau transgenic mouse brains causes tau reduction and rescues deficits in long term potentiation (LTP), but pseudophosphorylated (3xS/D) Hsp27 causes accumulation of tau and fails to rescue LTP [134]. From these observations, it is clear that the roles of Hsp27 in tau homeostasis are complex. To better understand this

process, we investigated the binding of Hsp27 to the tau microarray. While unphosphorylated Hsp27 binding to tau arrays was successful, attempts to characterize binding of a pseudophosphorylated Hsp27 mutant (Hsp27 (3xS/D)) were unsuccessful, resulting in high background and no clear signal.

The binding profile we obtained for Hsp27 was broader than that for any other chaperone tested (Figure 3.8). The identities of these peptides were also unique relative to other datasets. For example, the strongest sites for Hsp27 were two long continuous stretches of peptides located in the proline-rich domain and part of R1 (Figure 3.17) that are largely devoid of other chaperone interactions. These sites were quite large and continuous, suggesting that Hsp27 may interact with tau in a fundamentally different way. Strikingly, throughout the rest of the tau sequence (R2 to the C-terminus), the binding of Hsp27 is almost mutually exclusive with other chaperone interactions. For example, Hsp27 did not bind the frequently observed binding site 264-282 (containing the ^{275}VQIINKK^{281} motif) but bound a few peptides immediately up and downstream of this site. Furthermore, Hsp27 had a pronounced lack of binding to R3, a region also frequently identified for other chaperones. Finally, Hsp27 interacted extensively with the C-terminus from 364 onwards, where no other interactions have been observed. This binding profile suggests that Hsp27 might not directly compete with other chaperones and, further, that its binding might help maintain tau in a state competent for binding to other chaperones.

Another unique feature of Hsp27 binding was that it bound to 4 of the 7 phosphomimetic peptides (Figure 3.17). These peptides included mutations mimicking phosphorylation at

T205, S262, S356, and S404. Hsp27 is known to interact with phosphorylated tau [51], which is consistent with these findings. However, Hsp27 also bound the native version of all of these peptides. Interestingly, two of these phosphorylation sites are proline-directed (T205, S404), while the others are KXGS motifs (S262, S356), suggesting that Hsp27 does not discriminate between the two types like the CHIP-mediated chaperone degradation machinery does. In fact, Hsp27 overexpression has been correlated with an increase in pS262 levels, an effect that could play a role in pathology by preventing tau degradation by CHIP [135].

Hsp27 also bound regions bearing several FTDP-17 mutations that were not bound by any other chaperone. Notably, Hsp27 bound all four peptides that included A152, the site of the A152T mutation recently identified as a risk factor for tauopathies (see Section 3.3.21) [133]. Hsp27 also bound regions containing four mutations in the repeat domain: three in R1 (K257T, I260V, and L266V) and one in R4 (K369I). All four mutations impair microtubule assembly and enhance aggregation [34]. Finally, Hsp27 binds peptides near the C-terminus containing the mutation R406W; however, this mutation has only a minor effect on microtubule assembly and does not enhance tau aggregation. Together, these findings suggest that alteration of Hsp27 binding, particularly in the proline-rich domain, may play a role in tauopathies.

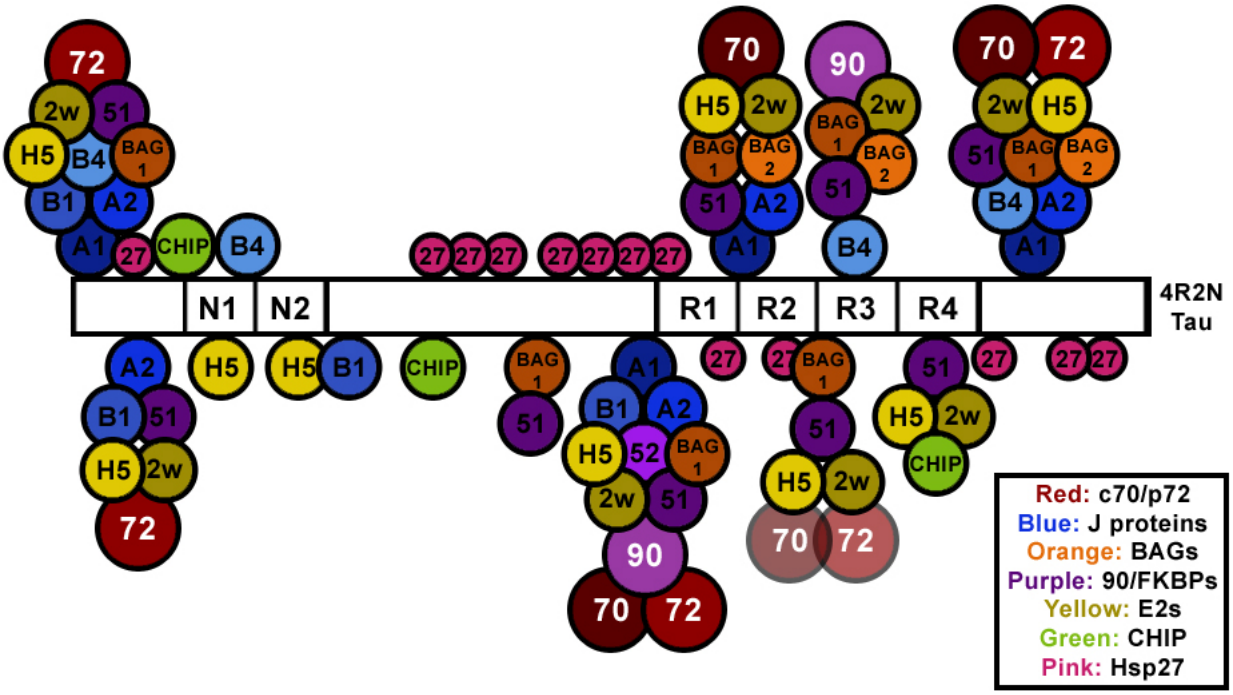

Figure 3.18. Model of chaperones binding to tau. Based on our microarray data, a model of chaperones (color-coded by class as in Figure 3.8) binding tau is shown. Chaperones cluster on a series of "hotspots": the N-terminus, a phosphorylation-rich region immediately upstream of the repeat domain, the beginning of repeats R2 and R3, and a phosphorylation-rich site near the C-terminus. Hsp27 is the exception and interacts with most of the proline-rich region as well as the C-terminus. Some chaperones have unique binding sites that are discussed in the text. In the first R3 binding site (including ^{306}VQIVYK) Hsc70 and Hsp72 are faded because this interaction has been shown previously (Sarkar 2008) but it was not observed in our experiments.

3.4 Discussion

We have used a peptide microarray platform to develop the first detailed model of chaperones binding to tau (Figure 3.18). These results suggested that nearly the entire length of tau is bound by at least one chaperone. Additionally, chaperones appeared to converge on a limited set of "hotspots" and these locations tended to be functionally important. A repeating theme in these studies was that "pro-degradation" chaperones and "pro-retention" chaperones share identical binding sites. In particular, the stabilizing chaperones (BAG-1 and FKBP51) and degradation chaperones (CHIP, Ube2w, UbcH5) all shared binding sites.

Similarly, Hsc70 (pro-stabilization) and DNAJA1/Hsp72/Hsp90 (pro-degradation) share some binding sites. These results suggest that competition for binding sites is one powerful mechanism for guiding the fate of tau in the chaperone system. Because these sites are also the sites of microtubule binding, post-translational modification and aggregation, the broader competition of chaperones for other cellular factors is likely to be central for tau homeostasis. These results highlight the importance of protein-protein interactions in protein quality control.

One of the most far-reaching implications of this model is the importance of the competition between chaperones, tau and microtubules. In the course of normal neuronal activity, tau must cycle on and off of microtubules. The binding sites of Hsc70 suggest that this chaperone protects the aggregation-prone regions from forming aberrant interactions during the times when tau is free in the cytosol.

Another important outcome of these studies is the interplay between chaperone binding and tau phosphorylation. In previous studies, Hsc70, Hsp90 and Hsp27 were all found to preferentially bind hyperphosphorylated tau, while CHIP only ubiquitinates tau derived from AD brain [47, 51, 127]. In our studies, only Hsp27 interacted extensively with the phosphomimetic peptides, binding 4 of 7. Generally, other chaperones didn't bind either the native or phosphomimetic peptides containing these residues. The exception was peptide 388, containing Ser396, which was bound by most of the chaperones tested, while the corresponding phosphomimetic (P6) was never bound (except by DNAJB4). Taken together, these findings suggest that the preferential binding of chaperones to

hyperphosphorylated tau observed previously is not due to direct interactions with phosphorylated regions. Rather, the conformational implications of phosphorylation might be an important feature. Indeed, phosphorylation has been shown to directly influence tau conformation, with the combination of three known pathological phosphorylated epitopes leading to compaction of the tau "paperclip" and increased reactivity with the MC-1 antibody [106]. Interestingly, tau incubation with Hsc70 *in vitro* leads to development of the MC-1 conformation, while MC-1 tau is one of the types preferentially degraded by upregulation of the chaperone machinery [89, 95]. Therefore, it appears that hyperphosphorylation of the whole tau molecule, not phosphorylation of individual residues, is important in regulating chaperone interactions. Peptide arrays do not permit insight into this particular question, so additional studies will be required.

One exception to this model may be MARK phosphorylation at the KXGS motif containing Ser356. Tau phosphorylated by MARK is resistant to chaperone-mediated degradation [89]. One of the three ubiquitination sites identified in PHF tau from AD brain, K353, is actually a part of this KXGS motif. We find that a peptide containing this motif, 344-358, is bound by the E3 ubiquitin ligase CHIP, the E2 ubiquitin conjugating enzymes Ube2w and UbcH5, and the tau stabilizing co-chaperone FKBP51. These chaperones must therefore compete with MARK for binding to this region of tau. Phosphorylation of Ser356 may directly inhibit CHIP and/or UbcH5 interaction with this site, thus preventing ubiquitination and proteasomal degradation. Alternatively, Ser356 phosphorylation may promote the interaction of FKBP51 with this site, also preventing CHIP binding and ubiquitination. Our data does not provide specific evidence for or against these hypotheses, as the

phosphomimetic peptide containing S356E corresponds with peptide 348, which was not bound by any chaperone. Further experiments are necessary to measure the relative affinities of the different chaperones for peptide 344-358, determine the minimal binding site in this region, and evaluate the effect of Ser356 phosphorylation.

The use of peptide microarrays to investigate chaperone binding to tau has allowed us to examine specific interactions in the absence of confounding variables such as tau phosphorylation, conformation state, and other interacting partners. Therefore, this dataset likely represents a "maximum" interaction profile that is limited and controlled by many other variables *in vivo.* This profile provides a starting point for investigations using targeted point mutations and deletions within tau to elucidate the relative contribution of different interactions in various contexts. The regulation of tau by chaperones may provide a valuable therapeutic opportunity, and a more detailed understanding of the interactions involved will allow for more rational development of selective therapeutic agents.

3.5 Experimental Methods

3.5.1 Protein Purification

Hsp70s (DnaK, Hsc70, Hsp70, NBD constructs; Hsp70 NBD (1-383), Hsc70 NBD (1-383), and Hsc70 NBD+linker (1-394)) were purified as previously described [136]. Likewise, Hsp90, J-domain (1-108), and DnaJ were purified as previously described [136, 137], with the addition of a Superdex 200 size exclusion column (GE Healthcare, Pittsburg, PA) as the last step of the J-domain purification. N-terminal His6x-tagged DNAJA1, DNAJA2, and DNAJB1 were purified as previously described [10]. Hsc70SBD (394-540) was expressed in

BL21 cells from a pMCSG7 vector encoding an N-terminal His6x tag under ampicillin selection. Cells were lysed by sonication into His6x-binding buffer (50 mM Tris pH 8.0, 10 mM imidazole, 500 mM NaCl, protease inhibitors) and purified using Ni-NTA resin (Novagen, Darmstadt, Germany). Protein was eluted with His6x-elution buffer (50 mM Tris, 300 mM imidazole, 300 mM NaCl), 2 mM EDTA added, and protein concentrated to ~6 mg/mL. Protein was further purified on a HiLoad Superdex 75 16/600 size exclusion column into storage buffer (50 mM Tris, 250 mM NaCl). Pure fractions were combined, concentrated, flash frozen and stored at -80ºC. Hsp27, Hsp22, αB □crystallin, expressed in Rosetta cells using the pMCSG7 vector. Cells were lysed by sonication into lysis buffer (20 mM Tris pH 8.0, 100 mM NaCl, 6 M urea, 5 mM β-mercaptoethanol, 15 mM imidazole) and purified by standard denaturing his purification using Ni-NTA resin. Proteins were eluted with 150 mM imidazole. Following elution EDTA was added to 5 mM and protein was concentrated to ~20 mg/ml. Protein was refolded upon injection on a Superdex 200 size exclusion column (GE Healthcare, Pittsburg, PA) with refolding buffer (20 mM NaP_i pH 7.2, 100 mM NaCl). The protein was flash frozen and stored at -80 ºC. Finally, FKBP51 was purified by using a standard His purification with Ni-NTA resin (Novagen) followed by separation using a superdex 200 size exclusion column in (10mM NaPi, 2mM KPi pH 7.4, 137 mM NaCl, 2.7 mM KCl, 1 mM DTT). The following proteins were purchased as follows; Clusterin (Enzo Life Sciences, 201-335-C050, Farmingdale, NY), PDI (PROSPEC, enz-262-b, East Burnswick, NJ), FKBP12 (PROSPEC, enz-347-c). MycF was a kind gift from Janet Smith (University of Michigan); nanobody80 was a kind gift from Roger Sunahara (University of Michigan).

3.5.2 Peptide Microarrays

A peptide microarray consisting of a variety of peptides experimentally evaluated for their ability to form fibrils was designed (Appendix A.1). Empty spots and process controls were used as negative controls. The microarrays were printed on single microscope slides in triplicate with peptides covalently immobilized at the N-terminus (Jenrin Peptide Technologies, Berlin, Germany). Binding was tested per manufacturer's protocol using 10 μM of His6x-tagged protein in binding buffer (25 mM HEPES pH 7.2, 150 mM NaCl, 20 mM KCl, 5 mM $MgCl_2$, 0.01% Tween20). Binding was detected using 1:1,000 titer of HiLyte555 anti-His6x antibody (Anaspec, Fremont, CA) in TBS-T with 1% bovine serum albumin (Sigma) and scanning the microarrays using a GenePix 4100A Microarray Scanner (Molecular Devices, Sunnyvale, CA) and an excitation wavelength of 532 nm. Binding was defined using a previously described peptide microarray analysis program, Rapmad, to identify bound peptides while excluding false positives identified in the Hsp70 NBD experiment [138]. The optional random forest procedure to remove potentially unreliable peptide spots was excluded from the analysis. Odds ratios (OR) were calculated for each individual experiment using the following equation;

$$OR = (FB*NN)/(NB*FN) \qquad \text{(Equation 1)}$$

FB indicates fibril forming peptides found to bind the chaperone, FN indicates fibril forming peptides found to not bind, NB indicates non-fibril forming peptides found to bind, and NN indicates non-fibril forming peptides found to not bind. Further, for proteins tested more than once, an OR was calculated for the combined data. In combining the data binding was defined as peptides found to bind in ≥ 2/3 of experiments for that chaperone (see Appendix A.3 for full results).

3.6 Appendix

Appendix 3.1 Luciferase Array Peptides

Luciferase	Peptide
1	MEDAKNIKKGPAPFY
5	KNIKKGPAPFYPLED
9	KGPAPFYPLEDGTAG
13	PFYPLEDGTAGEQLH
17	LEDGTAGEQLHKAMK
21	TAGEQLHKAMKRYAL
25	QLHKAMKRYALVPGT
29	AMKRYALVPGTIAFT
33	YALVPGTIAFTDAHI
37	PGTIAFTDAHIEVNI
41	AFTDAHIEVNITYAE
45	AHIEVNITYAEYFEM
49	VNITYAEYFEMSVRL
53	YAEYFEMSVRLAEAM
57	FEMSVRLAEAMKRYG
61	VRLAEAMKRYGLNTN
65	EAMKRYGLNTNHRIV
69	RYGLNTNHRIVVCSE
73	NTNHRIVVCSENSLQ
77	RIVVCSENSLQFFMP
81	CSENSLQFFMPVLGA
85	SLQFFMPVLGALFIG
89	FMPVLGALFIGVAVA
93	LGALFIGVAVAPAND
97	FIGVAVAPANDIYNE
101	AVAPANDIYNERELL
105	ANDIYNERELLNSMN
109	YNERELLNSMNISQP
113	ELLNSMNISQPTVVF
117	SMNISQPTVVFVSKK
121	SQPTVVFVSKKGLQK
125	VVFVSKKGLQKILNV
129	SKKGLQKILNVQKKL
133	LQKILNVQKKLPIIQ
137	LNVQKKLPIIQKIII
141	KKLPIIQKIIIMDSK
145	IIQKIIIMDSKTDYQ
149	IIIMDSKTDYQGFQS
153	DSKTDYQGFQSMYTF
157	DYQGFQSMYTFVTSH
161	FQSMYTFVTSHLPPG
165	YTFVTSHLPPGFNEY
169	TSHLPPGFNEYDFVP
173	PPGFNEYDFVPESFD
177	NEYDFVPESFDRDKT
181	FVPESFDRDKTIALI
185	SFDRDKTIALIMNSS
189	DKTIALIMNSSGSTG
193	ALIMNSSGSTGLPKG
197	NSSGSTGLPKGVALP
201	STGLPKGVALPHRTA
205	PKGVALPHRTACVRF
209	ALPHRTACVRFSHAR
213	RTACVRFSHARDPIF
217	VRFSHARDPIFGNQI
221	HARDPIFGNQIIPDT
225	PIFGNQIIPDTAILS
229	NQIIPDTAILSVVPF
233	PDTAILSVVPFHHGF
237	ILSVVPFHHGFGMFT
241	VPFHHGFGMFTTLGY
245	HGFGMFTTLGYLICG
249	MFTTLGYLICGFRVV
253	LGYLICGFRVVLMYR
257	ICGFRVVLMYRFEEE
261	RVVLMYRFEEELFLR
265	MYRFEEELFLRSLQD
269	EEELFLRSLQDYKIQ
273	FLRSLQDYKIQSALL
277	LQDYKIQSALLVPTL
281	KIQSALLVPTLFSFF
285	ALLVPTLFSFFAKST
289	PTLFSFFAKSTLIDK
293	SFFAKSTLIDKYDLS
297	KSTLIDKYDLSNLHE
301	IDKYDLSNLHEIASG
305	DLSNLHEIASGGAPL
309	LHEIASGGAPLSKEV
313	ASGGAPLSKEVGEAV
317	APLSKEVGEAVAKRF
321	KEVGEAVAKRFHLPG
325	EAVAKRFHLPGIRQG
329	KRFHLPGIRQGYGLT

333	LPGIRQGYGLTETTS
337	RQGYGLTETTSAILI
341	GLTETTSAILITPEG
345	TTSAILITPEGDDKP
349	ILITPEGDDKPGAVG
353	PEGDDKPGAVGKVVP
357	DKPGAVGKVVPFFEA
361	AVGKVVPFFEAKVVD
365	VVPFFEAKVVDLDTG
369	FEAKVVDLDTGKTLG
373	VVDLDTGKTLGVNQR
377	DTGKTLGVNQRGELC
381	TLGVNQRGELCVRGP
385	NQRGELCVRGPMIMS
389	ELCVRGPMIMSGYVN
393	RGPMIMSGYVNNPEA
397	IMSGYVNNPEATNAL
401	YVNNPEATNALIDKD
405	PEATNALIDKDGWLH
409	NALIDKDGWLHSGDI
413	DKDGWLHSGDIAYWD
417	WLHSGDIAYWDEDEH
421	GDIAYWDEDEHFFIV
425	YWDEDEHFFIVDRLK
429	DEHFFIVDRLKSLIK
433	FIVDRLKSLIKYKGY

437	RLKSLIKYKGYQVAP
441	LIKYKGYQVAPAELE
445	KGYQVAPAELESILL
449	VAPAELESILLQHPN
453	ELESILLQHPNIFDA
457	ILLQHPNIFDAGVAG
461	HPNIFDAGVAGLPDD
465	FDAGVAGLPDDDAGE
469	VAGLPDDDAGELPAA
473	PDDDAGELPAAVVVL
477	AGELPAAVVVLEHGK
481	PAAVVVLEHGKTMTE
485	VVLEHGKTMTEKEIV
489	HGKTMTEKEIVDYVA
493	MTEKEIVDYVASQVT
497	EIVDYVASQVTTAKK
501	YVASQVTTAKKLRGG
505	QVTTAKKLRGGVVFV
509	AKKLRGGVVFVDEVP
513	RGGVVFVDEVPKGLT
517	VFVDEVPKGLTGKLD
521	EVPKGLTGKLDARKI
525	GLTGKLDARKIREIL
529	KLDARKIREILIKAK
533	RKIREILIKAKKGGK
536	REILIKAKKGGKSKL

Appendix 3.2 Tau Array Peptides

PNS	4R2N	Peptide Sequence
1	**1**	**MAEPRQEFEVMEDHA**
5	**5**	**RQEFEVMEDHAGTYG**
9	**9**	**EVMEDHAGTYGLGDR**
13	**13**	**DHAGTYGLGDRKDQG**
17	**17**	**TYGLGDRKDQGGYTM**
21	**21**	**GDRKDQGGYTMHQDQ**
25	**25**	**DQGGYTMHQDQEGDT**
29	**29**	**YTMHQDQEGDTDAGL**
33	**33**	**QDQEGDTDAGLKESP**
37	**37**	**GDTDAGLKESPLQTP**
41	**41**	**AGLKESPLQTPTEDG**
45	**45**	**ESPLQTPTEDGSEEP**
49	**49**	**QTPTEDGSEEPGSET**
53	**53**	**EDGSEEPGSETSDAK**
57	**57**	**EEPGSETSDAKSTPT**
61	**61**	**SETSDAKSTPTAEDV**
65	**65**	**DAKSTPTAEDVTAPL**
69	**69**	**TPTAEDVTAPLVDEG**
73	**73**	**EDVTAPLVDEGAPGK**
77	**77**	**APLVDEGAPGKQAAA**
81	**81**	**DEGAPGKQAAAQPHT**
85	**85**	**PGKQAAAQPHTEIPE**
89	**89**	**AAAQPHTEIPEGTTA**
93	**93**	**PHTEIPEGTTAEEAG**
97	**97**	**IPEGTTAEEAGIGDT**
101	**101**	**TTAEEAGIGDTPSLE**
105	**105**	**EAGIGDTPSLEDEAA**
109	**109**	**GDTPSLEDEAAGHVT**
113	**113**	**SLEDEAAGHVTQ**EPE
117	**117**	**EAAGHVTQ**EPESGKV
121		HVTQEPESGKVVQEG
125		EPESGKVVQEGFLRE
129		GKVVQEGFLREPGPP
133		QEGFLREPGPPGLSH
137		LREPGPPGLSHQLMS
141		GPPGLSHQLMSGMPG
145		LSHQLMSGMPGAPLL
149		LMSGMPGAPLLPEGP
153		MPGAPLLPEGPREAT
157		PLLPEGPREATRQPS
161		EGPREATRQPSGTGP
165		EATRQPSGTGPEDTE
169		QPSGTGPEDTEGGRH
173		TGPEDTEGGRHAPEL
177		DTEGGRHAPELLKHQ
181		GRHAPELLKHQLLGD
185		PELLKHQLLGDLHQE
189		KHQLLGDLHQEGPPL
193		LGDLHQEGPPLKGAG
197		HQEGPPLKGAGGKER
201		PPLKGAGGKERPGSK
205		GAGGKERPGSKEEVD
209		KERPGSKEEVDEDRD
213		GSKEEVDEDRDVDES
217		EVDEDRDVDESSPQD
221		DRDVDESSPQDSPPS
225		DESSPQDSPPSKASP
229		PQDSPPSKASPAQDG
233		PPSKASPAQDGRPPQ
237		ASPAQDGRPPQTAAR
241		QDGRPPQTAAREATS
245		PPQTAAREATSIPGF
249		AAREATSIPGFPAEG
253		ATSIPGFPAEGAIPL
257		PGFPAEGAIPLPVDF
261		AEGAIPLPVDFLSKV
265		IPLPVDFLSKVSTEI
269		VDFLSKVSTEIPASE
273		SKVSTEIPASEPDGP
277		TEIPASEPDGPSVGR
281		ASEPDGPSVGRAKGQ
285		DGPSVGRAKGQDAPL
289		VGRAKGQDAPLEFTF
293		KGQDAPLEFTFHVEI
297		APLEFTFHVEITPNV

301		FTFHVEITPNVQKEQ
305		VEITPNVQKEQAHSE
309		PNVQKEQAHSEEHLG
313		KEQAHSEEHLGRAAF
317		HSEEHLGRAAFPGAP
321		HLGRAAFPGAPGEGP
325		AAFPGAPGEGPEARG
329		GAPGEGPEARGPSLG
333		EGPEARGPSLGEDTK
337		ARGPSLGEDTKEADL
341		SLGEDTKEADLPEPS
345		DTKEADLPEPSEKQP
349		ADLPEPSEKQPAAAP
353		EPSEKQPAAAPRGKP
357		KQPAAAPRGKPVSRV
361		AAPRGKPVSRVPQLK
365		GKPVSRVPQLKARMV
369		SRVPQLKARMVSKSK
373	**125**	QLK**ARMVSKSKDGTG**
377	**126**	**RMVSKSKDGTGSDDK**
381	**130**	**KSKDGTGSDDKKAK**T
385	**134**	**GTGSDDKKAK**TSTRS
389		DDKKAKTSTRSSAKT
393		AKTSTRSSAKTLKNR
397		TRSSAKTLKNRPCLS
401		AKTLKNRPCLSPKLP
405		KNRPCLSPKLPTPGS
409		CLSPKLPTPGSSDPL
413		KLPTPGSSDPLIQPS
417		PGSSDPLIQPSSPAV
421		DPLIQPSSPAVCPEP
425		QPSSPAVCPEPPSSP
429		PAVCPEPPSSPKHVS
433		PEPPSSPKHVSSVTS
437		SSPKHVSSVTSRTGS
441		HVSSVTSRTGSSGAK
445		VTSRTGSSGAKEMKL
449		TGSSGAKEMKLKGAD
453		GAKEMKLKGADGKTK
457	**143**	MKL**KGADGKTKIATP**

461	**144**	**GADGKTKIATPRGAA**
465	**148**	**KTKIATPRGAAPPGQ**
469	**152**	**ATPRGAAPPGQKGQA**
473	**156**	**GAAPPGQKGQANATR**
477	**160**	**PGQKGQANATRIPAK**
481	**164**	**GQANATRIPAKTPPA**
485	**168**	**ATRIPAKTPPAPKTP**
489	**172**	**PAKTPPAPKTPPSSG**
493	**176**	**PPAPKTPPSSGEPPK**
497	**180**	**KTPPSSGEPPKSGDR**
501	**184**	**SSGEPPKSGDRSGYS**
505	**188**	**PPKSGDRSGYSSPGS**
509	**192**	**GDRSGYSSPGSPGTP**
513	**196**	**GYSSPGSPGTPGSRS**
517	**200**	**PGSPGTPGSRSRTPS**
521	**204**	**GTPGSRSRTPSLPTP**
525	**208**	**SRSRTPSLPTPPTRE**
529	**212**	**TPSLPTPPTREPKKV**
533	**216**	**PTPPTREPKKVAVVR**
537	**220**	**TREPKKVAVVRTPPK**
541	**224**	**KKVAVVRTPPKSPSS**
545	**228**	**VVRTPPKSPSSAKSR**
549	**232**	**PPKSPSSAKSRLQTA**
553	**236**	**PSSAKSRLQTAPVPM**
557	**240**	**KSRLQTAPVPMPDLK**
561	**244**	**QTAPVPMPDLKNVKS**
565	**248**	**VPMPDLKNVKSKIGS**
569	**252**	**DLKNVKSKIGSTENL**
573	**256**	**VKSKIGSTENLKHQP**
577	**260**	**IGSTENLKHQPGGGK**
581	**264**	**ENLKHQPGGGKVQII**
585	**268**	**HQPGGGKVQIINKKL**
589	**272**	**GGKVQIINKKLDLSN**
593	**276**	**QIINKKLDLSNVQSK**
597	**280**	**KKLDLSNVQSKCGSK**
601	**284**	**LSNVQSKCGSKDNIK**
605	**288**	**QSKCGSKDNIKHVPG**
609	**292**	**GSKDNIKHVPGGGSV**
613	**296**	**NIKHVPGGGSVQIVY**
617	**300**	**VPGGGSVQIVYKPVD**

621	**304**	**GSVQIVYKPVDLSKV**
625	**308**	**IVYKPVDLSKVTSKC**
629	**312**	**PVDLSKVTSKCGSLG**
633	**316**	**SKVTSKCGSLGNIHH**
637	**320**	**SKCGSLGNIHHKPGG**
641	**324**	**SLGNIHHKPGGGQVE**
645	**328**	**IHHKPGGGQVEVKSE**
649	**332**	**PGGGQVEVKSEKLDF**
653	**336**	**QVEVKSEKLDFKDRV**
657	**340**	**KSEKLDFKDRVQSKI**
661	**344**	**LDFKDRVQSKIGSLD**
665	**348**	**DRVQSKIGSLDNITH**
669	**352**	**SKIGSLDNITHVPGG**
673	**356**	**SLDNITHVPGGGNKK**
677	**360**	**ITHVPGGGNKKIETH**
681	**364**	**PGGGNKKIETHKLTF**
685	**368**	**NKKIETHKLTFRENA**
689	**372**	**ETHKLTFRENAKAKT**
693	**376**	**LTFRENAKAKTDHGA**
697	**380**	**ENAKAKTDHGAEIVY**
701	**384**	**AKTDHGAEIVYKSPV**
705	**388**	**HGAEIVYKSPVVSGD**
709	**392**	**IVYKSPVVSGDTSPR**
713	**396**	**SPVVSGDTSPRHLSN**
717	**400**	**SGDTSPRHLSNVSST**
721	**404**	**SPRHLSNVSSTGSID**
725	**408**	**LSNVSSTGSIDMVDS**
729	**412**	**SSTGSIDMVDSPQLA**
733	**416**	**SIDMVDSPQLATLAD**
737	**420**	**VDSPQLATLADEVSA**
741	**424**	**QLATLADEVSASLAK**
744	**427**	**TLADEVSASLAKQGL**
P1	P1	**GYSSPGEPGEPGSRS**
P2	P2	**GYSSPGEPGTPGSRS**
P3	P3	**PGSPGEPGSRSRTPS**
P4	P4	**VKSKIGETENLKHQP**
P5	P5	**DRVQSKIGELDNITH**
P6	P6	**HGAEIVYKEPVVSGD**
P7	P7	**SPVVSGDTEPRHLSN**

3.7 References

[1] Schroder H, Langer T, Hartl FU, Bukau B. DnaK, DnaJ and GrpE form a cellular chaperone machinery capable of repairing heat-induced protein damage. EMBO J, 1993; 12: 4137-44.

[2] Minami Y, Hohfeld J, Ohtsuka K, Hartl FU. Regulation of the heat-shock protein 70 reaction cycle by the mammalian DnaJ homolog, Hsp40. J Biol Chem, 1996; 271: 19617-24.

[3] Lu Z, Cyr DM. The conserved carboxyl terminus and zinc finger-like domain of the co-chaperone Ydj1 assist Hsp70 in protein folding. J Biol Chem, 1998; 273: 5970-8.

[4] Szabo A, Langer T, Schroder H, Flanagan J, Bukau B, Hartl FU. The ATP hydrolysis-dependent reaction cycle of the Escherichia coli Hsp70 system DnaK, DnaJ, and GrpE. Proc Natl Acad Sci U S A, 1994; 91: 10345-9.

[5] Szabo A, Korszun R, Hartl FU, Flanagan J. A zinc finger-like domain of the molecular chaperone DnaJ is involved in binding to denatured protein substrates. EMBO J, 1996; 15: 408-17.

[6] Lu Z, Cyr DM. Protein folding activity of Hsp70 is modified differentially by the hsp40 co-chaperones Sis1 and Ydj1. J Biol Chem, 1998; 273: 27824-30.

[7] Fan CY, Lee S, Ren HY, Cyr DM. Exchangeable chaperone modules contribute to specification of type I and type II Hsp40 cellular function. Mol Biol Cell, 2004; 15: 761-73.

[8] Summers DW, Douglas PM, Ren HY, Cyr DM. The type I Hsp40 Ydj1 utilizes a farnesyl moiety and zinc finger-like region to suppress prion toxicity. J Biol Chem, 2009; 284: 3628-39.

[9] Bhangoo MK, Tzankov S, Fan AC, Dejgaard K, Thomas DY, Young JC. Multiple 40-kDa heat-shock protein chaperones function in Tom70-dependent mitochondrial import. Mol Biol Cell, 2007; 18: 3414-28.

[10] Tzankov S, Wong MJ, Shi K, Nassif C, Young JC. Functional divergence between co-chaperones of Hsc70. J Biol Chem, 2008; 283: 27100-9.

[11] Hageman J, van Waarde MA, Zylicz A, Walerych D, Kampinga HH. The diverse members of the mammalian HSP70 machine show distinct chaperone-like activities. Biochem J, 2011; 435: 127-42.

[12] Goedert M, Jakes R, Crowther RA, Hasegawa M, Smith MJ, Spillantini MG. Intraneuronal filamentous tau protein and alpha-synuclein deposits in neurodegenerative diseases. Biochem Soc Trans, 1998; 26: 463-71.

[13] Spillantini MG, Goedert M. Tau protein pathology in neurodegenerative diseases. Trends Neurosci, 1998; 21: 428-33.

[14] Williams DR. Tauopathies: classification and clinical update on neurodegenerative diseases associated with microtubule-associated protein tau. Intern Med J, 2006; 36: 652-60.

[15] Drechsel DN, Hyman AA, Cobb MH, Kirschner MW. Modulation of the dynamic instability of tubulin assembly by the microtubule-associated protein tau. Mol Biol Cell, 1992; 3: 1141-54.
[16] Drubin DG, Feinstein SC, Shooter EM, Kirschner MW. Nerve growth factor-induced neurite outgrowth in PC12 cells involves the coordinate induction of microtubule assembly and assembly-promoting factors. J Cell Biol, 1985; 101: 1799-807.
[17] Butner KA, Kirschner MW. Tau protein binds to microtubules through a flexible array of distributed weak sites. J Cell Biol, 1991; 115: 717-30.
[18] Kidd M. Paired helical filaments in electron microscopy of Alzheimer's disease. Nature, 1963; 197: 192-3.
[19] Wischik CM, Novak M, Edwards PC, Klug A, Tichelaar W, Crowther RA. Structural characterization of the core of the paired helical filament of Alzheimer disease. Proc Natl Acad Sci U S A, 1988; 85: 4884-8.
[20] Wille H, Drewes G, Biernat J, Mandelkow EM, Mandelkow E. Alzheimer-like paired helical filaments and antiparallel dimers formed from microtubule-associated protein tau in vitro. J Cell Biol, 1992; 118: 573-84.
[21] Friedhoff P, Schneider A, Mandelkow EM, Mandelkow E. Rapid assembly of Alzheimer-like paired helical filaments from microtubule-associated protein tau monitored by fluorescence in solution. Biochemistry, 1998; 37: 10223-30.
[22] Friedhoff P, von Bergen M, Mandelkow EM, Davies P, Mandelkow E. A nucleated assembly mechanism of Alzheimer paired helical filaments. Proc Natl Acad Sci U S A, 1998; 95: 15712-7.
[23] Braak H, Braak E. Staging of Alzheimer's disease-related neurofibrillary changes. Neurobiol Aging, 1995; 16: 271-8; discussion 278-84.
[24] Ramsden M, Kotilinek L, Forster C, Paulson J, McGowan E, SantaCruz K, Guimaraes A, Yue M, Lewis J, Carlson G, Hutton M, Ashe KH. Age-dependent neurofibrillary tangle formation, neuron loss, and memory impairment in a mouse model of human tauopathy (P301L). J Neurosci, 2005; 25: 10637-47.
[25] Santacruz K, Lewis J, Spires T, Paulson J, Kotilinek L, Ingelsson M, Guimaraes A, DeTure M, Ramsden M, McGowan E, Forster C, Yue M, Orne J, Janus C, Mariash A, Kuskowski M, Hyman B, Hutton M, Ashe KH. Tau suppression in a neurodegenerative mouse model improves memory function. Science, 2005; 309: 476-81.
[26] Hardy J, Selkoe DJ. The amyloid hypothesis of Alzheimer's disease: progress and problems on the road to therapeutics. Science, 2002; 297: 353-6.
[27] Tanzi RE, Bertram L. Twenty years of the Alzheimer's disease amyloid hypothesis: a genetic perspective. Cell, 2005; 120: 545-55.
[28] Roberson ED, Halabisky B, Yoo JW, Yao J, Chin J, Yan F, Wu T, Hamto P, Devidze N, Yu GQ, Palop JJ, Noebels JL, Mucke L. Amyloid-beta/Fyn-induced synaptic, network, and cognitive impairments depend on tau levels in multiple mouse models of Alzheimer's disease. J Neurosci, 2011; 31: 700-11.
[29] Vossel KA, Zhang K, Brodbeck J, Daub AC, Sharma P, Finkbeiner S, Cui B, Mucke L. Tau reduction prevents Abeta-induced defects in axonal transport. Science, 2010; 330: 198.

[30] Ittner LM, Ke YD, Delerue F, Bi M, Gladbach A, van Eersel J, Wolfing H, Chieng BC, Christie MJ, Napier IA, Eckert A, Staufenbiel M, Hardeman E, Gotz J. Dendritic function of tau mediates amyloid-beta toxicity in Alzheimer's disease mouse models. Cell, 2010; 142: 387-97.
[31] Ittner LM, Gotz J. Amyloid-beta and tau--a toxic pas de deux in Alzheimer's disease. Nat Rev Neurosci, 2011; 12: 65-72.
[32] Goedert M, Spillantini MG. Tau mutations in frontotemporal dementia FTDP-17 and their relevance for Alzheimer's disease. Biochim Biophys Acta, 2000; 1502: 110-21.
[33] van Swieten J, Spillantini MG. Hereditary frontotemporal dementia caused by Tau gene mutations. Brain Pathol, 2007; 17: 63-73.
[34] Gasparini L, Terni B, Spillantini MG. Frontotemporal dementia with tau pathology. Neurodegener Dis, 2007; 4: 236-53.
[35] Spires-Jones TL, Stoothoff WH, de Calignon A, Jones PB, Hyman BT. Tau pathophysiology in neurodegeneration: a tangled issue. Trends Neurosci, 2009; 32: 150-9.
[36] Maeda S, Sahara N, Saito Y, Murayama M, Yoshiike Y, Kim H, Miyasaka T, Murayama S, Ikai A, Takashima A. Granular tau oligomers as intermediates of tau filaments. Biochemistry, 2007; 46: 3856-61.
[37] Hanger DP, Anderton BH, Noble W. Tau phosphorylation: the therapeutic challenge for neurodegenerative disease. Trends Mol Med, 2009; 15: 112-9.
[38] Grundke-Iqbal I, Iqbal K, Tung YC, Quinlan M, Wisniewski HM, Binder LI. Abnormal phosphorylation of the microtubule-associated protein tau (tau) in Alzheimer cytoskeletal pathology. Proc Natl Acad Sci U S A, 1986; 83: 4913-7.
[39] Stoothoff WH, Johnson GV. Tau phosphorylation: physiological and pathological consequences. Biochim Biophys Acta, 2005; 1739: 280-97.
[40] Bhaskar K, Yen SH, Lee G. Disease-related modifications in tau affect the interaction between Fyn and Tau. J Biol Chem, 2005; 280: 35119-25.
[41] Wang Y, Garg S, Mandelkow EM, Mandelkow E. Proteolytic processing of tau. Biochem Soc Trans, 2010; 38: 955-61.
[42] Zilka N, Kovacech B, Barath P, Kontsekova E, Novak M. The self-perpetuating tau truncation circle. Biochem Soc Trans, 2012; 40: 681-6.
[43] Mandelkow EM, Mandelkow E. Biochemistry and cell biology of tau protein in neurofibrillary degeneration. Cold Spring Harb Perspect Med, 2012; 2: a006247.
[44] Sahara N, Maeda S, Yoshiike Y, Mizoroki T, Yamashita S, Murayama M, Park JM, Saito Y, Murayama S, Takashima A. Molecular chaperone-mediated tau protein metabolism counteracts the formation of granular tau oligomers in human brain. J Neurosci Res, 2007; 85: 3098-108.
[45] Koren J, 3rd, Jinwal UK, Lee DC, Jones JR, Shults CL, Johnson AG, Anderson LJ, Dickey CA. Chaperone signalling complexes in Alzheimer's disease. J Cell Mol Med, 2009; 13: 619-30.
[46] Miyata Y, Koren J, Kiray J, Dickey CA, Gestwicki JE. Molecular chaperones and regulation of tau quality control: strategies for drug discovery in tauopathies. Future Med Chem, 2011; 3: 1523-37.
[47] Dickey CA, Kamal A, Lundgren K, Klosak N, Bailey RM, Dunmore J, Ash P, Shoraka S, Zlatkovic J, Eckman CB, Patterson C, Dickson DW, Nahman NS, Jr.,

Hutton M, Burrows F, Petrucelli L. The high-affinity HSP90-CHIP complex recognizes and selectively degrades phosphorylated tau client proteins. J Clin Invest, 2007; 117: 648-58.
[48] Thompson AD, Scaglione KM, Prensner J, Gillies AT, Chinnaiyan A, Paulson HL, Jinwal UK, Dickey CA, Gestwicki JE. Analysis of the tau-associated proteome reveals that exchange of Hsp70 for Hsp90 is involved in tau degradation. ACS Chem Biol, 2012; 7: 1677-86.
[49] Dou F, Netzer WJ, Tanemura K, Li F, Hartl FU, Takashima A, Gouras GK, Greengard P, Xu H. Chaperones increase association of tau protein with microtubules. Proc Natl Acad Sci U S A, 2003; 100: 721-6.
[50] Abisambra JF, Jinwal UK, Suntharalingam A, Arulselvam K, Brady S, Cockman M, Jin Y, Zhang B, Dickey CA. DnaJA1 antagonizes constitutive Hsp70-mediated stabilization of tau. J Mol Biol, 2012; 421: 653-61.
[51] Shimura H, Miura-Shimura Y, Kosik KS. Binding of tau to heat shock protein 27 leads to decreased concentration of hyperphosphorylated tau and enhanced cell survival. J Biol Chem, 2004; 279: 17957-62.
[52] Sarkar M, Kuret J, Lee G. Two motifs within the tau microtubule-binding domain mediate its association with the hsc70 molecular chaperone. J Neurosci Res, 2008; 86: 2763-73.
[53] von Bergen M, Friedhoff P, Biernat J, Heberle J, Mandelkow EM, Mandelkow E. Assembly of tau protein into Alzheimer paired helical filaments depends on a local sequence motif ((306)VQIVYK(311)) forming beta structure. Proc Natl Acad Sci U S A, 2000; 97: 5129-34.
[54] von Bergen M, Barghorn S, Li L, Marx A, Biernat J, Mandelkow EM, Mandelkow E. Mutations of tau protein in frontotemporal dementia promote aggregation of paired helical filaments by enhancing local beta-structure. J Biol Chem, 2001; 276: 48165-74.
[55] Mukrasch MD, Biernat J, von Bergen M, Griesinger C, Mandelkow E, Zweckstetter M. Sites of tau important for aggregation populate {beta}-structure and bind to microtubules and polyanions. J Biol Chem, 2005; 280: 24978-86.
[56] Wang Y, Martinez-Vicente M, Kruger U, Kaushik S, Wong E, Mandelkow EM, Cuervo AM, Mandelkow E. Tau fragmentation, aggregation and clearance: the dual role of lysosomal processing. Hum Mol Genet, 2009; 18: 4153-70.
[57] Jinwal UK, Akoury E, Abisambra JF, O'Leary JC, 3rd, Thompson AD, Blair LJ, Jin Y, Bacon J, Nordhues BA, Cockman M, Zhang J, Li P, Zhang B, Borysov S, Uversky VN, Biernat J, Mandelkow E, Gestwicki JE, Zweckstetter M, Dickey CA. Imbalance of Hsp70 family variants fosters tau accumulation. FASEB J, 2012.
[58] Katz C, Levy-Beladev L, Rotem-Bamberger S, Rito T, Rudiger SG, Friedler A. Studying protein-protein interactions using peptide arrays. Chem Soc Rev, 2011; 40: 2131-45.
[59] Rudiger S, Germeroth L, Schneider-Mergener J, Bukau B. Substrate specificity of the DnaK chaperone determined by screening cellulose-bound peptide libraries. EMBO J, 1997; 16: 1501-7.
[60] Rudiger S, Schneider-Mergener J, Bukau B. Its substrate specificity characterizes the DnaJ co-chaperone as a scanning factor for the DnaK chaperone. EMBO J, 2001; 20: 1042-50.

[61] Rodriguez F, Arsene-Ploetze F, Rist W, Rudiger S, Schneider-Mergener J, Mayer MP, Bukau B. Molecular basis for regulation of the heat shock transcription factor sigma32 by the DnaK and DnaJ chaperones. Mol Cell, 2008; 32: 347-58.
[62] Terada K, Oike Y. Multiple molecules of Hsc70 and a dimer of DjA1 independently bind to an unfolded protein. J Biol Chem, 2010; 285: 16789-97.
[63] Rudiger S, Buchberger A, Bukau B. Interaction of Hsp70 chaperones with substrates. Nat Struct Biol, 1997; 4: 342-9.
[64] Kota P, Summers DW, Ren HY, Cyr DM, Dokholyan NV. Identification of a consensus motif in substrates bound by a Type I Hsp40. Proc Natl Acad Sci U S A, 2009; 106: 11073-8.
[65] Tapia V, Bongartz J, Schutkowski M, Bruni N, Weiser A, Ay B, Volkmer R, Or-Guil M. Affinity profiling using the peptide microarray technology: a case study. Anal Biochem, 2007; 363: 108-18.
[66] Baldi P, Long AD. A Bayesian framework for the analysis of microarray expression data: regularized t -test and statistical inferences of gene changes. Bioinformatics, 2001; 17: 509-19.
[67] Baldi P, Hatfield GW. DNA microarrays and gene expression. Cambridge University Press: Cambridge, UK ; New York, NY 2002.
[68] Ikai A. Thermostability and aliphatic index of globular proteins. J Biochem, 1980; 88: 1895-8.
[69] Kyte J, Doolittle RF. A simple method for displaying the hydropathic character of a protein. J Mol Biol, 1982; 157: 105-32.
[70] Bjellqvist B, Hughes GJ, Pasquali C, Paquet N, Ravier F, Sanchez JC, Frutiger S, Hochstrasser D. The focusing positions of polypeptides in immobilized pH gradients can be predicted from their amino acid sequences. Electrophoresis, 1993; 14: 1023-31.
[71] Mukrasch MD, Markwick P, Biernat J, Bergen M, Bernado P, Griesinger C, Mandelkow E, Zweckstetter M, Blackledge M. Highly populated turn conformations in natively unfolded tau protein identified from residual dipolar couplings and molecular simulation. J Am Chem Soc, 2007; 129: 5235-43.
[72] Mukrasch MD, Bibow S, Korukottu J, Jeganathan S, Biernat J, Griesinger C, Mandelkow E, Zweckstetter M. Structural polymorphism of 441-residue tau at single residue resolution. PLoS Biol, 2009; 7: e34.
[73] Goode BL, Denis PE, Panda D, Radeke MJ, Miller HP, Wilson L, Feinstein SC. Functional interactions between the proline-rich and repeat regions of tau enhance microtubule binding and assembly. Mol Biol Cell, 1997; 8: 353-65.
[74] Reynolds CH, Garwood CJ, Wray S, Price C, Kellie S, Perera T, Zvelebil M, Yang A, Sheppard PW, Varndell IM, Hanger DP, Anderton BH. Phosphorylation regulates tau interactions with Src homology 3 domains of phosphatidylinositol 3-kinase, phospholipase Cgamma1, Grb2, and Src family kinases. J Biol Chem, 2008; 283: 18177-86.
[75] Ding H, Matthews TA, Johnson GV. Site-specific phosphorylation and caspase cleavage differentially impact tau-microtubule interactions and tau aggregation. J Biol Chem, 2006; 281: 19107-14.
[76] Zhou XZ, Lu PJ, Wulf G, Lu KP. Phosphorylation-dependent prolyl isomerization: a novel signaling regulatory mechanism. Cell Mol Life Sci, 1999; 56: 788-806.

[77] Lu PJ, Wulf G, Zhou XZ, Davies P, Lu KP. The prolyl isomerase Pin1 restores the function of Alzheimer-associated phosphorylated tau protein. Nature, 1999; 399: 784-8.
[78] Barghorn S, Zheng-Fischhofer Q, Ackmann M, Biernat J, von Bergen M, Mandelkow EM, Mandelkow E. Structure, microtubule interactions, and paired helical filament aggregation by tau mutants of frontotemporal dementias. Biochemistry, 2000; 39: 11714-21.
[79] Fischer D, Mukrasch MD, von Bergen M, Klos-Witkowska A, Biernat J, Griesinger C, Mandelkow E, Zweckstetter M. Structural and microtubule binding properties of tau mutants of frontotemporal dementias. Biochemistry, 2007; 46: 2574-82.
[80] Min SW, Cho SH, Zhou Y, Schroeder S, Haroutunian V, Seeley WW, Huang EJ, Shen Y, Masliah E, Mukherjee C, Meyers D, Cole PA, Ott M, Gan L. Acetylation of tau inhibits its degradation and contributes to tauopathy. Neuron, 2010; 67: 953-66.
[81] Cohen TJ, Guo JL, Hurtado DE, Kwong LK, Mills IP, Trojanowski JQ, Lee VM. The acetylation of tau inhibits its function and promotes pathological tau aggregation. Nat Commun, 2011; 2: 252.
[82] Derkinderen P, Scales TM, Hanger DP, Leung KY, Byers HL, Ward MA, Lenz C, Price C, Bird IN, Perera T, Kellie S, Williamson R, Noble W, Van Etten RA, Leroy K, Brion JP, Reynolds CH, Anderton BH. Tyrosine 394 is phosphorylated in Alzheimer's paired helical filament tau and in fetal tau with c-Abl as the candidate tyrosine kinase. J Neurosci, 2005; 25: 6584-93.
[83] Vega IE, Cui L, Propst JA, Hutton ML, Lee G, Yen SH. Increase in tau tyrosine phosphorylation correlates with the formation of tau aggregates. Brain Res Mol Brain Res, 2005; 138: 135-44.
[84] Tremblay MA, Acker CM, Davies P. Tau phosphorylated at tyrosine 394 is found in Alzheimer's disease tangles and can be a product of the Abl-related kinase, Arg. J Alzheimers Dis, 2010; 19: 721-33.
[85] Otvos L, Jr., Feiner L, Lang E, Szendrei GI, Goedert M, Lee VM. Monoclonal antibody PHF-1 recognizes tau protein phosphorylated at serine residues 396 and 404. J Neurosci Res, 1994; 39: 669-73.
[86] Abraha A, Ghoshal N, Gamblin TC, Cryns V, Berry RW, Kuret J, Binder LI. C-terminal inhibition of tau assembly in vitro and in Alzheimer's disease. J Cell Sci, 2000; 113 Pt 21: 3737-45.
[87] Ferrari A, Hoerndli F, Baechi T, Nitsch RM, Gotz J. beta-Amyloid induces paired helical filament-like tau filaments in tissue culture. J Biol Chem, 2003; 278: 40162-8.
[88] Haase C, Stieler JT, Arendt T, Holzer M. Pseudophosphorylation of tau protein alters its ability for self-aggregation. J Neurochem, 2004; 88: 1509-20.
[89] Dickey CA, Dunmore J, Lu B, Wang JW, Lee WC, Kamal A, Burrows F, Eckman C, Hutton M, Petrucelli L. HSP induction mediates selective clearance of tau phosphorylated at proline-directed Ser/Thr sites but not KXGS (MARK) sites. FASEB J, 2006; 20: 753-5.
[90] Murrell JR, Spillantini MG, Zolo P, Guazzelli M, Smith MJ, Hasegawa M, Redi F, Crowther RA, Pietrini P, Ghetti B, Goedert M. Tau gene mutation G389R causes a tauopathy with abundant pick body-like inclusions and axonal deposits. J Neuropathol Exp Neurol, 1999; 58: 1207-26.

[91] Moore CL, Huang MH, Robbennolt SA, Voss KR, Combs B, Gamblin TC, Goux WJ. Secondary nucleating sequences affect kinetics and thermodynamics of tau aggregation. Biochemistry, 2011; 50: 10876-86.
[92] Yanagawa H, Chung SH, Ogawa Y, Sato K, Shibata-Seki T, Masai J, Ishiguro K. Protein anatomy: C-tail region of human tau protein as a crucial structural element in Alzheimer's paired helical filament formation in vitro. Biochemistry, 1998; 37: 1979-88.
[93] Jeganathan S, von Bergen M, Brutlach H, Steinhoff HJ, Mandelkow E. Global hairpin folding of tau in solution. Biochemistry, 2006; 45: 2283-93.
[94] Horowitz PM, LaPointe N, Guillozet-Bongaarts AL, Berry RW, Binder LI. N-terminal fragments of tau inhibit full-length tau polymerization in vitro. Biochemistry, 2006; 45: 12859-66.
[95] Jinwal UK, O'Leary JC, 3rd, Borysov SI, Jones JR, Li Q, Koren J, 3rd, Abisambra JF, Vestal GD, Lawson LY, Johnson AG, Blair LJ, Jin Y, Miyata Y, Gestwicki JE, Dickey CA. Hsc70 rapidly engages tau after microtubule destabilization. J Biol Chem, 2010; 285: 16798-805.
[96] Hayashi S, Toyoshima Y, Hasegawa M, Umeda Y, Wakabayashi K, Tokiguchi S, Iwatsubo T, Takahashi H. Late-onset frontotemporal dementia with a novel exon 1 (Arg5His) tau gene mutation. Ann Neurol, 2002; 51: 525-30.
[97] Poorkaj P, Muma NA, Zhukareva V, Cochran EJ, Shannon KM, Hurtig H, Koller WC, Bird TD, Trojanowski JQ, Lee VM, Schellenberg GD. An R5L tau mutation in a subject with a progressive supranuclear palsy phenotype. Ann Neurol, 2002; 52: 511-6.
[98] Gamblin TC, Berry RW, Binder LI. Tau polymerization: role of the amino terminus. Biochemistry, 2003; 42: 2252-7.
[99] Combs B, Gamblin TC. FTDP-17 tau mutations induce distinct effects on aggregation and microtubule interactions. Biochemistry, 2012; 51: 8597-607.
[100] Magnani E, Fan J, Gasparini L, Golding M, Williams M, Schiavo G, Goedert M, Amos LA, Spillantini MG. Interaction of tau protein with the dynactin complex. EMBO J, 2007; 26: 4546-54.
[101] Horowitz PM, Patterson KR, Guillozet-Bongaarts AL, Reynolds MR, Carroll CA, Weintraub ST, Bennett DA, Cryns VL, Berry RW, Binder LI. Early N-terminal changes and caspase-6 cleavage of tau in Alzheimer's disease. J Neurosci, 2004; 24: 7895-902.
[102] Rohn TT, Rissman RA, Davis MC, Kim YE, Cotman CW, Head E. Caspase-9 activation and caspase cleavage of tau in the Alzheimer's disease brain. Neurobiol Dis, 2002; 11: 341-54.
[103] Carmel G, Mager EM, Binder LI, Kuret J. The structural basis of monoclonal antibody Alz50's selectivity for Alzheimer's disease pathology. J Biol Chem, 1996; 271: 32789-95.
[104] Jicha GA, Bowser R, Kazam IG, Davies P. Alz-50 and MC-1, a new monoclonal antibody raised to paired helical filaments, recognize conformational epitopes on recombinant tau. J Neurosci Res, 1997; 48: 128-32.
[105] Weaver CL, Espinoza M, Kress Y, Davies P. Conformational change as one of the earliest alterations of tau in Alzheimer's disease. Neurobiol Aging, 2000; 21: 719-27.

[106] Jeganathan S, Hascher A, Chinnathambi S, Biernat J, Mandelkow EM, Mandelkow E. Proline-directed pseudo-phosphorylation at AT8 and PHF1 epitopes induces a compaction of the paperclip folding of Tau and generates a pathological (MC-1) conformation. J Biol Chem, 2008; 283: 32066-76.
[107] LaPointe NE, Morfini G, Pigino G, Gaisina IN, Kozikowski AP, Binder LI, Brady ST. The amino terminus of tau inhibits kinesin-dependent axonal transport: implications for filament toxicity. J Neurosci Res, 2009; 87: 440-51.
[108] Kanaan NM, Morfini GA, LaPointe NE, Pigino GF, Patterson KR, Song Y, Andreadis A, Fu Y, Brady ST, Binder LI. Pathogenic forms of tau inhibit kinesin-dependent axonal transport through a mechanism involving activation of axonal phosphotransferases. J Neurosci, 2011; 31: 9858-68.
[109] Patterson KR, Ward SM, Combs B, Voss K, Kanaan NM, Morfini G, Brady ST, Gamblin TC, Binder LI. Heat shock protein 70 prevents both tau aggregation and the inhibitory effects of preexisting tau aggregates on fast axonal transport. Biochemistry, 2011; 50: 10300-10.
[110] Kanaan NM, Morfini G, Pigino G, LaPointe NE, Andreadis A, Song Y, Leitman E, Binder LI, Brady ST. Phosphorylation in the amino terminus of tau prevents inhibition of anterograde axonal transport. Neurobiol Aging, 2012; 33: 826 e15-30.
[111] Amadoro G, Ciotti MT, Costanzi M, Cestari V, Calissano P, Canu N. NMDA receptor mediates tau-induced neurotoxicity by calpain and ERK/MAPK activation. Proc Natl Acad Sci U S A, 2006; 103: 2892-7.
[112] Usardi A, Pooler AM, Seereeram A, Reynolds CH, Derkinderen P, Anderton B, Hanger DP, Noble W, Williamson R. Tyrosine phosphorylation of tau regulates its interactions with Fyn SH2 domains, but not SH3 domains, altering the cellular localization of tau. FEBS J, 2011; 278: 2927-37.
[113] Reynolds MR, Berry RW, Binder LI. Site-specific nitration and oxidative dityrosine bridging of the tau protein by peroxynitrite: implications for Alzheimer's disease. Biochemistry, 2005; 44: 1690-700.
[114] Reynolds MR, Berry RW, Binder LI. Site-specific nitration differentially influences tau assembly in vitro. Biochemistry, 2005; 44: 13997-4009.
[115] Horiguchi T, Uryu K, Giasson BI, Ischiropoulos H, LightFoot R, Bellmann C, Richter-Landsberg C, Lee VM, Trojanowski JQ. Nitration of tau protein is linked to neurodegeneration in tauopathies. Am J Pathol, 2003; 163: 1021-31.
[116] Reynolds MR, Reyes JF, Fu Y, Bigio EH, Guillozet-Bongaarts AL, Berry RW, Binder LI. Tau nitration occurs at tyrosine 29 in the fibrillar lesions of Alzheimer's disease and other tauopathies. J Neurosci, 2006; 26: 10636-45.
[117] Elliott E, Tsvetkov P, Ginzburg I. BAG-1 associates with Hsc70.Tau complex and regulates the proteasomal degradation of Tau protein. J Biol Chem, 2007; 282: 37276-84.
[118] Elliott E, Laufer O, Ginzburg I. BAG-1M is up-regulated in hippocampus of Alzheimer's disease patients and associates with tau and APP proteins. J Neurochem, 2009; 109: 1168-78.
[119] Carrettiero DC, Hernandez I, Neveu P, Papagiannakopoulos T, Kosik KS. The cochaperone BAG2 sweeps paired helical filament- insoluble tau from the microtubule. J Neurosci, 2009; 29: 2151-61.

[120] Barik S. Immunophilins: for the love of proteins. Cell Mol Life Sci, 2006; 63: 2889-900.
[121] Kang CB, Hong Y, Dhe-Paganon S, Yoon HS. FKBP family proteins: immunophilins with versatile biological functions. Neurosignals, 2008; 16: 318-25.
[122] Cao W, Konsolaki M. FKBP immunophilins and Alzheimer's disease: a chaperoned affair. J Biosci, 2011; 36: 493-8.
[123] Jinwal UK, Koren J, 3rd, Borysov SI, Schmid AB, Abisambra JF, Blair LJ, Johnson AG, Jones JR, Shults CL, O'Leary JC, 3rd, Jin Y, Buchner J, Cox MB, Dickey CA. The Hsp90 cochaperone, FKBP51, increases Tau stability and polymerizes microtubules. J Neurosci, 2010; 30: 591-9.
[124] Chambraud B, Belabes H, Fontaine-Lenoir V, Fellous A, Baulieu EE. The immunophilin FKBP52 specifically binds to tubulin and prevents microtubule formation. FASEB J, 2007; 21: 2787-97.
[125] Chambraud B, Sardin E, Giustiniani J, Dounane O, Schumacher M, Goedert M, Baulieu EE. A role for FKBP52 in Tau protein function. Proc Natl Acad Sci U S A, 2010; 107: 2658-63.
[126] Jinwal UK, Miyata Y, Koren J, 3rd, Jones JR, Trotter JH, Chang L, O'Leary J, Morgan D, Lee DC, Shults CL, Rousaki A, Weeber EJ, Zuiderweg ER, Gestwicki JE, Dickey CA. Chemical manipulation of hsp70 ATPase activity regulates tau stability. J Neurosci, 2009; 29: 12079-88.
[127] Shimura H, Schwartz D, Gygi SP, Kosik KS. CHIP-Hsc70 complex ubiquitinates phosphorylated tau and enhances cell survival. J Biol Chem, 2004; 279: 4869-76.
[128] Petrucelli L, Dickson D, Kehoe K, Taylor J, Snyder H, Grover A, De Lucia M, McGowan E, Lewis J, Prihar G, Kim J, Dillmann WH, Browne SE, Hall A, Voellmy R, Tsuboi Y, Dawson TM, Wolozin B, Hardy J, Hutton M. CHIP and Hsp70 regulate tau ubiquitination, degradation and aggregation. Hum Mol Genet, 2004; 13: 703-14.
[129] Salminen A, Ojala J, Kaarniranta K, Hiltunen M, Soininen H. Hsp90 regulates tau pathology through co-chaperone complexes in Alzheimer's disease. Prog Neurobiol, 2011; 93: 99-110.
[130] Love S, Saitoh T, Quijada S, Cole GM, Terry RD. Alz-50, ubiquitin and tau immunoreactivity of neurofibrillary tangles, Pick bodies and Lewy bodies. J Neuropathol Exp Neurol, 1988; 47: 393-405.
[131] Cripps D, Thomas SN, Jeng Y, Yang F, Davies P, Yang AJ. Alzheimer disease-specific conformation of hyperphosphorylated paired helical filament-Tau is polyubiquitinated through Lys-48, Lys-11, and Lys-6 ubiquitin conjugation. J Biol Chem, 2006; 281: 10825-38.
[132] Scaglione KM, Zavodszky E, Todi SV, Patury S, Xu P, Rodriguez-Lebron E, Fischer S, Konen J, Djarmati A, Peng J, Gestwicki JE, Paulson HL. Ube2w and ataxin-3 coordinately regulate the ubiquitin ligase CHIP. Mol Cell, 2011; 43: 599-612.
[133] Coppola G, Chinnathambi S, Lee JJ, Dombroski BA, Baker MC, Soto-Ortolaza AI, Lee SE, Klein E, Huang AY, Sears R, Lane JR, Karydas AM, Kenet RO, Biernat J, Wang LS, Cotman CW, Decarli CS, Levey AI, Ringman JM, Mendez MF, Chui HC, Le Ber I, Brice A, Lupton MK, Preza E, Lovestone S, Powell J, Graff-Radford N, Petersen RC, Boeve BF, Lippa CF, Bigio EH, Mackenzie I, Finger E, Kertesz A, Caselli RJ, Gearing M, Juncos JL, Ghetti B, Spina S, Bordelon YM, Tourtellotte

WW, Frosch MP, Vonsattel JP, Zarow C, Beach TG, Albin RL, Lieberman AP, Lee VM, Trojanowski JQ, Van Deerlin VM, Bird TD, Galasko DR, Masliah E, White CL, Troncoso JC, Hannequin D, Boxer AL, Geschwind MD, Kumar S, Mandelkow EM, Wszolek ZK, Uitti RJ, Dickson DW, Haines JL, Mayeux R, Pericak-Vance MA, Farrer LA, Ross OA, Rademakers R, Schellenberg GD, Miller BL, Mandelkow E, Geschwind DH. Evidence for a role of the rare p.A152T variant in MAPT in increasing the risk for FTD-spectrum and Alzheimer's diseases. Hum Mol Genet, 2012; 21: 3500-12.

[134] Abisambra JF, Blair LJ, Hill SE, Jones JR, Kraft C, Rogers J, Koren J, 3rd, Jinwal UK, Lawson L, Johnson AG, Wilcock D, O'Leary JC, Jansen-West K, Muschol M, Golde TE, Weeber EJ, Banko J, Dickey CA. Phosphorylation dynamics regulate Hsp27-mediated rescue of neuronal plasticity deficits in tau transgenic mice. J Neurosci, 2010; 30: 15374-82.

[135] Bjorkdahl C, Sjogren MJ, Zhou X, Concha H, Avila J, Winblad B, Pei JJ. Small heat shock proteins Hsp27 or alphaB-crystallin and the protein components of neurofibrillary tangles: tau and neurofilaments. J Neurosci Res, 2008; 86: 1343-52.

[136] Chang L, Thompson AD, Ung P, Carlson HA, Gestwicki JE. Mutagenesis reveals the complex relationships between ATPase rate and the chaperone activities of Escherichia coli heat shock protein 70 (Hsp70/DnaK). J Biol Chem, 2010; 285: 21282-91.

[137] Southworth DR, Agard DA. Species-dependent ensembles of conserved conformational states define the Hsp90 chaperone ATPase cycle. Mol Cell, 2008; 32: 631-40.

[138] Renard BY, Lower M, Kuhne Y, Reimer U, Rothermel A, Tureci O, Castle JC, Sahin U. rapmad: Robust analysis of peptide microarray data. BMC Bioinformatics, 2011; 12: 324.

Chapter 4

Characterizing the Interaction of Hsc70 with Amyloidogenic Substrates

4.1 Abstract

A number of untreatable neurodegenerative diseases, including Alzheimer's and Huntington's diseases, are characterized by the deposition of amyloid fibrils. Amyloids are formed by the aggregation of misfolded proteins. Several molecular chaperones are able to prevent amyloid formation, both *in vivo* and *in vitro*. To better understand how chaperones interact with amyloids, we developed a peptide microarray consisting of ~60 fibril-forming peptides and ~60 sequences that are unable to form amyloids. These sequences were matched for their hydrophobicity, length and number of aromatic residues to focus the study on whether chaperones might be able discriminate between normal and amyloid-forming peptides. We then measured binding of 20 different chaperones to these arrays, which suggested that Hsp70s, Hsp90, and some J proteins have a slight preference for amyloid-forming sequences. We selected 10 peptides from this dataset and investigated their binding to the substrate-binding domain (SBD) of Hsc70 using fluorescence polarization (FP) and isothermal titration calorimetry (ITC). We confirmed some of the Hsc70-peptide interactions and also identified a number of false negatives and positives. Together, these results suggest that some amyloid-prone sequences are good Hsc70 "clients', but that other physicochemical properties are also critical.

4.2 Introduction

4.2.1 Amyloid fibers share a common structure

At least 25 diseases are characterized by the assembly of misfolded proteins into rigid amyloid fibrils. The proteins that form these amyloids, such as tau (see Chapter 3), huntingtin and amyloid-β (Aβ), are diverse in sequence but they all form fibrils that are rich in β-sheet content and have similar dimensions [1, 2]. Further, all amyloids bind tightly to histological stains, such as Congo Red and Thioflavin T. Recent structural studies have revealed that amyloid cores contain "dry steric zippers". These structures are characterized by the tight interdigitation of amino acid side chains and the exclusion of water [3]. For example, the hexapeptide sequences VQIINK and VQIVYK at the core of tau amyloids align in anti-parallel β-sheets, with the side chains tightly packed [4]. The Eisenberg laboratory has solved the structures of thousands of steric zippers and developed an algorithm, ZipperDB, that is able to predict amyloid propensity in sequences [5]. The identification of these sequences provides a new focus for therapeutic approaches.

4.2.2 Chaperones prevent amyloid formation and protect against disease

In vitro, Hsp70, J proteins and other chaperones potently suppress the formation of many amyloids, including those formed from tau (see Chapter 3), amyloid-β (Alzheimer's disease), α-synuclein (Parkinson's disease), polyQ-expanded huntingtin (Huntington's disease), amylin (type 2 diabetes) and insulin (injection amyloidosis) [6] [7-15]. Hsp70 appears to block amyloid formation by directly binding to the amyloidogenic protein and

blocking its aggregation This activity is sometimes dependent on ATPase activity but some J proteins also inhibit aggregation in the absence of enzymatic activity

One fascinating aspects of these previous findings is that individual chaperones, such as Hsp70, are able to prevent amyloid formation by peptides that are widely divergent in sequence and physicochemical properties. For example, Hsp70 is a potent suppressor of amyloid formation by highly polar polyglutamine sequences and largely hydrophobic KLVFF-based amyloids [7, 8]. These types of observations suggest that Hsp70 can identify both of these "dangerous" sequences even though they share no similar physicochemical characteristics. What these sequences share in common is the ability to form steric zippers. Thus, we wondered whether chaperones, especially Hsp70 and J proteins, might be able to discriminate between innocuous and "dangerous" sequences. We also wanted to explore whether all chaperones share this ability or whether some chaperones were more "attuned" to finding amyloids. Moreover, we wondered whether these chaperones might bury the amyloid sequences into their substrate-binding domains (SBDs) to prevent the recruitment of additional monomers. An understanding of this mechanism may provide insight into how chaperones normally protect against amyloid formation and toxicity.

4.3 Results

4.3.1 Amyloid peptide microarray

To study chaperone binding to amyloid-prone sequences, Dr. Andrea Thompson and Dr. Atta Ahmad designed a peptide microarray consisting of 120 peptides derived from 33 proteins (Appendix 4.1). The microarray was comprised of ~60 amyloidogenic (e.g. fibril-

Table 4.1 Odds ratio analysis of chaperones binding fibril-forming peptides

Sample type	Human Chaperone	Replicates	Odds Ratio	95% CI
Negative control	Hsp70 NBD	4	0.942	0.308-2.882
Hsp70/Hsp90	Hsc70 (HSPA8)	4	2.063	0.920-4.625
	Hsc70SBD	1	1.884	0.767-4.627
	DnaK (*E. coli*)	1	1.803	0.767-4.235
	Hsp70 (HSPA1B)	1	1.722	0.783-3.789
	Hsp90 (HSP90AA1)	2	2.150	0.737-6.271
Small Hsps	Hsp27 (HSPB1)	1	1.488	0.615-3.600
	Hsp22 (HSPB8)	2	0.939	0.180-0.489
	ab crystallin (HSPB5)	2	0.887	0.304-2.586
Negative control	J-domain DnaJ (*E.coli*)	2	1.472	0.392-5.519
Co-chaperones	DNAJA2	4	2.343	1.025-5.356
	DnaJ (*E.coli*)	1	2.844	1.145-7.066
	DNAJA1	1	2.418	0.893-6.541
	DNAJB1	2	2.263	0.871-5.877
	CHIP	2	2.090	0.661-6.606
	FKBP51 (FKBP5)	3	1.720	0.754-3.974
	DNAJB4	1	0.519	0.083-3.246
	Hop	1	no binding	
Other chaperones	FKBP12	2	no binding	
	PDI	1	0.404	0.095-1.712
	clusterin	1	1.026	0.473-6.079
Ub-conj enzymes	Ube2w	1	1.667	0.376-7.385
	UbcH5c	1	0.576	0.130-2.544
More negative controls	MycF	1	1.804	0.316-10.314
	nano80	1	1.044	0.348-3.126
	Antibody alone	3	0.461	0.040-5.250

Odds ratios (OR) and 95% confidence intervals were calculated based on binding data from chaperones on the amyloid peptide microarrays. An odds ratio greater than one indicates a preference for binding fibril-forming peptides over non-fibril forming. Dark grey indicates chaperones that exhibited a preference for fibril-forming peptides. Light grey indicates chaperones that had an OR > 1.5 but did not reach significance using a 95% CI. Some chaperones (e.g. Ube2w) had a reasonably high OR but due to binding very few peptides had a broad 95% CI and were thus not considered to represent a real preference.

forming) and ~60 non-amyloidogenic peptides. The pools of peptides were matched for their physicochemical properties, including their hydrophobicity, number of aromatic residues, length, molecular mass and overall charge (Appendix 4.2). The amyloid-forming

sequences were chosen from the literature, especially the structural studies of the Eisenberg group and, when possible, the non-amyloid forming peptides were chosen from non-amyloid forming sequences in the same proteins. Chaperone binding to this array was detected using the same procedure outlined in Chapter 3.

4.3.2 A subset of chaperones preferentially bind amyloidogenic peptides

We tested binding of chaperones from a range of structural classes, including Hsp70s, Hsp90s, J proteins, other co-chaperones, small heat shock proteins and components of the ubiquitin-proteasome system. For each chaperone, we calculated an odds ratio (OR) and used a 95% confidence interval to determine whether it could discriminate between amyloid and non-amyloid peptides (OR > 1.0 indicates a preference for binding fibril-forming peptides; see Section 4.5 for details). By this analysis, two co-chaperones – DNAJA2 and *E. coli* DnaJ – bound preferentially to amyloid-forming sequences. However, the relatively small size of the dataset limited its statistical power, so many chaperones, including Hsc70/Hsp72, DnaK, Hsp90, DNAJA1, DNAJB1, CHIP and FKBP51, had OR values consistently above 1 but they failed to reach significance. Other chaperones, particularly the small heat shock proteins and E2 ubiquitin-conjugating enzymes, did not show any preference for fibril forming peptides.

It is worth emphasizing that even the chaperones with a tendency to bind amyloid-forming sequences also bound other peptides. This result is not surprising given the known promiscuity of Hsp70 and other chaperones. In fact, it is quite remarkable that any chaperones showed a preference in this format, given the wide range of activities that

chaperones such as Hsp70 carry out. Thus, these data suggest that some chaperones are able to directly identify amyloid-prone sequences and that some chaperones are even able to differentiate these sequences from other, chemically similar sequences. However, no chaperone appeared able to bind all amyloids.

4.3.3 Hsc70SBD binding of peptides using fluorescence polarization

To further explore the amyloid-chaperone interactions, we divided the sequences into four categories: fibril-forming binders, fibril forming non-binders, non-fibril forming binders and non-fibril forming non-binders. "Binders" were characterized as peptides bound by DNAJA1, DNAJA2, DNAJB1, Hsc70/Hsc70$_{SBD}$, Hsp72 and Hsp90 (at least 5 of these 6). The raw binding results were also examined to ensure that the peptides chosen for further study were robust and from disease-associated proteins (Table 4.2).

Table 4.2 Peptides selected for binding studies

Category	Peptide	Parent Protein	FP IC_{50} (μM)[a]	Reference
Fibril-forming Binders	LVEALY	Insulin	43 ± 9	[4, 16, 17]
	SLYQLENY	Insulin	7 ± 2	[18]
	VQIVYK	Tau	33 ± 10	[4, 19]
Non-fibril-forming Binders	EALYLV	b2-microglobulin	8 ± 3	[16, 17]
	GERGFF	Insulin	> 200	[16, 17]
Fibril-forming Non-binders	KLVFFAED	Amyloid-b	> 200	[20, 21]
	GSIAAT	a-synuclein	39 ± 9	[4]
Non-fibril-forming Non-binders	KSNFLN	b2-microglobulin	32 ± 4	[16, 17]
	VQPVYK	Tau (mutant)	> 200	[19]
	HLVEAL	Insulin	140 ± 70	[16, 17]

[a]IC_{50} values of peptides competing with 5Fam-labeled LVEALY (20 nM) for binding to Hsc70$_{SBD}$ as measured by fluorescence polarization (FP)

The microarray study is only semi-quantitative and binding is measured at a liquid-solid interface. To study these interactions in solution by a distinct platform, we developed a fluorescence polarization (FP) assay. For these studies, we focused on $Hsc70_{SBD}$ and employed the known fluorescent tracer, LVEALY [17] (Figure 4.1). We found that the peptide bound with comparable affinity (~1 μM) to two different $Hsc70_{SBD}$ constructs, 394-540 and 394-509, the latter of which has the helical "lid" domain removed. The smaller construct was designed for NMR structural studies. Because both proteins yielded similar affinity for the tracer, we conducted the remainder of our studies with the 394-540 construct. Unfortunately, we were unable to detect binding of this tracer to any of the J proteins..

The ability of the peptides to compete with 20 nM 5Fam-LVEALY for binding to $Hsc70_{SBD}$ was evaluated (Figure 4.2) and IC_{50} values estimated (Table 4.2). As expected, unlabeled LVEALY competed with the labeled tracer, with the disparity between the affinity of the tracer (1.7 μM) and the IC_{50} value of the unlabeled peptide (42 μM) likely attributable to affinity contributed by the fluorophore. The other two fibril-forming binders (SLYQLENY and VQIVYK) also competed with the tracer, with SLYQLENY having an appreciably lower IC_{50} than LVEALY. Of the two non-fibril-forming binders, one competed well (EALYLV) and the other (GERGFF) did not. The result with GERGFF suggested that the array finding

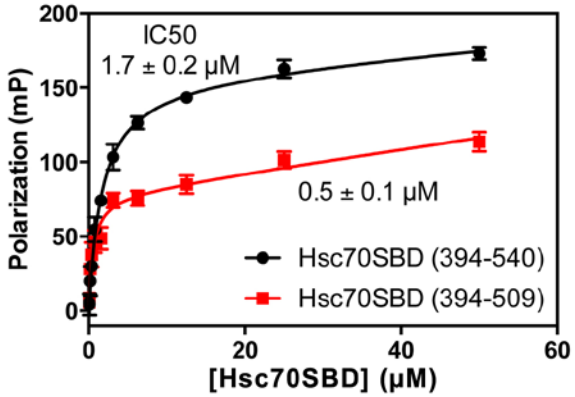

Figure 4.1. Hsc70SBD constructs bind LVEALY with the same affinity. Hsc70SBD binding of 5Fam-labeled LVEALY (20 nM) measured by fluorescence polarization (ex/em 485/528). IC50 values are indicated next to the corresponding curves.

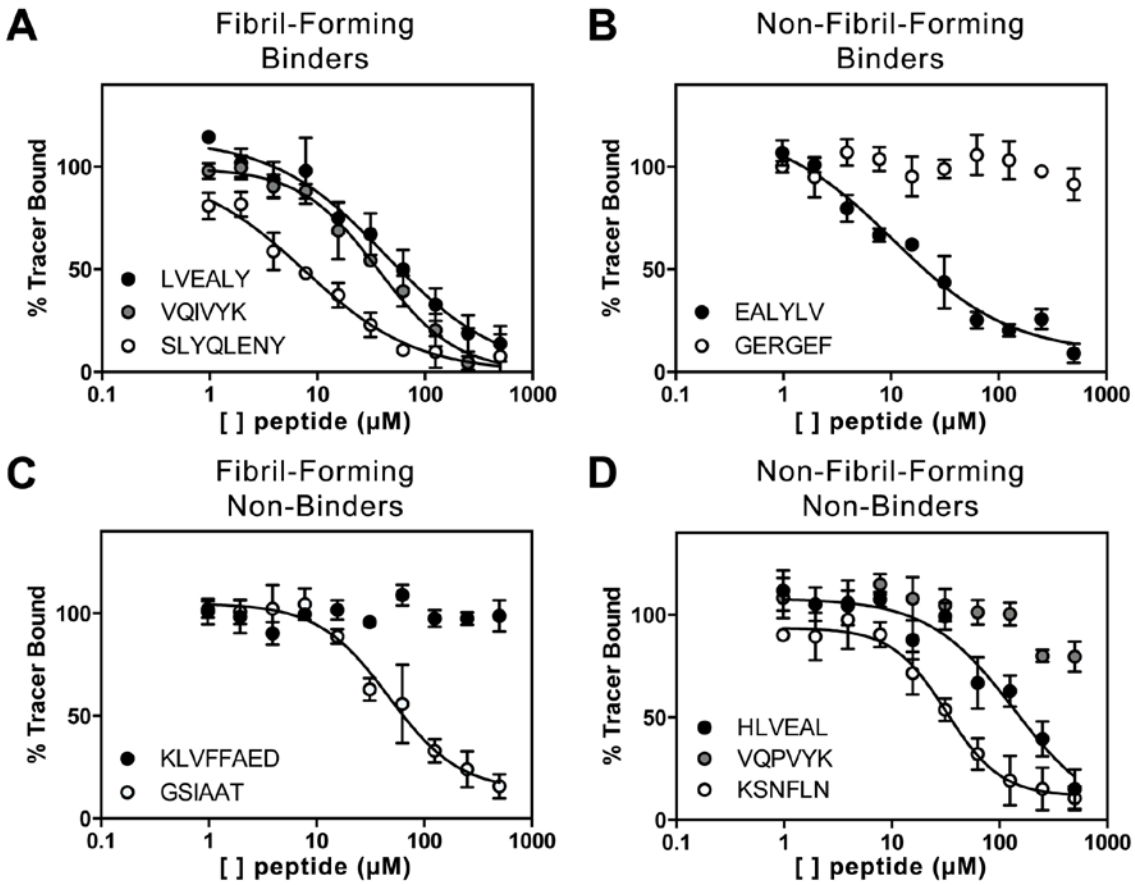

Figure 4.2. Competition of peptides with LVEALY for binding to Hsc70SBD by fluorescence polarization. Peptides selected from the microarray experiments as either Hsc70 binders or non-binders (see Table 4.2) were evaluated for competition with 5Fam-labeled LVEALY (20 nM) for binding to Hsc70SBD (394-540).

was either a false positive or that the chaperone recognized some feature of the immobilized peptide that was not replicated in the solution FP format (e.g. solubility, secondary structure, local concentration, etc). Similarly, one fibril-forming non-binder competed well (GSIAAT) and the other did not (KLVFFAED). Finally, one non-fibril forming non-binder competed well (KSNFLN) while the others did not (HLVEAL and VQPVYK). Although the sample size of this dataset is small, these results suggest that the arrays predicted ~70% of the chaperone interactions with Hsc70..

LVEALY, EALYLV, and HLVEAL were selected for further study in part because they have similar sequences yet disparate fibril-forming properties and behavior on the arrays. LVEALY and EALYLV are highly similar, but EALYLV doesn't form amyloids. Nevertheless, $Hsc70_{SBD}$ bound the two peptides with similar affinity, confirming previous suggestions that physicochemical characteristics play a major role in Hsp70 binding [22]. However, a one-residue shift from LVEALY to HLVEAL nearly abolished binding by $Hsc70_{SBD}$ in both the microarray and FP platforms. This result is in contrast to the known preference of Hsp70 for binding positively charged residues flanking a hydrophobic core [22]. This result suggests that the Phe residue at the end of LVEALY may be important for interaction with Hsc70 and may allow the chaperone to identify this "dangerous" sequence.

As discussed in Chapter 3, the tau sequence, VQIVYK (aka PHF6), is required for forming PHFs and this hexapeptide forms fibrils consisting of steric zippers [4]. VQPVYK is a closely related peptide that contains a point mutation (Ile to Pro) known to abolish amyloid formation [19]. Interestingly, this point mutant also abolished Hsc70 binding in our FP and microarray experiments. This finding could be due to a requirement for the Ile side chain in the binding interaction or a loss of β-sheet propensity altering the conformational dynamics of the peptide.

Together these data provide evidence that Hsc70 has a mild, global preference for fibril-forming peptides over non-fibril forming and that this preference is particularly strong for some amyloid-forming sequences.

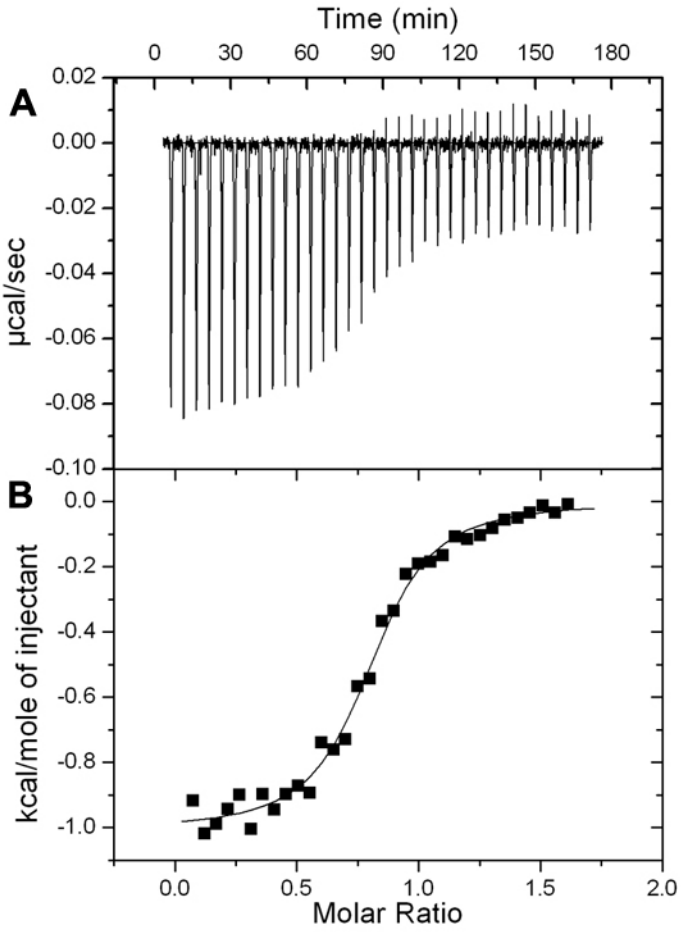

Figure 4.3 Calorimetric titration of VQIVYK with Hsc70SBD. Titration consisted of 5 µL injects of VQIVYK (400 µM) into sample cell containing Hsc70SBD (30 µM) at 25 °C. The buffer used was 25 mM HEPES, 5 mM $MgCl_2$, 10 mM KCl, 4% DMSO, pH 7.4. (A) Differences between sample cell and reference cell containing water. (B) Enthalpy per mole of injectant plotted as a function of molar ratio (peptide/protein). Data was fit as a single set of identical sites using ORIGIN (Microcal).

4.3.4 Characterizing Hsc70SBD-peptide binding by isothermal titration calorimetry

Next, we measured binding of the peptides to $Hsc70_{SBD}$ by ITC. We pursued these studies because the FP assay was designed to measure competition between the peptides and the fluorescent tracer, so we also wanted to test whether the peptides might bind a distinct site on the SBD. Briefly, a solution of peptide (400 µM) was injected into a buffer-matched solution of $Hsc70_{SBD}$ (30 µM) and the thermodynamic binding parameters determined using

MicroCal software (Figure 4.3 and Appendix 4.3). Some of these studies required addition of up to 4% DMSO to both the protein and peptide samples, a process which resulted in buffer mismatch issues and thus the high background observed in some titrations.

Of the ten peptides, one was not soluble enough to yield accurate measurements and these results were discarded (Table 4.3). Of the remaining peptides, each bound to $Hsc70_{SBD}$ with varying affinity (ΔG values between -7 and -8.5 kcal mol^{-1}). The binding of all peptides was enthalpically and entropically favorable. The low n-values (0.4-0.9 peptides/$Hsc70_{SBD}$) are likely due to the $Hsc70_{SBD}$ binding pocket being partially occupied by co-purified peptides/proteins. However, the variation among the n-values suggests that the peptide concentrations may be imprecise; future experiments should employ techniques to precisely determine peptide concentration in solution, such as amino acid analysis, in order to obtain completely accurate affinities and n-values. For this reason, we consider these data to be simply indications of binding or non-binding, while future studies will determine relative affinities.

Table 4.3 Thermodynamic parameters for association of $Hsc70_{SBD}$ with peptides[a]

	K_a (M^{-1})	K_D (μM)	ΔH (cal mol^{-1})	ΔS (cal mol^{-1} K^{-1})	ΔG [b] (kcal mol^{-1})	n
LVEALY	$2.05 \times 10^5 \pm 6.8 \times 10^4$	6 ± 2	-746 ± 137	22	-7.18	0.7
SLYQLENY	$2.78 \times 10^5 \pm 4.7 \times 10^4$	3.6 ± 0.6	-4548 ± 282	9.6	-7.42	0.5
VQIVYK	$1.53 \times 10^6 \pm 2.1 \times 10^5$	0.65 ± 0.09	-1008 ± 16	24.9	-8.43	0.8
EALYLV	$4.29 \times 10^5 \pm 5.0 \times 10^4$	2.3 ± 0.3	-2263 ± 108	18.2	-7.69	0.4
GERGFF	$5.04 \times 10^5 \pm 4.5 \times 10^4$	2.0 ± 0.2	-1450 ± 22	21.2	-7.77	0.9
KLVFFAED	insoluble					
GSIAAT	$5.1 \times 10^5 \pm 1.5 \times 10^5$	2.0 ± 0.6	-319 ± 25	25	-7.77	0.5
KSNFLN	$5.66 \times 10^5 \pm 1.4 \times 10^5$	1.8 ± 0.5	-1218 ± 63	22.2	-7.83	0.6
VQPVYK	$6.87 \times 10^5 \pm 1.2 \times 10^5$	1.5 ± 0.3	-351 ± 11	25.5	-7.95	0.8
HLVEAL	no binding					

[a]Values are for 25 mM HEPES, 5 mM $MgCl_2$, 10 mM KCl, 0-4% DMSO, pH 7.4, 25 ^oC
[b]$\Delta G = \Delta H - T\Delta S$

Comparing these results to the FP assay findings, it appeared that more peptides were positive binders. For example, both GERGFF and VQPVYK bound Hsc70, yet these peptides failed to compete with the LVEALY tracer. Thus, these peptides might have a non-canonical binding site on the SBD. Consistent with the FP study, HLVEAL did not bind strongly to $Hsc70_{SBD}$.

4.4 Discussion

We have used a peptide microarray to study binding of chaperones to fibril-forming peptides. This study is important because many chaperones, especially Hsp70 and small heat shock proteins, and co-chaperones, such as J proteins, have been strongly linked to preventing amyloid formation and toxicity. The previous studies had suggested that some chaperones might be able to identify the regions of amyloid-prone proteins critical for amyloid formation, yet there was little structural or biophysical evidence for such as model. Accordingly, we used peptide microarrays, FP and ITC to investigate these interactions, with a special focus on Hsc70. The array studies suggested a mild preference of a subset of the chaperones. This result is surprising and interesting because it suggests that some chaperones might be able to find "dangerous" sequences independent of their other commonly evaluated physicochemical properties. With FP, we evaluated the ability of a set of 10 peptides to compete with a fluorescent LVEALY tracer for binding to $Hsc70_{SBD}$. This assay yielded a 70% confirmation rate, with both false positives and negatives identified. Because of these false positives and negatives, the odds ratios originally calculated from the microarray data may not fully reflect the binding preferences of chaperones. Further, these results suggest that the peptides may be forming structures on the array surface that are not represented in solution, although this model remains to be tested. Finally, using ITC, we

elucidated the thermodynamic parameters of $Hsc70_{SBD}$ binding to 8 of these peptides. We found that one peptide did not bind and that the others bound with similar affinities. The ability of GERGFF and VQPVYK to bind Hsc70 by ITC, but not FP, suggest that these peptides do not share a binding site with the LVEALY tracer. To address this possibility, studies are underway using NMR to investigate the binding of peptides to $Hsc70_{SBD}$. Initial results with LVEALY suggest that the peptide interacts with disordered loops in the SBD and not the β-strands. Further investigations will hopefully clarify the possibility of multiple sites. Further, computational and experimental studies are ongoing in collaboration with the lab of David Eisenberg to evaluate whether chaperones can form "heterosteric zippers" with amyloid sequences.

4.5 Experimental Methods

4.5.1 Protein purification

Hsp70s (DnaK, Hsc70, Hsp70, NBD constructs; Hsp70 NBD (1-383), Hsc70 NBD (1-383), and Hsc70 NBD+linker (1-394)) were purified as previously described [23]. Likewise, Hsp90, J-domain (1-108), and DnaJ were purified as previously described [23, 24], with the addition of a Superdex 200 size exclusion column (GE Healthcare, Pittsburg, PA) as the last step of the J-domain purification. N-terminal His6x-tagged DNAJA1, DNAJA2, and DNAJB1 were purified as previously described [25]. Hsc70SBD (394-540) was expressed in BL21 cells from a pMCSG7 vector encoding an N-terminal His6x tag under ampicillin selection. Cells were lysed by sonication into His6x-binding buffer (50 mM Tris pH 8.0, 10 mM imidazole, 500 mM NaCl, protease inhibitors) and purified using Ni-NTA resin (Novagen, Darmstadt, Germany). Protein was eluted with His6x-elution buffer (50 mM

Tris, 300 mM imidazole, 300 mM NaCl), 2 mM EDTA added, and protein concentrated to ~6 mg/mL. Protein was further purified on a HiLoad Superdex 75 16/600 size exclusion column into storage buffer (50 mM Tris, 250 mM NaCl). Pure fractions were combined, concentrated, flash frozen and stored at -80°C. Hsp27, Hsp22, αB □crystallin, expressed in Rosetta cells using the pMCSG7 vector. Cells were lysed by sonication into lysis buffer (20 mM Tris pH 8.0, 100 mM NaCl, 6 M urea, 5 mM β-mercaptoethanol, 15 mM imidazole) and purified by standard denaturing his purification using Ni-NTA resin. Proteins were eluted with 150 mM imidazole. Following elution EDTA was added to 5 mM and protein was concentrated to ~20 mg/ml. Protein was refolded upon injection on a Superdex 200 size exclusion column (GE Healthcare, Pittsburg, PA) with refolding buffer (20 mM NaP_i pH 7.2, 100 mM NaCl). The protein was flash frozen and stored at -80 °C. Finally, FKBP51 was purified by using a standard His purification with Ni-NTA resin (Novagen) followed by separation using a superdex 200 size exclusion column in (10mM NaPi, 2mM KPi pH 7.4, 137 mM NaCl, 2.7 mM KCl, 1 mM DTT). The following proteins were purchased as follows; Clusterin (Enzo Life Sciences, 201-335-C050, Farmingdale, NY), PDI (PROSPEC, enz-262-b, East Burnswick, NJ), FKBP12 (PROSPEC, enz-347-c). MycF was a kind gift from Janet Smith (University of Michigan); nanobody80 was a kind gift from Roger Sunahara (University of Michigan).

4.5.2 Peptide microarrays

A peptide microarray consisting of a variety of peptides experimentally evaluated for their ability to form fibrils was designed (Appendix A.1). Empty spots and process controls were used as negative controls. The microarrays were printed on single microscope slides in triplicate with

peptides covalently immobilized at the N-terminus (Jenrin Peptide Technologies, Berlin, Germany). Binding was tested per manufacturer's protocol using 10 μM of His6x-tagged protein in binding buffer (25 mM HEPES pH 7.2, 150 mM NaCl, 20 mM KCl, 5 mM $MgCl_2$, 0.01% Tween20). Binding was detected using 1:1,000 titer of HiLyte555 anti-His6x antibody (Anaspec, Fremont, CA) in TBS-T with 1% bovine serum albumin (Sigma) and scanning the microarrays using a GenePix 4100A Microarray Scanner (Molecular Devices, Sunnyvale, CA) and an excitation wavelength of 532 nm. Binding was defined using a previously described peptide microarray analysis program, Rapmad, to identify bound peptides while excluding false positives identified in the Hsp70 NBD experiment [26]. The optional random forest procedure to remove potentially unreliable peptide spots was excluded from the analysis. Odds ratios (OR) were calculated for each individual experiment using the following equation;

$$OR = (FB*NN)/(NB*FN) \qquad \text{(Equation 1)}$$

FB indicates fibril forming peptides found to bind the chaperone, FN indicates fibril forming peptides found to not bind, NB indicates non-fibril forming peptides found to bind, and NN indicates non-fibril forming peptides found to not bind. Further, for proteins tested more than once, an OR was calculated for the combined data. In combining the data binding was defined as peptides found to bind in ≥ 2/3 of experiments for that chaperone (see Appendix A.3 for full results).

4.5.3 Fluorescence polarization

Fluorescence polarization experiments were performed in 384-well, black, low volume, round-bottom plates (Corning) using a BioTek Synergy 2 plate reader (Winooski, VT). To each well was added increasing amounts of protein and the 5-carboxyfluorescein (5-Fam)

labeled LVEALY tracer (20 nM) to a final volume of 20 uL in the assay buffer (50 mM HEPES, 75 mM NaCl, 0.01% Triton X-100, pH 7.4). The plate was allowed to incubate at room temperature for 1 h to reach equilibrium. The polarization values in millipolarization units (mP) were measured at an excitation wavelength at 485 nm and an emission wavelength at 528 nm. An equilibrium binding isotherm was constructed by plotting the FP reading as a function of the protein concentration at a fixed concentration of tracer (20 nM). All experimental data were analyzed using Prism 5.0 software (Graphpad Software, San Diego, CA) and the inhibition constants (IC50) were determined by nonlinear curve fitting to identify the concentration of protein at which 50% of the tracer (ligand) was bound.

4.5.4 Isothermal titration calorimetry

Hsc70SBD (394-540) was dialyzed extensively into Buffer A (25 mM HEPES, 5 mM $MgCl_2$, 10 mM KCl, pH 7.4) and buffer from the dialysis was saved for concentration adjustment. Peptide (400 μM) and Hsc70SBD (30 μM) solutions were made fresh with 0-4% DMSO (as required for peptide solubility) and degassed for 10-20 minutes. Peptide was titrated into Hsc70SBD (5 μL injections, stirring 310 RPM, 25-35 injections) at 25 °C. Experiments were carried out on a VP-ITC instrument (MicroCal, Northampton, MA) and data was analyzed using the Origin 7 software package. All binding isotherms were fit using the single set of identical sites model.

Notes

Andrea Thompson and Atta Ahmad designed the amyloid peptide microarray. Andrea Thompson, Amanda Wong, and Anne Gillies carried out the microarray experiments and

data analysis. Victoria Assimon carried out the FP experiments and data analysis. Anne Gillies carried out the ITC experiments and data analysis. Andrea Thompson, Anne Gillies, Victoria Assimon, and Jason Gestwicki contributed intellectually to this work.

4.6 Appendix

Appendix 4.1 Peptide microarray design

ID #	Name	Protein	Fibril/Non-Fibril	Location
1	GGVLVN	248PAP286	Fibril [27]	cytoplasm
2	SLFLIG	AIM1	non-Fibril [28]	membrane
3	VGGAVVTGV	α synuclein	Fibril [4, 20]	cytoplasm
4	GSIAAT	α synuclein	Fibril [4]	cytoplasm
5	GVATVA	α synuclein	Fibril [4]	cytoplasm
6	GGAVVT	α synuclein	predicted Fibril [16]	cytoplasm
7	AEKTKQ	α synuclein	predicted non-fibril [16]	cytoplasm
8	MPVDPD	α synuclein	predicted non-fibril [16]	cytoplasm
9	NFGAIL	amylin	Fibril [16, 20, 29, 30]	secreted/extra
10	FLVHSS	amylin	Fibril [16, 31]	secreted/extra
11	TNVGSNTY	amylin	Fibril [32]	secreted/extra
12	QRLANFLVH	amylin	Fibril [33]	secreted/extra
13	SSTNVG	amylin	Fibril [4]	secreted/extra
14	LIAGFN	amylin	non-Fibril [16]	secreted/extra
15	NLGPVL	amylin	non-Fibril [16]	secreted/extra
16	KLVFFAED	Aβ	Fibril [20, 21]	extra
17	AIIGLMVGGVV	Aβ	Fibril [4]	extra
18	GGVVIA	Aβ	Fibril [4]	extra
19	*MVGGVV*	Aβ	Fibril [4]	extra
20	*DGVVIA*	Aβ	non-fibril FL [34]	extra
21	*LVGGVV*	Aβ	non-fibril FL [34, 35]	extra
22	GFVVIA	Aβ	non-fibril FL [35]	extra
23	FFKRAA	AR	predicted non-fibril [16]	cytoplasm, nucleus
24	AVFIIY	ASPM	Fibril [28]	nucleus, cytoplasm
25	GRGHGG	ataxin-1 (ATXN1)	predicted non-fibril [16]	cytoplasm
26	DWSFYLLYYTEFT	b2-microglobulin	Fibril [4, 36]	secreted/extra
27	KDWSFY	b2-microglobulin	Fibril [17]	secreted/extra
28	KIVKWD	b2-microglobulin	Fibril [17]	secreted/extra
29	*FYLLYY*	b2-microglobulin	Fibril [17]	secreted/extra
30	LLYYTE	b2-microglobulin	Fibril [17]	secreted/extra
31	NHVTLS	b2-microglobulin	Fibril [4, 16, 17, 37]	secreted/extra
32	FHPSDIEVDLLK	b2-microglobulin	non-Fibril [36]	secreted/extra
33	IQRTPKIQVYSRHPAE	b2-microglobulin	non-Fibril [36]	secreted/extra
34	LSQPKIVKWDRDM	b2-microglobulin	non-Fibril [36]	secreted/extra
35	NGERIEKVEHSDLSFS KD	b2-microglobulin	non-Fibril [36]	secreted/extra
36	NGKSNFLNCYVSG	b2-microglobulin	non-Fibril [36]	secreted/extra
37	PTGKDEYACRVNHVT	b2-microglobulin	non-Fibril [36]	secreted/extra
38	YVSGFH	b2-microglobulin	non-Fibril [16, 17]	secreted/extra
39	VYSRHP	b2-microglobulin	non-Fibril [16, 17]	secreted/extra

40	KSNFLN	b2-microglobulin	non-Fibril [16, 17]	secreted/extra
41	RTPKIQ	b2-microglobulin	non-Fibril [16, 17]	secreted/extra
42	VTLSQP	b2-microglobulin	non-Fibril [16, 17]	secreted/extra
43	TEFTPT	b2-microglobulin	non-Fibril [16, 17]	secreted/extra
44	SRHPAE GGSGGSGGGSDYKD	b2-microglobulin	non-Fibril [16, 17]	secreted/extra
45	DDDK		process control	
46	EALYLV	b2-microglobulin	non-Fibril [16, 17]	secreted/extra
47	DFNKFH	Calcitonin	Fibril [4, 38]	secreted

ID #	Name	Protein	Fibril/Non-Fibril	Location
48	NFVNYS	CELR3	Fibril [28]	membrane
49	VTFTIQ	CPNE5	Fibril [28]	cytoplasm, membrane
50	YLVNFT	ECM1	Fibril [28]	extra membrane
51	NEFIIT	EMBP	non-Fibril [28]	secreted; cytoplasmic vesicles
52	YLVLIM	Fibulin-1	non-Fibril [28]	secreted/extra
53	MIFFIY	GCYB2	non-Fibril [28]	cytoplasm
54	SAILTA	gelsolin (GSN)	predicted Fibril [16]	cytoplasm, extracellular
55	TMSVSL	gelsolin (GSN)	predicted Fibril [16]	cytoplasm, extracellular
56	LYNYRH	gelsolin (GSN)	predicted non-fibril [16]	cytoplasm, extracellular
57	IRDNER	gelsolin (GSN)	predicted non-fibril [16]	cytoplasm, extracellular
58	LYVLIV	GRP21	Fibril [28]	membrane
59	QQSLFQ	HNRPD	Fibril [28]	Nucleus, cytoplasm
60	EIDFIL	Huntington (HTT)	predicted non-fibril [16]	cytoplasm
61	QQQQQQ	Huntington, ATXN1, ATXN2, AR	Fibril [4]	cytoplasm
62	*S**LYQLENY***	Insulin	Fibril [18]	extracellular
63	***LVEALYL**V*	Insulin	Fibril [18]	extracellular
64	L***VEALY***	Insulin	Fibril [4, 16, 17]	extracellular
65	***VEALY**L*	Insulin	Fibril [4, 16, 17]	extracellular
66	*LY**QLEN***	Insulin	Fibril [4, 16, 17]	extracellular
67	***YQLENY***	Insulin	Non-Fibril [16, 17]	extracellular
68	FVNQHL	Insulin	Non-Fibril [16, 17]	extracellular
69	*GSH**LVE***	Insulin	Non-Fibril [16, 17]	extracellular
70	***H**LVEAL***	Insulin	Non-Fibril [16, 17]	extracellular
71	FYTPKT	Insulin	Non-Fibril [16, 17]	extracellular
72	GERGFF	Insulin	Non-Fibril [16, 17]	extracellular
73	GVWWFF	Integrin beta-1	Fibril [28]	membrane
74	GIFNIK	LASS2	Fibril [28]	membrane
75	IFQINS	Lysozyme	Fibril [4, 20]	cytoplasm
76	TFQINS	Lysozyme-Hu	Fibril [4]	cytoplasm
77	NRLLLTG	model substrate	Unknown	NA
78	AGAAAAGA	Prion	Fibril [39, 40]	extra membrane
79	SNQNNF	Prion	Fibril [4]	extra membrane
80	VHDCVNITIK	Prion 180-193	Fibril [20, 41]	extra membrane
81	NITIKQHTVT	Prion 180-193	Non-Fibril [20, 41]	extra membrane
82	QHTVTTTKG	Prion 180-193	Non-Fibril [20, 41]	extra membrane
83	TTTKGENFTE	Prion 180-193	Non-Fibril [20, 41]	extra membrane
84	MIHFGND	Prion(Mu)	Fibril [4]	extra membrane
85	SMVLFSSPPV	Prion141-150	Fibril [20, 41]	extra membrane

86	EDRYYRENMH	Prion144-154	non-Fibril [20, 41]	extra membrane
87	FGSDYEDRYY	Prion144-154	non-Fibril [20, 41]	extra membrane
88	SSEITT	PTMA	predicted Fibril [16]	cytoplasm
89	EVDEEE	PTMA	predicted non-fibril [16]	cytoplasm
90	AA		process control	
91	KRAAED	PTMA	predicted non-fibril [16]	cytoplasm
92	*SSTSAASSSNY*	Rnase	Fibril [5]	cytoplasm
93	KHIIVA	Rnase	Fibril [5]	cytoplasm
94	SYSTMS	Rnase	Fibril [5]	cytoplasm
95	*SSTSAA*	Rnase	Fibril [4]	Cytoplasm
ID #	**Name**	**Protein**	**Fibril/Non-Fibril**	**Location**
96	*ASSSNY*	Rnase	Fibril [5]	cytoplasm
97	RNLTKD	Rnase	Non-Fibril [5]	cytoplasm
98	IHKAQN	Rnase, scrambled	Non-Fibril [5]	cytoplasm
99	ISMTTS	Rnase, scrambled	Non-Fibril [5]	cytoplasm
100	FERQHM	Rnase, scrambled	Non-Fibril [5]	cytoplasm
101	GNNQQNY	Sup35	Fibril [4]	Yeast fibril
102	NNQQNY	Sup35	Fibril [4]	Yeast fibril
103	VQIVYK	Tau (PHF6)	Fibril [4, 19]	cytoplasm
104	VQIPYK	Tau	Non-Fibril [19]	cytoplasm
105	VQPVYK	Tau	Non-Fibril [19]	cytoplasm
106	GQVEVSKE	Tau	Non-Fibril [20]	cytoplasm
107	VQEVYK	Tau	unknown	cytoplasm
108	VQYK	Tau	unknown	cytoplasm
109	VVRTPPKSPSSAKSR	Tau	unknown	cytoplasm
110	VQIINK	Tau	Fibril [42]	cytoplasm
111	VDLSKVTSK	Tau	Non-Fibril [20]	cytoplasm
112	PGGGKVQIVYKPV	Tau (K19)	Fibril [20]	cytoplasm
113	PGGKVYKPV	Tau (K19d)	Non-Fibril [20]	cytoplasm
114	QTAPVPMPD	Tau (K19Glu78)	Non-Fibril [20]	cytoplasm
115	GISVHI	TDP-43	predicted Fibril [16]	cytoplasm
116	GEVLMV	TDP-43	predicted Fibril [16]	cytoplasm
117	LRYRNP	TDP-43	predicted non-fibril [16]	cytoplasm
118	VFFFIG	TRHDE	non-Fibril [28]	membrane
119	WTVNYS	WDR36	Fibril [28]	cytoplasm
120	FIVNIV	XRP2	Fibril [28]	membrane

Appendix 4.2 Microarray peptide characteristics

	Fibril		**Non-Fibril**		**Unknown**	
Number of Peptides	59		56		5	
Experimentally validated	54		49		NA	
disease related	39		44		3	
hexamers	43		41		1	
< or > hexamers	16		15		2	
average length peptide	7.22	3.26	6.91	1.58	6.25	0.50
average MW	822.51	351.41	807.69	196.87	775.53	95.89
average pI	5.80	1.37	5.83	1.72	5.83	0.61
average pos charge	0.29	0.56	0.73	1.06	0.25	0.50

average neg charge	0.25	0.54	0.45	0.66	0.25	0.50
average instability index	26.95	42.76	36.36	43.30	21.26	16.23
average aliphatic index	108.06	68.01	88.49	73.19	16.25	32.50
average GRAVY	0.48	1.47	-0.26	1.46	-1.74	1.66

Appendix 4.3 Hsc70SBD binding to peptides by ITC

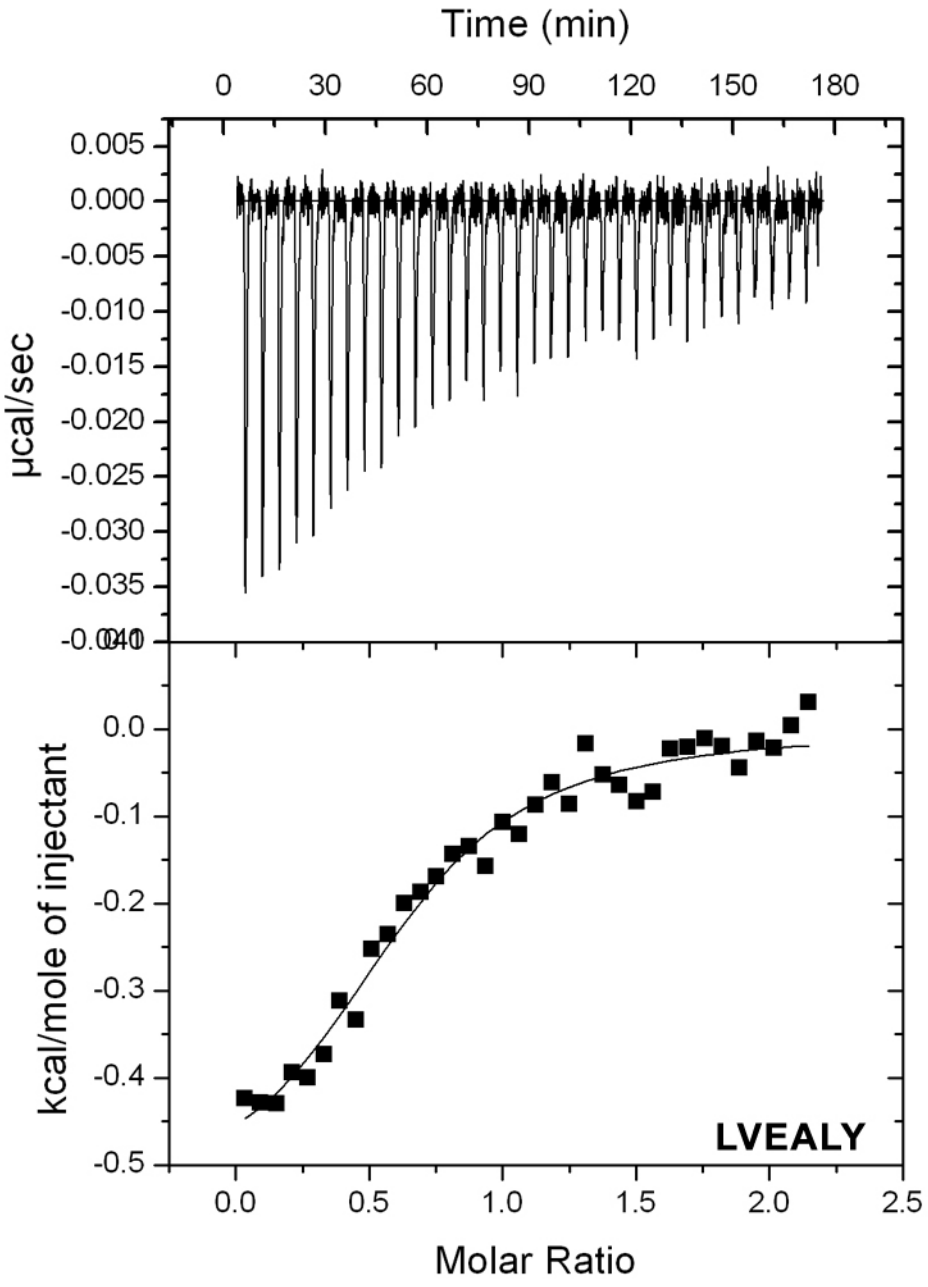

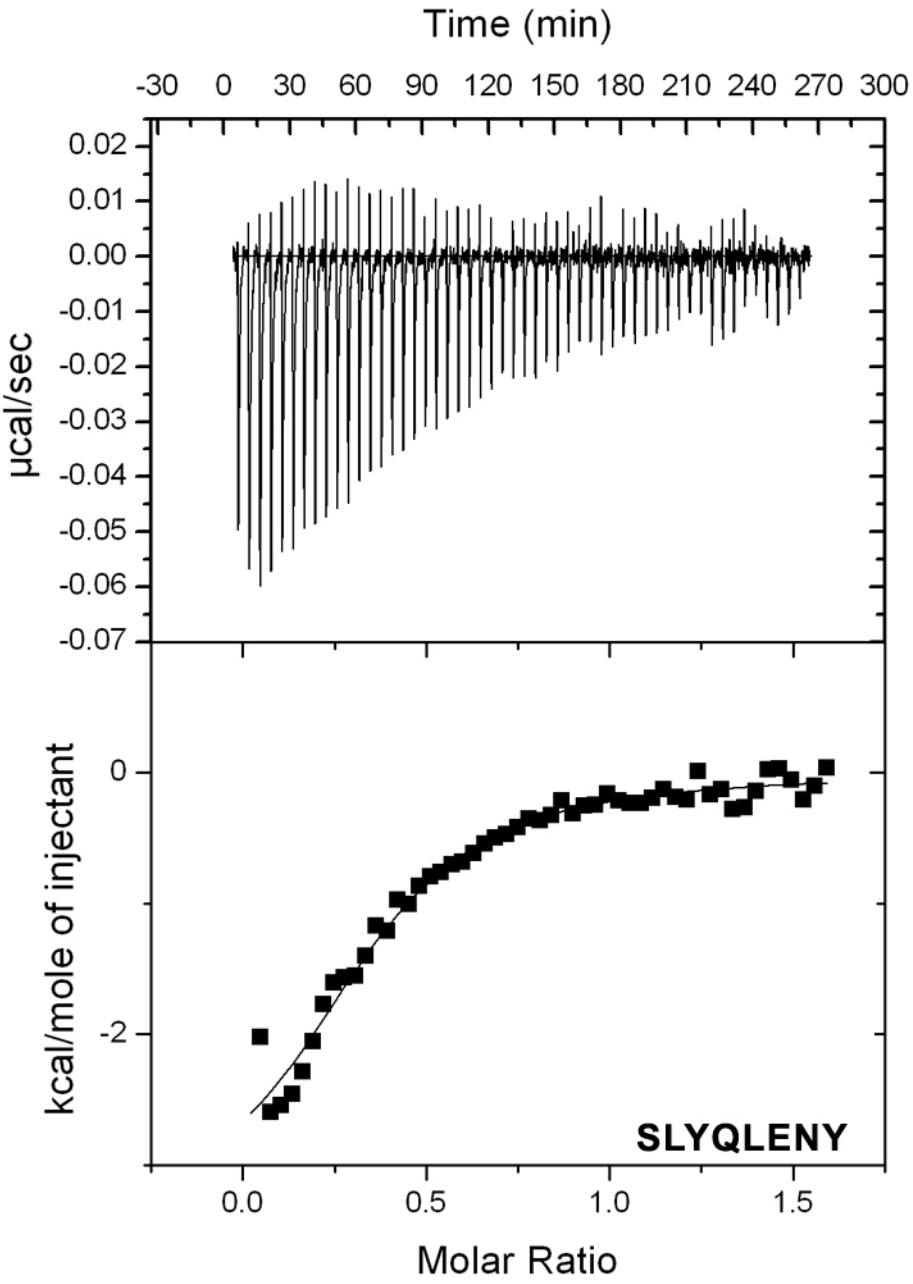
Time (min)
-30 0 30 60 90 120 150 180 210 240 270 300
0.02
0.01
0.00
-0.01
-0.02
-0.03
-0.04
-0.05
-0.06
-0.07
µcal/sec
0
-2
kcal/mole of injectant
SLYQLENY
0.0 0.5 1.0 1.5
Molar Ratio

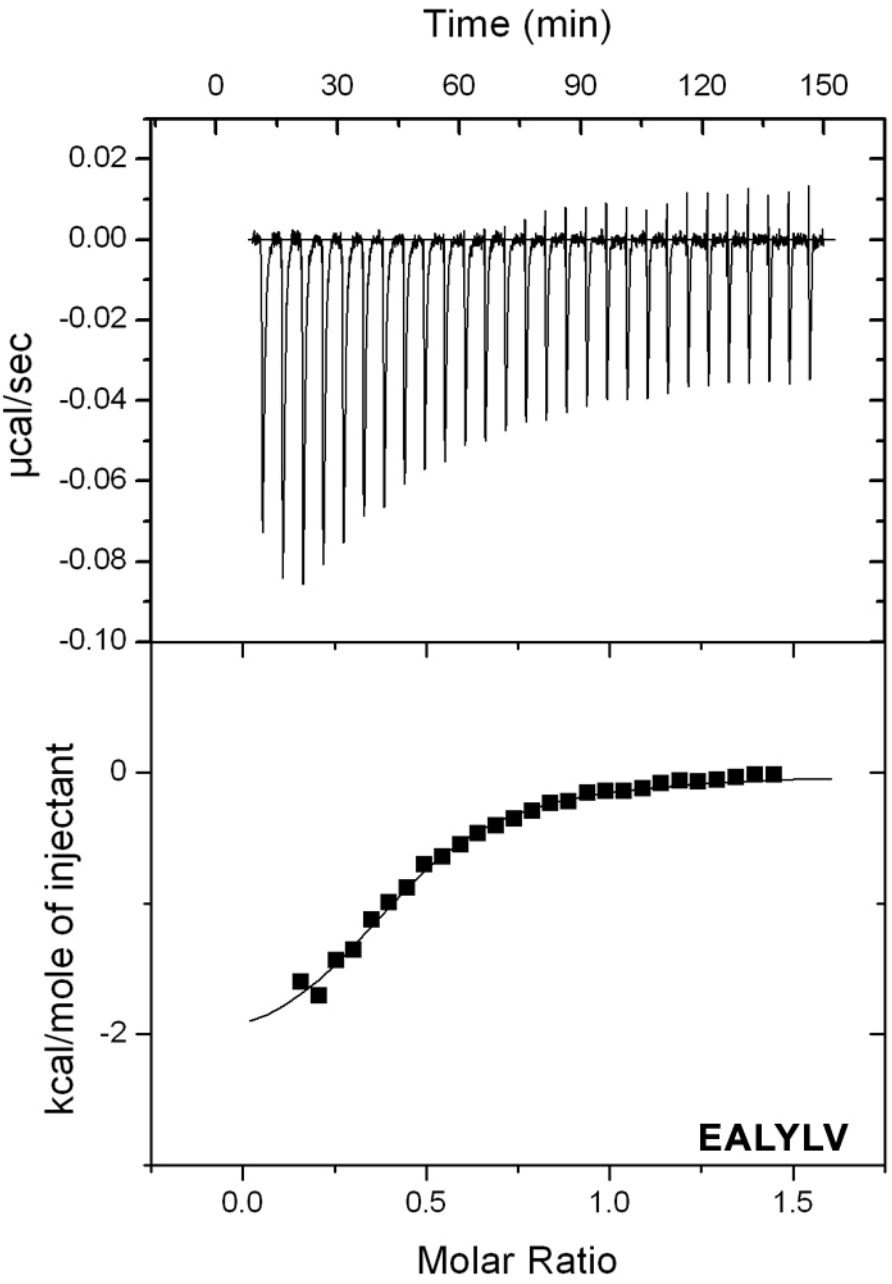
Time (min)
0
30
60
90
120
150
0.02
0.00
-0.02
-0.04
-0.06
-0.08
-0.10
µcal/sec
0
-2
kcal/mole of injectant
EALYLV
0.0
0.5
1.0
1.5
Molar Ratio

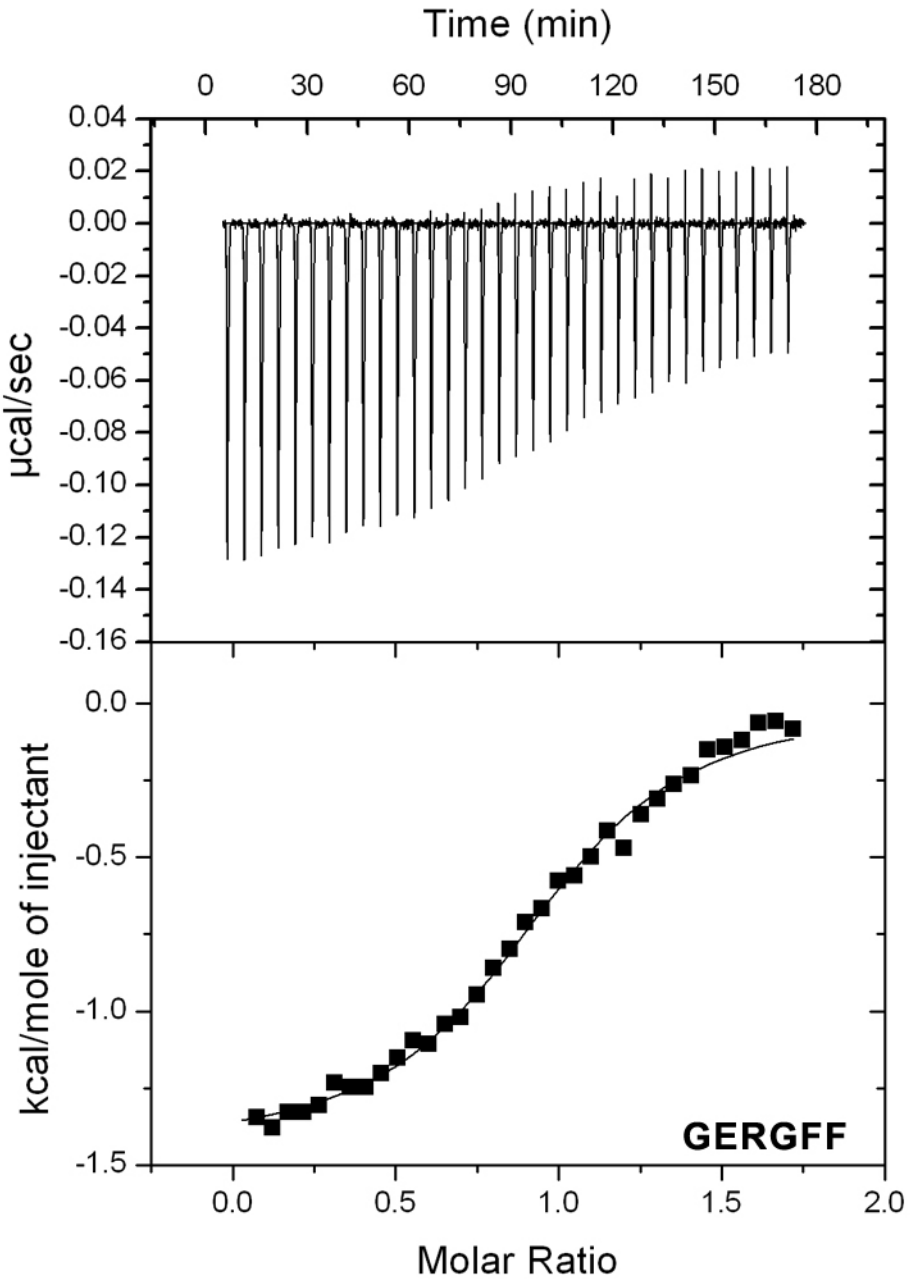
Time (min)
0
30
60
90
120
150
180
0.04
0.02
0.00
-0.02
-0.04
-0.06
-0.08
-0.10
-0.12
-0.14
-0.16
µcal/sec
0.0
-0.5
-1.0
-1.5
kcal/mole of injectant
GERGFF
0.0
0.5
1.0
1.5
2.0
Molar Ratio

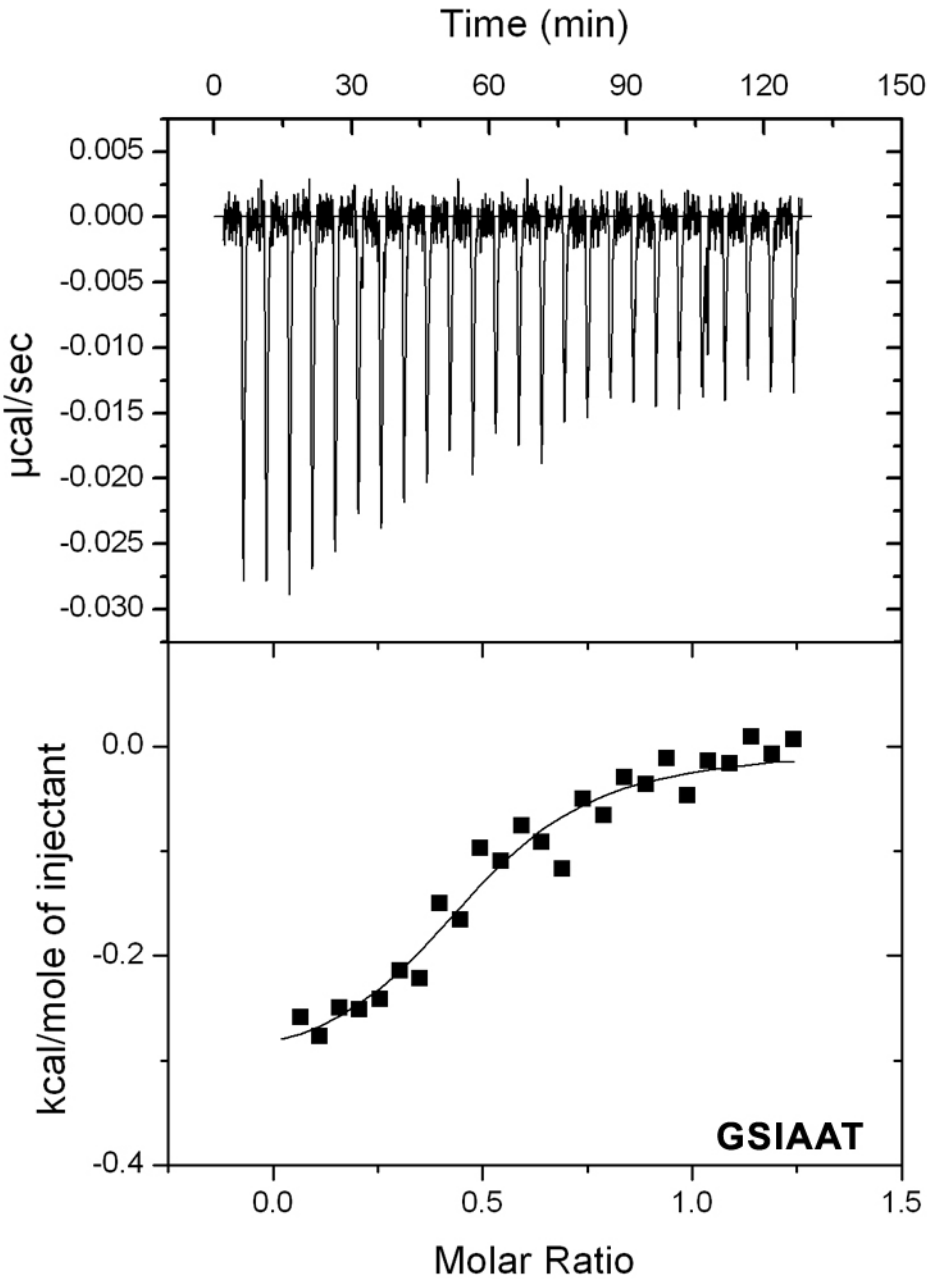
Time (min)
0
30
60
90
120
150
0.005
0.000
-0.005
-0.010
-0.015
-0.020
-0.025
-0.030
µcal/sec
0.0
-0.2
-0.4
kcal/mole of injectant
GSIAAT
0.0
0.5
1.0
1.5
Molar Ratio

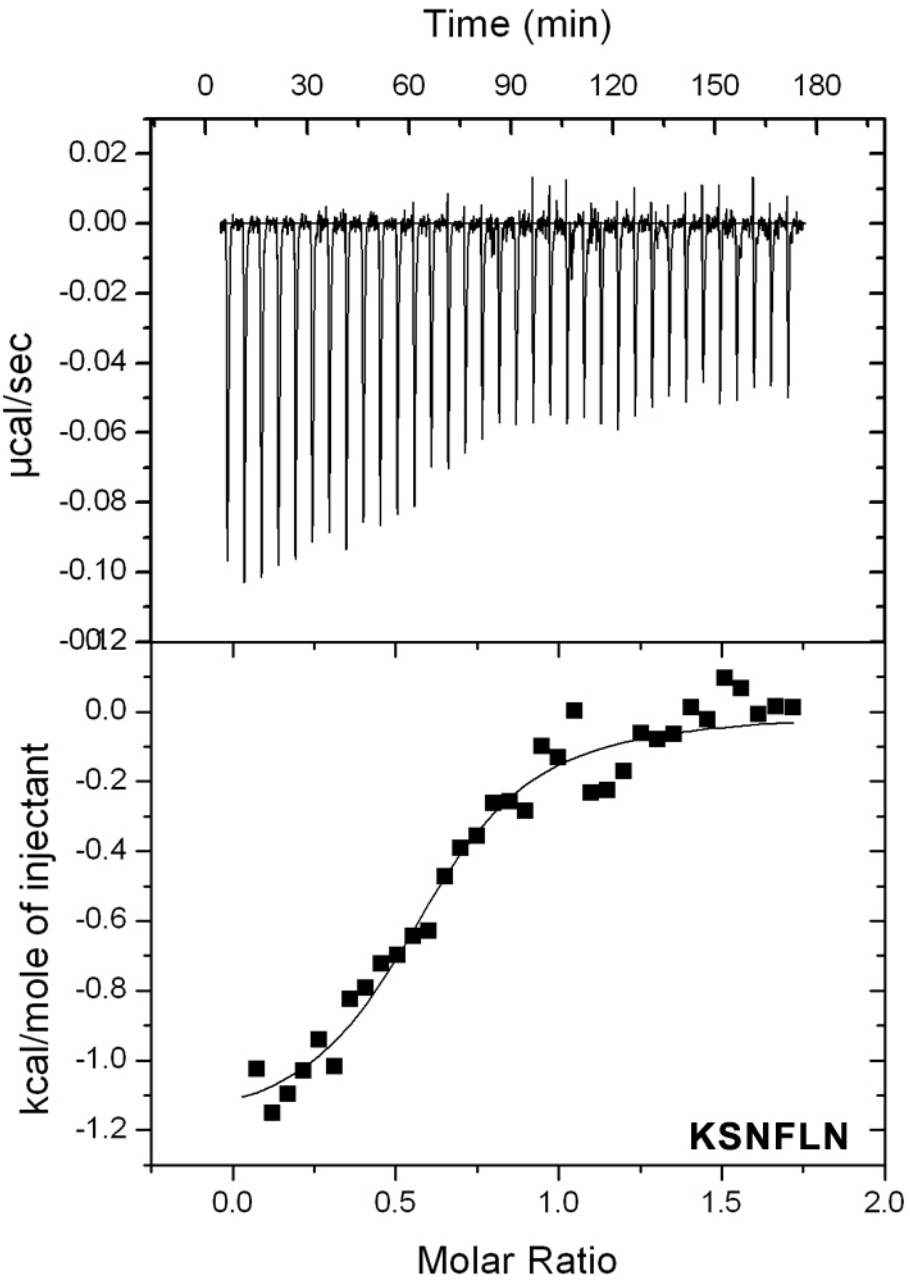
Time (min)
0
30
60
90
120
150
180
0.02
0.00
-0.02
-0.04
-0.06
-0.08
-0.10
-0.12
µcal/sec
0.0
-0.2
-0.4
-0.6
-0.8
-1.0
-1.2
kcal/mole of injectant
KSNFLN
0.0
0.5
1.0
1.5
2.0
Molar Ratio

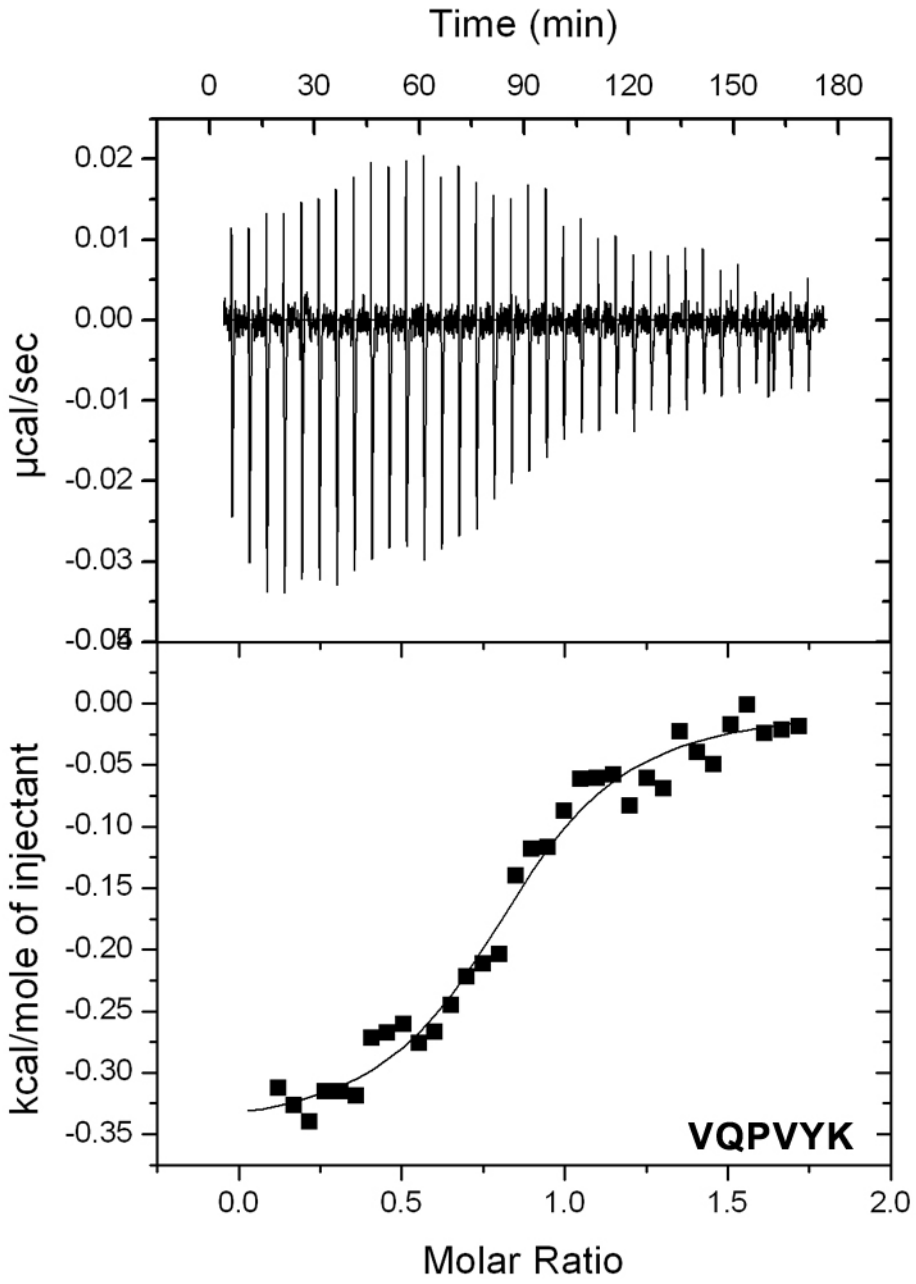
Time (min)
0
30
60
90
120
150
180
µcal/sec
0.02
0.01
0.00
-0.01
-0.02
-0.03
kcal/mole of injectant
0.00
-0.05
-0.10
-0.15
-0.20
-0.25
-0.30
-0.35
VQPVYK
0.0
0.5
1.0
1.5
2.0
Molar Ratio

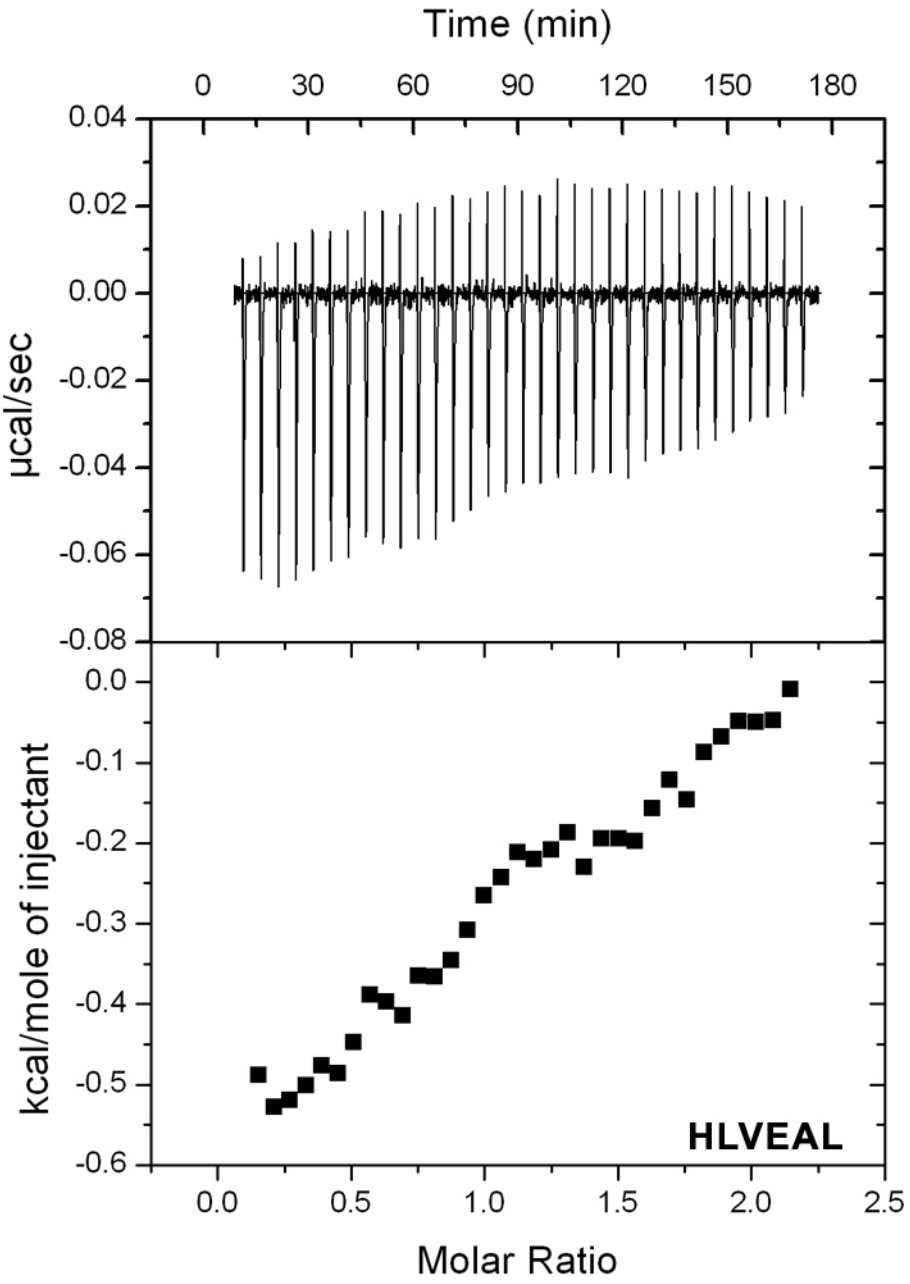
Time (min)
0
30
60
90
120
150
180
0.04
0.02
0.00
-0.02
-0.04
-0.06
-0.08
µcal/sec
0.0
-0.1
-0.2
-0.3
-0.4
-0.5
-0.6
kcal/mole of injectant
HLVEAL
0.0
0.5
1.0
1.5
2.0
2.5
Molar Ratio

4.7 References

[1] Chiti F, Dobson CM. Protein misfolding, functional amyloid, and human disease. Annu Rev Biochem, 2006; 75: 333-66.

[2] Eisenberg D, Jucker M. The amyloid state of proteins in human diseases. Cell, 2012; 148: 1188-203.

[3] Nelson R, Sawaya MR, Balbirnie M, Madsen AO, Riekel C, Grothe R, Eisenberg D. Structure of the cross-beta spine of amyloid-like fibrils. Nature, 2005; 435: 773-8.

[4] Sawaya MR, Sambashivan S, Nelson R, Ivanova MI, Sievers SA, Apostol MI, Thompson MJ, Balbirnie M, Wiltzius JJ, McFarlane HT, Madsen AO, Riekel C, Eisenberg D. Atomic structures of amyloid cross-beta spines reveal varied steric zippers. Nature, 2007; 447: 453-7.

[5] Goldschmidt L, Teng PK, Riek R, Eisenberg D. Identifying the amylome, proteins capable of forming amyloid-like fibrils. Proc Natl Acad Sci U S A, 2010; 107: 3487-92.

[6] Broadley SA, Hartl FU. The role of molecular chaperones in human misfolding diseases. FEBS Lett, 2009; 583: 2647-53.

[7] Muchowski PJ, Schaffar G, Sittler A, Wanker EE, Hayer-Hartl MK, Hartl FU. Hsp70 and hsp40 chaperones can inhibit self-assembly of polyglutamine proteins into amyloid-like fibrils. Proc Natl Acad Sci U S A, 2000; 97: 7841-6.

[8] Evans CG, Wisen S, Gestwicki JE. Heat shock proteins 70 and 90 inhibit early stages of amyloid beta-(1-42) aggregation in vitro. J Biol Chem, 2006; 281: 33182-91.

[9] Wacker JL, Zareie MH, Fong H, Sarikaya M, Muchowski PJ. Hsp70 and Hsp40 attenuate formation of spherical and annular polyglutamine oligomers by partitioning monomer. Nat Struct Mol Biol, 2004; 11: 1215-22.

[10] Dedmon MM, Christodoulou J, Wilson MR, Dobson CM. Heat shock protein 70 inhibits alpha-synuclein fibril formation via preferential binding to prefibrillar species. J Biol Chem, 2005; 280: 14733-40.

[11] Luk KC, Mills IP, Trojanowski JQ, Lee VM. Interactions between Hsp70 and the hydrophobic core of alpha-synuclein inhibit fibril assembly. Biochemistry, 2008; 47: 12614-25.

[12] Ballet T, Brukert F, Mangiagalli P, Bureau C, Boulange L, Nault L, Perret T, Weidenhaupt M. DnaK prevents human insulin amyloid fiber formation on hydrophobic surfaces. Biochemistry, 2012; 51: 2172-80.

[13] Patterson KR, Ward SM, Combs B, Voss K, Kanaan NM, Morfini G, Brady ST, Gamblin TC, Binder LI. Heat shock protein 70 prevents both tau aggregation and the inhibitory effects of preexisting tau aggregates on fast axonal transport. Biochemistry, 2011; 50: 10300-10.

[14] Ahmad A. DnaK/DnaJ/GrpE of Hsp70 system have differing effects on alpha-synuclein fibrillation involved in Parkinson's disease. Int J Biol Macromol, 2010; 46: 275-9.

[15] Chien V, Aitken JF, Zhang S, Buchanan CM, Hickey A, Brittain T, Cooper GJ, Loomes KM. The chaperone proteins HSP70, HSP40/DnaJ and GRP78/BiP suppress misfolding and formation of beta-sheet-containing aggregates by human

amylin: a potential role for defective chaperone biology in Type 2 diabetes. Biochem J, 2010; 432: 113-21.
[16] Thompson MJ, Sievers SA, Karanicolas J, Ivanova MI, Baker D, Eisenberg D. The 3D profile method for identifying fibril-forming segments of proteins. Proc Natl Acad Sci U S A, 2006; 103: 4074-8.
[17] Ivanova MI, Thompson MJ, Eisenberg D. A systematic screen of beta(2)-microglobulin and insulin for amyloid-like segments. Proc Natl Acad Sci U S A, 2006; 103: 4079-82.
[18] Ivanova MI, Sievers SA, Sawaya MR, Wall JS, Eisenberg D. Molecular basis for insulin fibril assembly. Proc Natl Acad Sci U S A, 2009; 106: 18990-5.
[19] von Bergen M, Friedhoff P, Biernat J, Heberle J, Mandelkow EM, Mandelkow E. Assembly of tau protein into Alzheimer paired helical filaments depends on a local sequence motif ((306)VQIVYK(311)) forming beta structure. Proc Natl Acad Sci U S A, 2000; 97: 5129-34.
[20] Fernandez-Escamilla AM, Rousseau F, Schymkowitz J, Serrano L. Prediction of sequence-dependent and mutational effects on the aggregation of peptides and proteins. Nat Biotechnol, 2004; 22: 1302-6.
[21] Landau M, Sawaya MR, Faull KF, Laganowsky A, Jiang L, Sievers SA, Liu J, Barrio JR, Eisenberg D. Towards a pharmacophore for amyloid. PLoS Biol, 2011; 9: e1001080.
[22] Rudiger S, Buchberger A, Bukau B. Interaction of Hsp70 chaperones with substrates. Nat Struct Biol, 1997; 4: 342-9.
[23] Chang L, Thompson AD, Ung P, Carlson HA, Gestwicki JE. Mutagenesis reveals the complex relationships between ATPase rate and the chaperone activities of Escherichia coli heat shock protein 70 (Hsp70/DnaK). J Biol Chem, 2010; 285: 21282-91.
[24] Southworth DR, Agard DA. Species-dependent ensembles of conserved conformational states define the Hsp90 chaperone ATPase cycle. Mol Cell, 2008; 32: 631-40.
[25] Tzankov S, Wong MJ, Shi K, Nassif C, Young JC. Functional divergence between co-chaperones of Hsc70. J Biol Chem, 2008; 283: 27100-9.
[26] Renard BY, Lower M, Kuhne Y, Reimer U, Rothermel A, Tureci O, Castle JC, Sahin U. rapmad: Robust analysis of peptide microarray data. BMC Bioinformatics, 2011; 12: 324.
[27] Sievers SA, Karanicolas J, Chang HW, Zhao A, Jiang L, Zirafi O, Stevens JT, Munch J, Baker D, Eisenberg D. Structure-based design of non-natural amino-acid inhibitors of amyloid fibril formation. Nature, 2011; 475: 96-100.
[28] Maurer-Stroh S, Debulpaep M, Kuemmerer N, Lopez de la Paz M, Martins IC, Reumers J, Morris KL, Copland A, Serpell L, Serrano L, Schymkowitz JW, Rousseau F. Exploring the sequence determinants of amyloid structure using position-specific scoring matrices. Nat Methods, 2010; 7: 237-42.
[29] Azriel R, Gazit E. Analysis of the minimal amyloid-forming fragment of the islet amyloid polypeptide. An experimental support for the key role of the phenylalanine residue in amyloid formation. J Biol Chem, 2001; 276: 34156-61.
[30] Tenidis K, Waldner M, Bernhagen J, Fischle W, Bergmann M, Weber M, Merkle ML, Voelter W, Brunner H, Kapurniotu A. Identification of a penta- and

hexapeptide of islet amyloid polypeptide (IAPP) with amyloidogenic and cytotoxic properties. J Mol Biol, 2000; 295: 1055-71.
[31] Mazor Y, Gilead S, Benhar I, Gazit E. Identification and characterization of a novel molecular-recognition and self-assembly domain within the islet amyloid polypeptide. J Mol Biol, 2002; 322: 1013-24.
[32] Nilsson MR, Raleigh DP. Analysis of amylin cleavage products provides new insights into the amyloidogenic region of human amylin. J Mol Biol, 1999; 294: 1375-85.
[33] Jaikaran ET, Higham CE, Serpell LC, Zurdo J, Gross M, Clark A, Fraser PE. Identification of a novel human islet amyloid polypeptide beta-sheet domain and factors influencing fibrillogenesis. J Mol Biol, 2001; 308: 515-25.
[34] Kanski J, Varadarajan S, Aksenova M, Butterfield DA. Role of glycine-33 and methionine-35 in Alzheimer's amyloid beta-peptide 1-42-associated oxidative stress and neurotoxicity. Biochim Biophys Acta, 2002; 1586: 190-8.
[35] Luhrs T, Ritter C, Adrian M, Riek-Loher D, Bohrmann B, Dobeli H, Schubert D, Riek R. 3D structure of Alzheimer's amyloid-beta(1-42) fibrils. Proc Natl Acad Sci U S A, 2005; 102: 17342-7.
[36] Jones S, Manning J, Kad NM, Radford SE. Amyloid-forming peptides from beta2-microglobulin-Insights into the mechanism of fibril formation in vitro. J Mol Biol, 2003; 325: 249-57.
[37] Ivanova MI, Sawaya MR, Gingery M, Attinger A, Eisenberg D. An amyloid-forming segment of beta2-microglobulin suggests a molecular model for the fibril. Proc Natl Acad Sci U S A, 2004; 101: 10584-9.
[38] Reches M, Porat Y, Gazit E. Amyloid fibril formation by pentapeptide and tetrapeptide fragments of human calcitonin. J Biol Chem, 2002; 277: 35475-80.
[39] Gasset M, Baldwin MA, Lloyd DH, Gabriel JM, Holtzman DM, Cohen F, Fletterick R, Prusiner SB. Predicted alpha-helical regions of the prion protein when synthesized as peptides form amyloid. Proc Natl Acad Sci U S A, 1992; 89: 10940-4.
[40] Sambashivan S, Liu Y, Sawaya MR, Gingery M, Eisenberg D. Amyloid-like fibrils of ribonuclease A with three-dimensional domain-swapped and native-like structure. Nature, 2005; 437: 266-9.
[41] Thompson A, White AR, McLean C, Masters CL, Cappai R, Barrow CJ. Amyloidogenicity and neurotoxicity of peptides corresponding to the helical regions of PrP(C). J Neurosci Res, 2000; 62: 293-301.
[42] von Bergen M, Barghorn S, Li L, Marx A, Biernat J, Mandelkow EM, Mandelkow E. Mutations of tau protein in frontotemporal dementia promote aggregation of paired helical filaments by enhancing local beta-structure. J Biol Chem, 2001; 276: 48165-74.

Chapter 5

Future Directions: Developing a Deeper Understanding of Chaperone Networks

5.1 Abstract

In this thesis, I have presented findings that address how chaperones function in networks of competing and cooperating elements. Our results highlight the diversity of functions found within a single class of co-chaperones, J proteins. We have additionally demonstrated that chaperones interact with substrates in different ways to achieve specific outcomes such as refolding, stabilization, degradation, or aggregation prevention. However, there is much yet to learn about the details of chaperone networks, particularly as they relate to disease pathologies. A more focused evaluation of individual J protein functions may provide useful insights into the Hsp70 machinery and its many roles. Additionally, many questions remain about how chaperones interact with tau in both healthy brains and tauopathies. Finally, our findings suggest that direct binding of amyloidogenic sequences by chaperones may play a key role in the prevention of amyloid formation, and a mechanistic understanding of this interaction may contribute to our understanding of protein misfolding in disease.

5.2 Conclusions

Chaperones have emerged as an exciting area of research that touches on many diverse aspects of biology. These ubiquitous proteins have long been silent actors in otherwise well-

understood processes, but their importance in normal cell function is beginning to be appreciated. At the same time, the role of chaperones in prevalent and challenging diseases, notably neurodegeneration and cancer, as well as their potential as therapeutic targets is being recognized. In recent years, our understanding of chaperones has improved by leaps and bounds at the mechanistic and systemic levels, but there is still much to be learned.

The goal of this thesis was to study chaperones as a network of interconnected actors. I was particularly intrigued by the diversity of J proteins, a co-chaperone class that has been dramatically expanded by evolution to support ever more complex organisms. Similarly, other classes of chaperones and co-chaperones have multiple members whose unique and shared functions are beginning to be elucidated. In order to obtain novel insights into the nature of these cooperative networks, I employed two techniques: chemical genetics and peptide microarrays. In Chapter 2 I describe the use of chemical genetics to study the effect of the loss of a specific J protein on *S. cerevisiae*. Overall, the deletion of individual chaperones had minimal effects on *S. cerevisiae* viability, suggesting either that the cell has compensatory mechanisms in the absence of a single J protein or that the full complement of J proteins is unnecessary in ideal growing conditions. However, when the cells were challenged with stressors, differences between the J proteins became clearly apparent. Some, like Ydj1 and Zuo1, appear to be generalists required for overall cellular health because deletion of these genes conferred sensitivity to many different stressors targeting functions ranging from cell wall synthesis to TOR signaling. The majority of the J proteins appear to have more specialized roles, though the lack of clear-cut functional divisions suggests that individual J protein deletion may have a domino effect on multiple pathways. Still others

did not confer any observable phenotype upon deletion, suggesting either that the cell can fully compensate for their absence or that they have specific roles not tested by our stressors. These experiments allowed for the novel identification of specific functional roles for J proteins that had only been minimally characterized previously. The dataset also supports an appreciation for the complexity of the J protein network and its involvement in a wide range of crucial cellular functions.

In Chapter 3, I describe a more mechanistic approach to understanding chaperone activities, both alone and in concert. I developed a peptide microarray platform in our lab in order to simultaneously measure many chaperone-substrate interactions. Peptide microarrays are particularly useful to study chaperone interactions as chaperones generally bind unfolded proteins, of which isolated peptides are a reasonably good mimic. I first used this technique to ask how chaperones converge on the substrates firefly luciferase and human tau. Extensive work has been done to characterize the activity of chaperones on these substrates: Hsp70 and co-chaperones can refold luciferase *in vitro* and *in vivo*, while many chaperones reduce tau aggregation and toxicity. However, the mechanistic details of these processes have proven challenging to untangle. For example, it is unknown why the human J protein, DNAJA2, is competent to catalyze luciferase refolding by Hsc70, while its close homologue DNAJA1 is not. Our data suggests that it is not a difference of luciferase binding sites for these J proteins that leads to the disparity, as originally hypothesized, but rather the ability of Hsc70 to stimulate binding of DNAJA2 to a β-sheet located between the two domains of luciferase. This finding suggests a new model of luciferase refolding by Hsc70 and a J protein. It is known that a J protein must first bind luciferase and recruit Hsc70, not vice

versa [1]. Our data suggests that when DNAJA2 recruits Hsc70, Hsc70 in turn stabilizes the interaction of DNAJA2 with a particular site and that this reciprocal cooperativity is what allows for productive luciferase refolding. This finding is reminiscent of the cooperative inhibition of a transcription factor, σ^{32}, by bacterial chaperones. It has been found that simultaneous binding of *E. coli* DnaK and DnaJ to σ^{32} is required for effective inhibition, that DnaK specifically destabilizes a region of σ^{32} to make it available for DnaJ binding, and that DnaJ stimulation of DnaK ATPase activity is optimal when both are bound to the substrate [2, 3]. Further work is required to achieve similar mechanistic understanding of the refolding of luciferase by chaperones, as will be discussed below.

Though many chaperones have been shown to influence tau biology in both healthy and diseased systems, little is known about direct interactions between chaperones and tau. I therefore took a broad, model-generating approach to map the interaction of many chaperones with tau using peptide microarrays. This approach was highly fruitful and yielded a rich, complex dataset from which many hypotheses can be developed. A broad feature of this dataset was that competition between pro-stabilizing and pro-degradation chaperones for binding to the same sites on tau likely plays an important role in tau homeostasis. Additionally, chaperones may compete with kinases, microtubules, and other tau molecules for tau interactions, thus playing an integral role in tau biology. The underlying cause of lowered chaperone levels in neurodegenerative disease is unclear, but a major consequence appears to be the disregulation of tau, which may contribute significantly to the pathological cascade. For example, hyperphosphorylation of tau may be due in part to the loss of chaperone competition with kinases for binding to many

phosphorylation-rich sites on tau. Chapter 3 explores the tau binding dataset in detail and draws connections to what is already known about the function, modification, and aggregation of tau.

In Chapter 4, we used the peptide microarray platform to address another question: can chaperones prevent amyloid formation by directly binding amyloidogenic sequences? This question was prompted by the observation that Hsp70 can abrogate the formation of amyloid fibrils comprised of steric zippers formed by peptides with widely divergent physicochemical properties. My co-workers, Dr. Andrea Thompson and Dr. Atta Ahmad, carefully designed the amyloid array to include both amyloid-forming and normal peptides with equivalent average physicochemical characteristics in order to test amyloidogenicity as a determinant of chaperone binding. Surprisingly, our experiments revealed that some chaperones – Hsp70s, Hsp90, DnaJ, DNAJA1/A2/B1, and CHIP – demonstrate preferential binding to amyloidogenic peptides, while others do not, suggesting that these particular chaperones – and perhaps others not tested – have evolved certain mechanism(s) to detect "dangerous" sequences and prevent amyloid formation. We selected ten peptides from this dataset for further study and evaluated their binding by the substrate binding domain of Hsc70 ($Hsc70_{SBD}$) using two methods: fluorescence polarization (FP) and isothermal titration calorimetry (ITC). By FP, we found that 4 of the 5 "binders" (as determined by the array data) were able to compete with the insulin peptide LVEALY for binding to $Hsc70_{SBD}$, while only 2 of 5 "non-binders" were able to compete, yielding a 70% confirmation rate for our array data. Similarly, using ITC I observed $Hsc70_{SBD}$ binding of all of the binders and 3 of the 5 non-binders. Interestingly, all interactions had comparable

affinities and were both enthalpically and entropically favorable. These results do not specifically identify a mechanism by which Hsc70 might preferentially identify amyloid-forming peptides. However, they are promising and continuing work in this area may yet shed light on this question.

5.3 Future Directions

5.3.1 Specific roles of J proteins in *S. cerevisiae* and beyond

The chemical genetics study of J proteins in *S. cerevisiae* suggests both specific investigation avenues and a general need to better understand the roles of individual J proteins in cells. Our data points to a role of Swa2, a J protein involved in clathrin removal from vesicles, in the cell's ability to mount a cell wall integrity (CWI) reponse. An investigation into whether these two functions are directly connected or distinct aspects of Swa2 biology may provide insights into clathrin uncoating and/or the CWI pathway and the involvement of chaperones in these processes. Another finding that merits further investigation is the role of Jjj3, an iron-bearing enzyme that participates in redox processes, as a redox partner for a wide array of pathways beyond its originally identified role in diphthamide synthesis. The finding that Apj1, a low-copy J protein that may be localized to the mitochondria, has synthetic lethal interactions suggests an unexpectedly important role for this J protein that cannot be compensated for by endogenous levels of other J proteins and deserves further interrogation. More broadly, this dataset highlights the diversity of J protein functions and their roles and relative importance to cell viability in *S. cerevisiae*. A growing body of literature supports this as a general feature of J protein co-chaperone networks in various organisms: they are diverse in both structure and function and have evolved to take on

many different roles, with the J domain functioning as a link to the Hsp70 chaperone machinery [4]. Our data contributes to this finding and underscores the importance of considering individual J proteins as unique actors within a given system, not a homogenous group.

5.3.2 Mechanism of chaperone-mediated luciferase refolding

Our experiments with a luciferase peptide microarray in Chapter 3 suggest that Hsc70 stimulates DNAJA2 binding to a luciferase β-sheet comprising residues 413-439. However, as these results were obtained with isolated peptides, further work is necessary to determine whether this stimulated binding occurs in the context of full-length luciferase and whether it is relevant for the mechanism of luciferase refolding by these chaperones and others. One useful technique might be hydrogen-deuterium exchange followed by mass spectrometry to identify regions of unfolded luciferase protected in the presence of DNAJA2 and/or Hsc70. Further, enzyme-linked immunosorbent assays (ELISAs) might be used to determine whether DNAJA2 can bind to the identified peptide in solution and whether the presence of Hsc70 increases the affinity of this interaction. This experiment could also be performed with full-length unfolded luciferase in order to determine whether Hsc70 increases the affinity of DNAJA2 for the whole protein. Parallel studies would be carried out with DNAJA1 to control for interactions that do not promote luciferase refolding. The ELISA platform could also be used to test different peptides within the identified region and perhaps identify the minimal binding site that DNAJA2 is stimulated to bind by Hsc70. Using this information, point mutations of luciferase could be studied for their effect on Hsc70/DNAJA2-mediated refolding. Our lab has determined that other J proteins,

DNAJB1 and DNAJB4, are also competent to catalyze luciferase refolding (Jennifer Rauch, unpublished data). Therefore, if point mutants are identified that do impact the ability of DNAJA2 to refold luciferase, it would be informative to test whether they also affect refolding by these other J proteins, as well as the bacterial refolding system (DnaK/DnaJ/GrpE), in order to determine whether this mechanism is universal to all chaperone-catalyzed luciferase refolding. The insights thus gained could be expanded to develop hypotheses about the mechanism of chaperone refolding of other substrates.

5.3.3 Testing models for tau regulation developed from peptide microarrays

One of the major findings of the tau microarray experiments was that chaperones of different classes share many binding "hotspots" on tau. The logical conclusion from this finding is that chaperones compete with one another as part of the tau triage process. Further work will be needed to elucidate which interactions are actually competitive, which dominate in certain contexts, and how modification of specific binding sites might affect binding affinities and therefore tau fate decisions. In the final stages of my thesis work, I attempted to confirm and elaborate upon the J protein results. I designed a set of tau constructs to include or exclude specific binding sites

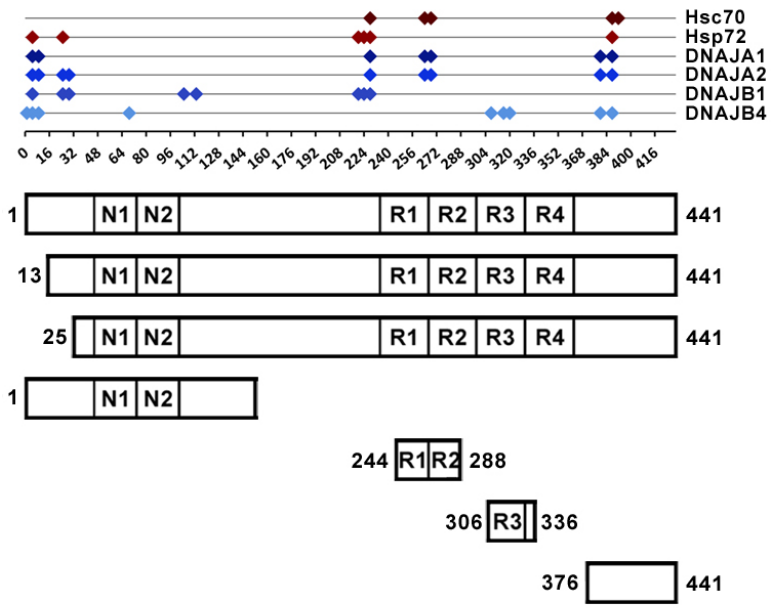

Figure 5.1. Truncations designed for ELISA studies of tau interactions with chaperones (J proteins and Hsp70s)

identified for the J proteins and Hsp70s (Figure 5.1). I then attempted to develop an ELISA platform to measure J protein binding to both full length tau and these constructs. Unfortunately, these efforts were unsuccessful, largely due to instability of the component proteins and the lack of reproducibility. One interesting finding of this work was that tau truncated at Asp25 was highly unstable, degrading into many smaller products after the normal purification procedure, further pointing to a key role of the N-terminus in tau biology, as discussed in Chapter 3.

Similar work moving forward will be valuable to identify what interactions identified on the array are important in the context of the full tau protein. Specifically, competition between pro-stabilizing (BAG1, FKBP51) and pro-degradation (BAG2, FKBP52, UbcH5, Ube2w, CHIP) chaperones for binding to full length tau and shorter constructs will be informative. Additionally, the effect of tau modifications, such as phosphorylation and FDTP-17 linked mutations, on chaperone interactions should be explored in order to understand how chaperone-tau contacts may be modified in disease contexts and the role this may have in pathology. Specifically, the influence of MARK phosphorylation at Ser356 on UbcH5/CHIP ubiquitination of tau, especially at Lys353, may explain the resistance of MARK-phosphorylated tau to proteasomal degradation.

Two specific "hotspots" that bear further investigation are the N-terminus and the polyproline helix/phosphorylation-rich site in the proline rich domain. As described in Chapter 3, the N-terminus has been found to have at least two effects in neurons: inhibition of anterograde fast axonal transport (FAT) and induction of exitotoxicity. As multiple

chaperones were found to bind the N-terminus, the effect of these chaperones (all four J proteins, Hsp72, BAG1, FKBP51, Ube2w, and UbcH5) on FAT inhibition and excitotoxicity should be explored. Additionally, the ability of these chaperones to bind N-terminally cleaved tau (at Asp13 or Asp25, the two caspase cleavage sites identified in this region) should be tested to understand how chaperone interactions with tau may be affected by N-terminal cleavage events during disease progression. Also, due to the involvement of the N-terminus of tau in its conformational dynamics, it may be informative to use NMR and FRET to explore the effect of chaperones on the occupation of different conformational states of tau, particularly in the presence of different phosphorylation patterns. The polyproline helix immediately upstream of the repeat domain is another intriguing site of interest that emerged from this dataset. It is already known that Pin-1, a peptidyl-prolyl isomerase, interacts with tau at this site and influences the affinity of tau for microtubules. It appears that other chaperones may also use this site to regulate tau's contacts and functions. Further experiments using point mutations or deletions are necessary to identify what feature(s) of this region are important for chaperone binding, such as the polyproline helix, the PXXP motif, or the many phosphorylated residues within this peptide. The influence of phosphorylation of these residues on chaperone interactions may also provide useful insights.

It is likely that the tau array dataset represents a maximum set of possible interactions, and further work will be necessary to identify what interactions play important roles in tau biology in both healthy and diseased systems. Experiments carried out based on this dataset will likely lead to the discovery of even more interesting aspects of chaperone-tau

interactions. A better understanding of this system may eventually lead to more rationally targeted therapies for tauopathies.

5.3.4 Understanding chaperone recognition of amyloidogenic sequences

Current work is in progress in collaboration with the lab of David Eisenberg to further explore the mechanism by which chaperones, particularly Hsc70, may recognize amyloidogenic peptides preferentially, as suggested by our peptide microarray data. We are exploring the possibility that Hsc70 could interdigitate its own sidechains with those of an amyloidogenic peptide, thereby forming a heterosteric zipper and preventing the formation of homosteric zippers and therefore amyloid fibrils. The Eisenberg lab is computationally assessing the ability of the Hsc70 substrate binding pocket to form heterosteric zippers with all of the peptides included on the amyloid array. They are also attempting to co-crystallize amyloidogenic peptides with the $Hsc70_{SBD}$ in the hopes of obtaining structural information about such an interaction, which has yet to be achieved. In our lab, Dr. Atta Ahmad has developed an $Hsc70_{SBD}$ construct that can be used to map the binding site of peptide substrates. He has successfully observed the interaction of LVEALY with the canonical substrate binding groove in the SBD. He is going to investigate the binding of other amyloidogenic peptides that were observed to bind by ITC, such as VQIVYK. He will also investigate the possibility of multiple binding sites on the SBD using peptides that were unable to compete with LVEALY but did bind by ITC, such as KSNFLN. The finding that Hsc70 and other chaperones can preferentially bind amyloid-forming sequences is a highly intriguing one and may point to a fundamental mechanism of cellular protection that is somehow lost in the course of diseases of protein misfolding. Further work to understand

this mechanism may prove vital to understanding the underlying pathology of these diseases.

5.4 Therapeutic Perspective

The insights gained through this work about chaperone interactions with tau and amyloidgenic peptides suggest that chaperone-substrate or chaperone-chaperone interactions may constitute viable therapeutic targets, but only when we have developed a much more detailed understanding of chaperone networks and their roles in disease. Based on our evidence from the peptide microarray platform, chaperone-tau interactions seem to be an integral part of the complex and subtle system of tau regulation. Further work will expand our understanding of the role of each specific interaction. With this knowledge in hand, we can identify protein-protein contacts that may be beneficial to inhibit, or even promote, using small molecules. Alternatively, developing an understanding of how relative chaperone levels influence tau regulation may allow us to productively alter specific chaperone expression levels in order to change the fate of tau. For example, the finding that Hsp72 levels are unexpectedly low in the highly stressed environment of AD suggests that promoting expression of Hsp72, which consigns tau for proteasomal degradation, may be a productive approach. Overall, it seems clear that chaperones are intimately involved in many disease processes, and further work to understand their roles in pathology, either through gain or loss of function, will bring us closer to developing effective therapies for some of the most challenging and destructive diseases affecting society.

5.5 Concluding Thoughts

With the work presented in this thesis, I attempted to advance our understanding of chaperone networks by developing complex datasets that provide evidence for many models. These datasets will serve as valuable starting points for future projects that in turn lead to a deeper understanding of how chaperone networks function. It is my hope that such work will allow for better characterization of the pathology of protein misfolding diseases, such as Alzheimer's disease, and in turn lead to more rational and effective therapies.

5.5 References

[1] Szabo A, Langer T, Schroder H, Flanagan J, Bukau B, Hartl FU. The ATP hydrolysis-dependent reaction cycle of the Escherichia coli Hsp70 system DnaK, DnaJ, and GrpE. Proc Natl Acad Sci U S A, 1994; 91: 10345-9.

[2] Rodriguez F, Arsene-Ploetze F, Rist W, Rudiger S, Schneider-Mergener J, Mayer MP, Bukau B. Molecular basis for regulation of the heat shock transcription factor sigma32 by the DnaK and DnaJ chaperones. Mol Cell, 2008; 32: 347-58.

[3] Suzuki H, Ikeda A, Tsuchimoto S, Adachi K, Noguchi A, Fukumori Y, Kanemori M. Synergistic binding of DnaJ and DnaK chaperones to heat shock transcription factor sigma32 ensures its characteristic high metabolic instability: implications for heat shock protein 70 (Hsp70)-Hsp40 mode of function. J Biol Chem, 2012; 287: 19275-83.

[4] Kampinga HH, Craig EA. The HSP70 chaperone machinery: J proteins as drivers of functional specificity. Nat Rev Mol Cell Biol, 2010; 11: 579-92.